X-921-74-145
PREPRINT

GODDARD EARTH MODELS (5 AND 6)

F. J. LERCH
C. A. WAGNER
J. A. RICHARDSON
J. E. BROWND

DECEMBER 1974

GSFC
GODDARD SPACE FLIGHT CENTER
GREENBELT, MARYLAND

For information concerning availability
of this document contact:

Technical Information Division, Code 250
Goddard Space Flight Center
Greenbelt, Maryland 20771

(Telephone 301-982-4488)

X-921-74-145

GODDARD EARTH MODELS (5 AND 6)

Francis J. Lerch
Carl A. Wagner
Geodynamics Branch. GSFC

James A. Richardson
Joseph E. Brownd
Computer Sciences Corp.. Silver Spring, Md.

December 1974

* Results presented at the 55th Annual Meeting of the American Geophysical Union, April 8-12, 1974, Washington, D.C.

GODDARD SPACE FLIGHT CENTER
Greenbelt, Maryland

GODDARD EARTH MODELS 5 AND 6

ABSTRACT

A comprehensive earth model has been developed at the Goddard Space Flight Center to satisfy requirements of the National Geodetic Satellite Program. The model consists of two complementary gravitational fields (in spherical harmonics) and center-of-mass locations for 134 tracking stations on the earth's surface. One gravitational field (Goddard Earth Model 5) is derived solely from satellite tracking data. This data on 27 satellite orbits is the most extensive used for such a solution. It includes 120,000 precisely reduced optical observations on 23 satellites, 160,000 one way doppler observations on 5 satellites, 10,000 laser ranges to 6 satellites, 100,000 S-band range and range-rate measurements to 1 satellite, 4,000 C-band ranges to 1 satellite and 3,000 radio interferometric (Minitrack) measurements on 4 satellite orbits. A second (combination) solution (GEM 6) uses this data with 13,400 simultaneous events from satellite camera observations, and 1654 5° x 5° surface gravimetric anomalies. This solution consists of 134 geocentric station locations, 328 spherical harmonics of gravity, the radius of the earth and the equatorial constant of gravity. The derived gravitational field is complete to (16,16) with resonant and zonal terms to 22nd degree. The derived mean equatorial radius of the earth is 6378144 meters. The satellite-only solution as a whole is accurate to about 4.5 milligals as judged by the surface gravity data. The majority of the station coordinates are accurate to better than 10 meters as judged by independent results from geodetic surveys and by doppler tracking of both distant space probes and near earth orbits. Both of these figures serve to meet requirements of the national program.

PREFACE

Over the period of the National Geodetic Satellite Program numerous people have contributed to the development of the program systems which led ultimately to the models for GEM 5 and 6. A list of these people and their areas of contribution is presented in a section under acknowledgments. For the current report, special acknowledgment is given to Thomas V. Martin, of Wolf Research and Development Corporation and to Barbara H. Putney, of GSFC, for the preparation of written material in Appendix A on the orbital theory employed in the GEODYN (Geodynamics) program. Special acknowledgment is given to James S. Reece, of Computer Sciences Corporation, for his contributions to the geometric theory and related program for the adjustment of station coordinates from simultaneous observations. Wayne A. Taylor, of Computer Sciences Corporation, was instrumental for the data processing and Barbara H. Putney for the management and integrity of the computer program system. Finally, we extend appreciation to Professor R. H. Rapp, of The Ohio State University for his work in the preparation of the surface gravity data employed and related techniques for applications.

ACKNOWLEDGMENT

The following contributors and their contributions to the development of the Goddard Earth Models have been recognized and are gratefully acknowledged. There are five periods for this development leading to the GEM 5 and 6 NGSP solutions:

1. 1965-1966; the development of the GEOS-A flash schedule using data types for all major geodetic systems.

2. 1966-1968; GEOS A and B Tracking system intercomparisons: the initiation of the NONAME orbit determination system.

3. 1967-1969; multi-satellite operations: the development of NONAME to handle all satellites and tracking formats.

4. 1968-1971; GEOSTAR development and preliminary solutions: geodetic parameter and station recovery capability from satellite tracking achieved from extended NONAME with MERGE and SOLVE programs.

5. 1971-1974; Goddard Earth Models solutions (1-6) from satellite and surface gravity data.

The period of the contribution is indicated by a superscript on the contributor's name. Four types of contributions are recognized: P—programming, development, and computer operations; RW—report writing; I—significant ideas; M—management operations (including project and data supply). These codes follow the contributor's name.

The following list is by no means exhaustive, and is broken down by organization for convenience.

Goddard Space Flight Center

F. Vonbun$^{2-5}$(M), J. Siry$^{1-4}$(I,P,M), D. Smith^{4,5}(I), F. Lerch$^{1-5}$(I,RW,P,M), E. Doll$^{1-3}$(I,M,RW), J. Marsh$^{1-3,5}$(I,RW,M,P), M. Velez^{3,4}(I,P,RW), G. Brodsky^{3,4}(P,RW), V. Laczo^{3,4}(I,P), W. Kahn^{3,4}(I,M), B. Putney$^{3-5}$(I,RW, P,M), C. Wagner^{4,5}(I,P,M,RW), T. Felsentreger^{3,4}(I), J. Murphy^{3,4}(I), J. Berbert$^{1-3}$(I,RW), C. Looney^{1}(I,M), J. Zegalia^{1,2}(M), R. Mather^{5}(I,P), M. Khan^{5}(I,P), E. Watkins$^{2-5}$(M), D. Rose$^{2-5}$(M).

Wolf Research and Development Corporation

R. Sandifer[1,2](I,RW,P), S. Moss[1-3](I,M), W. Wells[1-3](I), C. Martin[2,3](I,P, RW), T. Martin[2,3,5](I,P), H. Kahler[1,2](I,P,M), E. Mullins[5](RW), C. Goad[2,3] (P,I), J. Serelis[5](P), R. Williamson[1-3,5](P,I), V. Der[5](I,P), J. Diamante[5] (I,P), J. Vetter[1-3](P,I), S. Klosko[5](I), P. Dunn[2,3](I,P,RW), B. Brown[2,3](P, I), M. Willoughby[1,2](P), N. Roy[1,2](I,RW), M. D'Aria[1,2](I,RW), B. O'Neill[1,2] (I,RW), Ms. Willoughby[1,2](P), B. Douglas[5](I), M. Kaiser[1](P,I,RW), R. Gotz[2,3] (I,RW,P), R. Brooks[1,2](I,RW).

Computer Sciences Corporation

K. Nickerson[4,5](I,P,M,RW), W. Taylor[4,5](I,P,RW), D. McGraw[4](P), H. Dennis[4](P), H. Rainey[4](P), D. Weiss[4](P), C. Engrum[4](P), L. Williams[4](P), C. Kenworthy[4](P), K. Tasaki[4](P), K. Lamars[4](I), R. Grant[4,5](I,P), M. Sandson[5](I,RW,M), R. Brown[5](I,P), J. Brownd[5](I,P,RW,M), W. Strange[4,5](I,M), J. Richardson[5](I,P,RW,M), J. Reece[5](I,P,RW), R. Taylor[4,5](M), M. Harrison[5](P), A. Euler[5](P).

IBM

F. Green[4](I,M), R. Greene[4](I,M), G. Finley[3,4](P), Y. Sawanobori[4](P)

Computer Usage Corporation

C. Sheffield[4](I), R. Hamblen[4](P), J. Morris[4](P).

Computer and Software, Inc. (and CSTA)

P. Gibbs[5](P), D. Miller[5](P), D. Mentges[4,5](P), D. Mathews[4](P), H. Huston[5](P).

NASA Headquarters and Contracts through Headquarters

J. Rosenberg[1,2](I,M), W. Kaula[4,5](I), R. Rapp[5](I,M), I. Mueller[2](I), H. Schmid[5](M).

Smithsonian Astrophysical Observatory

B. Miller[4,5](M).

CONTENTS

	Page
ABSTRACT	iii
PREFACE	iv
ACKNOWLEDGMENTS	v
1. INTRODUCTION	1
2. DATA EMPLOYED	9
2.1 GEM 5 Data, Satellite Dynamic Solution	9
2.2 GEM 6 Data, Combination Solution	9
3. MODELING AND ANALYSIS	19
3.1 Geopotential	19
3.2 Techniques in Modeling the Data	20
3.3 Satellite Sensitivity to the Potential	22
3.4 Error Estimates for Geopotential Coefficients (GEM 5)	28
3.4.1 Formulation of Error Estimates for Geoid Height and Gravity Anomaly	28
3.4.2 Adjusted Error Estimates of Potential Coefficients	31
3.5 Relative Weighting and Error Estimates for Combined Solution (GEM 6)	33
3.6 Verification of Error Estimates	34
4. RESULTS	43
4.1 Gravitational Potential for GEM 5 and 6	43

CONTENTS (continued)

Page

4.1.1 Zonal Harmonics 43

4.1.2 Comparison with Gravity Anomalies 43

4.1.3 Comparison with Satellite Data 52

4.1.4 Geoid Height 62

4.2 Station Coordinates for GEM 6 65

4.2.1 Comparison with Other Solutions 72

4.2.2 Comparison with Mean Sea Level Heights 77

4.2.3 Comparison with Positions on National Datums 80

4.2.4 Displacements in Mean Pole and Greenwich Meridian 83

4.2.5 Summary of Results for Station Coordinates 83

4.3 Geodetic Parameters 89

5. SUMMARY AND CONCLUSIONS 93

REFERENCES 97

APPENDIX A—METHODS EMPLOYED A-1

A1. Orbit Theory for GEODYN A1-1

A2. Geometric Method for Simultaneous Observations Including Constraints from Datum Survey A2-1

A3. Gravimetric Method for Mean Anomaly Data A3-1

A4. Method of Combined Solution A4-1

APPENDIX B—SATELLITE AND GRAVITY DATA DISTRIBUTIONS . . B-1

LIST OF ILLUSTRATIONS

Figure		Page
2-1	Distribution of Stations in GEM 6	12
2-2	BC-4 Baselines and Ties	14
3-1	Average (rms) Coefficient Value by Degree	23
3-2	Satellite Sensitivity to Potential Terms (30 x 30)	26
3-3	Stochastic Satellite Sensitivity	27
3-4	Average (rms) Standard Deviation Per Degree n for GEM 5 and Gravimetry Solutions	29
3-5	Percent Accuracy of GEM 5 Coefficients by Degree	33
3-6	Percent Reduction in Error Variances of GEM 5 Due to the Effect of Combining Gravimetry Data in GEM 6	35
3-7	Comparison of Geoid Profile Derived from Altimetry and GEM 6	38
3-8	Comparison of Error Estimates for Coefficients of Degree n	39
4-1	GEM 5 Gravity Anomaly Contours	53
4-2	GEM 6 Gravity Anomaly Contours	54
4-3	GEM 5 Geoidal Heights	55
4-4	GEM 6 Geoidal Heights	56
4-5	Geoid Height Zonal Profile	63
4-6	Station Height above Geoid Computed by GEM 6 vs Surveyed Height	79
4-7	Displacement of the Greenwich Meridian and Pole as Shown through Comparisons with GEM 6	87

LIST OF TABLES

Table		Page
1-1	Description of Goddard Earth Models	5
2-1	Orbital Parameters on 27 Satellites and Distribution of Data for Satellite Arcs Using Optical Data Only	10
2-2	Distribution of Data for Satellite Arcs Using a Variety of Tracking Systems	11
2-3	Simultaneous Observations Used for Geometrical Station Adjustment	15
2-4	Baseline Constraints from Survey (BC-4 Stations)	15
2-5	Basic Geodetic Reference Parameters	16
2-6	Standard Deviations of Tracking Observations	16
3-1	Satellite Data and Sensitivity Level	24
3-2	Average (rms) Error Estimates for Potential Coefficients of Degree n for GEM 6	35
3-3	Station Coordinate Error Estimates for Tracking Systems in GEM 6	36
4-1	GEM 5 Normalized Coefficients	44
4-2	GEM 6 Normalized Coefficients	45
4-3	Comparison of Zonal Coefficients	46
4-4	Comparison of Terrestrial 5° Anomalies with Anomalies Computed from Various Models	48
4-5	Statistical Error Estimates for Gravity Models Based upon 5° Terrestrial Anomalies	49
4-6	Gravity Anomaly Degree Variances	51
4-7	RMS Value of Residuals of Two-Way Doppler for USB Tracking on Daily Arcs of ERTS-1	57

LIST OF TABLES (continued)

Table		Page
4-8	Weighted RMS of Observation Residuals in Camera Observations for a Weekly Arc on Each of 23 Satellites . . .	58
4-9	RMS of Residuals from Laser System Measurements of Short Arcs of BE-C	60
4-10	Comparison of Models for Long-Term Zonal Perturbations	60
4-11	Summary of Gravity Model Comparisons with Satellite and Gravimetry Data	61
4-12	Major Geoid Features	62
4-13	Global RMS of Geoid Height Differences with the GEM 6 Model	64
4-14	Constraints on Relative Position (Survey Ties)	66
4-15	Constraints on Baseline Distance	68
4-16	GEM 6 Station Coordinates	69
4-17	Comparison with JPL's DSS (Deep Space Stations).	73
4-18	Direct Comparison of Spin Axis Distance and Longitude (GEM 6-JPL)	73
4-19	Comparisons of GEM 6 with GEM 4 Station Positions	75
4-20	GEM 6-GSFC 73 Station Coordinates	76
4-21	Station Comparisons of GEM 6-SAO SE III	76
4-22	Station Comparisons of GEM 6-NWL 9D	78
4-23	GEM 6-OSU WN4 Station Comparisons	78
4-24	Comparisons of Δy (coordinate differences) for Selected BC-4 Stations	78

LIST OF TABLES (continued)

Table		Page
4-25	Station Comparisons of GEM 6-Mean Sea Level Height . . .	82
4-26	Adopted Origins Used for Solutions of Seven Parameters on Survey Datum	82
4-27	Solutions for Relation of GEM 6 to Major Datums	84
4-28	Differences between Coordinates of Stations in GEM 6 and other Major Datums	85
4-29	Datum Shifts to GEM 6 System	88

SECTION I . . . . . INTRODUCTION

SECTION I . . . . . INTRODUCTION

GODDARD EARTH MODELS 5 AND 6

1. INTRODUCTION

The 10 year National Geodetic Satellite Program (NGSP) had its start in 1964. A principal goal was to determine a gravitational field for the earth complete to (15,15) in spherical harmonics and with an overall accuracy of about 4 milligals for this field. A complementary goal was to develop a worldwide geodetic system. The geocentric position of a large number of surface stations on continents and islands were to be found to within 10 meters.

At that time the long wavelength components of the field were virtually unknown, apart from the earth's oblateness and a few other low degree zonal terms. Until these could be found, the bulk of the last 100 meters of the earth's shape would remain unknown. Prior to the satellite era the positions of continents and ocean islands themselves were not known to better than a kilometer with respect to each other. These goals, while stated in terms of classical geodesy (the measure of the earth), were of equal utility to the space program.

Roughly speaking, the uncertainties of the earth's shape (the geoid) map with a magnification of about ten to one into the periodic deviations of a close satellite's orbit in a day's time. Similarly, the uncertainties in tracking station positions map roughly one to one into periodic orbit errors. Thus, in the early 1960's the tracking error within a well-observed one day arc, just from the uncertainties in the gravity field and surface locations, was of the order of a kilometer. This was an intolerable situation when the trackers available at the time had accuracies as much as two orders of magnitude better than this. But even before the national program began Izsak (1963) at the Smithsonian Astrophysical Observatory, Anderle (1965) at the Naval Weapons Laboratory, Guier (1963) at the Applied Physics Laboratory, and Kaula (1963) at Goddard Space Flight Center had used camera and radio doppler tracking data to derive complex fields and begin the reduction of these orbit errors. The methods available for orbit computation in this early work were analytic and numeric; not essentially different from those used now. Where only sparse camera data was used (and ultimate accuracy was not required) Kaula and Izsak showed that simple linear perturbation theory for the geopotential, lunar-solar gravity and radiation pressure, augmented by empirical terms to account for atmospheric drag, could achieve acceptable results. They demonstrated the importance of solving for the tracking station positions in conjunction with the gravitational field and orbit parameters. Anderle and Guier, using dense doppler data in short arcs, computed their orbits numerically to high precision (but with long computer times). Guier saved some computation time by computing the gravitational field "partial derivatives" analytically. But he did not work with as high a tracking density as Anderle.

Two other features of this early phase of the national program should be noted. All solutions for the zonal harmonics came from independent long arc analyses using the well known secular and long period orbit perturbations of these terms. Secondly, even by the mid 1960's, combination solutions for the geopotential were attempted with more than one data type, from both satellites and surface gravity [Kaula (1966a,b), Kohnlein (1967), Bjerhammar (1967), and Rapp (1968)]. Formally, these gave the first complete (15,15) fields, but the data coverage, both at the surface and on the satellites, was not yet sufficient to give accurate results. Nevertheless, the computer techniques for large scale combination-data solutions (using the least squares adjustment process) were established by 1968. At this time Goddard Space Flight Center undertook the task of producing an earth model to the full specifications of the program with use of all available data (Lerch and Kahn, 1968).

Goddard's approach, similar to Anderle's (1965), was to use numerical integration for all orbit and "partials" computation, irrespective of satellite data type. In this way formal orbit computation accuracies of better than one meter (for extended arcs) could be achieved, looking forward to the 1970's when the more stringent requirements of the earth and ocean physics program would have to be met [Kaula (1969)]. The unique feature of Goddard's approach (besides the comprehensive data use) was to allow as free and simultaneous an adjustment as possible for all the orbit, station, tracking and field parameters. In particular, the zonal geopotential was to be adjusted from the data simultaneously with the other field coefficients. It was expected that such an unconstrained and fully correlated solution, employing a large data base and accurate orbit perturbations, would find the most accurate values for the earth model parameters.

In support of this approach there is available at Goddard the computing capability of the IBM 360/95 data processor with approximately 5 megabytes of core storage. As an example of its speed, a weekly orbital ephemeris is generated in less than one minute with accuracy better than a meter for a complete 15 x 15 geopotential field. Also an orbital data processing system was already available as a result of intercomparison studies, performed for NGSP, of major geodetic tracking systems observing the GEOS-I and II satellites (Lerch et al., 1967; Lerch and Kahn, 1968). This system formed the basis for the results obtained here, and its present development is described in the appendix of this report.

In 1971, a preliminary satellite field to (8,8) was derived at Goddard (Lerch, et al., 1971) from camera observations on 12 satellite orbits by numerical integration. Tests indicated that this model was not as accurate as the first Smithsonian Standard Earth (SE 1) (Lundquist and Veis, 1966) which used almost the same data. Modeling for atmospheric drag perturbations, particularly for the low altitude satellites, needed improvement. In 1972, the first of the Goddard Earth Models (GEM 1 and 2) was produced; GEM 1 (complete to (12,12)) using

only camera observations on 21 orbits (none of low inclination), and GEM 2 (complete to (16,16)) combining this data with surface gravity information (anomalies). The locations of 46 tracking stations (world-wide) was an adjunct of these first models. These models proved fully competitive with the second Smithsonian Standard Earth (SE 2) (Gaposchkin and Lambeck, 1970). They were found to be surprisingly better in tests with (1 meter) laser data on certain well known orbits. Most remarkably, the zonals (of GEM 2) were accurate enough to give significantly improved results over the Smithsonian SE 2 on two new orbits of low inclination.

In 1972 (also), GEM 3 and 4 were derived from an extended data base using electronic observations (doppler, S-band range and range-rate, Minitrack and laser range measurements). Again GEM 3 (odd numbered) was a satellite-only field (complete to (12,12)). GEM 4 was a combination solution (complete to (16,16)) with data from GEM 3 and surface gravity, and it included the geocentric locations of 61 tracking stations. Satellite data on 27 orbits (including 2 of low inclination) were included in these solutions. Tests with surface gravity data showed improved results for GEM 3 over GEM 1 and SE 2. Models of GEM 1 through 4 are referenced in Lerch et al., 1972a,b.

In 1973, simultaneous observations on the high altitude PAGEOS satellite became available from the BC-4 cameras of the NOS network (Schmid, 1974). Additional laser and simultaneous MOTS* camera observations on the GEOS I and II satellites (Reece and Marsh, 1973) were also utilized for an extended solution. The simultaneous observations provided the first opportunity for purely geometric station recovery similar to the solutions pioneered by Veis (1963). In all, 134 tracking stations could be colocated with the earth's center using survey ties between some of the BC-4 sites and the previous satellite trackers on the close orbits. New surface gravity data, in the form of world-wide 300 x 300 mile equal area mean anomalies, were obtained from Rapp (1972). These proved much smoother than the data in GEM 2 and 4, and used geophysical model anomalies as well as statistical prediction for the data in the world's unsurveyed areas (66 percent of the total). All this new data was combined with the data previously processed for GEM 3 to produce the satellite-only field (GEM 5) and the new combination model (GEM 6), as the Goddard Space Flight Center's final contribution to the NGSP. These final solutions are fully described in this report.

An overall summary of the contents of the GEM solutions is presented in Table 1-1. The subsequent sections of the report are organized as follows:

2. Description of Data
3. Modeling and Analysis

*Minitrack Optical Tracking System

4. Results

5. Summary and Conclusions

Important aspects of the modeling are described and analyzed in Section 3. A detailed account of the mathematical equations and methods for processing the data is organized in Appendix A as follows:

A1 - satellite dynamic (orbital) data
A2 - satellite geometric (simultaneous) data
A3 - gravimetric (surface) data
A4 - combination of above data

Finally, a detailed set of tabulations describing satellite and gravimetric data is presented in Appendix B.

Table 1-1

Description of Goddard Earth Models (GEM)

Solution	Spherical* Harmonics	Stations' Coordinates	Tracking Data	Gravimetric Data
GEM 1	12 x 12		120,000 Camera Obs. on 23 Satellites, MINITRACK Obs. on 2 Satellites	
GEM 2	16 x 16	46 Stations	GEM 1 Data	1707 5° x 5° Mean Gravity-Anomalies Based on 21,000 1° x 1° Values
GEM 3	12 x 12		400,000 Camera, Laser DME and Electronic Obs. on 27 Satellites Including Data from SAS and PEOLE at Low Inclination	
GEM 4	16 x 16	61 Stations	GEM 3 Data	1707 5° x 5° Mean Gravity-Anomalies Based on 21,000 1° x 1° Values
GEM 5	12 x 12		GEM 3 Data with Different Weighting	
GEM 6	16 x 16	134 Stations	GEM 5 Data Plus Geometric Data from BC-4 Camera, Laser and MOTS Camera Systems	Rapp's 5° Equal Area Mean Gravity-Anomalies Based on 23,000 1° x 1° Values

*Harmonics include zonal and satellite resonant coefficients to degree 22.

SECTION II . . . . . DATA EMPLOYED [redacted]

SECTION II . . . . . DATA EMPLOYED

2. DATA EMPLOYED

2.1 GEM 5 Data, Satellite Dynamic Solution

Goddard Earth Model 5 has been computed from observations taken by camera, electronic and laser systems on 27 close-earth satellites. The tracking systems providing observational data included: Baker-Nunn cameras, Minitrack Interferometer, Minitrack Optical Tracking System (MOTS) cameras, laser DME, Goddard Range and Range-Rate (GRARR) systems, C-band radar systems, and Tranet Doppler systems. The satellite orbital geometry and data are presented in Tables 2-1 and 2-2.

In brief, the data processed in the orbit computations of GEM 5 is as follows:

- 294 7-day-long optical data arcs consisting of approximately 120,000 observations on 23 satellites (See Table 2-1),
- 68 7-day long arcs with electronic, laser, and additional optical data consisting of approximately 294,000 observations among 10 satellites (Minitrack data was employed to support analysis for zonal and satellite resonant terms.),
- 100 one- and two-day arcs of GEOS data employed for improvement of stations' coordinates.

A more complete description of the data distribution, summarized by station and by satellite arc in chronological order, is presented in Appendix B, Tables B-1 to B-5.

2.2 GEM 6 Data, Combination Solution

GEM 6 has been computed from a combination of GEM 5 with surface gravimetric data and BC-4, laser DME, and MOTS simultaneous observations. In addition, terrestrial baselines and local survey ties between stations were employed in the form of statistical constraints. In all, data was processed for a worldwide network of 134 tracking stations. A map illustrating the distribution of tracking stations is presented in Figure 2-1. Stations and/or observations employed in the orbit mode of computation are referred to as a dynamic set and those employed in the simultaneous mode, as with the BC-4 network, are referred to as a geometric set. Lines connecting the BC-4 stations in Figure 2-1 correspond to simultaneous observations and show how the BC-4 network is connected geometrically throughout the world. Geometric data for the MOTS and laser systems was employed principally in the area of the U.S., and this is not illustrated in the above figure since these stations are also a part of the dynamic system. Geometric data for the BC-4 stations was observed on the PAGEOS satellite and that for the MOTS and laser systems was observed on the GEOS-I and II satellites.

Table 2-1

Orbit Parameters on 27 Satellites and Distribution of Data for Satellite Arcs Using Optical Data Only

294 Weekly Opt. Arcs (Primarily SAO Baker-Nunn)

Satellite Name		A (Meters)	E	I (Deg)	Perigee Height (km)	Mean Motion (Rev/Day)	No. Arcs	No. Obs.
TELSTAR-1	620291	9669530.1	0.2421	44.79	951.3	9.13	16	1946
GEOS-I	650891	8067353.6	0.0725	59.37	1107.5	11.98	35	45555*
SECOR-5	650631	8154869.9	0.0801	69.23	1140.1	11.79	4	290
OV1-2	650781	8314700.2	0.1835	144.27	414.8	11.45	4	910
ECHO-1RB	600092	7968879.1	0.0121	47.22	1501.0	12.20	18	2240
DI-D	670141	7641681.9	0.0842	39.45	589.0	13.07	9	6386
BE-C	650321	7503563.5	0.0252	41.17	941.9	13.36	22	4947
DI-C	670111	7344163.4	0.0526	40.00	586.6	13.79	4	902
ANNA-1B	620601	7504950.8	0.0070	50.13	1075.8	13.35	40	4183
GEOS-II	680021	7710806.6	0.0308	105.79	1114.2	12.82	24	25315*
OSCAR-7	660051	7404041.3	0.0242	89.70	847.7	13.63	4	1780
5BN-2	630492	7463226.9	0.0058	89.95	1062.5	13.47	5	355
COURIER-1B	600131	7473289.0	0.0174	28.34	988.5	13.44	12	3375
GRS	630261	7228289.3	0.0604	49.72	421.3	14.13	5	369
TRANSIT-4A	610151	7321521.7	0.0079	66.83	806.0	13.86	14	1316
BE-B	640841	7364785.0	0.0143	79.70	901.8	13.74	4	469
OGO-2	650811	7345633.6	0.0739	87.37	424.8	13.79	7	461
INJUN-1	610162	7312542.4	0.0076	66.81	895.0	13.88	9	768
AGENA-RB	640011	7297251.5	0.0010	69.91	920.2	13.93	7	1005
MIDAS-4	610281	9995760.5	0.0121	95.84	1504.8	8.69	20	14879
VAN-2RB	590012	8496759.8	0.1832	32.89	562.0	11.09	11	379
VAN-2	590011	8309120.5	0.1648	32.87	562.2	11.46	5	615
VAN-3	590071	8511504.6	0.1906	33.35	517.9	11.06	15	996
SAS	701071	6922505.3	0.0030	3.03	523.5	15.07	--	--
PEOLE	701091	7006154.9	0.0162	15.01	515.4	14.80	--	--
TIROS-9	650041	8020761.2	0.1167	96.42	706.7	12.09	--	--
ALOU-2	650981	8097474.4	0.1508	79.83	502.0	11.91	--	--
						Totals	294	119441

*MOTS OBS.: GEOS-I-34000, GEOS-II-22000.

Table 2-2

Distribution of Data for Satellite Arcs Using a Variety of Tracking Systems

Satellite Electronic, Laser, and Additional Optical Data (68 Weekly Orbital Arcs)

	DI-C	BE-B	BE-C	DI-D	GEOS-I	GEOS-II	SAS	PEOLE	TIROS 9	ALOU 2	Total
Baker-Nunn	450 (80)*	60 (20)	160 (50)	500 (80)	2780 (500)	550 (120)					4,500 (850)
MOTS					2700 (350)	3300 (550)					6,000 (900)
GRARR (S-Band)						103000 (300)					103,000 (300)
Laser	680 (7)	100 (5)	160 (7)	1410 (5)		7350 (35)		200 (21)			9,900 (80)
Doppler		12200 (550)	14000 (850)		99500 (2700)	37700 (1400)					163,400 (5500)
C-Band						4000 (100)					4,000 (100)
Mini-Track							700 (85)	500 (65)	1500 (679)	600 (296)	3,300 (1125)
Total	1130 (87)	12360 (575)	14320 (970)	1910 (85)	104980 (3550)	155900 (2500)	700 (85)	700 (85)	1500 (679)	600 (296)	294,100 (8875)
No. of Arcs	2	6	6	1	13	12	4	4	14	6	68

*Observations (passes)

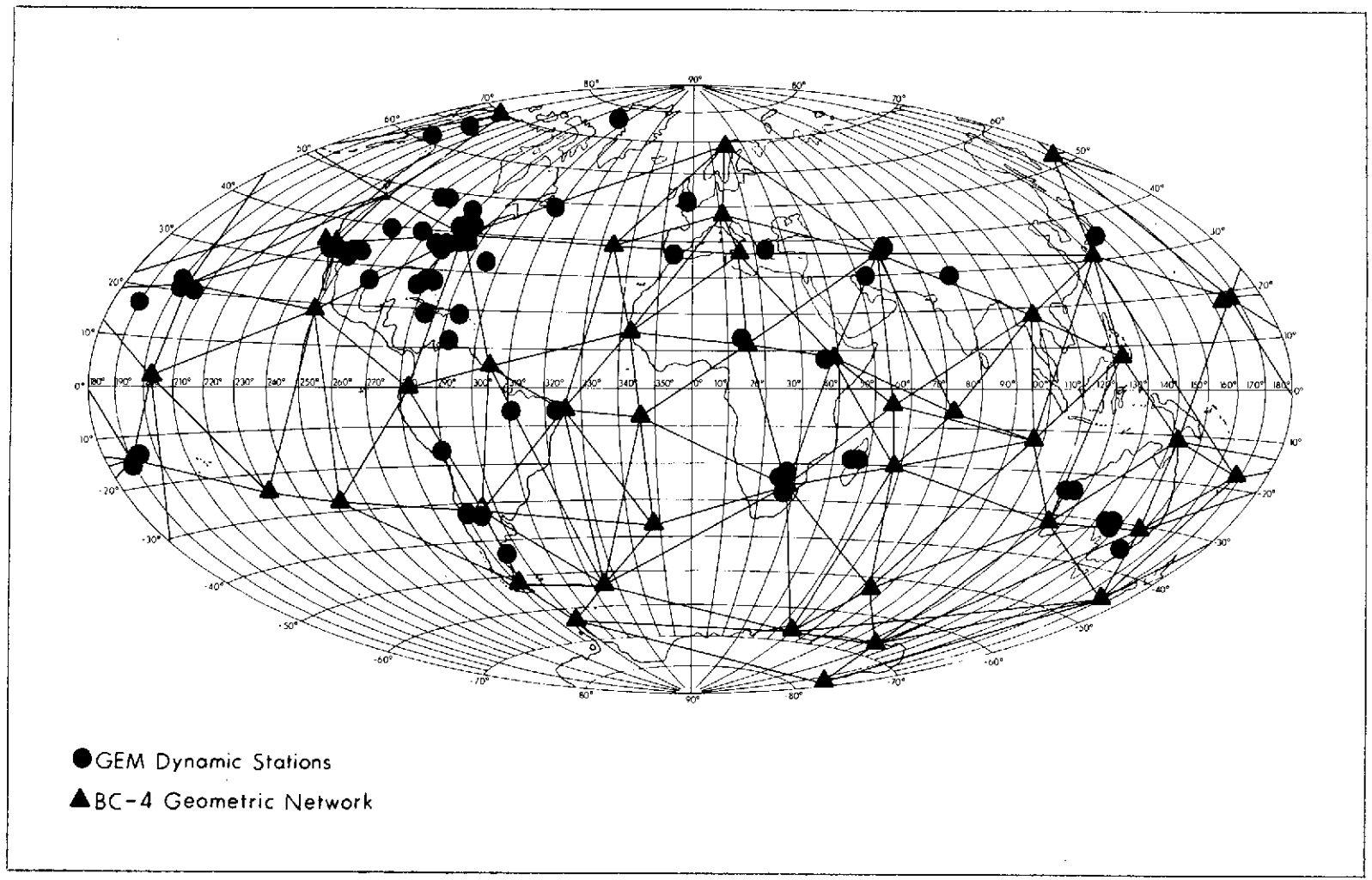

Figure 2-1. Distribution of Stations in GEM 6

Data used in GEM 6 in addition to GEM 5 data are listed with associated tables and figures for reference as follows:

- Global surface gravity data in the form of 5° equal area (300 n.m. sq.) anomalies computed by Rapp (1972). Table B-10 of Appendix B.
- Geometric data of two-, three-, four-camera, and laser/two-camera events from the MOTS-SPEOPT-Laser Network (primarily in the U.S.). Table 2-3.
- 48 relative position constraints computed from local datum surveys. (These constraints are used in order to combine the dynamic and geometrically determined networks, and to cause closely situated stations to adjust in a statistically constrained manner.) Figure 2-2.
- Eight baseline distance constraints, employed with the BC-4 data (2 in U.S., 3 in Europe, 2 in Australia, and 1 in Africa). Figure 2-2 and Table 2-4.

A complete listing, identifying the participating stations of some 13,000 simultaneous events in Table 2-3, is presented in Tables B-6 to B-8 of Appendix B. A listing of 48 survey ties employed for stations is presented in Table B-9.

The gravimetry data included 1654 values of mean gravity anomalies for 5° equal area blocks covering the whole earth. Of these, 1283 were predicted anomalies based upon observed gravity measurements and 371 were modeled anomalies as described by Rapp (1972). The predicted anomalies ranged from 1 to 15 mgal in accuracy and modeled anomalies were estimated with an accuracy of 20 mgal. This data is listed in Table B-10 along with the number of 1° equal area blocks of observed anomalies that were used to predict the 5° mean anomaly. An overall view of coverage of the gravity data may be seen by Figure B-1, where the distribution of the 5° equal area blocks is illustrated.

The accuracy estimate of the predicted anomaly is assigned to each block in Figure B-1. Generally small values of this quantity correspond to strong coverage of observed gravity data and larger values to poor coverage. Blocks with blank entries correspond to the modeled anomalies, and these are seen to be quite prevalent in the southern hemisphere.

Basic geodetic constants describing the reference ellipsoid of the earth and its gravity are given in Table 2-5. Table 2-6 shows the standard deviations assigned the various observations among the tracking systems. The inverse square of the standard deviations were used as weights for the observations in the least squares normal equations.

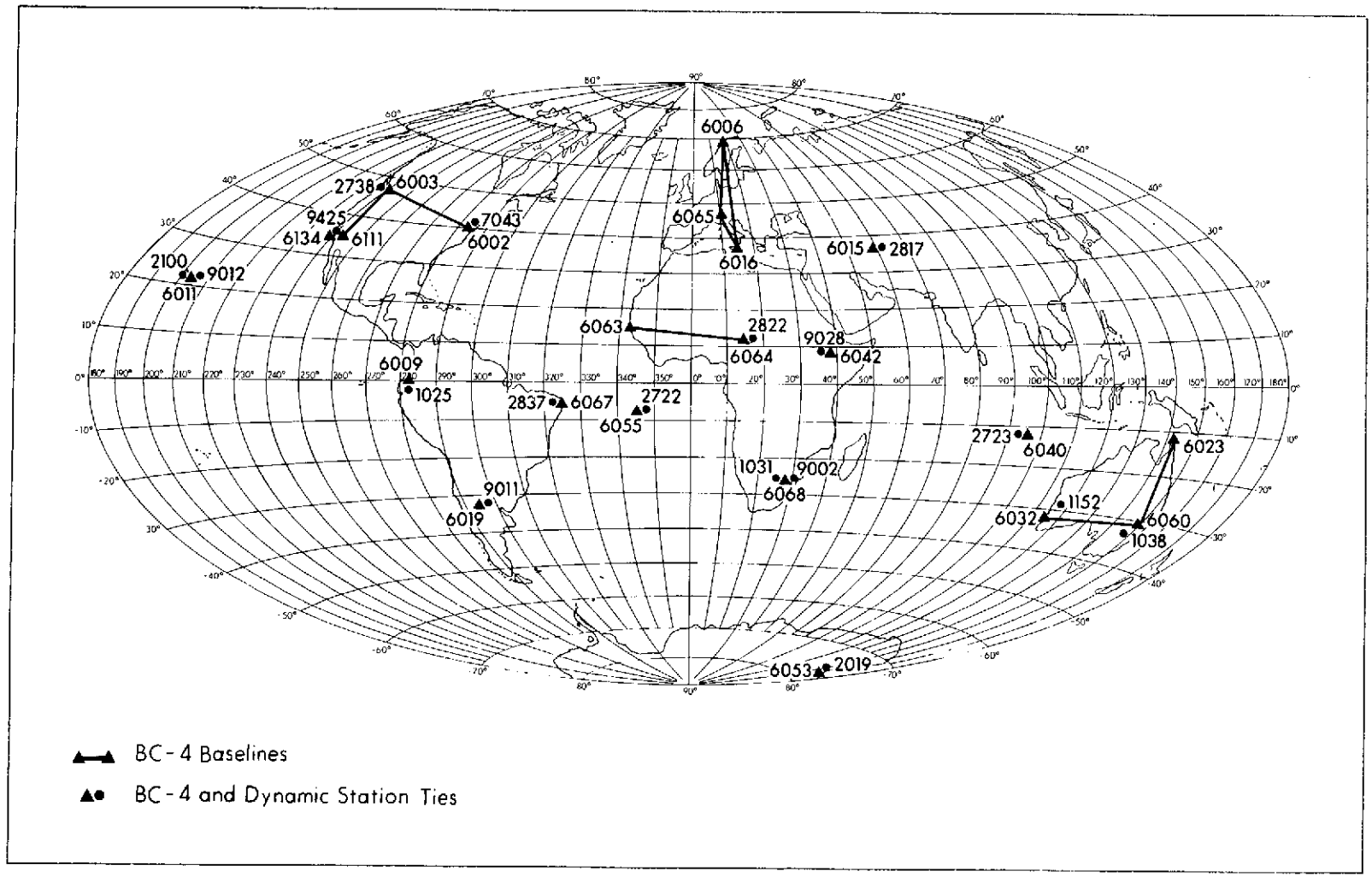

Figure 2-2. BC-4 Baselines and Ties

Table 2-3

Simultaneous Observations Used for Geometrical Station Adjustment

MOTS-SPEOPTS-Laser Data

Event Type	Number of Events*
Two-Camera	3870
Three-Camera	1614
Four-Camera	584
Laser/Two-Camera	42

*Each event pertains to a single flash from lamps on GEOS-I or II.

BC-4 Photographic Events*

Event Type	Number of Events
Two-Camera	5896
Three-Camera	1332
Four-Camera	99

*Each photographic event consists of 7 points of satellite image of PAGEOS.

Table 2-4

Baseline Constraints from Survey
(BC-4 Camera Stations)

Station Baseline	Distance (meters)	Estimated Standard Deviation PPM
6002-6003	3 485 363.23	1.00
6006-6016	3 545 871.56	1.00
6006-6065	2 457 765.81	0.70
6016-6065	1 194 793.60	0.85
6023-6060	2 300 209.80	0.50
6032-6060	3 163 623.87	1.00
6063-6064	3 485 550.76	0.85
6003-6111	1 425 876.45	0.90

Table 2-5

Basic Geodetic Reference Parameters

Mean equatorial radius,	a_e	= 6378155 meters
Flattening,	f	= 1/298.255
Rotation rate,	ω	= .7292115146 x 10^{-4} radians/second
Geocentric gravitational constant,	GM	= 3.986013 x 10^{14} meters^3/second^2
Mean equatorial gravity	g_e	= 978029.1 milligals

Table 2-6

Standard Deviations of Tracking Observations

Observation	Standard Deviation
GRARR: range	10 meters
: range-rate	3 cm/sec
Laser: range	1 meter
Camera: declination (δ)	2 seconds of arc
: right ascension ($\alpha \cos\delta$)	2 seconds of arc
MINITRACK: direction cosines	3 x 10^{-4}
NWL Doppler: range-rate	4 cm/sec
C-Band radar: range	8 meters

SECTION III . . . . . MODELING AND ANALYSIS

3. MODELING AND ANALYSIS

The gravity potential of the earth (geopotential) is given as the sum of a centrifugal potential and the gravitational potential expressed in an infinite series of spherical harmonics. The gravitational potential is truncated and this effect will be analyzed in terms of the geoid, orbits and data sensitivity. The spherical coordinates of the potential and the station coordinates are given in a center of mass reference system which is oriented to the mean pole (CIO) of 1900-1905, Bomford (1971). Satellite orbital motion provides the basis of a center of mass origin. Orientation to the CIO pole is provided through use of polar motion data distributed by the Bureau of International de l'Heure (BIH). Station observations are processed in two modes: geometrically with only simultaneous events used, as with the BC-4 world triangulation network, and dynamically using the computed orbits. Stations processed geometrically are tied to those processed dynamically through the use of local datum coordinates as shown in Figure 2-2. Scale for the station coordinates is principally determined from the reference value of GM, Table 2-5, which provides scale for the satellite orbits through the gravitational potential. However the 8 baseline distances in Table 2-4 for the BC-4 network contribute somewhat to this scale in the combination solution, GEM 6.

3.1 Geopotential

The gravity potential of the earth or geopotential is

$$W = V + \Phi \tag{3.1}$$

where V is the gravitational potential, and Φ the centrifugal potential, and where

$$V = \frac{GM}{r}\left[1 + \sum_{n=2}^{\infty}\sum_{m=0}^{n}\left(\frac{a_e}{r}\right)^n \bar{P}_n^m(\sin\varphi)\,(\bar{C}_{nm}\cos m\lambda + \bar{S}_{nm}\sin m\lambda)\right],$$

$$\Phi = \frac{1}{2}(r\,\omega\cos\varphi)^2, \tag{3-2}$$

for which r, φ, λ are spherical coordinates of radial distance, latitude, and longitude, $\bar{P}_n^m(\sin\varphi)$ is the associated normalized Legendre polynomial of degree n, order m with argument $\sin\varphi$, $\bar{C}_{nm}$, $\bar{S}_{nm}$ are normalized spherical harmonic coefficients, and ω is the rotational velocity of the earth. The coefficients are termed zonals ($\bar{C}_{n0}$, $\bar{S}_{n0} = 0$), tesserals ($\bar{C}_{nm}$, $\bar{S}_{nm}$, $n \neq m$), and sectorials ($\bar{C}_{nn}$, $\bar{S}_{nn}$, $n = m$). $\bar{C}_{10}$, $\bar{C}_{11}$ and $\bar{S}_{11}$ are equal to zero for a center of mass reference system, and the coefficients $\bar{C}_{21}$ and $\bar{S}_{21}$ correspond to a shift in position of the mean pole. For an offset of 5 meters these coefficients ($\bar{C}_{21}$, $\bar{S}_{21}$) would be of the order of 10^{-9}, and cannot be reliably determined. However,

values for these coefficients are estimated in the solution to serve as a measure of the accuracy for the low degree and order coefficients.

The gravitational potential V is employed in computing satellite motion, and the potential W, set equal to a constant W_0 on the geoid, is employed for processing the gravimetric data. The constant W_0 is a function of the reference parameters GM, a_e, f and ω whose initial values are presented in Table 2-5. An adjustment to the mean earth ellipsoidal parameters, a_e and f, are made through use of values of $\bar{C}_{20}$, the leading oblateness coefficient, and g_e, a value of equatorial gravity, both of which are derived in GEM 6. Formulation for this adjustment of g_e, a_e and f is given in Section A3 of Appendix A on gravimetric methods. An alternate adjustment of a_e through use of mean sea level height from station survey data is presented in Section 4 on results. Results for geodetic parameters are summarized in Section 4.3.

The coefficients determined in the satellite solution for the GEM 5 model are as follows: $\bar{C}_{no}$ for degrees 2 through 22, $\bar{C}_{nm}$ and $\bar{S}_{nm}$ complete to degree and order 12, and for satellite resonant coefficients of order 12, 13, and 14 n is complete to 22, and of resonant order 9 n extends to 15. The number of satellites resonant for a given order m may be seen from the orbital mean motions listed in Table 2-1. Analysis for this particular truncation of the harmonics, including terms to degree and order 30, is given in Section 3.3. In the GEM 6 solution additional coefficients are determined by combining surface gravity data with the satellite tracking data. GEM 6 is complete to degree and order 16. The relative effects of these two sources of data in estimating the coefficients will be described later where a solution based upon surface gravity data only is employed.

3.2 Techniques in Modeling the Data

The mathematical modeling for processing the satellite orbital data, the geometric and gravimetric data, including the weighted least squares normal equations, and the method of combining the data for solution of the geodetic parameters are presented in Appendix A. The material presented there for the satellite dynamics is quite extensive, and a brief account of it is described here since the orbital data provides the main contribution to the geodetic model. Further the material covered in the appendix in this area is more general than our application, whereas the description given here is restricted to our geodetic problem.

The orbital force equations are integrated numerically in an inertial reference system with a uniform time (A1). The reference system is oriented in the celestial frame of the true equator and equinox of date, at the beginning of a weekly arc of satellite data. An 11th order Cowell type of numerical integration is employed with a stepsize to provide for better than one meter of accuracy in satellite position on the modeled forces. These forces include the effects of the

gravitational potential of the earth, sun and moon, solar radiation pressure, and atmospheric drag based upon the Jacchia-Nicholet model (Jacchia, 1965).

Certain coordinate transformations and time conversions are employed to process the forces, the observations, and station positions. Luni-solar precession and nutation of the earth, the rotation of the earth (UT-1 time), and polar motion transformations are applied. Time system conversions between A1, UT-1, and UTC (transmitted time) are provided in BIH circulars along with polar motion data in x, y angles. Polar motion data is applied to station coordinates referenced to the mean CIO pole. Observation data are preprocessed, corrected, and transformed to A1 time at the satellite for the observation equations. Data types are generally time tagged in UTC but will vary in the time system and with the corrections to be applied. For instance, MOTS optical data for right ascension and declination are in a true of date celestial system and time tagged with UTC. On the other hand, Baker-Nunn optical data are received from SAO in a reference system of the mean equator and equinox of 1950.0 and time tagged in SAO atomic time at the station. The SAO observations are transformed to the true equator and equinox of date, corrected for diurnal aberration and parallactic refraction, and adjusted to A1 time at the satellite by accounting for the travel time of light to the station. The various processing for the different data types may be seen in the appendix.

The variational equations for the orbital state parameters, drag force parameters, and potential coefficients are integrated numerically along with the force equations for a weekly arc span of satellite data. The orbits are initially converged to the observations through the process of differential corrections for the satellite state and drag force parameters. This process is based upon a weighted least squares adjustment, where the weights are the inverse of the variances of the observation errors (Table 2-6). For certain electronic tracking systems, a bias parameter is modeled for the data in a given satellite tracking pass at a station. Since the number of modeled bias parameters may become large in a weekly arc of data, each bias parameter is eliminated from the least squares normal equations at the end of each tracking pass of data through the back substitution process. After convergence of the orbit a final iteration is made to produce the normal equations for all parameters including the geodetic parameters for adjustments of the potential coefficients and station coordinates from initial values.

All non-geodetic parameters are eliminated from the normal equations through the technique of back substitution. The reduced normal equations are then combined for all of the orbital arcs on the 27 satellites. The combined set of normal equations are then solved separately for the satellite only (GEM 5) solution. They are also reserved for combination with the normal equations for the geometric and gravimetric data to provide the solution for GEM 6. The GEM 6 solution

contains 730 geodetic parameters, consisting of 134 station positions and 328 potential coefficients.

In order to effect some control on the distribution of satellite data in GEM 5 certain groups of satellite data arcs were proportionately downweighted. Excluding GEOS-I and II which contain 60% of the optical data in Table 2-1, an average of 2500 observations per satellite exist on the remaining 21 satellites. GEOS-I and II optical data arcs were downweighted to give an effective average of about 10,000 observations per satellite. Similarly the 40 data arcs (principally electronic data) on the first six satellites in Table 2-2 were downweighted to give an effective average of about 4000 observations per satellite. In addition to this consideration a standard error of unit weight was applied for each data arc based upon the weighted observation residuals. The latter consideration was employed to account principally for degradation in orbital accuracy, particularly for effects of atmospheric drag on low altitude satellites.

3.3 Satellite Sensitivity to the Potential

The coefficients of the gravitational potential, excluding $\bar{C}_{20}$ which is of order 10^{-3}, gradually decrease in size with degree n. A rule given by Kaula for the average (rms) size coefficient ($\bar{C}_{nm}$, $\bar{S}_{nm}$) for a given degree is

$$s_n \equiv \sigma\left\{\bar{C}_{nm}, \bar{S}_{nm}\right\} = 10^{-5}/n^2, \text{ for } m = 0 \text{ to } n,$$

which may be seen from Figure 3-1 to compare reasonably with the GEM 5 coefficients. This rule, with the use of orbital perturbation theory, from Kaula (1966 b), was employed in a harmonic analysis program to estimate the potential perturbation of the satellite for individual terms in the gravitation potential. The 27 satellite orbits employed in GEM 5 were evaluated for the effects of terms to degree and order 30. The number of different satellites that have sensitivity to a given potential term gives a qualitative measure of resolution for that term. The result provides information to estimate where the satellite potential should be truncated.

This technique was employed by Strange (1968), and it requires a measure of satellite orbital sensitivity representative of the accuracy in the satellite observational data. The satellites and associated data are listed in Tables 2-1 and 2-2 including their orbital parameters, and the accuracy of the data is listed in Table 2-6. A fixed sensitivity level per satellite was used in this analysis as an along-track threshold, representative of the accuracy in the observation data. Although the radial and cross track perturbations are also significant, the predominant component is generally the along-track one. Each potential term in V gives rise to a spectrum of harmonics in orbital perturbations (Kaula, 1966 b,

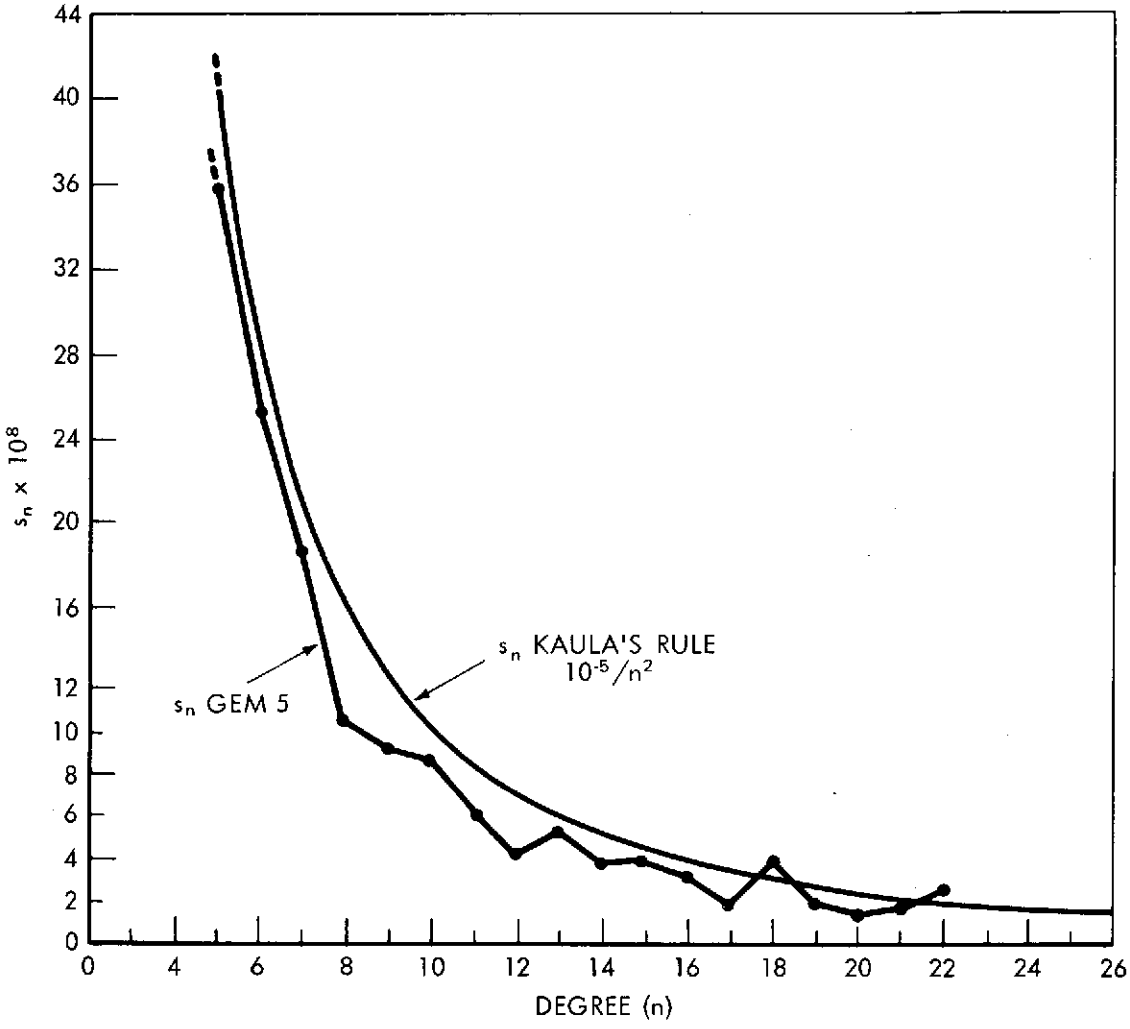

Figure 3-1. Average (rms) Coefficient Value by Degree

pg. 40). These were transformed to the along-track position component and then summed (rss) for a net effect.

The satellite sensitivity levels and pertinent information are listed in Table 3-1. For the satellites containing just optical data in the solution the sensitivity level varies from 8 to 35 meters. Only two (high altitude) satellites have values greater than 19 meters. Three satellites with only Minitrack data have sensitivity levels of over 100 meters; two of these contribute principally to the resolution of satellite resonant terms and the third, SAS (3° inclination), contributes mainly to the zonal terms. Seven satellites (affected by drag) have range and/or range-rate data in the solution. Six of these with laser range data were assigned sensitivity levels of 5 meters, even though the data is accurate to one meter, whereas the seventh one was assigned 10 meters.

Table 3-1

Satellite Data and Sensitivity Level

Satellite Name	Data Type*	Sensitivity Level (Meters)	A (Kilometers)	E	I (Degrees)	Mean Motion (Rev/Day)	Primary Resonant Period (Days)
AGENA	O	8.9	7297.	0.0010	69.91	13.92	5.0
ALOU-2	M	517.0	8100.	0.1505	79.82	11.90	6.2
ANNA-1B	O	10.9	7501.	0.0082	50.12	13.37	4.8
BE-B	L,RR,O	5.0	7354.	0.0135	79.69	13.76	3.0
BE-C	L,RR,O	5.0	7507.	0.0257	41.19	13.35	5.6
COURIER	O	10.6	7469.	0.0161	28.31	13.46	3.8
DI-C	L,O	5.0	7341.	0.0532	39.97	13.81	2.5
DI-D	L,O	5.0	7622.	0.0848	39.46	13.05	8.4
ECHO-1RB	O	16.4	7966.	0.0118	47.21	12.21	11.9
GEOS-A	RR,O	16.4	8075.	0.0719	59.39	11.96	7.0
GEOS-B	L,R,RR,O	5.0	7711.	0.0330	105.79	12.82	5.7
GRS	O	8.3	7239.	0.0598	49.76	14.10	10.7
INJUN	O	9.1	7316.	0.0079	66.82	13.87	3.8
MIDAS-4	O	35.1	9995.	0.0112	95.83	8.69	3.0
OGO-2	O	9.3	7341.	0.0752	87.37	13.79	3.8
OSCAR-7	O	10.0	7411.	0.0224	89.70	13.60	2.2
OVI-2	O	18.8	8317.	0.0184	144.27	11.45	2.2
PEOLE	L,M	5.0	7006.	0.0164	15.01	14.82	2.1
SAS	M	163.0	6923.	0.0035	3.04	15.09	4.6
SECOR-5	O	17.2	8151.	0.0793	69.22	11.79	3.4
TELSTAR	O	31.9	9669.	0.2429	44.79	9.13	14.9
TIROS-9	M	494.0	8024.	0.1173	96.41	12.07	19.5
TRANSIT-4A	O	9.2	7322.	0.0076	66.82	13.85	3.5
VAN2ROC	O	20.5	8496.	0.1832	32.92	11.09	294.3
VAN2SAT	O	18.6	8298.	0.1641	32.89	11.49	2.7
VAN3SAT	O	20.7	8508.	0.1901	33.34	11.07	187.6
5BN-2	O	10.5	7462.	0.0058	89.95	13.46	2.4

*L - Laser Range, R - Range, RR - Range Rate, O - Optical, M - Minitrack

Two figures are presented to summarize the results. Figure 3-2 displays the number of satellites (satellite count) for each harmonic coefficient out to degree and order 30 that have perturbations larger than the sensitivity level listed in Table 3-1. Figure 3-3 is similar, except that the sensitivity level is reduced by one-fifth of the above size. The latter figure is used as a measure of stochastic sensitivity, that is, resolution statistically. The solution passing through the mean of the observations is more accurate than any given observation.

In each of the two (sensitivity) figures the distribution pattern in the satellite count is quite large for the low degree and order terms. Beyond a certain degree there is only good observability for the zonal terms, satellite resonant terms, and low order terms. The satellites that are resonant of order m (m = 9, 11 through 14) can be seen from their mean motion in Table 3-1 by taking the nearest integer value in revolutions per day. Also a satellite count is seen for certain orders m of twice the above values. These correspond to secondary resonance effects. Formulation for resonant analysis is given by Kaula (1966 b, pp. 49-56). The primary beat periods associated with the satellite resonant effects are listed in Table 3-1.

Satellite perturbations for some of the potential terms are in the region of kilometers, particularly for long period zonal terms with periods of several months and for some satellite resonant terms. Because weekly satellite arcs are employed in the solution, each harmonic perturbation in the analysis whose period exceeded one week was proportionately reduced as the harmonic amplitude is proportional to its period. Similarly secular perturbations of the even zonal terms were computed for a weekly time span and these contribute principally to the large satellite count for the even zonals.

In Figure 3-2 the satellite count for the bulk of the coefficients, excluding the zonal and resonant terms, is associated principally with the m-daily terms (of m cycles per day). However, in Figure 3-3 for the lower sensitivity level, short period terms (less than one satellite revolution) also contribute to the satellite sensitivity. Orbital perturbation formulas including the m-daily and short period terms may be found on page 40 of Kaula (1966).

Based upon the above results the truncation for the low order terms (m = 0, 1 and 2) could be extended beyond the point employed in GEM 5. Coefficients for satellite resonant order 15 could be included. The general point of truncation at degree 12 is probably satisfactory. The stochastic sensitivity level indicates good resolution in harmonics of degree 12. However, since a number of the 12th degree terms are void in Figure 3-2, the recovery of these terms are based upon small perturbations. It is shown later that, with use of error estimates for the potential coefficients, the 12th degree terms have about 40% accuracy. Thus, in all, it does not appear very beneficial to extend the general truncation of the harmonics beyond degree 12 for the satellite solution.

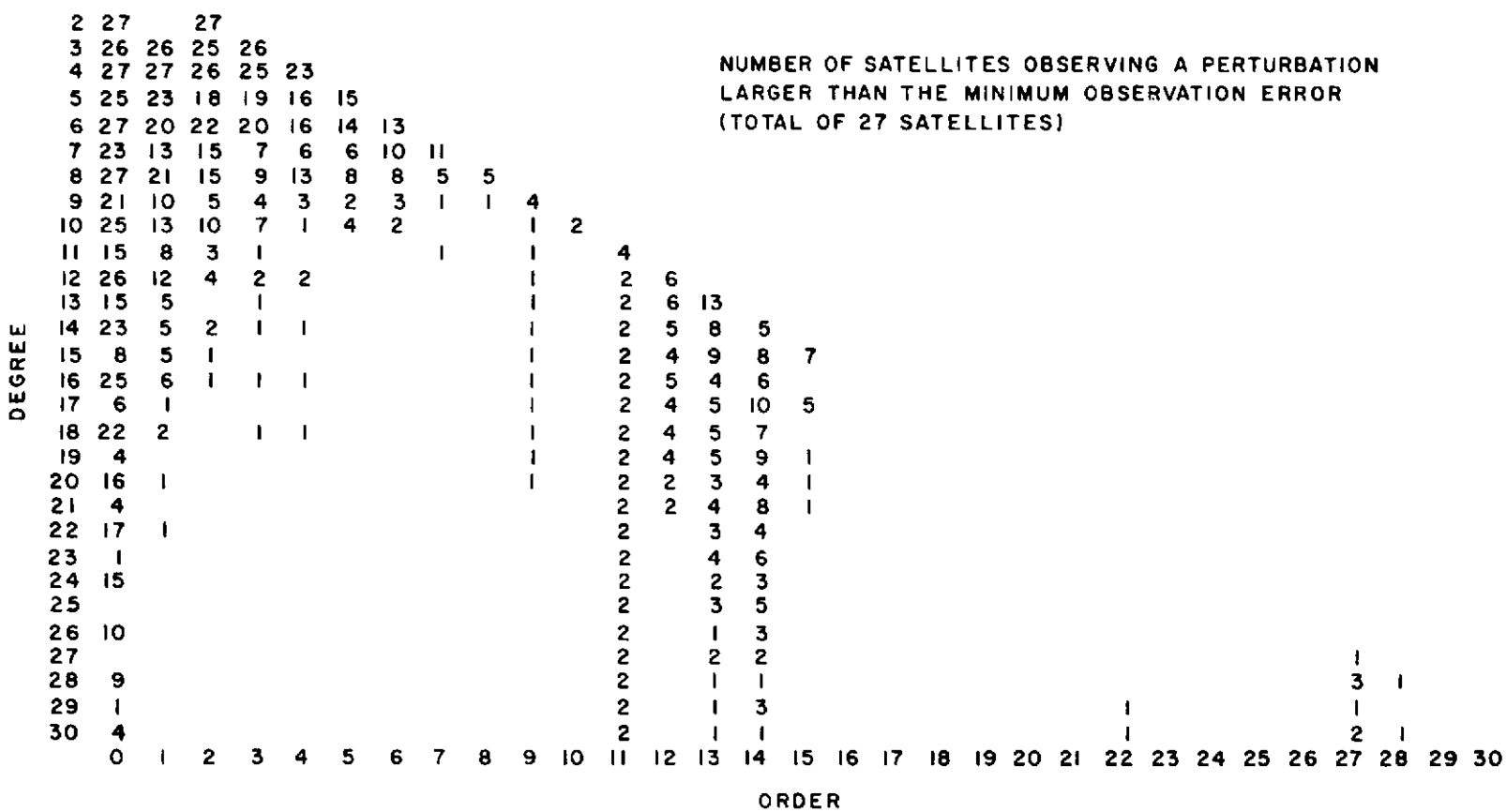

Figure 3-2. Satellite Sensitivity to Potential Terms (30 x 30)

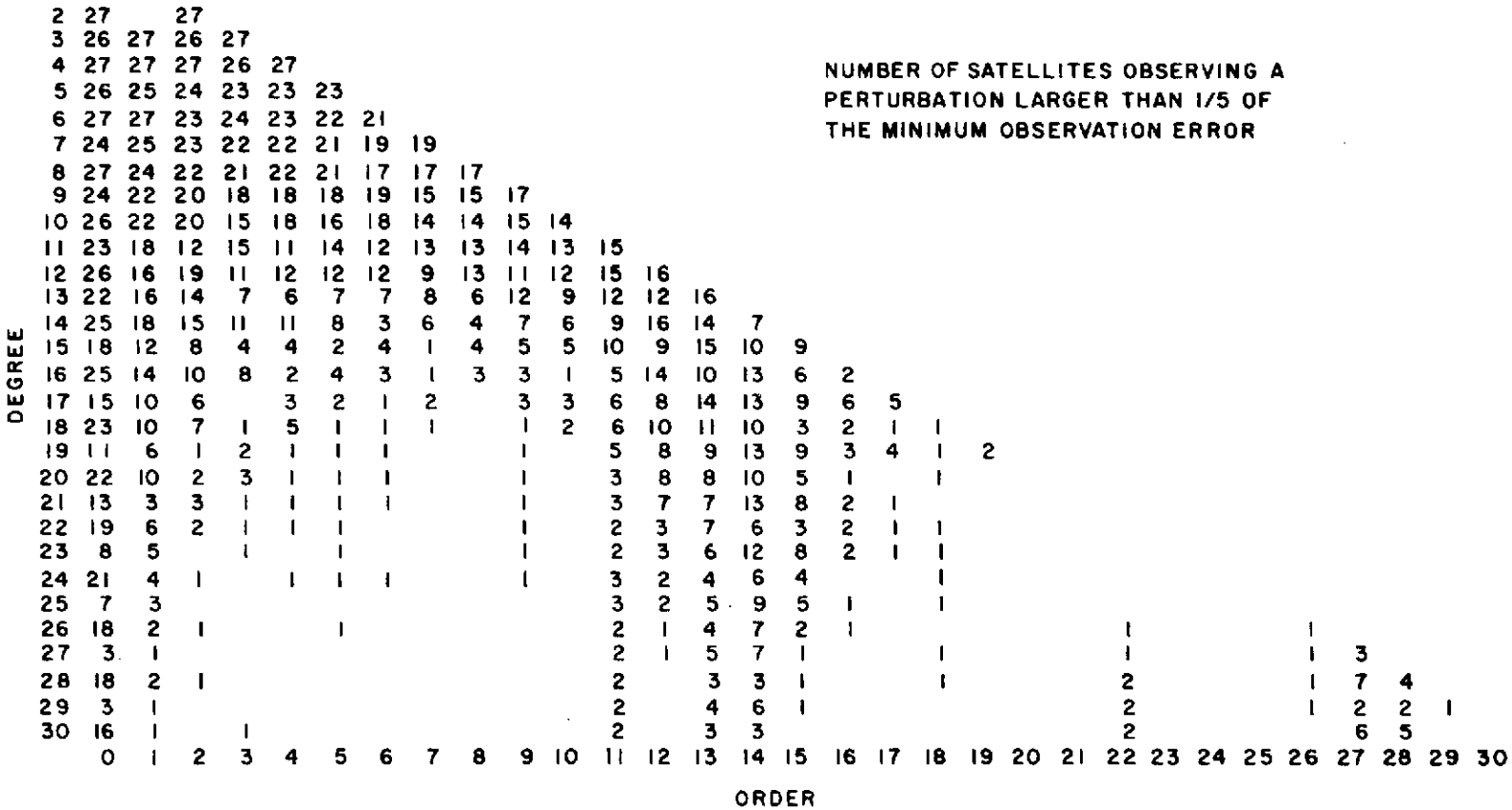

Figure 3-3. Stochastic Satellite Sensitivity

3.4 Error Estimates for Geopotential Coefficients of GEM 5

The average standard deviation (σ_n) per degree n for the potential coefficients are plotted in Figure 3-4 for both the satellite solution, GEM 5, and a gravimetric solution derived from the 5° mean gravity anomalies. Judging from these formal error estimates the strength of the combination solution will predominantly depend upon GEM 5. Analysis is presented to calibrate this information in GEM 5 according to outside data sources.

The formal standard deviations are obtained from the inverse matrix of the normal equations with observation weighting of $1/\sigma^2_{OBS}$. Such results generally provide optimistic error estimates without some upward adjustment. Relative values of the standard deviations are generally considered meaningful, and hence the adjusted values may be derived through a calibration factor. This factor is usually applied as a standard error of unit weight based upon the observations employed in the solution. This factor has already been included in a priori form for each data arc of GEM 5. A calibration factor for GEM 5 will be derived below based upon gravimetry data not employed in the solution. It is expected that this will provide realistic error estimates for the GEM 5 coefficients. Use will be made of the calibration factor for GEM 5 in the error estimates for GEM 6.

3.4.1 Formulation of Error Estimates for Geoid Height and Gravity Anomaly— The gravity anomaly Δg and geoid height h_g may be represented, from Heiskanen and Moritz (1967), for a point (r, ϕ, λ) on the geoid as follows:

$$\Delta g = \frac{GM}{r^2} \sum_{n=2}^{N} (n-1) \sum_{m=0}^{n} H_{nm} \tag{3.3}$$

$$h_g = \frac{GM}{\gamma r} \sum_{n=2}^{N} \sum_{m=0}^{n} H_{nm} \tag{3.4}$$

where

$$H_{nm} = \left(\frac{a_e}{r}\right)^n \bar{P}_{nm} (\sin\phi) (\bar{C}^*_{nm} \cos m\lambda + \bar{S}_{nm} \sin m\lambda)$$

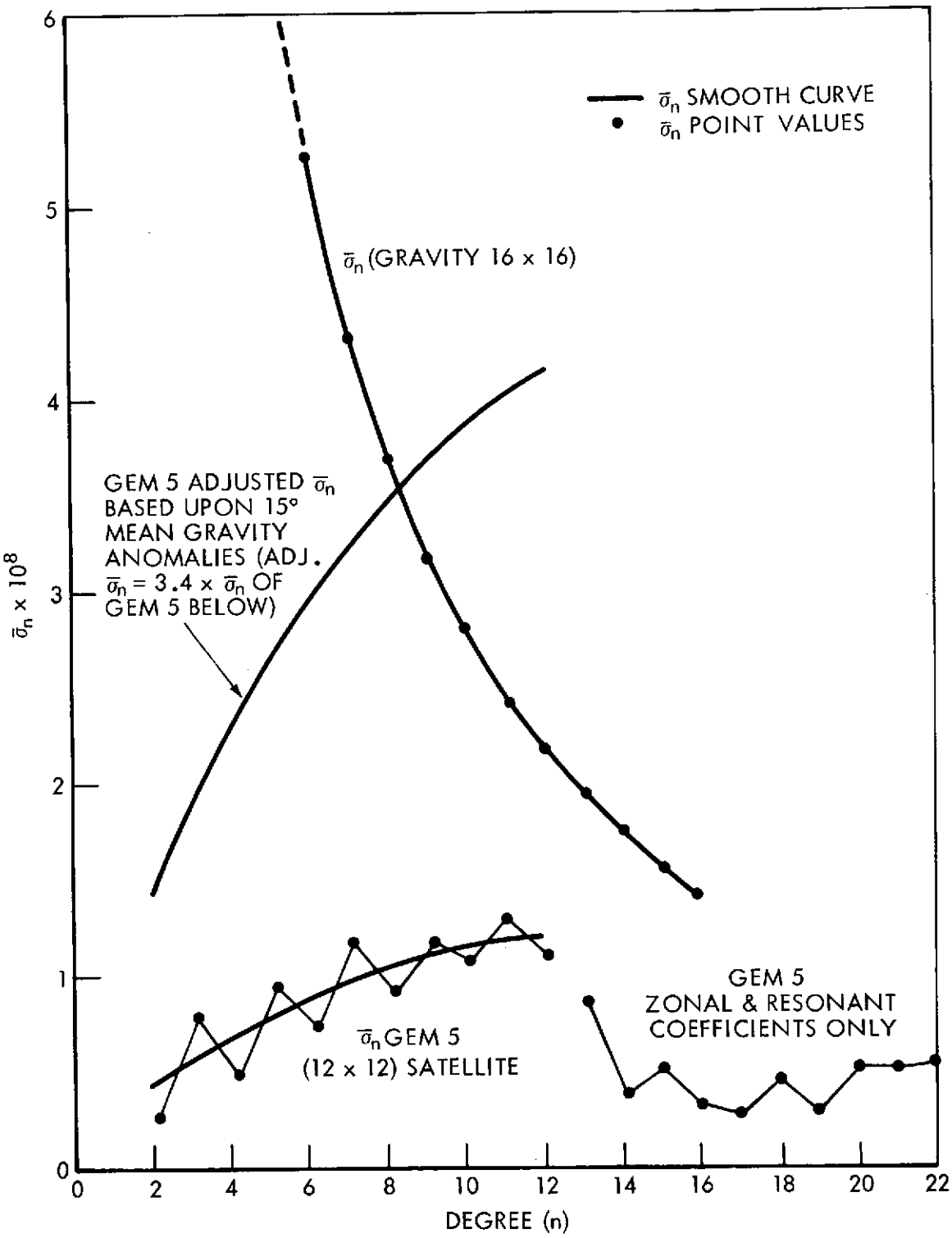

Figure 3-4. Average (rms) Standard Deviation Per Degree n ($\bar{\sigma}_n$) for GEM 5 and Gravimetry Solutions

and $\bar{C}^*_{nm} = \bar{C}_{nm}$ except for even zonals for which $\bar{C}^*_{no} = C_{no} - \bar{C}'_{no}$ and $\bar{C}'_{no}$ are the oblate zonal coefficients for the reference ellipsoid. A mean square error estimate of Δg and h_g over the geoid, due to the uncertainty $\sigma_{nm}(\bar{C}, \bar{S})$ in the coefficients, may be estimated from equations (3.3) and (3.4) with use of a spherical approximation $r = R$, where R is the mean radius of the earth. These results are

$$\sigma^2_{\Delta g} = \bar{\gamma}^2 \sum_{n=2}^{N} (n-1)^2 \ \sigma^2_n \ (T) \tag{3.5}$$

$$\sigma^2_h = R^2 \sum_{n=2}^{N} \sigma^2_n \ (T) \tag{3.6}$$

$$\sigma^2_n \ (T) = \sum_{m=0}^{n} \left[\sigma^2_{nm} \ (\bar{C}) + \sigma^2_{nm} \ (\bar{S}) \right] \tag{3.7}$$

where $\bar{\gamma}$ is a mean value of gravity.

The average standard deviation per degree n ($\bar{\sigma}_n$) plotted in Figure 3-4 was computed from (3.7) as follows:

$$\bar{\sigma}^2_n = \frac{\sigma^2_n \ (T)}{2n+1} \tag{3.8}$$

for harmonic terms complete to degree and order n, and for terms not complete in degree n

$$\bar{\sigma}^2_n = \frac{\sigma^2_n \ (T_L)}{L} \tag{3.9}$$

where L is the number of coefficients determined in the solution for that degree. With use of the standard deviations for GEM 5, the error committed in the gravity anomaly from (3.5) due to the modeled coefficients is, with $\bar{\gamma} \sim 10^6$ mgal,

$$\sigma_{\Delta g} = 1.3 \text{ mgal.} \tag{3.10}$$

Similarly the formal uncertainty estimate of the average global geoid height is, from (3.6),

$$\sigma_h = .8\,\text{m} \tag{3.11}$$

3.4.2 Adjusted Error Estimates of Potential Coefficients—Comparisons of mean gravity anomaly computed from GEM 5 (G_c) with that computed (G_T) directly from terrestrial gravity data was made. The mean (free-air) gravity anomalies are values averaged over equal area blocks (s x s square) on the geoid, and the block size is given in terms of the geocentric angle θ subtended by the length s. A commensurate block size θ for mean gravity anomaly corresponding to a harmonic solution complete to degree and order N may be obtained from the half wavelength resolution of the harmonics, namely

$$\theta \sim \frac{180}{N} \text{ (degrees)}$$

Thus for N = 12, as in GEM 5, 15°(θ) equal area blocks of mean gravity anomaly were employed for a commensurate comparison.

A global set of such terrestrial anomalies were obtained from Hajela (1973) with error estimates for each 15° anomaly. A global error between G_T and G_c accounting for the errors in the gravimetry data gave

$$\sigma\,(G_T - G_c) = 4.4\,\text{mgal} \tag{3.12}$$

where a standard error (of unit weight) in the gravimetry data was 1.9 mgal. Note the discrepancy between (3.12) and that derived in (3.10) from the formal error estimates in the coefficients. Equating these results in the form

$$\sigma\,(G_T - G_c) = K\,\sigma_{\Delta g} \tag{3.13}$$

gives

$$4.4 = 1.3\,K$$

or

$$K = 3.4 \tag{3.14}$$

as a calibration factor for $\bar{\sigma}_n$ of GEM 5. An equivalent result to (3.12) is derived more indirectly in Section 4. with use of 5° mean anomalies, where the statistical techniques of Kaula are employed.

Thus $K\,\bar{\sigma}_n$ represents satellite coefficient errors that are more realistic as judged by the gravimetric data. Furthermore $K\,\bar{\sigma}_n$ may be used to check the average uncertainty in geoid height, σ_h in (3.11), with differences seen in comparisons between geoid heights derived from GEM 5 and those derived from

detailed gravity data and astrogeodetic deflections in major areas of survey. These comparisons yield an rms difference of approximately 5 meters. This result may be equated to a total predicted error as follows:

$$5 \simeq \left(K^2 \sigma_h^2 + \delta_h^2 \right)^{1/2} \tag{3.15}$$

σ_h : error in geoid height of .8 meter due to formal standard errors in GEM 5 coefficients

K : scale factor of 3.4 obtained from (3.14)

δ_h : error in geoid height due to coefficients not included in GEM 5.

The mean square error of omission, δ_h^2 due to coefficients not included in GEM 5, was estimated from (3.6) by using Kaula's value of $10^{-5}/n^2$ for the uncertainty in the omitted (unmodeled) coefficients. This result gave

$$\delta_h^2 = 22.6\,m^2, \tag{3.16}$$

and since $\sigma_h = .8$ m,

$$K^2 \sigma_h^2 = 7.4\,m^2. \tag{3.17}$$

Then the total predicted error for geoid height is

$$(K^2 \sigma_h^2 + \delta_h^2)^{1/2} = 5.5\,m. \tag{3.18}$$

The latter result is fairly consistent with the 5 meters in (3.15) which was obtained from the direct comparisons. It is noted that (3.18) does not provide a strong source of calibration since the omission error (3.16) is much larger than the commission error (3.17).

From the above results, principally (3.13), it would seem that a better error estimate for the standard deviations σ_i of the geopotential parameters of GEM 5 is

$$\sigma_i \text{ (error)} = K\, \sigma_i \text{ (computed)}$$

$$K = 3.4. \tag{3.19}$$

The adjusted errors ($K\, \bar{\sigma}_n$) by degree n are plotted in Figure 3-4. Based upon these adjusted errors the percent accuracy for coefficients of degree n for GEM 5 are plotted in Figure 3-5, where Kaula's rule (Figure 3-1) was used for the average size coefficient of degree n. In the combination solution (GEM 6) the gravimetry data should improve the relatively low accuracy in the high degree coefficients.

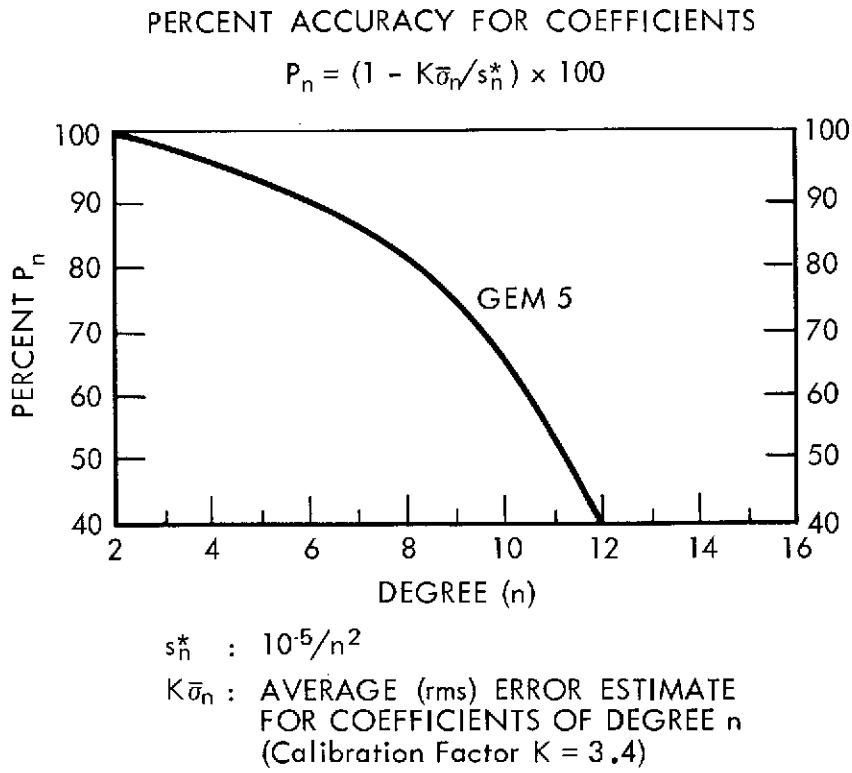

Figure 3-5. Percent Accuracy of GEM 5 Coefficients by Degree

3.5 Relative Weighting and Error Estimates for Combined Solution GEM 6

A relative weighting factor w was applied in the combination solution for GEM 6 as follows:

$$\bar{S} + \bar{M} + w\,\bar{G} = 0 \qquad (3.20)$$

where $\bar{S}$, $\bar{M}$, and $\bar{G}$ denote the normal matrix equations respectively for the satellite dynamic system (GEM 5), the geometric system, and the gravimetric system. $\bar{G}$ contains just geopotential parameters, $\bar{M}$ station coordinate parameters only, and $\bar{S}$ both station and geopotential parameters. Based upon the calibration results of the satellite solution, as in 3.19, it was decided that some additional weighting (w) for the gravimetry system $\bar{G}$ should be applied. Assuming the standard deviations from $\bar{G}$ are correct, w should be 11.4 (K^2) based upon the GEM 5 calibration.

A precise value for w, however, cannot be determined since the gravimetry solution has not been calibrated against an external reference as has GEM 5. In a previous combination solution for GEM 4 a relative weighting factor of w = 5 was

applied, and this value resulted in relatively poor comparisons for GEM 4 with satellite data as shown in Table 4-11 of Section 4. A conservative value of w = 2 was applied for GEM 6 and provided greatly improved results as shown in the same table.

The inverse matrix of the normal equations for each system, $\bar{G}$ and $\bar{S}$, has been employed to obtain the formal standard deviations for these systems. Similarly, the inverse matrix for the combined system (3.20), was used to provide those for GEM 6. Average (rms) error values for coefficients of degree n, $\bar{\sigma}_n$, were obtained for GEM 6. As with GEM 5 these were likewise scaled by 3.4 (K) and are presented in Table 3-2. A relationship between the two solutions GEM 5 and 6, showing the effect of combining the gravimetry data in GEM 6, is presented in Figure 3-6. The relationship gives the percent reduction of the coefficient errors (variances) of GEM 6 with respect to those of GEM 5, namely for each degree n

$$P_n = 1 - \bar{\sigma}_n^2 \text{ (GEM 6)} / \bar{\sigma}_n^2 \text{ (GEM 5)} \qquad (3.21)$$

Since $\bar{\sigma}_n$ is scaled by K in each solution the result for P_n does not depend upon K but it does depend upon the relative weighting factor w. The result for P_n shows that the gravimetry data in GEM 6 has progressively greater effect as n increases, with relatively little effect on the low degree coefficients, and reduces the variance of GEM 5 to 50% at about degree ten. Results are listed for n to degree 12, since GEM 5 contains just satellite resonant and zonal coefficients beyond this point.

Formal standard deviations for the station coordinates for GEM 6 also gave optimistic results. This was seen from numerous comparisons with station coordinates, including datum survey, which are given in Section 4.2. Again, as with the potential coefficients, relative values of the formal standard deviations for the station coordinates were considered generally meaningful. These values were scaled by a factor of three to provide a more realistic error estimate, consistent with the above comparisons. Error estimates are given in Table 4-16 of Section 4.2 for 134 tracking stations. A summary of the results is given in Table 3-3. These results show an average (rms) error of 6.6 meters for station coordinates. The BC-4 geometric system has the largest error among the tracking systems with a value of 8.5 m. The errors refer to the dispersion or noise in the coordinates and do not represent an overall scale error or orientation errors.

3.6 Verification of Error Estimates

The adjusted standard deviations of GEM 6 for geopotential and station coordinate parameters are used below to predict an error estimate for the average uncertainty in the computed height of station above mean sea level (geoid). The

Table 3-2

Average (rms) Error Estimates $\bar{\sigma}_n$ for Potential Coefficients of Degree n for GEM 6
(σ values scaled by 10^8)

n	$\bar{\sigma}_n$	Zonal* (σ_n)
2	.8	.1
3	2.4	.2
4	1.4	.2
5	2.7	.2
6	2.0	.4
7	2.9	.3
8	2.3	.4
9	2.6	.3
10	2.4	.5
11	2.6	.3
12	2.3	.6
13	3.2	.5

n	$\bar{\sigma}_n$	Zonal (σ_n)
14	3.0	.7
15	2.7	.5
16	2.3	.9
17	.7	.5
18	1.3	.8
19	.8	.6
20	1.6	.8
21	1.8	.7
22	1.8	1.1

Resonant and zonal coefficients only for n = 17 to 22.

ERROR ESTIMATES $\bar{\sigma}_n$:
$\bar{\sigma}_n$ (ERROR) = $3.4\bar{\sigma}_n$ (GEM 6)

*Zonal terms are better defined and listed for comparison

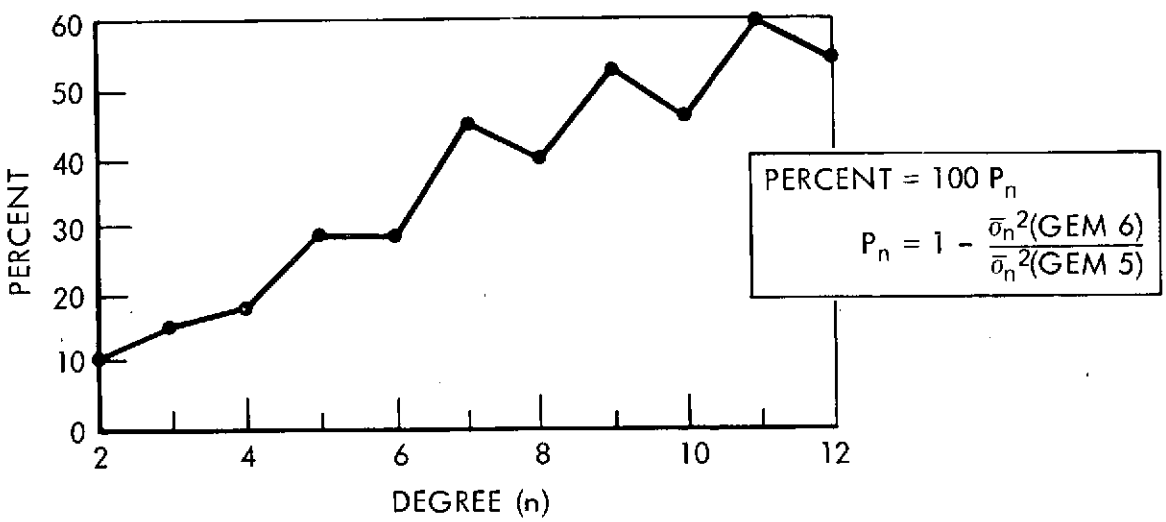

Figure 3-6. Percent Reduction in the Error Variances of GEM 5 Due to the Effect of Combining Gravimetry Data in GEM 6

Table 3-3

Station Coordinate Error Estimates for Tracking Systems in GEM 6

Tracking System	No. of Stations	RMS of Errors	No. of Stations Excluded*
NWL Doppler	17	6.9 m	1
GRARR	4	3.8	1
C-Band	7	6.2	0
Baker-Nunn	23	5.3	1
MOTS	30	4.9	0
BC-4	42	8.5	5
Laser	3	3.4	0
Total	126	6.6 m	8

*Eight stations with coordinate errors larger than 16 m were excluded.

differences in computed heights (MSLH) from GEM 6 and mean sea level heights (MSL) from survey are plotted in Figure 4-6 of Section 4.2.2. This data comparison result gave an average rms residual, from Table 4-25, as

$$\text{RMS (MSLH - MSL)} = 7.7\,\text{m}. \tag{3.22}$$

The residuals (MSLH-MSL) are referenced to a mean equatorial radius of the Earth of $a_e = 6378144$ m as shown in the table.

Based upon the calibrated values of the standard deviations of GEM 6, a predicted estimate for the average error of the computed heights (MSLH) of the stations is given as

$$\sigma_{\text{MSLH}} = \left(\sigma_R^2 + \sigma_{hg}^2\right)^{1/2} \tag{3.23}$$

where σ_R represents the overall dispersion in radial position errors for the stations and σ_{hg} represents a global error in geoid height. In Table 3-3 an rms error of 6.6 m was obtained for station coordinates. A global error in geoid height was obtained from (3.15) to (3.18) for GEM 5. A similar value, computed for GEM 6 is 4.5 m. Using $\sigma_{hg} = 4.5$ and $\sigma_R = 6.6$ m in (3.23), then

$$\sigma_{\text{MSLH}} = 8.0\,\text{m}, \tag{3.24}$$

which compares well with (3.22) obtained directly from the data.

An additional estimate for the average uncertainty in geoid height for GEM 6 has recently been obtained from experimental altimeter data taken on SKYLAB IV during one revolution of the earth. The ground track passed over nearly all ocean surface. Geoid heights derived from the altimetry data are plotted in Figure 3-7 along with those computed from GEM 6. These results were presented by C. Leitao of NASA (Wallops) at the International Symposium on Applications of Marine Geodesy, June 5, 1974, Columbus, Ohio. The reference for this presentation is listed under McGoogan (1974), principal investigator for the SKYLAB S-193 altimeter experiment. The rms of geoid height residuals in the figure is approximately 7.3 meters, for which variations as large as 15 meters may be seen in the southern area of the Atlantic Ocean. However, the orbital position error may account for part of the 15 meters since S-band tracking data coverage is lacking in this region.

A final comparison is made to check the estimated errors for the GEM 5 coefficients. The root mean square values for the differences in coefficients of degree n (RMS_n) between GEM 5 and a solution, SAT 16 x 16, are plotted in Figure 3-8. SAT 16 x 16 has been recently derived and is based upon satellite optical and ISAGEX laser data, and it is complete to degree and order 16 in harmonics. It contains the same satellites as in GEM 5 but does not include some 270,000 electronic observations contained in GEM 5. Values of $\bar{\sigma}_n$, average (rms) standare deviations for coefficients of degree n, have been calibrated for GEM 5 as previously discussed to represent realistic error estimates, and these are plotted in the figure for comparison. These error estimates compare favorably with the coefficient differences, including the oscillations seen between even and odd degree harmonics. For consecutive harmonics even degree terms have relatively larger orbital perturbations and hence these have smaller errors as shown in the figure.

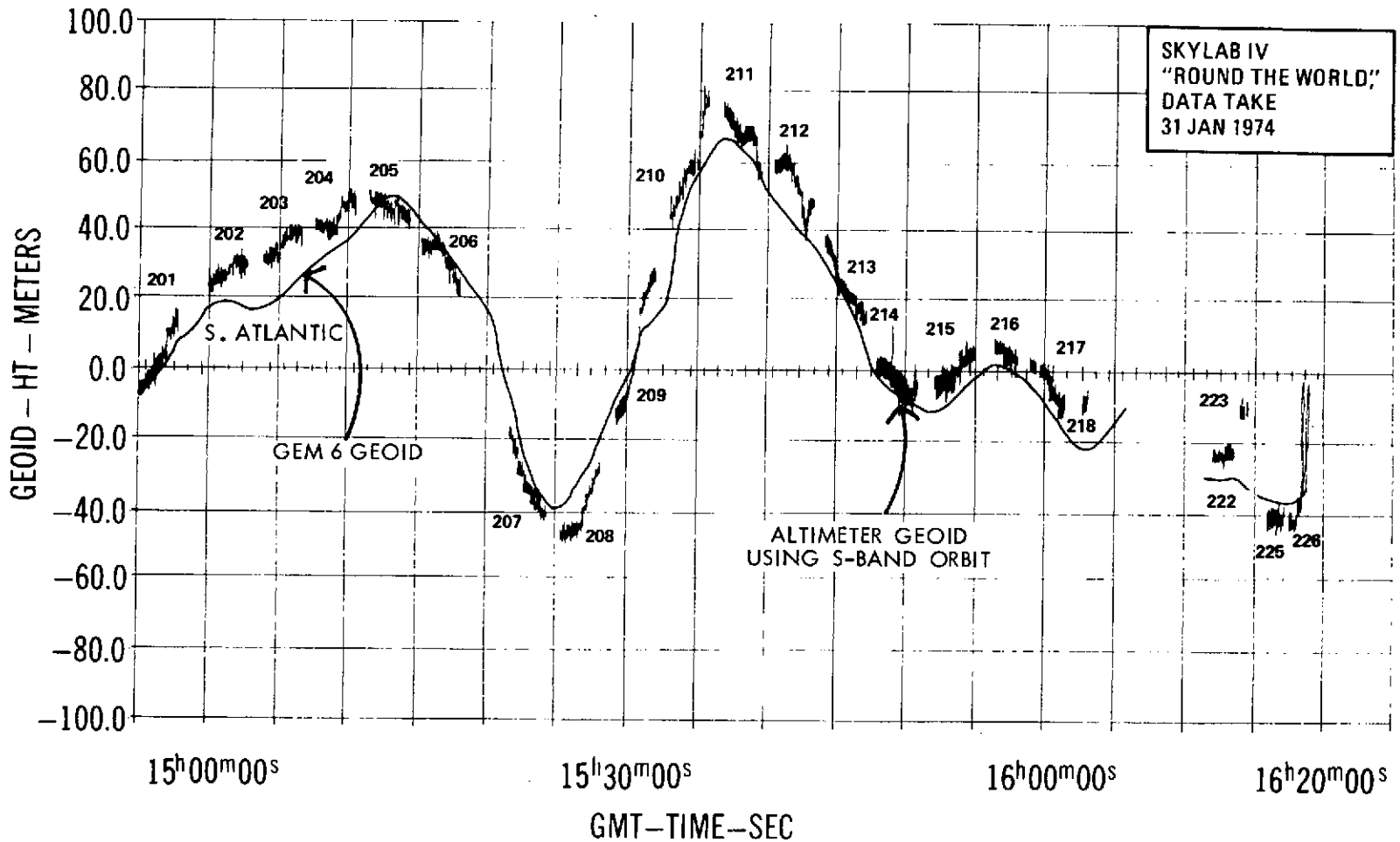

Figure 3-7. Comparison of GEOID Profile Derived from Altimetry and GEM 6

RMS_n : ROOT MEAN SQUARE OF DIFFERENCES IN COEFFICIENTS OF DEGREE n BETWEEN SOLUTIONS OF GEM 5 AND SAT 16 x 16

$K\bar{\sigma}_n$: AVERAGE (rms) OF ERROR ESTIMATES FOR COEFFICIENTS OF DEGREE n CALIBRATED FOR GEM 5 WITH K = 3.4

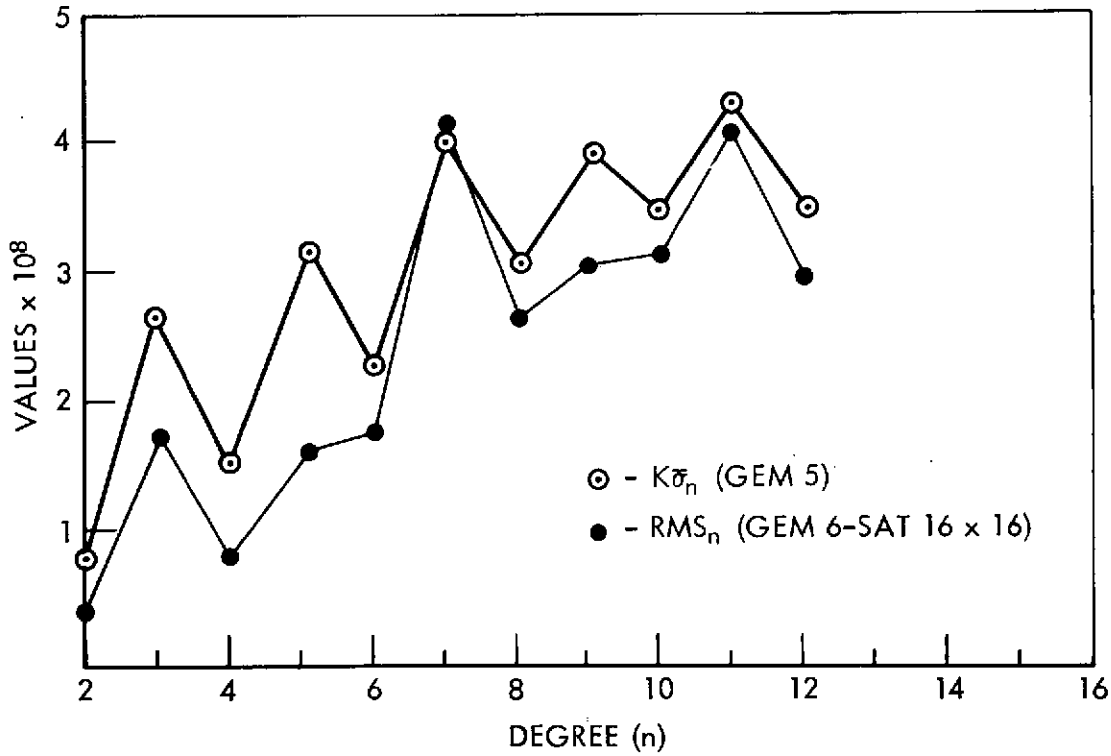

Figure 3-8. Comparison of Error Estimates for Coefficients of Degree n

SECTION IV . . . . . RESULTS (GEOPOTENTIAL AND STATIONS)

4. RESULTS

4.1 Gravitational Potential for GEM 5 and 6

Spherical harmonic coefficients, in terms of normalized values, are given in Table 4-1 for GEM 5 and Table 4-2 for GEM 6.

4.1.1 Zonal Harmonics—Coefficients of the zonal harmonics have been determined by Cazenave et al. (1971) and by Kozai (1969) by analyses of orbital perturbations of long periods, while GSFC, in its work on GEM, determines them by analysis of orbital perturbations on weekly arcs. The solution of Cazenave et al. (French 71) resulted by a combination of Kozai's normal equations with corresponding equations for three low-inclination satellites (SAS, PEOLE, DIAL). Kozai's solution was used in the Smithsonian Standard Earth II (SAO SE 2). Table 4-3 compares the zonal coefficients in GEM, the SAO SE 2, and the French 71. The rms differences from the coefficients of the French 71 are:

	Solutions with Data on Satellites of Low Inclination				Solutions without Data from Satellites of Low-Inclination*		
Solutions	GEM 3	GEM 4	GEM 5	GEM 6	SAO SE 2	GEM 1	GEM 2
rms x 10^9	9.5	7.6	8.9	7.4	16.3	22.5	9.1

*Solutions without low inclination satellite data employ satellites whose inclinations are greater than 28°.

The rms agreement with the French values is much better for the solutions that contain the data on low-inclination satellites than for the solutions that lack this data. The comparisons of the French coefficients with the GEM 1, 3, and 5 coefficients show progressively better agreement as do the comparisons with the GEM 2, 4, and 6 coefficients. The rms difference of 7.4 x 10^{-9} between GEM 6 and the French values is approaching the error estimates given for the zonals by each of the solutions. The rms of these error estimates is 4.5 x 10^{-9} for the French 71 and 5.7 x 10^{-9} for GEM 6, as obtained from Table 3-2. Hence these results serve to confirm the error estimates derived in GEM 6, for which the zonals are the best determined set. (From the values in Table 3-2 the average (rms) coefficient error is 27 x 10^{-9}, significantly larger than the zonal errors.)

Secular and long period zonal perturbations on 21 satellites are analyzed for the above models and presented in Section 4.1.3. In this analysis improved results are obtained for those solutions which include low inclination satellite data.

4.1.2 Comparison with Gravity Anomalies—Data on surface gravity were employed for testing models derived only from satellite tracking data and models

Table 4-1

Normalized Coefficients in GEM 5 (x 10^6)

ZONALS

INDEX N	M	VALUE	INDEX N	M	VALUE	INDEX N	M	VALUE	INDEX N	M	VALUE	INDEX N	M	VALUE
2	0	-484.1662	3	0	0.9605	4	0	0.5363	5	0	0.0659	6	0	-0.1457
7	0	0.0956	8	0	0.0430	9	0	0.0272	10	0	0.0587	11	0	-0.0547
12	0	0.0338	13	0	0.0498	14	0	-0.0260	15	0	-0.0081	16	0	-0.0046
17	0	0.0215	18	0	0.0052	19	0	0.0031	20	0	0.0152	21	0	-0.0101
22	0	-0.0121												

SECTORIALS AND TESSERALS

INDEX N	M	VALUE $\bar{C}$	$\bar{S}$	INDEX N	M	VALUE $\bar{C}$	$\bar{S}$	INDEX N	M	VALUE $\bar{C}$	$\bar{S}$
2	1	-0.0012	-0.0087	2	2	2.4282	-1.3602	3	1	2.0055	0.2449
3	2	0.9296	-0.6126	3	3	0.7285	1.4052	4	1	-0.5396	-0.4525
4	2	0.3495	0.6719	4	3	0.9794	-0.2201	4	4	-0.1691	0.3026
5	1	-0.0579	-0.0893	5	2	0.6533	-0.3110	5	3	-0.4403	-0.2440
5	4	-0.2996	0.0261	5	5	0.1373	-0.6877	6	1	-0.0756	-0.0145
6	2	0.0595	-0.3560	6	3	0.0284	-0.0095	6	4	-0.1018	-0.4537
6	5	-0.2858	-0.5174	6	6	0.0307	-0.2265	7	1	0.2535	0.1244
7	2	0.3409	0.1049	7	3	0.2740	-0.2104	7	4	-0.3044	-0.1071
7	5	0.0028	0.0708	7	6	-0.3299	0.1584	7	7	0.0275	0.0661
8	1	0.0099	0.1836	8	2	0.0469	0.0719	8	3	-0.0289	-0.0721
8	4	-0.2410	0.3562	8	5	-0.0814	0.0773	8	6	-0.0545	0.3172
8	7	0.0685	0.0604	8	8	-0.0976	0.0826	9	1	0.1598	0.0063
9	2	0.0170	0.0023	9	3	-0.1269	-0.1234	9	4	0.0056	0.0347
9	5	-0.0250	-0.1839	9	6	0.0630	0.2220	9	7	-0.0711	-0.0387
9	8	0.1595	-0.0350	9	9	-0.0389	0.0884	10	1	0.0883	-0.1740
10	2	-0.0434	-0.0330	10	3	-0.0503	-0.1219	10	4	-0.0740	-0.1015
10	5	-0.1163	-0.0480	10	6	-0.0056	-0.0795	10	7	-0.0135	-0.0247
10	8	0.0304	-0.1288	10	9	0.1117	-0.0542	10	10	0.0696	-0.0405
11	1	-0.0203	0.0215	11	2	0.0326	-0.0883	11	3	0.0052	-0.1343
11	4	0.0390	-0.1657	11	5	0.0181	0.0310	11	6	0.0003	0.0478
11	7	0.0125	-0.1086	11	8	-0.0246	0.0534	11	9	0.0195	0.0630
11	10	-0.0972	0.0036	11	11	0.0632	-0.0245	12	1	-0.0831	-0.0302
12	2	-0.0280	0.0225	12	3	0.0842	0.0576	12	4	0.0033	-0.0201
12	5	0.0100	0.0146	12	6	0.0681	0.0404	12	7	-0.0149	0.0160
12	8	-0.0230	-0.0160	12	9	0.0289	0.0426	12	10	-0.0071	0.0359
12	11	0.0036	0.0389	12	12	-0.0125	-0.0090	13	5	0.0952	0.0851
13	12	-0.0282	0.1002	13	13	-0.0598	0.0689	14	1	-0.0150	0.0053
14	9	0.0378	0.0644	14	11	0.0002	-0.0001	14	12	0.0070	-0.0366
14	13	0.0145	0.0264	14	14	-0.0455	-0.0045	15	9	0.0643	0.0588
15	12	-0.0348	0.0154	15	13	-0.0226	-0.0022	15	14	0.0037	-0.0191
16	12	0.0269	-0.0088	16	13	0.0009	-0.0132	16	14	-0.0217	-0.0406
17	12	0.0167	-0.0009	17	13	0.0104	0.0188	17	14	-0.0133	-0.0022
18	12	-0.0599	-0.1212	18	13	-0.0225	-0.0619	18	14	-0.0109	-0.0033
19	12	-0.0290	-0.0269	19	13	-0.0244	-0.0300	19	14	0.0002	0.0007
20	12	0.0073	-0.0000	20	13	-0.0020	-0.0317	20	14	0.0078	-0.0087
21	12	-0.0217	-0.0226	21	13	-0.0270	0.0108	21	14	0.0096	0.0073
22	12	-0.0399	-0.0053	22	13	-0.0412	-0.0159	22	14	-0.0080	0.0024

Table 4-2

Normalized Coefficients in GEM 6 (x 10^6)

ZONALS

INDEX N	M	VALUE	INDEX N	M	VALUE	INDEX N	M	VALUE	INDEX N	M	VALUE	INDEX N	M	VALUE
2	0	-484.1661	3	0	0.9607	4	0	0.5362	5	0	0.0661	6	0	-0.1451
7	0	0.0961	8	0	0.0426	9	0	0.0264	10	0	0.0606	11	0	-0.0528
12	0	0.0306	13	0	0.0470	14	0	-0.0206	15	0	-0.0045	16	0	-0.0077
17	0	0.0152	18	0	0.0091	19	0	0.0044	20	0	0.0143	21	0	-0.0098
22	0	-0.0138												

SECTORIALS AND TESSERALS

INDEX N	M	VALUE $\bar{C}$	$\bar{S}$	INDEX N	M	VALUE $\bar{C}$	$\bar{S}$	INDEX N	M	VALUE $\bar{C}$	$\bar{S}$
2	1	-0.0009	-0.0032	2	2	2.4251	-1.3883	3	1	2.0021	0.2482
3	2	0.9332	-0.6311	3	3	0.6969	1.4260	4	1	-0.5403	-0.4648
4	2	0.7461	0.6695	4	3	0.9655	-0.2073	4	4	-0.1636	0.3051
5	1	-0.0684	-0.0842	5	2	0.6651	-0.3112	5	3	-0.4656	-0.1947
5	4	-0.2485	0.0360	5	5	0.1845	-0.7119	6	1	-0.0734	0.0150
6	2	0.0643	-0.3740	6	3	0.0115	0.0059	6	4	-0.0867	-0.4655
6	5	-0.2747	-0.5464	6	6	0.0173	-0.2627	7	1	0.2501	0.1385
7	2	0.3463	0.0875	7	3	0.1988	-0.1844	7	4	-0.2867	-0.1408
7	5	0.0265	0.0228	7	6	-0.3074	0.1213	7	7	0.0624	0.0048
8	1	0.0102	0.0579	8	2	0.0610	0.0860	8	3	-0.0378	-0.0667
8	4	-0.2311	0.0284	8	5	-0.0570	0.0622	8	6	-0.0947	0.2528
8	7	0.0658	0.0819	8	8	-0.0832	0.0701	9	1	0.1426	0.0137
9	2	0.0552	-0.0216	9	3	-0.1299	-0.0727	9	4	-0.0125	-0.0147
9	5	-0.0036	-0.0686	9	6	0.0163	0.1267	9	7	-0.0566	-0.0037
9	8	0.2519	-0.0101	9	9	-0.0275	0.0873	10	1	0.0927	-0.1343
10	2	-0.0419	-0.0703	10	3	-0.0383	-0.0958	10	4	-0.0699	-0.1247
10	5	-0.0525	-0.0377	10	6	-0.0550	-0.1342	10	7	0.0174	-0.0237
10	8	0.0473	-0.1213	10	9	0.0960	-0.0749	10	10	0.1365	-0.0391
11	1	-0.0087	0.0431	11	2	-0.0123	-0.1176	11	3	-0.0334	-0.0841
11	4	-0.0263	-0.1033	11	5	0.0842	0.0406	11	6	-0.0421	-0.0353
11	7	0.0041	-0.1123	11	8	-0.0204	0.0714	11	9	-0.0349	0.0393
11	10	-0.0464	-0.0333	11	11	0.0696	-0.0356	12	1	-0.0717	-0.0477
12	2	-0.0530	0.0621	12	3	0.0694	0.0371	12	4	-0.0488	-0.0158
12	5	0.0624	0.0230	12	6	0.0531	0.0280	12	7	-0.0261	0.0127
12	8	-0.0187	-0.0031	12	9	-0.0002	0.0251	12	10	0.0231	-0.0012
12	11	0.0066	0.0359	12	12	-0.0123	-0.0103	13	1	-0.0157	-0.0816
13	2	-0.0464	-0.0867	13	3	-0.0460	0.0454	13	4	0.0298	-0.0670
13	5	0.0586	0.0469	13	6	-0.0848	0.0577	13	7	-0.0414	0.0482
13	8	-0.0055	-0.0347	13	9	0.0271	0.0588	13	10	-0.0240	-0.0044
13	11	-0.0576	-0.0830	13	12	-0.0261	0.0991	13	13	-0.0543	0.0722
14	1	-0.0038	0.0480	14	2	-0.0150	0.0429	14	3	0.0653	0.0032
14	4	0.0019	0.0010	14	5	-0.0144	-0.0216	14	6	0.0166	-0.0442
14	7	0.0426	0.0030	14	8	-0.0007	-0.0414	14	9	0.0140	0.0552
14	10	-0.0380	-0.0797	14	11	0.0614	-0.0313	14	12	0.0047	-0.0413
14	13	0.0211	0.0281	14	14	-0.0448	-0.0016	15	1	0.0333	-0.0224
15	2	0.0370	-0.0641	15	3	-0.0457	0.0279	15	4	-0.0070	0.0163
15	5	0.0136	0.0358	15	6	-0.0130	-0.1076	15	7	0.0751	0.0668
15	8	-0.0261	-0.0242	15	9	0.0116	0.0385	15	10	0.0351	-0.0480
15	11	-0.0090	-0.0106	15	12	-0.0338	0.0145	15	13	-0.0191	-0.0000
15	14	0.0036	-0.0189	15	15	-0.0444	0.0356	16	1	0.0321	-0.0091
16	2	-0.0200	0.0639	16	3	-0.0083	-0.0205	16	4	0.0252	0.0306
16	5	0.0120	0.0173	16	6	0.0321	0.0136	16	7	-0.0003	-0.0286
16	8	-0.0456	-0.0046	16	9	-0.0652	-0.0676	16	10	-0.0118	0.0386
16	11	0.0189	-0.0078	16	12	0.0197	-0.0195	16	13	0.0034	-0.0139
16	14	-0.0172	-0.0430	16	15	-0.0475	-0.0378	16	16	-0.0376	-0.0119
17	12	0.0137	-0.0012	17	13	0.0145	0.0204	17	14	-0.0111	-0.0013
18	12	-0.0636	-0.0269	18	13	-0.0137	-0.0560	18	14	-0.0127	-0.0006
19	12	-0.0309	-0.0300	19	13	-0.0205	-0.0251	19	14	-0.0006	0.0011
20	12	-0.0056	-0.0154	20	13	0.0114	-0.0282	20	14	0.0055	-0.0098
21	12	-0.0324	-0.0175	21	13	-0.0241	0.0108	21	14	0.0094	0.0078
22	12	-0.0425	-0.0065	22	13	-0.0324	-0.0151	22	14	-0.0077	-0.0007

Table 4-3

Comparison of Zonal Coefficients (Normalized Coefficients x 10^6)

Degree	Cazenave et al. French 1971	GEM-1	GEM-2	GEM 3	GEM-4	GEM-5	GEM-6	Kozai SAO SE 2
2	-484.170	-484.177	-484.167	-484.171	-484.169	-484.166	-484.166	-484.166
3	.961	.962	.955	.958	.957	.961	.961	.959
4	.540	.557	.537	.547	.541	.536	.536	.531
5	.068	.062	.073	.068	.069	.066	.066	.069
6	-.155	-.178	-.145	-.162	-.153	-.146	-.145	-.139
7	.094	.105	.087	.092	.091	.096	.096	.094
8	.051	.080	.040	.062	.051	.043	.043	.029
9	.027	.008	.033	.030	.031	.027	.026	.023
10	.051	.021	.065	.040	.050	.059	.061	.077
11	-.049	-.020	-.055	-.056	-.056	-.055	-.053	-.042
12	.038	.059	.021	.046	.039	.034	.031	.008
13	.039	.002	.043	.049	.048	.050	.047	.024
14	-.016	-.037	-.009	-.030	-.027	-.026	-.021	.014
15	.015	.047	.004	-.007	-.005	-.008	-.005	.031
16	-.008	-.013	-.026	-.012	-.009	-.005	-.008	-.033
17	.005	-.035	.007	.020	.017	.022	.019	.014
18	.023	.018	.023	.016	.011	.005	.009	.038
19	.018	.045	.015	.008	.009	.003	.004	.035
20	.014	-.002	-.001	.003	.009	.015	.014	.001
21	-.016	-.031	-.012	-.008	-.008	-.010	-.010	-.022
22				-.001	-.004	-.012	-.014	

Table 4-4

Comparisons of Terrestrial 5° Anomalies (G_T) with Anomalies (G_S) Computed from Various Models

$E\left[(G_T - G_S)^2\right]$ mgal^2				
Model (Harmonics)	1281 Blocks $n \geq 1$	1042 Blocks $n \geq 5$	562 Blocks $n \geq 15$	211 Blocks $n = 25$
GEM 1 (12 x 12)	157	161	166	173
SE 2 (16 x 16)	164	168	167	172
GEM 3 (12 x 12)	152	155	161	170
GEM 5 (12 x 12)	151	155	160	171
GEM 4 (16 x 16)	149	136	127	127
GEM 6 (16 x 16)	134	129	126	116
EXP (20 x 20)	125	117	96	83

Satellite-Derived Solutions–GEM 1, 3, 5.
Combined Solutions (satellite/gravimetry)–SE 2, GEM 4, 6, EXP.
All solutions contained higher degree zonal and selected resonance terms extending to degree 21 or 22, which were excluded from the computation of G_S.

Kaula (1966) provided a statistical technique for estimating the mean square of the errors (ϵ_T, ϵ_S, δ_g) in $E(G_T - G_S)^2$ for a given solution and a given set of gravity anomaly data. The derivation assumes independence in the solution and the data. The following quantities are defined for the statistical error estimates:

$E((G_T - G_S)^2)$ = mean square difference between the terrestrial anomaly G_T and the anomaly G_S computed from the solution

$E(G_T^2)$ = mean square of the terrestrial anomalies

$E(G_S^2)$ = mean square of anomaly computed from the solution

$E(G_T G_S)$ = estimate of the variance of G_H, the true contribution to G_S

$E(\epsilon_T^2)$ = mean square value of error in terrestrial anomaly

$E(\delta_g^2)$ = mean square value of neglected higher degree terms in the G_S set (omission error)

$E(\epsilon_S^2)$ = mean square error in the solution G_S (commission error).

derived by adding gravimetric data. Rapp's 5° equal-area (300 n.m. squares) (555 km) gravity anomalies are employed in the comparisons. These consist of the 1654 blocks of anomalies (Table B-10) of which 1283 of the 5° blocks were based upon actual measurements of gravity in a form of 1° equal-area anomalies. For these 1283 blocks, mean square differences, $E\left[(G_T - G_S)^2\right]$, between the 5° gravity anomaly (G_T) and the value (G_S) computed from the potential coefficients of various models, form the basis of comparison for results presented in Table 4-4. Values of G_S were computed for the harmonics that are complete through degree and order N as indicated in the table for the different models. Two blocks with values of G_T greater than 70 mgals were excluded from the comparisons, leaving a total of 1281 blocks.

Results for four subsets of the 1281 blocks are included in the table. These subsets are based upon the number (n) of 1° observed anomalies which were used to form the 5° mean terrestrial anomaly (G_T). The four samples selected for the comparisons consist of the 1281 blocks where $n \geq 1$, 1042 blocks for $n \geq 5$, 562 blocks for $n \geq 15$, and 211 blocks for $n = 25$.

Models are listed in the table in the order of increasing agreement with the data on surface gravity. The average reduction in $E\left[(G_T - G_S)^2\right]$ between GEM 1 and GEM 5 is about 5 $mgal^2$ for the four samples. This improvement is significant for satellite models considering that the total reduction for this quantity is about 33 $mgal^2$ when surface gravity data are included, as in the case of GEM 6.

GEM 6 was computed including the gravity data of Rapp in its solution. For this reason GEM 6 is in better agreement with the test data than GEM 4, which used a similar but different set than Rapp's data in its solution. The improvement in GEM 3 and GEM 5 relative to GEM 1 is attributed to the inclusion of electronic and laser DME data. The result in Table 4-4 for the SAO Standard Earth II (SAO SE 2) is somewhat unexpected since it used a set of surface gravity data in its solution. However these data were based upon an earlier collection and were fewer than Rapp's data.

The value $E(G_T - G_S)^2$ for the mean square gravity anomaly differences is due to: (1) errors (ϵ_S) of commission caused by errors in the potential coefficients in the solution, (2) errors (ϵ_T) in the data, and (3) errors (δ_g) of omission caused by excluding higher-degree coefficients from the solution. The solution (EXP in Table 4-4) is derived in a manner similar to GEM 6 except that the EXP solution is complete to degree and order 20 in spherical harmonics. This extension is obtained from the contributions of the surface-gravity data. Since 5° mean gravity anomalies correspond ideally to a model complete to degree and order 36 in harmonics, the primary source of the value for the total error is due to the omission errors δ_g. The EXP model shows a considerable reduction in $E(G_T - G_S)^2$ relative to GEM 6.

Table 4-5

Statistical Error Estimates for Gravity Models Based Upon 5° Terrestrial Anomalies G_T and Anomalies G_S Obtained from Potential Coefficients

	(mgal^2)						
	$E(G_T-G_S)^2$	$E(G_T G_S)$	$E(G_S^2)$	$E(G_T^2)$	$E(\epsilon_S^2)$	$E(\epsilon_T^2)$	$E(\delta_g^2)$
GEM 5 (12 x 12)							
n ≥ (blocks)							
10 (770)	156	183	207	315	24	19	113
15 (563)	160	188	209	326	21	16	123
20 (400)	151	181	198	315	17	14	120
GEM 6 (16 x 16)							
n ≥ (blocks)							
10 (771)	126	213	237	315	24	19	83
15 (563)	126	218	235	326	17	16	93
20 (401)	115	210	219	315	10	14	91
EXP (20 x 20)							
n ≥ (blocks)							
10 (771)	102	237	260	315	23	19	60
15 (563)	96	256	252	326	11	16	69
20 (401)	84	235	239	315	4	14	66

For a given argument Q, the preceding quantities E(Q) are computed from

$$E(Q) = \sum_{i=1}^{K} Q_i/K$$

where the subscript i corresponds to a 5° equal area block centered at a given latitude and longitude, and K is the number of blocks containing terrestrial gravity anomalies G_T.

Formulas for the mean square errors of ϵ_T and ϵ_S and the neglected higher degree terms of δ_g are

$$E(\epsilon_T^2) = E\left[\frac{E(G_T^2)}{n}\right],$$

$$E(\epsilon_S^2) = E(G_S^2) - E(G_H^2),$$

$$E(\delta_g^2) = E((G_T - G_S)^2) - E(\epsilon_T^2) - E(\epsilon_S^2).$$

where n is the number of 1° observed anomalies in a 5° block.

The statistical estimates were applied to three samples of the 5° test anomalies for the GEM 5, GEM 6, and EXP models. The resultant estimates are listed in Table 4-5. Samples of the 1281 blocks of observed data were chosen for $n \geq 10$, 15, and 20. The error estimates are expected to be most valid for GEM 5 since the solution is independent of the test data.

The estimate for $E(\delta_g^2)$ represents the amount of information that remains to be extracted from the gravity data corresponding to a given solution. For the three models in Table 4-5, the $E(\delta_g^2)$ averaged over the three samples reduces from 119 $mgal^2$ for the 12 x 12 GEM 5 model, to 89 $mgal^2$ for the 16 x 16 GEM 6 model, and to 65 $mgal^2$ for the 20 x 20 EXP model. These omission (or truncation) errors are decreasing by at least 24 $mgal^2$ as the maximum degree increases by 4. At this rate the truncation error would be exhausted for a field complete to degree 32. Ideally this would occur at degree 36 for a global set of 5° anomalies.

The mean square errors of commission $E(\epsilon_S^2)$, due to errors in the potential coefficients in the solution, are estimated more realistically for the GEM 5 satellite model since its solution is independent of the test data. The rms error is about 4.5 mgal for the three samples, which is consistent with the value derived from the 15° equal-area anomalies in equation (3.12) of Section 3.4.

Degree variances of gravity anomaly give a measure of the power spectrum corresponding to harmonic wavelengths of degree n. Gravity anomaly degree variances for the GEM 5, GEM 6, and EXP models are listed in Table 4-6. Values are quite consistent from degree 2 to 12 for the three solutions. For these coefficients, a maximum difference of 3 $mgal^2$ is seen at degree 7 between GEM 5 and each of the combination solutions. Degree variances are listed beyond degree 12 for the GEM 5 satellite model but these include only the effects of the zonal and selected satellite resonant terms. Similarly the results agree very well between the GEM 6 and the EXP model through degree 16. The sharp rise in the EXP (20 x 20) result for degrees 19 and 20 is probably related to the so-called "aliasing" effect. This effect is due to the truncation of the spherical harmonics. Some of the remaining information in the gravity anomaly (δ_g) for higher degree (>20) terms is absorbed into adjacent degree terms in the solution.

Table 4-6

Gravity Anomaly Degree Variances ($mgals^2$)

Degree n	GEM 5	GEM 6	EXP
0	—	9.0	9.0
2	7.3	7.3	7.3
3	33.5	33.6	33.5
4	19.5	19.3	19.3
5	20.4	21.6	21.1
6	18.6	20.0	19.7
7	20.1	17.4	17.1
8	10.5	8.4	8.4
9	10.0	8.8	8.5
10	10.8	11.4	10.7
11	7.1	7.7	7.5
12	4.0	4.1	4.2
13	5.2	10.6	9.3
14	1.7	5.9	6.2
15	1.9	8.5	6.7
16	0.7	6.8	7.5
17	0.3	0.3	5.5
18	2.4	2.4	7.7
19	1.0	1.0	12.5
20	0.5	0.5	10.9
21	0.8	0.9	0.8
22	1.6	1.5	1.5

Table 4-6 includes a value corresponding to the harmonic of degree zero, namely Δg_0, which was derived in the combination solutions as an adjustment for the reference value of equatorial gravity g_e. Since $\Delta g_0 = 3$ mgal, the reference value of g_e given in Table 2-5 is adjusted to 978032.1 mgal (g_e') so as to correspond to the observed gravity data. The observed and computed gravity anomalies used in the comparisons above referred to normal gravity with the adjusted g_e'.

Maps of gravity anomaly contours are presented in Figures 4-1 for GEM 5 and 4-2 for GEM 6. The differences in results are primarily due to the truncation at degree 12 in the GEM 5 model. The global RMS of the anomaly differences for the terms through degree 12 between the two models is 3 mgal and for terms beyond degree 12 it is 5.5 mgal. Maps of geoid height are given in Figure 4-3 for GEM 5 and 4-4 for GEM 6 and these are subsequently discussed in Section 4.1.4. The maps are based upon a reference ellipsoid with parameters listed in Table 2-5.*

4.1.3 Comparison with Satellite Data (Analysis of the Effects of Different Models of the Gravitation Potential on Satellite-Observation Residuals)—Orbits have been derived from several sets of tracking observations with use of various models of the gravitational field. The rms of the observation residuals found by use of the different models is used as a measure for comparing them. Results are presented in the following Tables:

Table 4-7 — USB tracking data on 11 daily arcs of the ERTS-1 satellite

Table 4-8 — 7-day arcs of camera data on 23 satellites

Table 4-9 — BE-C laser DME data on 22 short arcs

Table 4-10 — Long-term zonal perturbations on 21 satellites

The unified S-band (USB) tracking data were processed for 11 stations using each of the GEM models and SAO SE 2. The results are listed in Table 4-7. These data provided global coverage for the orbit on 11 daily arcs of the ERTS-1 satellite. For each daily arc the number of two-way Doppler range-rate observations and station passes are listed. The rms of the residuals are given for each arc along with the average for the 11 arcs corresponding to each of the

*A map of geoid height of GEM 6 referenced to an earth in hydrostatic equilibrium is given by Khan and O'Keefe, "Recommended Reference Figures for Geophysics and Geodesy," GSFC X-592-73-318 (Figure 2), October 1973.

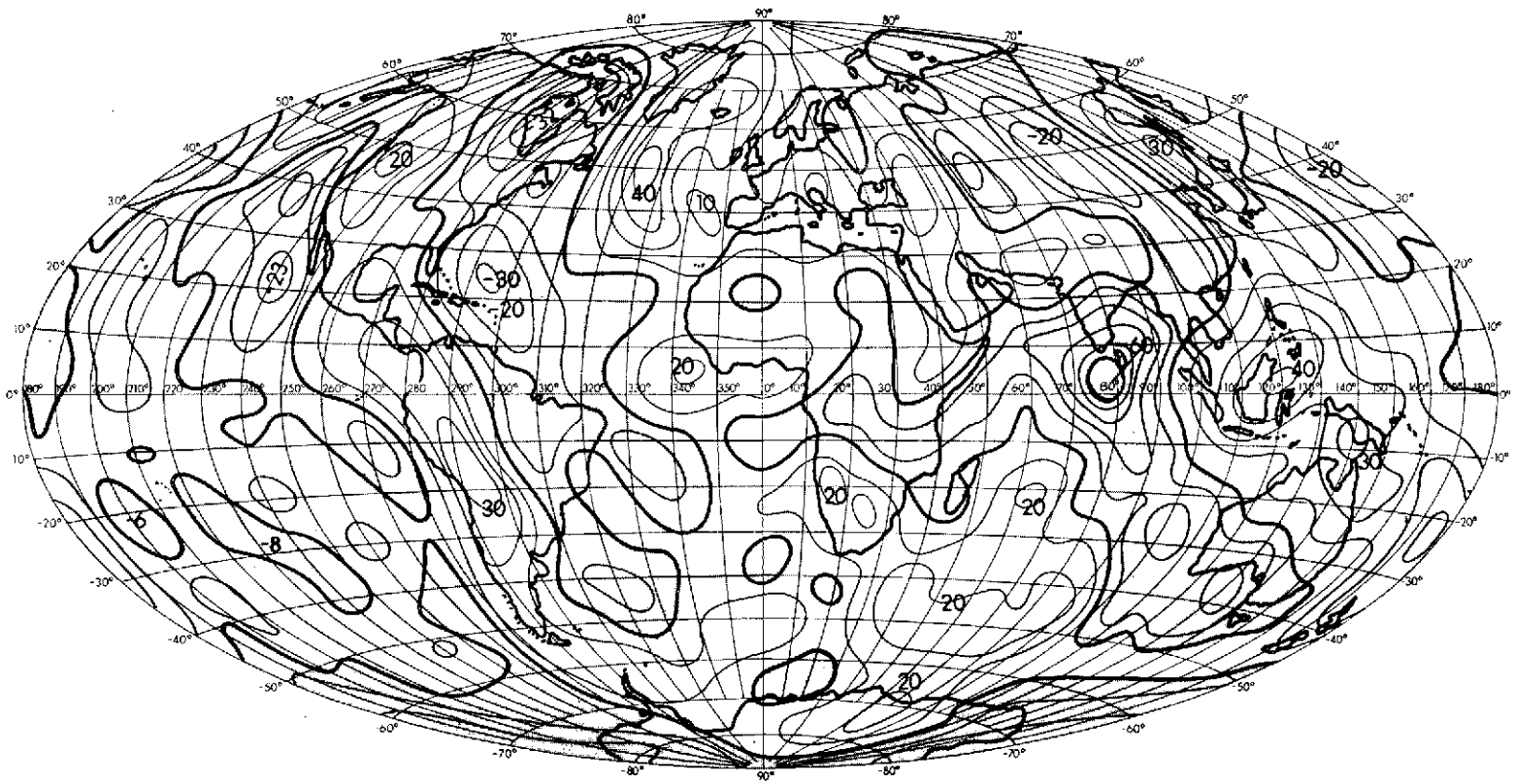

Figure 4-1. GEM 5 Gravity Anomaly Contours
(10mgal Interval)

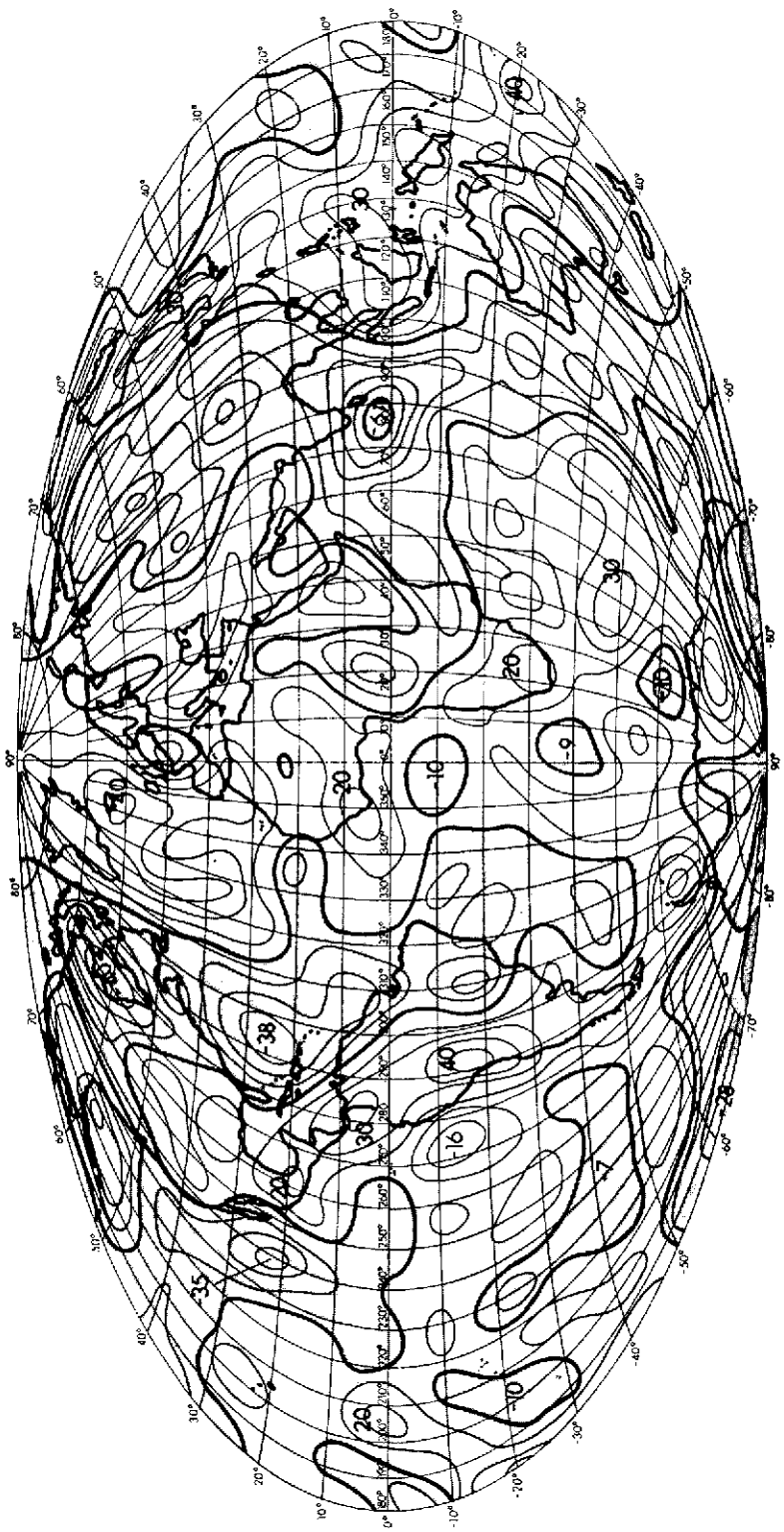

Figure 4-2. GEM 6 Gravity Anomaly Contours
(10mgal Interval)

Figure 4-3. GEM 5 Geoidal Heights
(10m Interval)

Figure 4-4. GEM 6 Geoidal Heights
(10m Interval)

Table 4-7

RMS (cm/sec) Value of Residuals of Two-Way Doppler for USB Tracking on Daily Arcs of ERTS-1

Daily Arc (1972)	No. of Obs. (passes)	GEM 1	GEM 3	GEM 4	GEM 5	GEM 6	SE 2
7/23	2610 (27)	4.9	6.2	10.3	5.6	6.4	9.1
7/28	1924 (19)	4.9	5.5	4.7	5.5	4.0	9.4
7/29	1183 (18)	5.3	5.3	4.8	5.5	4.3	11.2
7/30	1167 (17)	5.4	6.2	5.6	6.1	3.7	8.7
7/31	989 (15)	5.9	5.7	5.4	5.7	6.2	9.8
8/1	1280 (19)	6.8	5.9	6.0	6.0	6.1	10.4
8/2	1239 (20)	6.4	5.3	6.1	5.2	4.9	11.7
8/4	1176 (18)	7.4	6.0	6.3	6.4	5.5	13.0
8/8	1026 (17)	6.1	6.0	9.1	6.4	6.3	9.1
8/9	1309 (20)	6.2	7.0	10.5	6.8	6.3	10.4
8/10	1686 (20)	5.8	6.1	9.9	6.1	6.9	10.1
Average rms		5.9	5.9	7.2	5.9	5.5	10.3

Orbital elements: a = 7283207m., e = .0001, i = 99.12°.
11 USB Stations: ACN3, BDA3, CRO3, CYI3, GDS8, GDSA, GWM3, HAW3, HSK8, MAD8, MIL3.
Average of 7 stations participated per arc.

gravity models. The average rms shows the best result for GEM 6. The SE 2 is significantly poorer than the GEM's in this comparison with data not included in either solution.

Table 4-8 presents the weighted rms of observation residuals for a weekly arc on each of the 23 satellites that contain data from cameras (see Table 2-1). The rms values are weighted corresponding to the 2 arc second standard deviation representing the accuracy of the cameras' data. Ideally then the rms values should be close to unity (they may be scaled by a factor of 2 for conversion to arc seconds). The average rms value per satellite is listed at the bottom of the table for each of the gravity models in units of seconds of arc. The two solutions GEM 1 and 3 and the GEM 6 combination solution all agree to within 0.37 arc seconds of the GEM 5 value of 2.37 arc seconds (in the average rms value per satellite). The GEM 4 and SE 2 are 0.63 arc seconds and 1.07 arc seconds larger than the GEM 5 value, respectively. Again the GEM models give significantly better results than the SE 2.

Table 4-8

Weighted RMS of Observation Residuals in Camera Observations for a Weekly Arc on Each of 23 Satellites (Weight Based on 2 Seconds of Arc)

Satellite	GEM 1	GEM 2	GEM 3	GEM 4	GEM 5	GEM 6	SAO SE 2
TELSTAR	0.9	0.9	0.9	0.9	0.9	1.0	2.5
GEOS-A	0.8	1.0	0.9	0.8	0.8	0.8	1.0
SECOR	1.3	1.2	1.3	1.2	1.3	1.2	1.3
OVI-2	2.0	2.3	2.0	2.3	2.0	2.2	2.1
ECHO	1.1	1.1	1.1	1.3	1.1	1.1	1.3
DI-D	1.5	1.7	1.5	1.7	1.4	1.7	2.5
BE-C	0.9	1.0	0.9	1.0	0.9	1.0	1.1
DI-C	1.1	1.5	1.2	1.8	1.0	1.3	1.9
ANNA-1B	1.1	1.3	1.3	1.5	1.1	1.3	1.3
GEOS-B	0.9	0.9	0.8	0.9	0.9	0.9	1.2
OSCAR	1.0	1.2	1.4	1.6	1.0	1.1	1.2
5BN-2	2.5	1.6	4.1	3.3	1.4	1.8	2.7
COURIER	1.2	1.4	1.3	1.3	1.2	1.2	1.1
GRS	1.9	2.3	2.0	2.6	1.8	2.0	4.3
TRANSIT	1.0	1.0	1.0	1.1	1.0	1.1	1.1
BE-B	1.2	1.3	1.4	1.6	1.3	1.6	1.4
OGO-2	1.6	2.9	1.3	2.9	1.4	2.6	2.9
INJUN	1.1	1.3	1.1	1.6	1.0	1.3	1.5
AGENA	1.7	1.6	1.6	1.8	1.6	1.5	2.4
MIDAS	0.8	0.8	0.8	0.8	0.8	0.8	0.8
VANG-2R	0.8	0.8	0.8	0.8	0.8	0.9	0.8
VANG-2S	1.5	1.7	1.4	1.6	1.4	1.7	1.5
VANG-3S	1.3	1.3	1.2	1.3	1.2	1.4	1.7
Average rms (arc seconds)	2".54	2".79	2".71	3".10	2".37	2".74	3".44

Twenty-two short arcs on BE-C have been derived from laser data, which are independent of the GEM solutions. The BE-C arcs are 3 revolutions in length; each consists of four consecutive passes of data which were collected by the GSFC laser system (GODLAS) at Greenbelt during a 5-month period starting in July 1970. The rms of the residuals are listed in Table 4-9 for the individual arcs, along with an average rms per arc. The results agree to within .3 meter for the GEM 1, GEM 5, and GEM 6 models. These average rms values range from 1.33 to 1.65 meters. As shown in the table somewhat larger average rms values for GEM 3 (2.0 meters) and for the SE 2 model (2.51 meters) have been obtained and a value as large as 4.05 meters has been obtained for GEM 4. For short arcs derived from laser data on a single pass, all the above models generally give rms values of about 50 centimeters, corresponding closely to the estimate of the accuracy of GODLAS. A preliminary solution for the gravitational potential (PGS 2), which was based upon camera data as in the case of GEM 1 but which is complete to degree and order 16 in harmonics and includes a number of selected higher degree terms, gave an average rms value of 1.06 meters for the 22 four-pass arcs. Results for individual arcs for PGS 2 are listed in Table 4-9 along with the results for the other models.

Zonal solutions were tested on the orbits of 21 satellites, most of which were not used in the models being tested (e.g. Wagner, 1972). They include the low inclination satellites of SAS and PEOLE. Tests were for the long-term zonal effects on mean elements. Wagner uses as criteria the weighted rms of the mean element residuals of each solution, which represents a relative measure of accuracy. Results are listed in Table 4-10.

The solutions that contain the low inclination satellites, GEM 3 through 6 and French 71, compare favorably in this test. Considering that the GEM satellite solutions were based upon week-long orbital arcs and the French 71 solution was based upon satellite long-term zonal effects, it verifies that good zonal recovery may be achieved from short-term zonal effects. The SAO SE 2, GEM 1, and GEM 2 solutions do not compare as well in these tests because they do not contain the effects of low inclination satellites. Wagner's solution is expected to have the lowest rms since it was based entirely upon the test data.

Summary results of Tables 4-7 through 4-10 of this section and Table 4-4 of the previous section are presented in Table 4-11. The rms values of observation residuals for the different data categories show, on the average, better results for the GEM 5 and GEM 6 models. For purposes of ordering the models for evaluation a simplified ranking scheme was used, as described in the table, and was based upon the relative order of the rms values from the different comparisons. Using this method, GEM 5 and 6 rank highest while GEM 4 and the SE 2 model rank least.

Table 4-9

Rms(m) of Residuals from Laser System Measurements of Short Arcs of BE-C

DATE YYMMDD	TIME HHMMSS	NO. PTS.	GEM 1	GEM 3	GEM 4	GEM 5	GEM 6	SAO SE 2	PGS 2
700706	205829	493	1.2	3.4	3.9	2.0	1.4	1.4	0.9
700818	040000	1712	2.1	1.4	1.3	1.8	2.1	1.4	1.2
700822	040435	1777	1.7	2.3	5.2	2.2	1.2	3.7	0.8
700824	024423	1338	1.5	1.2	1.8	1.2	1.8	0.9	1.1
700825	035555	1197	1.2	2.4	5.5	1.3	3.0	1.4	1.3
700826	031510	1072	0.9	2.3	6.0	1.3	2.2	2.5	0.9
700827	023425	1498	1.3	2.7	5.3	2.0	1.3	3.1	0.8
700828	015324	1269	1.3	1.5	3.3	1.6	1.0	2.7	0.7
700829	011340	1579	1.3	0.9	0.8	1.1	1.2	1.1	1.0
700831	014527	1008	0.7	2.0	5.1	1.0	2.5	1.6	1.0
700901	010340	2001	1.2	3.3	7.5	2.0	2.4	3.6	1.0
700902	002214	1875	1.4	2.4	5.3	2.0	1.1	3.5	0.8
700902	230000	1567	1.2	1.1	2.1	1.4	0.7	1.9	0.8
700907	221312	1349	1.5	2.0	4.0	1.4	1.1	3.6	1.0
700911	193306	775	1.1	2.8	5.4	1.7	1.9	2.7	0.9
700929	140000	615	1.0	1.1	1.9	1.0	1.0	2.5	1.1
701001	130000	690	1.9	0.8	1.7	1.4	1.7	1.7	1.7
701003	135548	818	0.9	2.0	7.3	1.0	2.6	3.0	2.2
701017	080000	568	2.2	1.9	3.2	2.2	1.3	4.0	1.1
701116	222815	506	1.1	2.9	5.1	1.7	2.3	2.1	1.2
701117	214802	723	1.1	1.9	5.0	1.3	1.6	3.4	1.0
701124	185600	1285	1.5	1.6	2.5	1.6	0.9	3.4	0.9
Average rms			1.33	2.00	4.05	1.54	1.65	2.51	1.06

Table 4-10

Comparison of Models for Long-Term (Orbital) Zonal Perturbations

Solution	rms	Solution	rms	Solution	rms
SAO SE 2*	5.49	French 71	3.28	GEM 5	3.13
GEM 2*	4.80	GEM 3	2.92	GEM 6	2.97
GEM 1*	3.62	GEM 4	2.89	Wagner	1.50**

*These models did not include low inclination satellite in their solutions.
**This result was derived from direct use of the data.

Table 4-11

Summary of Gravity Model Comparisons with Satellite and Gravimetry Data
(RMS of Observation Residuals)

Models	Optical Data on Weekly Arcs for 23 Satellites (seconds of arc)	USB Doppler* Data on 11 Daily ERTS-1 Arcs (cm/sec)	Laser Data* on 22 BE-C Short Arcs (meters)	Long-Term Zonal Perturbations on 21 Satellites (relative measure)	5° Terrestrial Gravity Anomalies (mgal)	Average** Rank
GEM 1	2.54	5.9	1.33	3.62	13.3	2.3 (4)
GEM 3	2.71	5.9	2.00	2.92	13.0	2.2 (3)
GEM 4	3.10	7.2	4.05	2.89	12.1	2.8 (5)
GEM 5	2.37	5.9	1.54	3.13	13.0	1.6 (2)
GEM 6	2.74	5.5	1.65	2.97	11.7	1.4 (1)
SAO SE 2	3.44	10.3	2.51	5.49	13.3	4.6 (6)

*Data for these two categories were independent of the solutions for all models.

**Models were ranked in each category with a serial number (0, 1, 2, 3, 4, 5) corresponding respectively to increasing RMS values. The average rank for a given model was obtained as the mean of the individual rankings, and the mean was used to rank the models from 1 to 6 as shown in parentheses.

4.1.4 Geoid Height--Contour maps of geoidal heights relative to the reference ellipsoid are presented in Figures 4-3 and 4-4 for the GEM 5 and GEM 6 models, respectively. The major features of relative highs and lows are exhibited below for eight main features.

Table 4-12

Major Features of the Geoid

Number	Geographic Name	Approximate		Height	
		Latitude	Longitude	GEM 5	GEM 6
1	Solomon Island High	-10°	150°	73	77
2	Indian Low	0°	80°	-110	-110
3	British Isle High	50°	350°	64	70
4	Bahama Low	30°	290°	-53	-55
5	Antartica High	-55°	50°	46	50
6	North East Pacific Low	20°	240°	-47	-55
7	Antartica Low	-70°	200°	-60	-57
8	South America High	-20°	290°	32	35

There is a good agreement between the two models in the major features. The largest difference is 8 meters and occurs at the North East Pacific Low.

Some comparisons are made between the GEM 6 and other geoids. A zonal profile of geoidal height from GEM 6 is given in Figure 4-5. An rms of differences between geoidal heights computed from the zonal harmonic coefficients of Cazenave et al. (1971) and from those of GEM 6 is 0.2 meters; the maximum difference is less than a meter. In general a global rms of differences (Δh) in geoidal height between two models may be estimated using Bruns formula (Heiskanen and Moritz, 1967) and it is given as follows:

$$rms_{\Delta h} = \left[R_e^2 \sum_{n=2}^{N} \sum_{m=0}^{n} (\Delta \bar{C}_{nm}^2 + \Delta \bar{S}_{nm}^2) \right]^{1/2} \qquad (4.1)$$

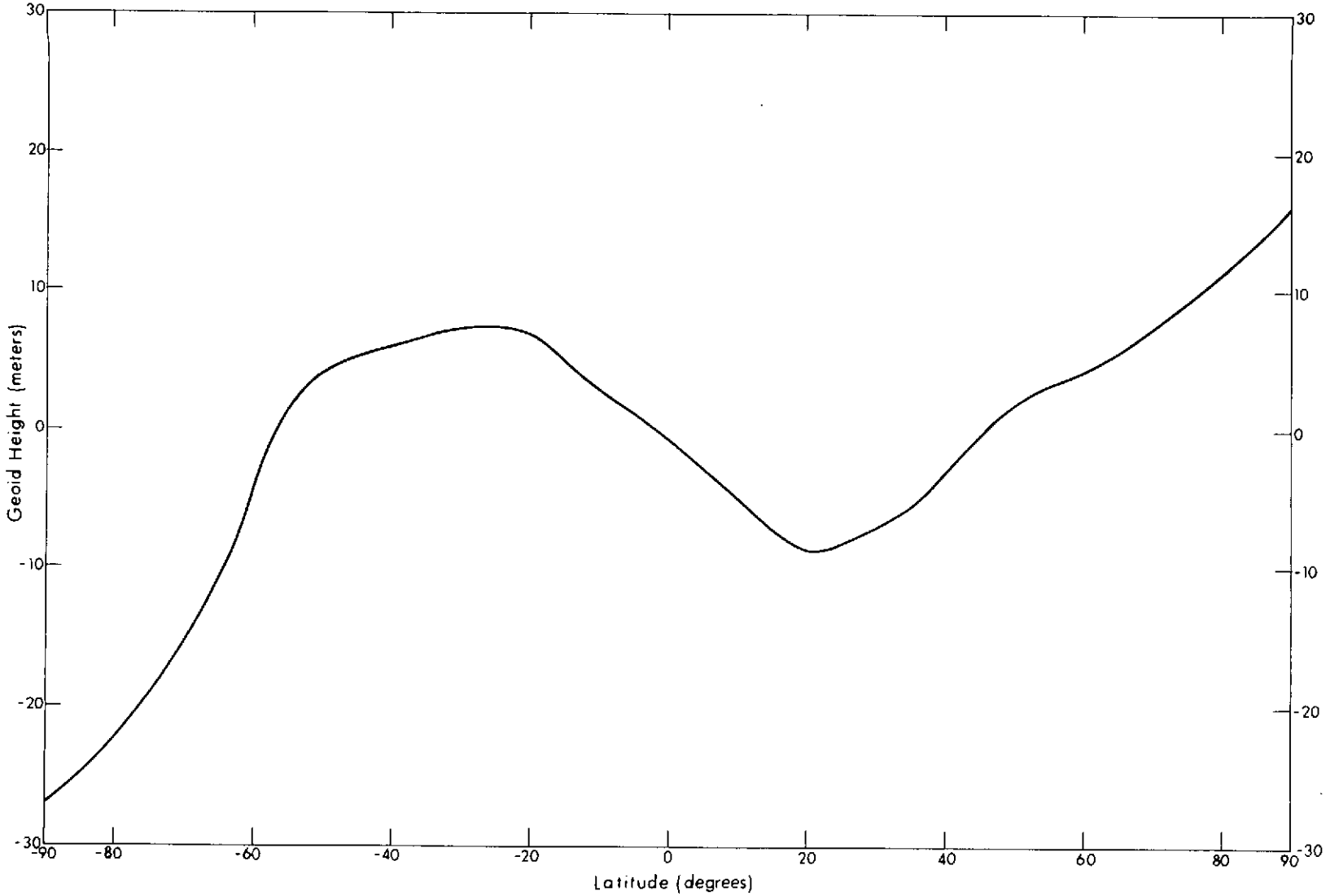

Figure 4-5. Profile of Geoidal Heights Using only Zonal Harmonics in GEM 6

where $\Delta\bar{C}$, $\Delta\bar{S}$ are normalized coefficient differences of degree n and order m between the two models, R_e is the mean radius for the earth, and N corresponds to the largest degree term in the models.

Using equation (4.1), comparisons between the GEM 6 solution and various models are listed as follows:

Table 4-13

Global RMS of Geoid Height Differences with the GEM 6 Model

	GEM 2	GEM 4	GEM 5	EXP (20 x 20)
rms (meters)	3	3	4	4

The effect of truncation on geoid height for coefficients beyond degree N may be estimated from use of Kaula's values ($10^{-5}/n^2$) for these coefficients. By extending (4.1) and replacing the differences with Kaula's values we obtain approximately

$$\text{rms}_{\Delta h}\ (n > N) = \frac{64}{N}\ \text{(meters)}. \tag{4.2}$$

Using the above result of 4 m for EXP (20 x 20) and a value of 3 m, obtained from (4.2) with N = 20, for the effect of truncation, a global (rms) error in geoid height for GEM 6 is estimated as

$$\sigma_{\Delta h}\ (\text{GEM 6}) = (4^2 + 3^2)^{1/2} = 5\ \text{m} \tag{4.3}$$

Errors in geoid height for GEM 6 may be expected to be smaller in areas of major survey where gravimetric data is more complete. For example, tests were made for GEM 6 with the use of a detailed geoid in North America, Eurasia, and Australia (Vincent et al., 1972) where 1°-by-1° gravity anomaly data were used. An rms of geoid height differences for these areas was about 3.5 meters. However large variations in geoid height exist in certain areas. For example, a difference of 12 meters exists in the vicinity of the Puerto Rican Trench.

The result in Table 4-13 of 4 m for the rms of geoid height differences between GEM 5 and 6 considers terms from degrees 12 to 16 that have not been included in the solution for GEM 5. For terms that are common to the two models the rms value for geoid height differences is 3 meters. This value compares closely to the value obtained from the error estimates of the coefficients in GEM 5, as may be seen from (3.17) of Section 3.

4.2 Station Coordinates for GEM 6

In conjunction with the derivation of the GEM 6 gravitational field, positions were derived for some 134 tracking stations. Positions for all stations except the BC-4 camera stations were derived dynamically. The positions of the BC-4 stations were derived by using the geometric theory of simultaneous observations between BC-4 cameras and using constraints on relative positions from ground surveys to tie a subset of BC-4 stations to other camera and Doppler stations. Also certain positions for MOTS and GSFC laser sites were derived using both the geometric and dynamic process.

In addition, constraints from geodetic networks were applied to the relative positions of certain pairs of stations. These relative position constraints, based on local datum survey coordinates, were applied to 47 pairs of stations, where in our judgment such ground survey ties would strengthen the solution. Table 4-14 lists the ties, the Δx, Δy, Δz survey differences, an estimated uncertainty used for weighting, and the residuals from the solution. Except for Doppler stations, uncertainties were estimated in a formal way from Simmons' Rule* as

$$\sigma = .029\ D^{2/3}\ \text{(meters)}$$

where D is the distance between the stations in kilometers. The Doppler stations are uncertain by an additional 3 meters due to a lack of information concerning the relationship of the surveyed point to the electrical (phase) center of the Doppler antennae. This weighting is not critical. A reasonable variation in weights results in nearly the same solution.

In arriving at the station positions, a set of chord distances between BC-4 stations, with associated error estimates, were also enforced. These chord distances, taken from Mueller (1973), together with the error estimates assigned in this solution are presented in Table 4-15. The observations used in the solution are described in Section 2 and the theory used in Appendix A.

The station coordinates were derived as part of the GEM 6 solution along with the geopotential, amounting to 729 unknown parameters. The solution of this large a set of normal equations required some attention to numerical accuracy. It was obtained by the Cholesky method with use of an iterative improvement process. A computed condition number indicated that the corrections to initial values were accurate to six digits. The average correction for station coordinates was of the order of 10 meters, except for a few Doppler stations where the corrections were of the order of 100 meters. Of the unknowns, 328 were corrections to coefficients of the Earth's gravitational potential, and 402 were corrections to assumed coordinates of 134 stations.

*Simmons, L. G., "How Accurate is First-Order Triangulation?", Journal of U.S. Coast and Geodetic Survey, April 1950.

Table 4-14

Constraints on Relative Position (Survey Ties)

Station Pair	Relative Position Constraints (Meters)			Est. Stand. Dev. (Meters)	Solution Residuals with Respect to Constrained Values (Meters)		
	Δx	Δy	Δz	σ	δx	δy	δz
2017 2117	-3.75	6.28	-2.02	4.23	6.03	3.19	10.73
2822 6064	-12.06	13.60	23.74	3.00	-1.66	2.03	1.07
2837 6067	46.13	290.25	-1248.20	3.00	-10.56	0.71	3.59
1038 6060	304147.18	114912.15	494900.60	2.04	-6.45	12.01	6.91
2019 6053	-130.35	808.62	87.15	3.00	-0.48	9.33	-3.28
2722 6055	-78.06	-172.20	-160.45	3.00	7.44	-6.64	2.98
2723 6040	19.71	0.69	14.10	3.00	1.93	-1.73	-3.74
1152 6032	-47149.40	-424141.91	676055.82	2.50	10.97	2.19	-3.32
6019 9011	-52.01	-37.07	18.82	0.01	0.01	0.00	0.00
1021 7043	12681.43	44984.51	51158.99	0.49	-1.48	-2.67	-2.86
1022 7071	168409.91	50582.89	45732.81	0.93	0.60	6.44	2.51
1034 7034	0.08	0.66	-0.74	0.01	0.00	0.00	0.00
1037 1042	-7.58	-0.59	0.50	0.01	0.00	0.00	0.00
7043 7050	-38.21	-36.26	-31.23	0.01	0.00	0.01	0.01
7043 7052	130836.64	-50256.13	-100969.38	0.90	3.61	-2.64	2.65
7043 7077	-652.92	-1710.84	-1877.61	0.06	0.01	0.00	0.00
7043 7078	130867.90	-50025.41	-100693.72	0.90	-0.77	-0.53	0.42
7071 7072	4.08	5.48	11.42	0.01	-0.20	0.04	0.72
7071 7073	10.32	6.62	9.32	0.01	0.19	-0.03	-0.72
7071 7074	11.03	8.97	15.81	0.01	0.00	0.00	0.00
2738 6003	3.96	-23.90	21.87	3.00	8.19	16.28	-4.58
1025 6009	17214.35	4034.43	58089.41	0.46	-0.01	0.05	0.04
2817 6015	7.76	4.05	-16.20	3.00	-11.17	-3.60	11.18

Table 4-14 (continued)

Station Pair	Relative Position Constraints (Meters)			Est. Stand. Dev. (Meters)	Solution Residuals with Respect to Constrained Values (Meters)		
	Δx	Δy	Δz	σ	δx	δy	δz
6111 6134	-53.77	-90.12	-305.26	0.01	0.00	0.00	0.00
6002 7043	-56.27	-499.54	-568.43	0.02	0.00	0.00	0.00
6011 9012	-49.58	118.93	-35.81	0.01	0.00	0.00	0.00
7071 9010	19.05	3.07	3.92	0.01	0.01	0.01	0.01
9003 9023	6011.64	-17986.56	-27467.42	0.30	-0.02	-0.04	0.42
4740 7039	-674.06	699.92	1476.31	0.04	0.00	0.00	0.00
4760 7039	-683.27	706.55	1488.25	0.04	0.00	0.00	0.01
1037 1126	-334.06	-403.53	-571.31	0.02	0.01	0.00	-0.01
1152 7054	54.96	-51.86	-135.62	0.01	0.00	0.00	0.00
2203 7052	-116.78	-336.48	-389.60	3.00	5.76	2.27	0.02
2115 4050	354.70	970.65	296.73	3.00	1.51	-3.76	3.73
4082 7071	65691.26	62291.57	137 735.55	0.87	-0.74	-0.31	-1.78
4840 4860	-2384.64	711.85	1660.19	0.06	0.00	-0.01	0.00
4840 7052	-2425.68	685.03	1630.22	0.06	-0.01	0.00	0.01
1024 4946	-21762.84	24680.80	54300.42	0.46	0.28	-0.20	-0.60
1031 6068	59.69	-55.46	51.19	0.01	0.00	0.00	0.00
6068 9002	28722.17	46167.12	-7673.38	0.42	0.50	-0.44	0.47
7072 9049	4.82	-3.60	-12.97	0.01	0.01	0.01	0.00
6111 9425	-1159.33	43554.59	52281.60	0.48	0.38	0.07	0.09
6042 9028	2992.55	-3032.66	-2462.26	0.08	0.00	0.01	0.00
2100 6011	32128.97	-180272.68	-83071.46	3.04	-12.07	1.62	5.85
9005 9025	36256.49	10061.56	30386.63	0.38	0.27	-0.11	0.52
7901 9001	0.0	0.0	0.0	4.23	-20.28	-1.41	7.34
2106 1035	-22330.33	23266.93	17999.44	3.02	-4.97	21.12	-1.57

Table 4-15

Constraints on Baseline Distance (BC-4 Stations)

	Distance (meters)	Estimated Standard Deviation PPM, (m)	Residual (meters)
6002-6003	3 485 363.23	1.00 (3.49)	6.58
6006-6016	3 545 871.56	1.00 (3.55)	1.68
6006-6065	2 457 765.81	0.70 (1.72)	-1.04
6016-6065	1 194 793.60	0.85 (1.02)	2.92
6023-6060	2 300 209.80	0.50 (1.15)	-1.72
6032-6060	3 163 623.87	1.00 (3.16)	-5.54
6063-6064	3 485 550.76	0.85 (2.96)	-2.32
6003-6111	1 425 876.45	0.90 (1.29)	-2.03

The station coordinate results are presented in Table 4-16 in the form of latitude, longitude, and geodetic height with respect to an ellipsoid having a semi-major axis of 6378155 meters and a flattening of 1/298.255.

Before discussing these results, the consequences of the applied constraints should be examined. First, comparisons of GEM 6 station coordinates with GEM 4 station coordinates, as well as with other solutions not involving the BC-4 stations, indicate that most positions derived dynamically are essentially unaffected by inclusion of the BC-4 network. The only exceptions are Doppler stations 2019, 2722, 2723, and 2738. Only a small amount of Doppler data was available for determination of the positions of these stations, and they are very weakly determined from calculations using dynamics. These stations were essentially determined from the BC-4 and baseline data used in the solution.

Secondly, the baseline constraints and the ties to the dynamic system both provide scale to the BC-4 network. The scale inferred by using the baselines only is approximately 2 ppm smaller than the dynamical results as discussed in Section 4.2.2. A comparison of combination solutions (BC-4 geometric and dynamical) with and without baselines shows essentially no change in scale for the BC-4 network, except for 8 of the 47 BC-4 stations that were tied in directly or

Table 4-16

GEM 6 Station Coordinates

STATION POSITIONS FOR BAKER-NUNN

STATION NAME	NUMBER	LATITUDE DEG	MN	SECOND	LONGITUDE DEG	MN	SECOND	HEIGHT METERS	SIGMA* METERS
1ORGAN	9001	32	25	25.079	253	26	48.996	1619.1	4.
1OLFAN	9002	-25	57	35.837	28	14	52.459	1559.0	3.
WOOMER	9003	-31	6	2.124	136	47	3.319	155.5	4.
1SPAIN	9004	36	27	46.818	353	47	36.958	60.0	3.
1TOKYO	9005	35	40	22.968	139	32	16.563	84.9	5.
1NATAL	9006	29	21	34.781	79	27	27.517	1871.0	4.
1QUIPA	9007	-16	27	56.628	288	30	24.604	2484.7	4.
1CURAC	9008	29	38	13.839	52	31	11.372	1580.3	5.
1SHRAZ	9009	12	5	25.186	291	9	44.532	-23.2	5.
1JUPTR	9010	27	1	14.120	279	53	13.357	-24.8	3.
1VILDO	9011	-31	56	34.597	294	53	36.609	625.1	4.
1MAUIO	9012	20	42	26.175	203	44	33.983	3042.8	4.
HOPKIN	9021	31	41	3.302	249	7	18.599	2341.0	6.
AUSBAK	9023	-31	23	25.694	136	52	43.649	134.0	4.
DODAIR	9025	36	0	20.304	139	11	31.565	883.7	5.
DEZEIT	9028	8	44	51.242	38	57	33.407	1904.1	5.
COMRIV	9031	-45	53	12.290	292	23	9.413	192.5	5.
JUPGEO	9049	27	1	13.948	279	53	12.993	-28.1	3.
AGASSI	9050	42	30	21.542	288	26	30.583	129.9	17.
GREECE	9091	38	4	44.849	23	55	58.658	487.2	5.
COLDLK	9424	54	44	34.634	249	57	23.125	669.4	12.
EDWAFB	9425	34	57	50.677	242	5	8.030	748.9	6.
OSLONR	9426	60	12	39.200	10	45	2.938	617.0	13.
JOHNST	9427	16	44	38.879	190	29	9.343	18.8	7.

STATION POSITIONS FOR GRARR

STATION NAME	NUMBER	LATITUDE DEG	MN	SECOND	LONGITUDE DEG	MN	SECOND	HEIGHT METERS	SIGMA
MADGAR	1122	-19	1	16.314	47	18	15.185	1349.6	38.
MADGAS	1123	-19	1	14.392	47	18	11.335	1387.6	5.
ROSRAN	1126	35	11	45.528	277	7	26.240	828.1	3.
ULASKR	1128	64	58	18.964	212	29	12.728	338.8	3.
CARVON	1152	-24	54	11.015	113	42	59.302	2.5	4.

STATION POSITIONS FOR C-BAND

STATION NAME	NUMBER	LATITUDE DEG	MN	SECOND	LONGITUDE DEG	MN	SECOND	HEIGHT METERS	SIGMA
ETRPRE	4050	-25	56	37.592	28	21	28.937	1588.6	12.
ETRMRT	4082	28	25	28.943	279	20	7.649	-30.7	5.
NBER34	4740	32	20	53.337	295	20	46.909	-26.9	4.
NWALI8	4840	37	50	29.160	284	30	53.007	-39.4	4.
NWALI3	4860	37	51	37.279	284	29	25.864	-36.4	4.
NBER05	4760	32	20	52.837	295	20	47.119	-24.9	4.
WOOR38	4946	-30	49	5.877	136	50	17.532	124.3	6.

*Error estimate for Cartesian coordinates.

a_e = 6378155 m

f = 1/298.255

Table 4-16 (continued)

STATION POSITIONS FOR DOPPLER

STATION NAME	STATION NUMBER	LATITUDE DEG	MN	SECOND	LONGITUDE DEG	MN	SECOND	HEIGHT METERS	SIGMA METERS
ANCHOR	2014	61	17	0.168	210	10	29.035	63.9	5.
TAFUNA	2017	-14	19	49.937	189	17	3.046	27.4	5.
THULEG	2018	76	32	19.344	291	13	54.033	51.9	8.
MCMRDO	2019	-77	50	52.257	166	40	25.770	-33.1	8.
WAHIWA	2100	21	31	15.531	202	0	10.436	395.6	4.
LACRES	2103	32	16	44.522	253	14	45.428	1150.7	5.
LASHM2	2106	51	11	9.367	358	58	25.532	217.8	4.
APLMND	2111	39	9	48.588	283	6	11.907	96.0	4.
PRETOR	2115	-25	56	48.272	28	20	52.046	1582.6	5.
ASAMOA	2117	-14	19	50.265	189	17	2.891	39.5	5.
WALDOP	2203	37	51	52.094	284	29	32.286	-38.0	9.
ASCION	2722	- 7	58	9.757	345	35	40.701	88.6	8.
COCOSL	2723	-12	11	44.560	96	50	3.054	-44.3	12.
MOSLAK	2738	47	11	7.247	240	39	43.766	338.3	12.
STNVIL	2745	33	25	32.087	269	5	9.799	-2.5	35.
MESHED	2817	36	14	26.485	59	37	44.239	950.8	5.
FRTLMY	2822	12	7	53.927	15	2	6.787	298.5	6.
NATLDP	2837	- 5	54	57.998	324	49	55.950	3.9	5.

STATION POSITIONS FOR MOTS

STATION NAME	STATION NUMBER	LATITUDE DEG	MN	SECOND	LONGITUDE DEG	MN	SECOND	HEIGHT METERS	SIGMA
1BPOIN	1021	38	25	50.253	282	54	48.699	-38.2	3.
1FTMYR	1022	26	32	53.359	278	8	4.161	-35.9	3.
1OOMER	1024	-31	23	24.970	136	52	15.455	128.6	5.
1QUITO	1025	- 0	37	21.567	281	25	16.401	3571.8	15.
1SATAG	1028	-33	8	58.448	289	19	53.576	709.3	5.
1MOJAV	1030	35	19	47.931	243	5	59.055	886.2	3.
1JOBUR	1031	-25	53	0.843	27	42	26.404	1537.2	3.
1NEWFL	1032	47	44	29.838	307	16	46.121	64.2	7.
1GFORK	1034	48	1	21.344	262	59	19.513	216.4	3.
1WNKFL	1035	51	26	46.148	359	18	8.330	97.3	5.
1ULASK	1036	64	58	37.046	212	28	31.715	284.1	7.
1ROSMN	1037	35	12	7.388	277	7	41.321	864.1	3.
1ORORL	1038	-35	37	32.106	148	57	14.825	943.5	4.
1ROSMA	1042	35	12	7.408	277	7	41.021	864.1	3.
1TANAN	1043	-19	0	31.860	47	17	59.360	1362.2	6.
1UNDAK	7034	48	1	21.344	262	59	19.513	215.4	3.
1EDINB	7036	26	22	46.743	261	40	7.459	20.9	3.
1COLBA	7037	38	53	36.207	267	47	40.940	227.4	3.
1BERMD	7039	32	21	49.826	295	20	35.069	-14.9	4.
1PURIO	7040	18	15	28.817	294	0	23.584	-10.4	3.
1GFSCP	7043	39	1	15.716	283	10	20.528	10.1	3.
1DENVR	7045	39	38	48.056	255	23	38.640	1757.8	3.
1JUM24	7071	27	1	14.010	279	53	12.657	-26.9	3.
1JUM40	7072	27	1	14.388	279	53	12.844	-26.1	3.
1JUPC1	7073	27	1	14.372	279	53	13.060	-26.6	3.
1JUBC4	7074	27	1	14.570	279	53	13.107	-25.9	3.
1SUDBR	7075	46	27	21.306	279	3	10.514	235.5	5.
1JAMAC	7076	18	4	34.700	283	11	27.038	417.9	5.
1GFSCN	7077	38	59	57.438	283	9	37.906	7.1	3.
WALMOT	7078	37	51	47.543	284	29	27.717	-39.6	5.

Table 4-16 (continued)

STATION POSITIONS FOR BC-4

STATION NAME	NUMBER	LATITUDE DEG	MN	SECOND	LONGITUDE DEG	MN	SECOND	HEIGHT METERS	SIGMA METERS
BELTSV	6002	39	1	39.706	283	10	27.538	0.1	3.
MOSELK	6003	47	11	6.660	240	39	43.768	331.6	7.
SHEMYA	6004	52	42	48.985	174	07	26.363	38.3	17.
TROMSO	6006	69	39	44.108	18	56	29.299	109.3	12.
TRCERA	6007	38	45	36.426	332	54	25.707	99.9	8.
PARMBO	6008	5	26	53.866	304	47	40.707	-30.2	12.
QUITO	6009	- 0	5	51.408	281	34	47.674	2685.5	13.
MAUIO	6011	20	42	27.235	203	44	38.433	3057.8	4.
WAKEIS	6012	19	17	28.643	166	36	39.443	-15.6	9.
KANOYA	6013	31	23	42.733	130	52	16.579	76.1	13.
CATNIA	6016	37	26	38.374	15	2	45.352	38.6	7.
MASHAD	6015	36	14	25.459	59	37	43.740	947.7	7.
VILDOL	6019	-31	56	35.317	294	53	38.999	625.1	4.
EASTER	6020	-27	10	36.330	250	34	22.636	199.6	17.
TUTILA	6022	-14	19	54.394	189	17	8.692	15.5	8.
THRUSD	6023	-10	35	3.276	142	12	39.420	107.9	8.
INVERC	6031	-46	24	58.309	168	19	31.502	-11.5	7.
CAVERS	6032	-31	50	25.036	115	58	31.671	-18.1	6.
SOCORO	6038	18	43	58.568	249	2	41.347	-23.0	8.
PITCRN	6039	-25	4	6.765	229	53	12.572	295.2	19.
COCOSI	6040	-12	11	43.990	96	50	2.460	-47.8	8.
ADISBA	6042	8	46	12.504	38	59	52.089	1865.2	5.
CERROS	6043	-52	46	52.600	290	46	34.090	78.3	8.
HEARDI	6044	-53	1	9.425	73	23	34.212	34.8	12.
MAURIT	6045	-20	13	52.901	57	25	31.944	133.1	8.
ZAMBGA	6047	6	55	20.395	122	4	8.907	59.3	11.
PALMER	6050	-64	46	26.371	295	56	53.697	23.1	12.
MAWSON	6051	-67	36	4.268	62	52	22.242	28.8	8.
WILKES	6052	-66	16	44.937	110	32	7.169	-5.5	8.
MCMRDO	6053	-77	50	41.846	166	38	31.279	-56.0	8.
ASCENS	6055	- 7	58	15.213	345	35	34.770	70.1	7.
XMASIL	6059	2	0	18.617	202	35	16.306	2.3	8.
CULGOA	6060	-30	18	34.411	149	33	40.993	226.2	5.
SGAISL	6061	-54	17	0.709	323	30	21.877	2.0	9.
DAKAR	6063	14	44	42.292	342	31	0.697	44.3	7.
FORTLY	6064	12	7	54.697	15	2	7.246	296.4	5.
HOHNBG	6065	47	48	3.758	11	1	25.916	970.1	9.
NATALB	6067	- 5	55	38.935	324	50	4.707	13.2	8.
JOBURG	6068	-25	52	58.963	27	42	23.644	1539.2	3.
TRSUNA	6069	-37	3	53.227	347	41	5.670	25.3	15.
CHIMAI	6072	18	46	10.593	98	58	2.372	245.9	11.
DGOGRA	6073	- 7	21	6.513	72	28	20.592	-77.9	9.
MAHE	6075	- 4	40	14.620	55	28	47.950	534.4	9.
PRTVLA	6078	-17	41	31.834	168	18	24.472	54.4	28.
WRIGHT	6111	34	22	54.548	242	19	5.990	2247.7	5.
PRBARW	6123	71	18	48.393	203	21	8.504	-34.0	18.
WRIGHT	6134	34	22	44.455	242	19	5.765	2161.8	5.

STATION POSITIONS FOR LASER

STATION NAME	NUMBER	LATITUDE DEG	MN	SECOND	LONGITUDE DEG	MN	SECOND	HEIGHT METERS	SIGMA
GODLAS	7050	39	1	14.387	283	10	18.638	11.1	3.
WALLAS	7052	37	51	36.199	284	29	23.965	-42.4	3.
CRMLAS	7054	-24	54	15.965	113	42	58.252	-3.5	4.

adjacent to the baselines (Table 4-15). Since the baselines are considered accurate to at least 1 ppm, this solution (GEM 6, with baselines) was retained as being better for the eight stations 6003, 6004, 6006, 6007, 6008, 6063, 6065, and 6111.

From the above considerations the overall scale for the GEM 6 stations including the BC-4 geometric network is essentially derived through the dynamic system. This means that scale is determined by the reference value of GM (398601.3 km^3/sec^2) employed in the satellite dynamics. Here, an adjustment (s) in scale for coordinates is related to GM as follows:

$$s = \frac{\Delta r}{r} = \frac{\Delta GM}{3GM} ,$$

where r is the radial distance to the station. A current value of GM = 398600.8 km^3/sec^2 (±0.4) has been obtained from analysis of Mariner 9 tracking data by Esposito and Wong (1972). Allowing for the new value of GM and its uncertainty, the scale would be reduced by 0.4 ppm (±0.3). Hence, the above reduction in scale of 2 ppm ($\Delta r = -13$ m), inferred by the 8 baselines from the geometric only solution, is not consistent with that inferred by recent estimates of GM.

4.2.1 Comparison with Other Solutions—Other solutions for station coordinates are compared with GEM 6 to assess the random and systematic differences between solutions. Coordinates of JPL's Deep Space Stations provide an independent source of comparison with GEM 6.

JPL's DSS solution (Mottinger, 1969) does not yield a station's complete position. The better determined parameters are distances from the spin-axis and differences between the longitudes of the stations. In order to compare GEM 6 with JPL's solution, only the x, y coordinates were used (Table 4-17). GEM 6's coordinates for the DSS sites were obtained by using the local datum connections between the camera stations and the DSS stations. In Table 4-18 direct comparisons are given with spin-axis distance (D) and longitude (λ). JPL employs a different reference for longitude than GEM 6 which accounts for the large offset of $\Delta\bar{\lambda} = 0.51''$. Removing this effect in longitude and an effect for scale on spin axis distance, the resulting residuals (reflecting random errors) agree very well as shown in Table 4-18. The scale difference of 1.4 ppm is not explained. However, removal of just one station (Woomera) from this small sample would reduce the scale to 0.9 ppm. The 3 m rms (Table 4-17) is within the estimate of random error given for both GEM 6 and the JPL DSS solutions.

In Tables 4-19 through 4-23, GEM 6 is compared with five other solutions. The five solutions are (1) GEM 4, (2) GSFC 73 (Marsh et al., 1973), (3) SAO SE III (Gaposchkin 1973), (4) NWL 9D (Anderle 1973), and (5) the Ohio State University

Table 4-17

Comparisons with JPL's DSS (Deep Space Stations)
Based Upon a Four Parameter Solution (GEM 6 - JPL)

Scale = 1.42×10^{-6} $\quad \Delta\lambda = -.50$ seconds

$\bar{\Delta}x = -3.2$ m $\quad \bar{\Delta}y = -0.8$ m

Site	Differences	
	Δx(m)	Δy(m)
Goldstone, Cal.	+1.4	+6.9
Woomera, Aus.	-3.3	+1.1
Tidbinbilla, Aus.	+1.6	-3.0
Johannesburg, RSA	+1.6	-2.3
Madrid, Spain	-0.0	-2.1
	rms(m):3.0	

Table 4-18

Direct Comparisons of Spin-Axis Distance (D) and Longitude (λ)
(GEM 6 - JPL)

Site	ΔD (m)	$\Delta D/D$ ($\times 10^{6}$)	$\Delta\lambda$ (sec)	$\Delta D - \Delta\bar{D}$ (m)	$\Delta\lambda - \Delta\bar{\lambda}$ (sec)
Goldstone, Cal.	2.8	0.5	-.67	-5.1	-.19
Woomera, Aus.	12.7	2.2	-.35	4.8	.16
Tidbinbilla, Aus.	6.7	1.3	-.34	-1.2	+.17
Johannesburg, RSA	5.4	0.9	-.57	-2.2	-.06
Madrid, Spain	4.4	0.9	-.63	-3.5	-.12
Average	7.9	1.2	-.51		

WN 4 (Mueller 1973). Systematic differences between the solutions were estimated using station positions common to both solutions by solving for a translation in space to make the origins coincide, three rotations about coordinate axes to orient the coordinate systems, and a scale difference. The systematic quantities are indicated in the tables together with the rms of the random differences after removal of the seven systematic parameters. The 7 parameter adjustment and related symbols are defined in Section 4.2.3, equation (4.4).

The comparison with GEM 4 shown in Table 4-19 was carried out by solving for seven parameters using 62 common stations of GEM 6 and GEM 4. Three additional seven-parameter solutions were made using subsets of the 62 stations common to the solutions, namely (1) 23 MOTS-SPEOPTS camera stations, (2) 13 Doppler stations, and (3) 19 Baker-Nunn cameras. The comparison indicates the coordinate system of GEM 6 and GEM 4 are referred to the same center of mass for all practical purposes, and that negligible differences of scale and rotation are involved. Hence, the coordinate systems of GEM 6 and GEM 4 are nearly identical, verifying that the addition of BC-4 geometric data has not significantly changed results from the dynamic system (GEM 4).

Table 4-20 presents results from seven-parameter solutions comparing GEM 6 with GSFC 73. This result using 43 stations shows that a significant difference occurs in rotation (ω) about the z-axis of 0.35" arc sec. The translation of origin, scale difference, and other rotation parameters are negligible. Although GSFC 73 is a solution based upon two day orbital arcs using optical data on two satellites only, the above discrepancy in the longitude origin is not expected.

Differences in orientation among the models are discussed in Section 4.2.4, where polar and longitude displacements are plotted in Figure 4-7. Models are seen to vary from one another in longitudinal reference by as much as one second of arc.

Although good agreement exists in orientation between GEM 6 and OSU WN4, Table 4-23, large scale (1.9 ppm) and translation (20 m) differences are seen in this comparison of BC-4 camera stations. The large systematic differences can be explained since WN-4 is a geometric only solution, which employs an arbitrary origin and derives scale from the eight baselines in Table 4-15. These large differences do not exist in the BC-4 station comparison in Table 4-22 between GEM 6 and NWL 9D, a solution whose results are derived dynamically from satellite doppler data. (The BC-4 station coordinates for NWL 9D were inferred from adjacent doppler stations through use of survey ties.)

Since SE III and GEM 6 employ similar data, the comparisons in Table 4-21 between these solutions should be closer. But the large systematic difference of 15 m in the z-coordinate of the Baker-Nunn stations between GEM 6 and SE III

Table 4-19

Station Comparisons of GEM 6 with GEM 4

	62 Stations	23 MOTS-SPEOPTS Camera Stations	19 BN Camera Stations	13 Doppler Stations
Δx (m)	.54±1.4	-.58±2.7	.30±2.4	.85±3.1
Δy (m)	-.44±1.4	-.13±2.7	.03±2.4	-.50±3.3
Δz (m)	.22±1.4	-.56±2.8	3.8±2.4	-1.5±3.1
s ($\times 10^6$)	-.02± .22	-.01± .42	.07± .37	-.01± .48
ϵ (sec)	.00± .05	.02± .10	.02± .09	-.10± .14
ψ (sec)	-.02± .05	-.08± .13	.02± .10	-.07± .11
ω (sec)	.04± .05	+.04± .12	.00± .86	+.06± .12
rms (m)	±3.3	±2.8	±.12	±3.7

Table 4-20

GEM 6 - GSFC 73 Station Coordinates

	43 Stations
Δx (m)	$0.5 \pm .7$
Δy (m)	$0.6 \pm .6$
Δz (m)	$2.1 \pm .7$
s ($x10^6$)	$.44 \pm .1$
ϵ (sec)	$.00 \pm .03$
ψ (sec)	$.04 \pm .03$
ω (sec)	$.35 \pm .03$
rms (m)	± 4.6

Table 4-21

Station Comparisons of GEM 6 - SAO Standard Earth III

	68 Stations	17 BN Stations	47 BC-4 Stations
Δx (m)	$+4.2 \pm 1.22$	1.9 ± 2.4	$+4.8 \pm 1.46$
Δy (m)	-5.3 ± 1.22	-3.5 ± 2.4	-6.2 ± 1.46
Δz (m)	$+9.5 \pm 1.22$	15.0 ± 2.4	$+7.4 \pm 1.46$
s ($x\ 10^6$)	$.49 \pm .05$	$.84 \pm .38$	$+.23 \pm .05$
ϵ (sec)	$+.19 \pm .05$	$-.01 \pm .09$	$+.23 \pm .05$
ψ (sec)	$-.08 \pm .05$	$-.10 \pm .11$	$-.09 \pm .06$
ω (sec)	$-.46 \pm .05$	$-.51 \pm .09$	$-.47 \pm .06$
rms (m)	± 10	± 8	± 10

does not exist in the comparisons with GEM 4 or GSFC 73. To agree with the overall scale difference (s = 0.49 ppm) for SE III, radial positions of GEM 6 should be adjusted downward by about 3 m, whereas to agree with NWL 9D the scale adjustment should be made upward by about 2.5 m. Hence scale agrees reasonably between GEM 6 and these solutions, all of which employ satellite dynamics and use a similar value for GM.

Although systematic differences in station coordinates may be removed between solutions through the 7 parameter adjustment, the resulting residuals are not always random. Such an effect is seen in the comparison between GEM 6 and WN4. The rms of the position differences is ±10 m after systematic differences are removed. Examination of residuals reveals a systematic trend between GEM 6 and the OSU WN4 solution in a series of stations in Europe, Africa and the South Atlantic. These stations are in the vicinity of the Greenwich meridian and tied closely to the baselines in Europe and North Africa (Figure 2-2). Table 4-24 compares Δy residuals from the seven parameter solutions for 9 BC-4 stations in this region. In the area of these comparisons Δy is nearly equivalent to longitude. Other Δy differences shown in Table 4-24 are from GEM 6-SAO Standard Earth III, and the GEM 6-BC 4 stations tied to NWL 9D by ground ties. This comparison indicates that a significant geometric problem exists for the chain of stations connected to the European and African baselines.

4.2.2 Comparison with Mean Sea Level Heights—Heights of stations above the geoid as determined from GEM 6 are compared in Figure 4-6 with heights above mean sea level determined by survey. The following difference is plotted for each of 134 tracking stations:

$$\Delta H = (h-N) - MSLH \text{ (meters)}$$

where

h is station's height above the ellipsoid used in GEM 6 based upon a reference a_e = 6378155 m, and 1/f = 298.255

N is the geoidal height derived from GEM 6

MSLH is the height above mean sea level from survey.

The differences ΔH are shown in Figure 4-6 by a symbol signifying the tracking system providing the data. A key for the symbol is given with the figure. The residuals are analyzed to derive a mean value of a_e for the ellipsoid and to estimate any systematic offset in center of mass.

Table 4-22

Station Comparisons of GEM 6-NWL 9D

	12 Doppler Stations	20 BC-4 Stations
Δx (m)	-6.2 ± 1.3	4.3 ± 2.3
Δy (m)	3.1 ± 1.5	1.4 ± 2.3
Δz (m)	8.3 ± 1.4	1.9 ± 2.3
s ($\times 10^6$)	$-.30 \pm .21$	$-.41 \pm .35$
ϵ (sec)	$.01 \pm .06$	$.30 \pm .09$
ψ (sec)	$-.03 \pm .06$	$.15 \pm .09$
ω (sec)	$-.59 \pm .06$	$-.65 \pm .09$
rms (m)	± 2.8	± 7.9

Table 4-23

GEM 6-OSU WN4
Station Comparisons

	45 BC-4 Stations
Δx (m)	$+20 \pm 1.5$
Δy (m)	$+12 \pm 1.5$
Δz (m)	-9 ± 1.5
s ($\times 10^6$)	$+1.9 \pm .23$
ϵ (sec)	$-.07 \pm .06$
ψ (sec)	$+.07 \pm .06$
ω (sec)	$+.08 \pm .06$
rms (m)	± 11

Table 4-24

Comparisons of Δy (coordinate differences) for Selected BC-4 Stations

	6006	6065	6007	6016	6063	6064	6055	6067	6069
GEM6-OSU WN4	32	28	26	24	26	12	22	12	20
GEM6-SAO SE III	22	21	8	17	11	8	9	-2	11
GEM6-Doppler BC-4 Ties	23	1	9	4	-2	-3	13	4	

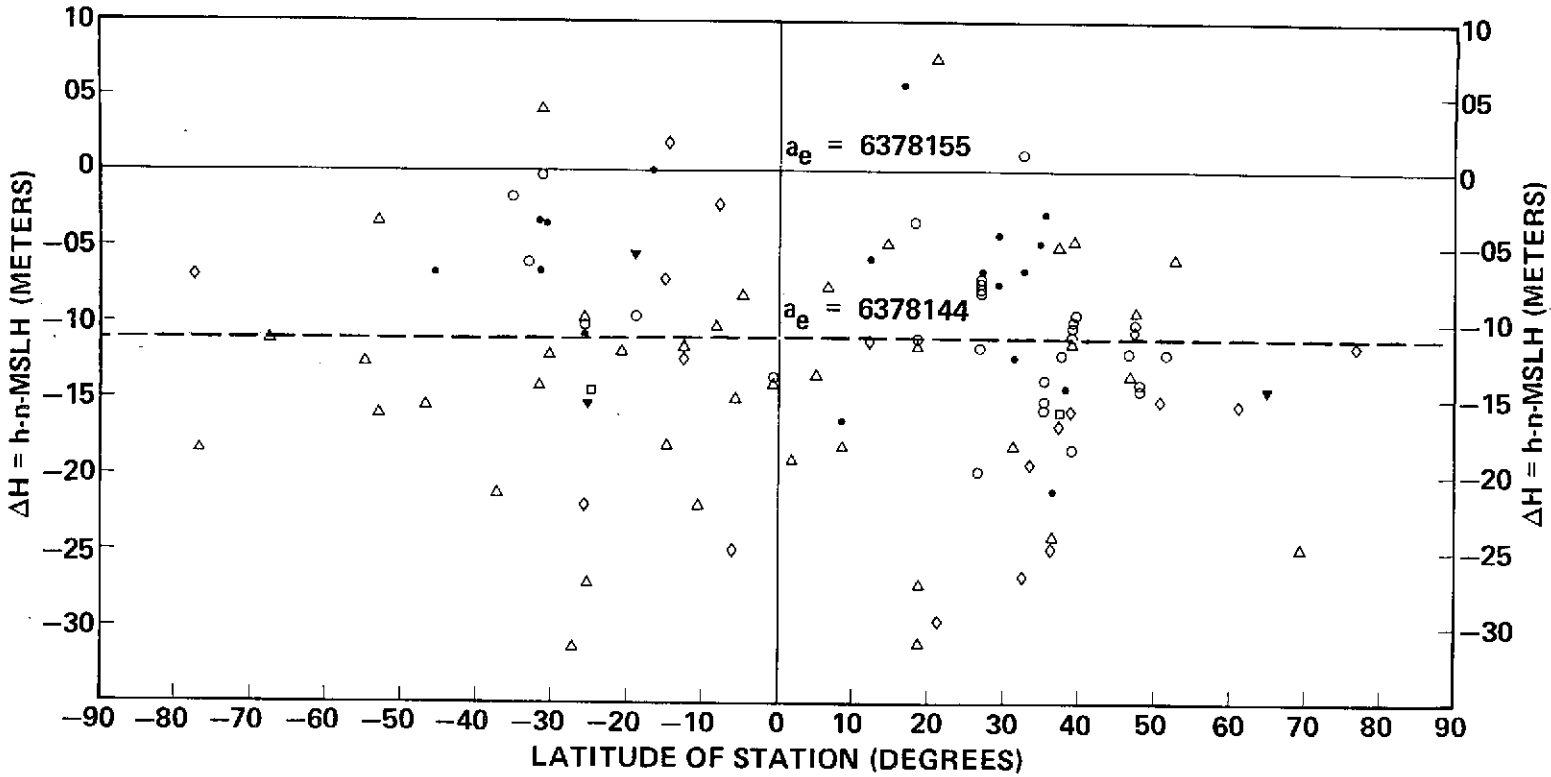

KEY TO STATIONS

- • BAKER-NUNN
- ◊ NWL TRANET DOPPLER
- ▼ GRARR
- □ LASER
- ○ MOTS
- △ BC-4

MSLH = HEIGHT OF STATION ABOVE MEAN SEA LEVEL (SURVEY)
h = ELLIPSOIDAL HEIGHT OF STATION FROM DYNAMIC SOLUTION (a_e = 6378155, 1/f = 298.255)
N = GEOID HEIGHT DYNAMIC SOLUTION GRAVITY FIELD
ΔH = h - N - MSLH

Figure 4-6. Station Height Above Geoid Computed by GEM 6 vs Surveyed Height

Table 4-25 shows solutions which estimate four systematic differences in the coordinate system based upon the comparison of MSL heights. Three of the parameters constitute a translation of the origin and the fourth is a change to the semi-major axis, a_e. Five solutions are presented in the table. Results are given first for 114 stations representing a combination of the various tracking systems used in GEM 6, followed by results from subsets of stations by data type as follows: 29 MOTS-SPEOPTS camera stations, 40 BC-4 camera stations, 19 Baker-Nunn camera (BN) stations, and 18 Doppler stations. The geoidal heights used in the solution were computed from GEM 6 as were the ellipsoidal heights.

The first solution (114 stations) shows a displacement of the origin of nearly 2.3 m and a best fitting equatorial radius a_e of 6378144 m. The next four solutions use subsets of stations to estimate the systematic differences. The derived semi-major axis ranges from 6378141 m to 6378149.3 m or a total excursion of nearly 8 m. The solutions using MOTS-SPEOPTS cameras and the BN cameras give the largest semi-major axes and the BC-4 network resulted in the smallest semi-major axis, with the Doppler station solution occupying a central position. Recall from Table 4-23 that the GEM 6-OSU WN4 gave a scale difference of 1.9 ppm, which when applied results in a derived semi-major axis for OSU WN4 by this method of 6378129 m. This agrees with an independent geometric adjustment which we have made using only the BC-4 camera and baseline data. Apparently the ties made between the BC-4 cameras and other tracking stations (dynamic system) dominated the terrestrial baselines in the solutions for the stations more removed from the baselines. The range of 8 m in determinations of a_e reflect systematic differences between the data from the tracking systems for which the comparisons were made. No significant effect in center of mass displacement (Δx, Δy, Δz) exists in the solution for the 114 stations. Some effect is seen in the subset solutions where the station distribution is not as well defined. These differences in the subset results reflect errors in the geoid computed from GEM 6 and the selection process due to spacing of the stations as well as the error in station height.

4.2.3 Comparison with Positions on National Datums—Stations' coordinates in GEM 6 are compared to coordinates in national or international datums by first computing the datum shifts involved and using these to transform the coordinates. We refer to coordinates in the national or international datums as surveyed coordinates.

Let λ_s φ_s h_s be the geodetic coordinates of a particular station as determined by survey on the ground. These are converted to rectangular coordinates x_s, y_s, z_s using the datum's specifications. x_s, y_s, z_s will be referred to as "surveyed" coordinates. The surveyed coordinates are transformed to the system of GEM 6 by the equation

$$\begin{pmatrix} x'_s \\ y'_s \\ z'_s \end{pmatrix} = \begin{pmatrix} \Delta x + x_o \\ \Delta y + y_o \\ \Delta z + z_o \end{pmatrix} + (1 + s) \begin{pmatrix} 1 & \omega & -\psi \\ -\omega & 1 & \epsilon \\ \psi & -\epsilon & 1 \end{pmatrix} \begin{pmatrix} x_s - x_o \\ y_s - y_o \\ z_s - z_o \end{pmatrix} \quad * \qquad (4.4)$$

where

$\begin{pmatrix} x'_s \\ y'_s \\ z'_s \end{pmatrix}$ are surveyed coordinates transformed to GEM 6's system,

$\begin{pmatrix} x_s \\ y_s \\ z_s \end{pmatrix}$ are surveyed coordinates in the original datum,

$\begin{pmatrix} x_o \\ y_o \\ z_o \end{pmatrix}$ are the coordinates of the adopted datum origin,

s is the scale difference,

ω is the rotation about the z-axis,

ψ is the rotation about the y-axis,

ϵ is the rotation about the x-axis.

Table 4-26 shows the adopted origins λ_o, ϕ_o, h_o, transformed to x_o, y_o, z_o for the calculations outlined above. With the exception of the NAD 1927 the adopted origin for our calculations do not agree with the origins of the 4 datums whose solutions are derived.

By including the coordinates of the datums' origin, the translation parameters (Δx, Δy, Δz) are then exactly equal to the shift of the local datum at the datum origin. Also the correlations between translational and rotational parameters are minimized.

*When used to compare GEM 6 with another geocentric solution the coordinates (x_o, y_o, z_o) are zero and the survey coordinates are replaced by those for the geocentric solution.

Table 4-25

Station Comparisons of GEM 6 - Mean Sea Level Height

	114 Stations	29 MOTS SPEOPTS Cameras	40 BC-4 Stations	19 BN Stations	18 Doppler Stations
Δx (m)	-1.5 ±1.8	-0.9 ±5.8	3.2 ±2.6	-8.9 ±4.0	-6.8 ±4.0
Δy (m)	-1.3 ±1.8	0.5 ±5.1	-1.1 ±2.7	-0.9 ±3.6	0.4 ±5.2
Δz (m)	-1.5 ±1.9	-4.8 ±5.8	0.5 ±3.0	-2.7 ±4.9	-4.8 ±4.9
Δa (m)	-11.3 ±1.0	-8.0 ±3.0	-14.0 ±1.6	-5.7 ±2.5	-11.7 ±2.7
rms (m)	±7.7	±4.3	±8.3	±4.3	±7.5
a_e(m)	6378143.7	6378147.0	6378141.0	6378149.3	6378143.0

Table 4-26

Adopted Origins Used for Solutions of Seven Parameters on the Survey Datum

Datum	λ_o Longitude	ϕ_o Latitude	h_o Height
NAD 1927	261° 27' 29.''494	39° 13' 26.''686	0
SAD 1969	290 0 0	-20 0 0	0
EUROPE	15 0 0	40 0 0	0
AUSTRALIA	124 0 0	-33 0 0	0

Table 4-27 presents solutions for seven parameters of four major datums using the coordinates of cameras and giving the rms of the differences with station coordinates. In each solution, individual stations are weighted equally. The average rms error for each datum is 4.5 meters. Coordinate differences for each station are shown in the table for the associated datum.

A special comment is needed for the European Datum (ED 50) solution. The solution is presented using only 5 stations for its determination. A number of other stations connected to the ED 50 were rejected because they did not fit with any reasonable hypothesis concerning the accuracy of the triangulation on ED 50.

4.2.4 Displacements in Mean Pole and Greenwich Meridian—In Figure 4-7 relative displacements of the Greenwich Meridian (the angle ω converted to meters) and the mean pole (the angles ϵ and ψ converted to meters at the pole) are plotted with GEM 6 referenced at the origin. The comparisons are made two ways, first by differencing the solutions with GEM 6 for stations derived from dynamic data and second, by differencing solutions for BC-4 stations with the GEM 6 BC-4 results. The NWL 9D solution is compared both ways, one by differencing twelve doppler stations directly with GEM 6 doppler stations and secondly, by converting the NWL 9D solution to coordinates of 30 BC-4 sites through local survey ties and differencing with GEM 6 BC-4 coordinates. An independent BC-4 geometric only solution, GEM 6I, was also compared with GEM 6 BC-4 results.

The comparisons for the stations derived from dynamic data tend to give more consistent results for the mean pole displacements than the comparisons for the BC-4 stations.

The diagram comparing displacements of the Greenwich Meridian shows close agreement between GEM 4, GEM 6, OSU WN-4 and the GEM 6 independent geometric solution. Two of the other solutions plotted, the JPL and NWL 9D solutions, use different longitude references, since Doppler and distance measurements contain no directional references.

4.2.5 Summary of Results for Station Coordinates—Coordinates of the 134 tracking stations computed in GEM 6 provide datum shifts for establishing a unified world geodetic system for 11 different datums. GEM 6 station position results are presented in Table 4-16 of Section 4.2, with respect to an ellipsoid having a semi-major axis of 6378155 m and a flattening of 1/298.255. Table 4-29 shows the datum translations for transforming 11 local datums to the GEM 6 system, and Table 4-27 gives the translation, scale difference, and 3 rotations to transform 4 major datums to the GEM 6 system.

Radial positions of GEM 6 station coordinates and mean sea level heights from survey indicate a mean radius a_e for the Earth of 6378143.7 meters. Results from this analysis have been presented in Table 4-25 and Figure 4-6 where variations ranging from 6378141.0 meters to 6378149.3 meters can be seen for subsets of the tracking systems. An independent geometric solution of the BC-4 data gives an a_e of 6378129.0 meters based upon DME baselines. However, it was shown that the latter result is inconsistent with recent estimates for GM. Further results in Table 4-25 for the total set of stations show that the center of mass is determined to within 2 meters for the GEM 6 system.

Table 4-27

Solutions for Relation of GEM 6 to Major Datums*

	GEM 6 - NAD	GEM 6 - AUS	GEM 6 - SAD	GEM 6 - ED 1950
No. Stations	33	10	9	5
Δx (m)	-24 $\pm$2.1	-135 $\pm$4.0	-63 $\pm$3.7	-83 $\pm$5.1
Δy (m)	151 $\pm$2.3	-39 $\pm$4.0	0 $\pm$3.6	-116 $\pm$5.1
Δz (m)	187 $\pm$2.1	133 $\pm$3.9	-32 $\pm$3.5	-120 $\pm$5.7
s ($\times 10^6$)	1.7$\pm$1.2	2.4$\pm$2.2	-1.3$\pm$1.2	-.3$\pm$1.6
ϵ (sec)	-.2$\pm$ .5	-1.0$\pm$ .7	.6$\pm$ .3	.6$\pm$ .6
ψ (sec)	.1$\pm$ .3	-1.2$\pm$ .6	-.2$\pm$ .3	.4$\pm$1.0
ω (sec)	-.8$\pm$ .3	.4$\pm$ .5	-.0$\pm$ .4	-.6$\pm$ .4
rms (m)	$\pm$4.0	$\pm$4.9	$\pm$6.0	$\pm$2.6

*The signs of Δx, Δy, Δz should be reversed to find the displacement of the coordinate origin.

Table 4-28

Differences Between Coordinates of Stations in GEM 6 Datum and Other Major Datums

NAD 1927 - GEM 6

Station	Meters		
	Δx	Δy	Δz
1021	4	0	-5
1022	-1	-2	3
1030	1	-4	3
1034	-2	1	3
1037	-1	0	7
1042	-1	0	7
1126	-1	0	7
2203	0	7	-5
4082	0	5	7
4840	6	-4	-5
4860	6	-4	-5
6002	2	-2	-7
6111	-2	2	-4
6134	-2	2	-4
7034	-2	1	3
7036	2	0	1
7037	0	1	5
7043	2	-2	-7
7045	-3	-5	2
7050	2	-2	-7
7052	6	-4	-5
7071	-1	5	5
7072	-1	5	6
7073	-0	5	5
7074	-1	5	5
7075	-2	-2	-1
7077	2	-2	-7
7078	2	-2	-7
9001	-8	2	-2
9010	-1	5	5
9021	-5	-5	-4
9049	-1	5	6
9425	-1	2	4
		rms 4.0	

Table 4-28 (continued)

SAD 1969 - GEM 6

Station	Meters		
	Δx	Δy	Δz
1025	-8	-8	-3
1028	13	-9	-4
2837	17	4	-5
6008	0	3	-1
6009	-7	-8	-3
6019	-3	3	8
6067	6	4	-2
9009	-9	8	-10
9011	-3	3	8
9031	-7	0	12
		rms 7.3	

AUS 1965 - GEM 6

Station	Meters		
	Δx	Δy	Δz
1024	3	-7	-3
1038	-3	0	-5
1152	-6	-1	4
4946	4	-7	-3
6023	3	5	9
6032	0	4	-3
6060	-7	10	6
7054	-6	-1	4
9003	6	-2	-5
9023	6	-2	-5
		rms 4.9	

ED 1950 - GEM 6

Station	Meters		
	Δx	Δy	Δz
1035	-6	-4	-8
6015	10	2	11
9004	6	1	10
9008	-8	-1	-9
9091	-1	1	-5
		rms 2.6	

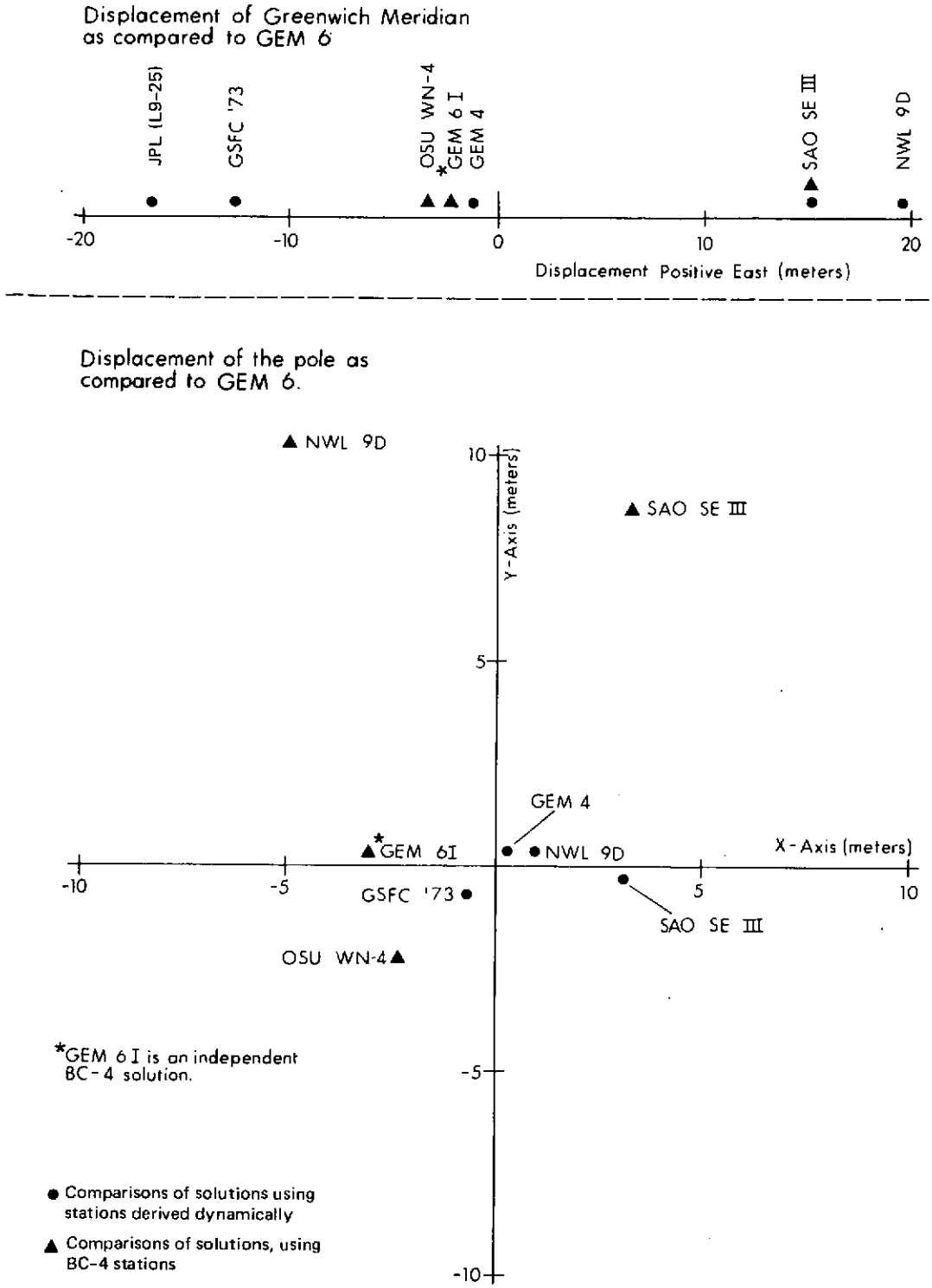

Figure 4-7. Displacement of the Greenwich Meridian and Pole as Shown Through Comparisons with GEM 6

Table 4-29

Datum Shifts to GEM 6 System*

Datum	No. of Sites	Meters		
		Δx	Δy	Δz
NAD 1927	33	-22	155	187
SAD 1969	10	-66	3	-33
EUROPE 1950	4	-81	-115	-122
AUSTRALIA 1965	10	-130	-41	134
ADIND	5	-147	-3	211
OLD HAWAIIAN	4	61	-284	-182
ARC	5	-126	-110	-296
TOKYO	3	-147	509	686
SAMOA	1	-114	124	426
MADAGASCAR	2	-172	-237	-119
JOHNSTON IS.	1	177	-80	-209

*The signs of Δx, Δy, Δz should be reversed to find the displacement of the coordinate origin.

Systematic differences of coordinates in dynamical solutions such as GEM 6, GSFC 73, the NWL 9D solution, and classical geodetic triangulation may be removed by estimating seven parameters. Three parameters are translations, three are rotations and one is a scale change. After removing systematic differences, coordinates of major tracking systems in GEM 6 such as MOTS-SPEOPTS cameras, Baker-Nunn cameras and laser DME stations agree with the GSFC 73 solution and with classical geodetic triangulations so well that these coordinates are believed to be known with an rms accuracy of about 5 m in each coordinate. Coordinates of Doppler stations are known in the GEM 6 system to an rms of about 7 m and BC-4 cameras are known to an rms of about 9 m in each coordinate.

Coordinates of BC-4 cameras derived through geometric theory by different investigators give relatively large dispersions in the magnitudes of the seven parameters used to estimate systematic differences in the solutions, compared with corresponding results from dynamic solutions. In addition relatively large dispersion exists after systematic differences are removed. The BC-4 camera network has relatively fewer observations per station on the average compared with stations in dynamical solutions. Stations derived through dynamical processing of observations are connected through orbital constraints with many other stations, providing a stronger set of global connections for stations than the simultaneous observations in the BC-4 network.

4.3 Geodetic Parameters

The reference values of the earth's ellipsoid and normal gravity are listed along with the corresponding adjusted values based upon the GEM solution as follows:

	Reference Value	Adjusted Value
a_e (equatorial radius)	6378155 m	6378144 m
f (flattening)	1/298.255	1/298.257
g_e (equatorial gravity)	978029.1 mgal	978032.1 mgal

The adjusted value for g_e was derived from the surface gravity data. The adjusted value of a_e was derived in Section 4.2.2 from analysis of the GEM 6 station coordinates and MSL heights of stations. Another estimate of a_e may be derived from the reference value of GM = 398601.3 km^3/sec^2 and the adjusted value of g_e (Lerch et al., 1972). This value for a_e is 6378142 m and it is well within the range of values of a_e associated with the results from subsets of stations as given in Table 4-25. Since scale for the station positions is enforced through GM, both estimates of a_e are referenced to the above value of GM.

The adjusted value for flattening is based principally on the leading oblateness coefficient $\bar{C}_{20}$, and the maximum effect of the adjustment (Δf) on ellipsoidal position is less than 0.2 m. Hence flattening f essentially remains the same.

SECTION V. . . . . SUMMARY AND CONCLUSIONS

5. SUMMARY AND CONCLUSIONS

The Goddard Earth Model (GEM 6) has been developed to satisfy requirements in the National Geodetic Satellite Program (NGSP) and to serve as a preliminary model for investigations in the Earth and Ocean Physics Applications Program (EOPAP). GEM 6 was derived from a comprehensive set of satellite tracking and surface gravity data. Its solution consists of a gravitational potential in spherical harmonics and a worldwide system of 134 tracking station locations. Harmonic terms of the potential are complete for coefficients through degree and order 16 and include some selected zonal and satellite resonant terms to degree 22. Terms through degree 16 represent broad features of the gravity field and provide resolution in wavelengths down to 2600 km on the geoid. These broad features are estimated to have a worldwide average accuracy of 4.5 mgal in gravity anomaly and 3 m in geoid height.

Tracking station coordinates in the model are referenced to a center of mass system, which is determined to better than 2 m. Transformations to this common reference system are given for 11 local datums throughout the world, thus providing for a unified geodetic system of stations. Coordinates in GEM 6 are estimated to have an average accuracy of 6.5 m, excluding possible rotation, translation, and scale errors. Of these only a scale error would affect the relative position of stations. Scale for the stations depends upon the value of GM employed. Current estimates of GM are consistent with a contraction of the GEM 6 earth of only about 3 m. Such an effect does not significantly increase the above error estimate for station coordinates. These accuracy figures specified for the stations and the geoid serve to meet the goals of the national program (NGSP).

In addition to the potential coefficients and station coordinates of GEM 6, certain basic parameters associated with the mean earth ellipsoid were derived. These are: a_e = 6378144 m for the semimajor axis, flattening f = 1/298.257, and g_e = 978032 mgal for equatorial gravity. The value of a_e was derived from analysis of radial coordinates of the tracking stations and their mean sea level heights from survey. The value of flattening is essentially unchanged from the initial reference value and the value of g_e was derived from the gravimetry data.

Along with GEM 6, a separate model of the gravitational potential (GEM 5) was derived based upon only the data processed dynamically among 27 satellites. Harmonics in GEM 5 are complete to degree and order 12, and include the selected zonal and satellite resonant terms to degree 22. Satellite data of GEM 5 formed the major contribution to the potential of GEM 6, controlling almost entirely the long wavelength terms of low degree and accounting for about 30% of the adjustment on the average for terms of degree 12 in GEM 6. The average

accuracy for the GEM 5 coefficients are shown to vary from better than 75% through degree 8 to 40% at degree 12. The accuracy of the high degree terms of GEM 6 is improved over GEM 5.

Error estimates for the GEM 6 coefficients show that the zonals are the best determined. Comparisons of zonal coefficients and their long-term perturbations on different satellite orbits verify the high accuracy of these terms in the GEM solutions.

The error of 3 m for geoid height given above for GEM 6 corresponds to the long wavelength terms for the coefficients through degree 16. The zonal contribution is less than 1/3 meter. Considering coefficients beyond degree 16 a total (rms) error in geoid heights is estimated as 5 m. A single global track of SKYLAB altimetry has shown a 7.3 m deviation (rms) from the GEM 6 geoid. Therefore, considerable improvement remains to be made to reduce the total error in the geoid to 1/2 meter for application in the EOPAP program.

REFERENCES

REFERENCES

1. Anderle, R. J., "Geodetic Parameter Set NWL-5-E-6 Based on Doppler Satellite Observations," NWL Report 1978, 1965.

2. Anderle, R. J., "Transformation of Terrestrial Survey Data to Doppler Satellite Datum," presented at the IAG Symposium on Computational Methods in Geometrical Geodesy, Oxford, England, September 1973.

3. Bjerhammar, A., "On a Coalescent World Geodetic System," Research Institute for Geodetic Sciences (GIMRADA), 1967.

4. Bomford, G., Geodesy, Oxford University Press, 1971.

5. Cazenave, A., F. Forestier, F. Novel, and J. Pieplu, "Improvement of Zonal Harmonics Using Observations of Low Inclination Satellites, DIAL SAS, and PEOLE," paper presented at AGH Meeting, Wash. D.C., April 1971.

6. Esposito, P. B., and S. K. Wong, "Geocentric Gravitational Constant Determined from Mariner 9 Radio Tracking Data," paper presented at the International Symposium on Earth Gravity Models and Related Problems, St. Louis, Missouri, 1972.

7. Gaposchkin, E. and K. Lambeck, "1969 Smithsonian Standard Earth (II)," SAO Special Report 315, 1970.

8. Gaposchkin, E. M., "Smithsonian Institution Standard Earth III," presented at American Geophysical Union Meeting, Washington, D.C., April 1973.

9. Guier, W. H., "Determination of the Nonzonal Harmonic of the Geopotential from Satellite Doppler Data," NATURE 200, 124-125, Oct. 12, 1963.

10. Hajela, D. P., "The Computation of 15° and 10° Equal Area Block Terrestrial Free Air Gravity Anomalies," Dept. of Geodetic Science, Report No. 178, Ohio State University, June 1972.

11. Heiskanen, W., and H. Moritz, Physical Geodesy, W. H. Freeman and Company, 1967.

12. Izsak, I. G., "Tesseral Harmonics in the Geopotential," NATURE 199, 137-139, July 13, 1963.

13. Kaula, W. M., "Improved Geodetic Results from Camera Observations of Satellites," J. Geophys. Res. 68, 5183-5189, Sept. 15, 1963.

14. Kaula, W. M., "Tests and Combinations of Satellite Determinations of the Gravity Field," J. Geophys. Res. 71, 5303-5314, 1966a.

15. Kaula, W. M., Theory of Satellite Geodesy, Blaisdell Press, Waltham, Mass., 1966b.

16. Kaula, W. M., (Chairman), "The Terrestrial Environment Solid Earth and Ocean Physics Applications of Space and Astronomic Techniques." Report of a Study at Williamstown, Mass. to the National Aeronautics and Space Administration, NASA CR-1579, August 1969.

17. Kohnlein, W., "The Earth's Gravitational Field as Derived from a Combination of Satellite Data with Gravity Anomalies," In: Smithsonian Astrophysical Observatory Special Report 264, 57-72, 1967.

18. Kozai, Y., "Revised Zonal Harmonics in the Geopotential," SAO Special Report 295, 1969.

19. Lerch, F., J. Marsh, and B. O'Neill, "Gravity Model Comparisons Using GEOS-1 Long Arc Orbital Solutions," GSFC X-552-68-71, December 1967.

20. Lerch, F., and W. Kahn, "Geodetic Parameter and Station Recovery (GEOSTAR) Plan," Goddard Space Flight Center, Greenbelt, Md., 1968.

21. Lerch, F. J., C. A. Wagner, B. H. Putney, and K. G. Nickerson, "Preliminary Goddard Geopotential Using Optical Tracking Data and a Comparison with SAO Models," GSFC X-552-71-143, October 1971.

22. Lerch, F., C. Wagner, D. Smith, M. Sandson, J. Brownd, and J. Richardson, "Gravitational Field Models for the Earth (GEM 1 and 2)," NASA TMX 65970, NTIS, Springfield, Va., May 1972a.

23. Lerch, F., C. Wagner, B. Putney, M. Sandson, J. Brownd, J. Richardson, and W. Taylor, "Gravitational Field Models GEM 3 and 4," NASA TMX 66207, NTIS, Springfield, Va., November 1972b.

24. Lerch, F. J., "Geometrical Geodesy Techniques in Goddard Earth Models," GSFC X-592-73-339, January 1974.

25. Lundquist, C. A., and G. Veis, "Geodetic Parameters for a 1966 Smithsonian Institution Standard Earth," Smithsonian Astrophysical Observatory Special Report 200, 1966.

26. Marsh, J., B. Douglas, and S. Klosko, "A Unified Set of Tracking Station Coordinates Derived from Geodetic Satellite Tracking Data," GSFC X-553-71-370, July 1971.

27. McGoogan, J., C. Leitao, L. Miller, and W. Wells, "Skylab S-193 Altimeter Experiment Performance, Results and Applications," Paper presented at the International Symposium on Applications of Marine Geodesy, Columbus, Ohio, June 1974.

28. Mottinger, N. A., "Status of DSS Location Solutions for Deep Space Probe Missions: Third Generation Orbit Determination Program Solutions for Mariner Mars 1969 Mission," JPL Space Program Summary 37-60, vol. II, November 30, 1969.

29. Mueller, Ivan I., "Free Geometric Adjustment of the OSU/NGSP Global Network (Solution WN-4)," presented at the First International Symposium of the Use of Artificial Satellites for Geodesy and Geodynamics in Athens, Greece, May 1973.

30. Rapp, R. H., "Further Studies in the Combination of Gravimetric and Satellite Data," Department of Geodetic Science Report No. 119, The Ohio State University, December 1968.

31. Rapp, R. H., "The Formation and Analysis of a 5° Equal Area Block Terrestrial Gravity Field," Reports of the Department of Geodetic Science No. 178, The Ohio State University Research Foundation, Columbus, Ohio, June 1972.

32. Rapp, R. H., "Current Estimates of Mean Earth Ellipsoid Parameters," Geophysical Research Letters, Vol. 1, No. 1, AGU, May 1974.

33. Reece, J., and J. Marsh, "Simultaneous Observation Solutions for NASA-MOTS and SPEOPT Station Positions on the North American Datum," GSFC X-592-73-170, June 1973.

34. Schmid, H. H., "Worldwide Satellite Triangulation Results and Analysis," Journal of Geophysical Research, Vol. 79, 5349, December 1974.

35. Smith, D. E., F. J. Lerch, and C. A. Wagner, "A Gravitational Field Model for the Earth," In: Space Research XIII, 11-20, Akademie-Verlag, Berlin, 1973.

36. Strange, W., F. Calabria, H. Rainey, and L. Gunshol, "Requirements for Resonant Satellites for Gravimetric Satellite Geodesy," Report prepared by Geonautics, Inc., for NASA under Contract NASW-1594, January 1968.

37. Veis, G., "The Determination of Absolute Directions in Space with Artificial Satellites," SAO Special Report 133, 1963.

38. Vincent, S., W. Strange, and J. Marsh, "A Detailed Gravimetric Geoid of North America, the North Atlantic, Eurasia, and Australia," NASA TMX 66238, NTIS, Springfield, Va., September 1972.

39. Wagner, C. A., "Earth Zonal Harmonics from Rapid Numerical Analysis of Long Satellite Arcs," NASA TMX 66039, Nat. Technical Information Service, Springfield, Va., 1972.

APPENDICES

APPENDIX A

METHODS EMPLOYED FOR DATA PROCESSING IN GEM 5 AND 6

CONTENTS

Appendix		Page
A1	ORBIT THEORY FOR GEODYN	A1-1
A2	GEOMETRIC METHODS FOR SIMULTANEOUS OBSERVATIONS INCLUDING CONSTRAINTS FROM DATUM SURVEY	A2-1
A3	GRAVIMETRIC METHOD FOR MEAN ANOMALY DATA	A3-1
A4	TECHNIQUES IN COMBINED SOLUTION	A4-1

APPENDIX A1 . . . . . ORBIT THEORY FOR GEODYN

APPENDIX A1

ORBIT THEORY FOR GEODYN

CONTENTS

		Page
A1-1.0	INTRODUCTION	A1-1
A1-2.0	COORDINATE SYSTEMS	A1-2
A1-2.1	Definition	A1-2
A1-2.2	Topocentric	A1-2
A1-2.3	Time Systems	A1-3
A1-2.4	Polar Motion	A1-4
A1-2.5	Coordinate Systems for Motions of the Earth	A1-6
A1-2.6	True of Date Coordinate System	A1-6
A1-2.7	Inertial Coordinate System	A1-6
A1-2.8	Earth-Fixed Coordinate System	A1-7
A1-2.9	Greenwich Hour Angle	A1-7
A1-2.10	Precession and Nutation	A1-7
A1-3.0	MEASUREMENT MODELING AND RELATED DERIVATIVES	A1-9
A1-3.1	Measurements	A1-9
A1-3.2	Variational Partials of the Measurements	A1-12
A1-3.3	Corrections to Measurements	A1-15

Page

A1-4.0 FORCE MODELS AND VARIATIONAL EQUATIONS A1-20

A1-4.1 The Geopotential Field of the Earth A1-22

A1-4.1.1 Solid Earth Tides A1-28

A1-4.2 Luni-Solar-Planetary Ephemeris A1-28

A1-4.3 Third-Body Gravitational Forces A1-29

A1-4.4 Solar Radiation Pressure A1-30

A1-4.5 Atmospheric Drag A1-30

A1-4.5.1 Atmospheric Density A1-32

A1-5.0 ADJUSTMENT PROCEDURES A1-34

A1-5.1 Bayesian Least Squares Method A1-34

A1-5.2 Measurement Bias Separation (Electronic Instruments) A1-35

A1-6.0 NUMERICAL INTEGRATION PROCEDURE A1-37

A1-6.1 Integration for Position and Velocity Components A1-37

A1-6.2 Integration for the Variational Equations A1-38

A1-6.3 Interpolation A1-39

REFERENCES A1-40

APPENDIX A1

ORBIT THEORY FOR GEODYN

A1-1.0 INTRODUCTION

Presented in this area are the procedures and mathematics used in processing satellite tracking observations for orbit determination and geodetic parameter estimation. The methods in the GEODYN (geodynamics) system have been chosen to give accurate results with a reasonable amount of computer time and memory requirements. There has been a continuous upgrading of modeling, satellite data type handling and computer application over the years. This Appendix represents the information as it was being applied at the end of 1972.

For GEM 5 the output of this system is a set of least squares normal equations for adjustments of geodetic parameters of station coordinates and potential coefficients and for the satellite orbital parameters. These normal equations are processed and combined as in A4 of the appendix.

A1-2.0 GEODETIC COORDINATE SYSTEMS

A1-2.1 Definition

The GEODYN program involves the use of several coordinate systems. It is convenient to define the station positions in a spherical coordinate system. This system uses an oblate spheroid or an ellipsoid of revolution as a model for the geometric shape of the earth. The earth is flattened slightly at the poles and bulges a little at the equator; thus, a cross section of the earth through the poles is approximately an ellipse. Rotating an ellipse about its shorter axis forms an oblate spheroid.

An oblate spheroid is uniquely defined by specifying two dimensions, conventionally, the semi-major axis a and the flattening f, where $f = (a-b)/a$, and b is the semi-minor axis.

The coordinates utilized in GEODYN are termed geodetic coordinates and are defined as follows: ϕ is the geodetic latitude, the acute angle between the semi-major axis and a line through the observer perpendicular to the spheroid, λ is the east longitude, the angle measured eastward in the equatorial plane between the Greenwich meridian and the observer's meridian, and h is the spheroid height, the perpendicular height of the observer above the reference spheroid.

Methods exist for the conversion from ϕ, λ, and h to X_e, Y_e, and Z_e, the earth-fixed cartesian coordinates, and for the inverse conversion.

A1-2.2 Topocentric

The observations of a spacecraft are usually referenced to the observer, and therefore an additional set of reference systems is used for this purpose. The origin of these systems, referred to as topocentric coordinate systems, is the observer on the surface of the earth.

Topocentric right ascension and declination are measured in an inertial system whose Z-axis and X-Y plane are parallel to those of the geocentric inertial system defined by the true of date coordinate system. The X-axis in this case also points toward the vernal equinox.

The other major topocentric system is the earth-fixed system determined by the zenith and the observer's horizon plane. This is an orthonormal system defined by $\hat{N}$, $\hat{E}$ and $\hat{Z}$, which are unit vectors which point in the same directions as vectors from the observer pointing north, east and toward the zenith.

Their definitions are:

$$\hat{N} = \begin{bmatrix} -\sin\phi\cos\lambda \\ -\sin\phi\sin\lambda \\ \cos\phi \end{bmatrix}, \hat{E} = \begin{bmatrix} -\sin\lambda \\ \cos\lambda \\ 0 \end{bmatrix}, \hat{Z} = \begin{bmatrix} \cos\phi\cos\lambda \\ \cos\phi\sin\lambda \\ \sin\phi \end{bmatrix},$$

where ϕ is the geodetic latitude and λ is the east longitude of the observer.

This latter system is the one to which such measurements as azimuth and elevation, X and Y angles, and direction cosines are related.

A1-2.3 Time Systems

Three principal time systems are currently in use: ephemeris time, atomic time, and universal time.

Ephemeris time is the independent variable in the equations of motion of the planets and their satellites; this time is the uniform mathematical time. The corrections that must be applied to universal time to obtain ephemeris time are published in the American Ephemeris and Nautical Almanac or alternatively by BIH, the "Bureau International de l'Heure."

Atomic time is a time referred to the oscillations of cesium in a zero gravitational field. In practice A1 time is based on the mean frequency of oscillation of several cesium standards as compared with the frequency of ephemeris time. This is the time system in which the satellite equations of motion are integrated by the program.

Universal time is determined by the rotation of the earth. UT1, the time reference system used in GEODYN to position the earth, is universal time that has been corrected for polar motion. UTC is the time of the transmitting clock of any of the synchronized transmitting time signals. The frequency of a UTC clock is pre-set to a predicted frequency of UT2 time, where UT2 time is universal time corrected for observed polar motion and extrapolated seasonal variation in the speed of the earth's rotation. The program output is given in UTC time.

One needs time system transformations between any combination of the A1, UT1, UT2, or UTC reference systems.

The time transformations between any input time system and any output time system is formed by addition and subtraction of the following set of time differences: UT2-UT1, A1-UT1, A1-UTC.

The following equation is used to calculate (UT2-UT1) for any year:

$$(UT2\text{-}UT1) = +^{s}.022 \sin 2\pi t - ^{s}.012 \cos 2\pi t - ^{s}.006 \sin 4\pi t + ^{s}.007 \cos 4\pi t$$

t = fraction of the tropical year elapsed from the beginning of the Besselian year for which the calculation is made. (1 tropical year = 365.2422 days.)

This difference, (UT2-UT1) is known by the name "seasonal variation." The time difference (A1-UT1) is computed by linear interpolation from a table of values. The spacing for the table is every 10 days, which matches the increment for the "final time of emission" data published by the U.S. Naval Observatory in the bulletin, "Time Signals." The differences for this table are determined by: (A1-UT1) = (A1-UTC) - (UT1-UTC). The values for (UT1-UTC) are obtained from "Circular D", BIH. The differences (A1-UTC) are determined according to the following procedure.

UTC contains discontinuities both in epoch and in frequency because an attempt is made to keep the difference between a UTC clock and a UT2 clock less than $^{s}.1$. When adjustments are made, by international agreement they are made in steps of $^{s}.1$ and only at the beginning of the month, i.e., at $0^{h}.0$ UT of the first day of the month. The general formula which is used to compute (A1-UTC) is $(A1\text{-}UTC) = a_0 + a_1 (t-t_0)$. Both a_0 and a_1 are recovered from tables. The values in the table for a_0 are the values of (A1-UTC) at the time of each particular step adjustment. The values in the table for a_1 are the values for the new rates of change between the two systems after each step adjustment. Values for a_0 and a_1 are published both by the U.S. Naval Observatory and BIH.

A1-2.4 Polar Motion

Consider the point P which is defined by the intersection of the earth's axis of rotation at some time t with the surface of the earth. At some time $t+\Delta t$, the intersection will be at some point P' which is different than P. Thus the axis of rotation appears to be moving relative to a fixed position on the earth; hence the term "motion of the pole."

A rectangular coordinate system has been established with its center at a point F fixed on the surface of the earth with F near the point P around 1900, and measurements have been taken of the rectangular coordinates of the point P during the period 1900.0 - 1906.0. It was observed that the point P moves in roughly circular motion in this coordinate system with two distinct periods, one period of approximately 12 months and one period of 14 months. The mean position of P during this period is defined to be the point P_0, the mean pole of 1900.0 - 1906.0.

The mean is taken over a six year period in order to average out both the 12 month term (6 periods) and the 14 month term (5 periods) simultaneously. The radius of this observed circle varies between 15 and 35 feet.

In addition to the periodic motion of P about P_o, by taking six year means of P in the years after 1900 - 1906, called P_m, there is seen to be secular motion of the mean position of the pole away from its original mean position P_o in the years 1900 - 1906 at the rate of approximately 0".0032/year in the direction of the meridian 60°W, and a libration motion of a period approximately 24 years with a coefficient of about 0".022. The short periodic motions over a period of six years average about 0".2 to 0".3.

This motion of the pole means that the observing stations are moving with respect to the "earth-fixed" coordinate system used in GEODYN. The station positions must be corrected for this effect.

The position of the instantaneous or true pole is computed by linear interpolation in a BIH table of observed values for the true pole relative to the mean pole of 1900 - 1906. The table increment is 10 days. The data in the table is in the form of the coordinates of the true pole relative to the mean pole measured in seconds of arc. This data was obtained from "Circular D" which is published by BIH.

Consider the station vector $\bar{X}$ in a system attached to the earth of the mean pole and the same vector $\bar{Y}$ in the "earth-fixed" system of GEODYN referred to the true pole of date. The transformation between $\bar{Y}$ and $\bar{X}$ consists of a rotation of x about the X_2 axis and a rotation of y about the X_1 axis; that is

$$\bar{Y} = R_1(y)\, R_2(x)\, \bar{X} = \begin{bmatrix} 1 & 0 & 0 \\ 0 & \cos y & \sin y \\ 0 & -\sin y & \cos y \end{bmatrix} \begin{bmatrix} \cos x & 0 & -\sin x \\ 0 & 1 & 0 \\ \sin x & 0 & \cos x \end{bmatrix} \bar{X}$$

Because x and y are small angles, their cosines are set to 1 and their sines equal to their values in radians. Consequently,

$$Y = \begin{bmatrix} 1 & 0 & -x \\ xy & 1 & y \\ x & -y & 1 \end{bmatrix} \bar{X}$$

A1-2.5 Coordinate Systems for Motion of the Earth

The choice of appropriate coordinate systems for the orbit prediction problem is controlled by several factors.

Firstly, in the case of a satellite moving in the earth's gravitational field, the most suitable reference system for orbit computation is a system with its origin at the earth's center of mass, referred to as a geocentric reference system.

Secondly, the satellite equations of motion are integrated in an inertial coordinate system.

Also, the earth is rotating at a rate $\dot{\theta}_g$, which is the time rate of change of the Greenwich hour angle. This angle is the hour angle of the true equinox of date with respect to the Greenwich meridian as measured in the equatorial plane.

Finally, the earth both precesses and nutates, thus changing the directions of both the earth's spin axis and the true equinox of date in inertial space.

A1-2.6 True of Date Coordinate System

At any given time, the spin axis of the Earth (+Z) and the direction of the true equinox of date (+X) may be used to define a right-handed geocentric coordinate system. This system is known as the true of date coordinate system. The other coordinate systems of the program will be defined in terms of this system.

A1-2.7 Inertial Coordinate System

The inertial coordinate system is the true of date coordinate system defined at $0^h.0$ of the reference day for each satellite. This is the system in which the satellite equations of motion are integrated. This is a right-handed, Cartesian, geocentric coordinate system with the X-axis directed toward the true equinox of $0^h.0$ of the reference day and with the Z-axis directed parallel to the earth's spin axis toward north at the same time. The Y-axis is defined so that the coordinate system is orthogonal.

It should be noted that the inertial system differs from the true of date system by the variation in time of the directions of the earth's spin axis and the true equinox of date. This variation is described by the effects of precession and nutation.

A1-2.8 Earth-Fixed Coordinate System

The earth-fixed coordinate system is geocentric, with the Z-axis pointing north parallel to the axis of rotation and with the X-axis parallel to the equatorial plane, pointing toward the Greenwich meridian. The system is orthogonal and right-handed; thus the Y-axis is automatically defined. This system is rotating with respect to the true of date coordinate system. The Z-axis, the spin axis of the earth, is common to both systems. The rotation rate is equal to the earth's angular velocity. Consequently, the hour angle θ_g of the true equinox of date with respect to the Greenwich meridian (measured westward in the equatorial plane) is changing at a rate of $\dot{\theta}_g$ equal to the angular velocity of the earth.

A1-2.9 Greenwich Hour Angle θ_g

The computation of the Greenwich hour angle is quite important because it provides the orientation of the earth relative to the true of data system. This angle is the major variable in relating the earth-fixed system to the inertial reference frame in which the satellite equations of motion are integrated.

The evaluation of θ_g is discussed in detail in the Explanatory Supplement,

$$\theta = \theta_{go} + \Delta t_1 \dot{\theta}_1 + \Delta t_2 \dot{\theta}_2 + \Delta\alpha$$

where Δt_1 is the integer number of days since January 0.0 UT of the reference year, Δt_2 is the fractional UT part of a day for the time of interest, θ_{go} is the Greenwich hour angle on January 0.0 UT of the reference year, $\dot{\theta}_1$ is the mean advance of the Greenwich hour angle per mean solar day, $\dot{\theta}_2$ is the mean daily rate of advance of Greenwich hour angle $(2\pi + \theta_1)$, and $\Delta\alpha$ is the equation of equinoxes (nutation in right ascension).

The initial θ_{go} is obtained from the proper table in the Nautical Almanac of values containing the Greenwich hour angle on January 0.0 for each year.

A1-2.10 Precession and Nutation

The inertial coordinate system of GEODYN, in which the equations of motion are integrated, is defined by the true equator and equinox of date for $0^h.0$ of the reference day. However, the earth-fixed coordinate system is related to the true equator and equinox of date at any given instant. Thus, it is necessary to consider the effects which change the orientation in space of the equatorial plane and the ecliptic plane. These phenomena are the combined gravitational effect of the moon and the sun on the earth's equatorial bulge, and the effect of the gravitational pulls of the various planets on the earth's orbit. The first of these affects the orientation of the equatorial plane; the second affects the orientation

of the ecliptic plane. Both affect the relationship between the inertial and earth fixed reference systems.

The effect of these phenomena is to cause precession and nutation, both for the spin axis of the earth and for the ecliptic pole. This precession and nutation provides the relationship between the inertial system defined by the true equator and equinox of the reference date and the "instantaneous" system defined by the true equator and equinox of date at any given instant.

The luni-solar effects cause the earth's axis of rotation to precess and nutate about the ecliptic pole. This precession will not affect the angle between the equatorial plane and the ecliptic (the "obliquity of the ecliptic") but will affect the position of the equinox in the ecliptic plane. Thus the effect of luni-solar precession is entirely in celestial longitude. The nutation will affect both, consequently we have nutation in longitude and nutation in obliquity.

The effect of the planets on the earth's orbit will cause both secular and periodic deviations. However, the ecliptic is defined to be the mean plane of the earth's orbit. Periodic effects are not considered to be a change in the orientation of the ecliptic; they are considered to be a perturbation of the earth's celestial latitude.

The secular effect of the planets on the ecliptic plane is separated into two parts: planetary precession and a secular change in obliquity. The effect of planetary precession is entirely in right ascension. As is the convention, all of these secular effects are considered under the heading, "precession." The periodic effects are, nutation in longitude, and nutation in obliquity.

A1-3.0 MEASUREMENT MODELING AND RELATED DERIVATIVES

A1-3.1 Measurements

It is necessary to provide the proper interaction between the observations and the needed computed values of the observations.

The observations are geometric in nature. The computed values for the observations are obtained by applying these geometric relationships to the computed values for the relative positions and velocities of the satellite and the observer at the desired time.

In addition to the geometric relationships, GEODYN allows for a timing bias and for a constant bias to be associated with a measurement type from a given station. Adjustment of these biases is optional.

The measurement model is therefore

$$C_{t+\Delta t} = f_t(\bar{r}, \dot{\bar{r}}, \bar{r}_{ob}) + b + \dot{f}_t(\bar{r}, \dot{\bar{r}}, \bar{r}_{ob}) \cdot \Delta t$$

where $C_{t+\Delta t}$, is the computed equivalent of the observation taken at time $t + \Delta t$, $\bar{r}$, is the earth-fixed position vector of the satellite, $\bar{r}_{ob}$, is the earth-fixed position vector of the station, $f_t(\bar{r}, \dot{\bar{r}}, \bar{r}_{ob})$, is the geometric relationship defined by the particular observation type at time t with the shortened notation f_t, b, is a constant bias on the measurement, and Δt, is the timing bias associated with the measurement. The functional dependence of f_t was explicitly stated for the general case. Many of the measurements are functions only of the position vectors and are hence not functions of the satellite velocity vector $\dot{\bar{r}}$.

One requires the partial derivatives of the computed values for the measurements with respect to the parameters being determined. These parameters are: the true of date position and velocity of the satellite epoch, the force model parameters, the earth-fixed station positions, and the measurement biases.

These parameters are implicitly divided into a set $\bar{\alpha}$ which are not concerned with the dynamics of satellite motion, and a set $\bar{\beta}$ which are.

The partial derivatives associated with the parameters $\bar{\alpha}$; i.e., station positions and measurement biases are computed directly at the given observation times. The partial derivatives with respect to the parameters $\bar{\beta}$; i.e., the epoch position and velocity and the force model parameters, must be determined according to a chain rule:

$$\frac{\partial C_{t+\Delta t}}{\partial \bar{\beta}} = \frac{\partial C_{t+\Delta t}}{\partial \bar{x}_t} \frac{\partial \bar{x}_t}{\partial \bar{\beta}} ,$$

where $\bar{x}_t$ is the vector which describes the satellite position and velocity in true of date coordinates. The partial derivatives $\partial C_{t+\Delta t}/\partial \bar{x}_t$ are computed directly at the given observation times, but the partial derivatives $\partial \bar{x}_t/\partial \bar{\beta}$ may not be so obtained. These latter relate the true of date position and velocity of the satellite at the given time to the parameters at epoch through the satellite dynamics. The specific parameters are described in 4.0.

The partial derivatives $\partial \bar{x}_t/\partial \bar{\beta}$ are called the variational partials and are obtained by direct numerical integration of the variational equations. These equations are analogous to the equations of motion.

First consider the partial derivatives of the computed values associated with the parameters in $\bar{\beta}$. We have

$$\frac{\partial C_{t+\Delta t}}{\partial \bar{\beta}} = \frac{\partial f_t}{\partial \bar{x}_t} \frac{\partial \bar{x}_t}{\partial \bar{\beta}} .$$

Note that we have dropped the partial derivative with respect to $\bar{\beta}$ of the differential product $\dot{f}_t \Delta t$. This is because we use first order Taylor series approximation in our error model and hence higher order terms are assumed negligible. This linearization is also completely consistent with the linearization assumptions made in the solution to the estimation equations.

The partial derivatives $\partial f_t/\partial \bar{x}_t$ are computed by transforming the partial derivatives $\partial f_t/\partial \bar{r}$ and $\partial f_t/\partial \dot{\bar{r}}$ from the earth-fixed system to the true of date system.

In summary, the partial derivatives required for computing the $\partial C_{t+\Delta t}/\partial \bar{\beta}$, the partial derivatives of the computed value for a given measurement, are the variational partials and the earth-fixed geometric partial derivatives.

The partial derivatives of the computed values with respect to the station positions are simply related to the partial derivatives with respect to the satellite position at time t:

$$\frac{\partial C_{t+\Delta t}}{\partial \bar{r}_{ob}} = \frac{\partial f_t}{\partial \bar{r}_{ob}} = - \frac{\partial f_t}{\partial \bar{r}}$$

where $\bar{r}$ is the satellite position vector in earth-fixed coordinates. This simple relationship is a direct result of the symmetry in position coordinates.

The partial derivatives with respect to the biases are,

$$\frac{\partial C_{t+\Delta t}}{\partial b} = 1, \quad \frac{\partial C_{t+\Delta t}}{\partial (\Delta t)} = \dot{f}_t$$

Let us consider the calculation of the geometric function f_t and its derivatives. These derivatives have been shown above to be the partial derivatives with respect to satellite position and velocity at time t and the time rate of change of the function f_t.

The basic types of observation are right ascension and declination, range, range-rate, direction cosines, l and m, angles x and y, and azimuth and elevation. The geometric relationship which corresponds to each of these observations follow. It should be noted that in addition to the earth-fixed or inertial coordinate systems, some of these use topocentric coordinate systems.

Range: Consider the station-satellite vector: $\bar{\rho} = \bar{r} - \bar{r}_{ob}$, where $\bar{r}$ is the satellite position vector (x, y, z) in the geocentric earth-fixed system, and $\bar{r}_{ob}$ is the station vector in the same system.

The (slant) range, ρ is then the magnitude of the $\bar{\rho}$ vector, which is one of the measurements.

Range-rate: The time rate of change of this vector $\bar{\rho}$ is $\dot{\bar{\rho}} = \dot{\bar{r}}$, since $\dot{\bar{r}}_{ob} = 0$. Let us consider that $\bar{\rho} = \rho\hat{u}$, where $\hat{u}$ is the unit vector in the direction of $\bar{\rho}$. Thus we have $\dot{\bar{\rho}} = \dot{\rho}\hat{u} + \rho\dot{\hat{u}}$. The quantity $\dot{\rho}$ in the above equations is the value for the range-rate and is determined by $\dot{\rho} = \hat{u} \cdot \dot{\bar{r}}$.

Right ascension and declination: The topocentric right ascension α and declination δ are inertial coordinate system measurements. GEODYN computes these angles from the components of the earth-fixed station-satellite vector and the Greenwich hour angle θ_g.

$$\alpha = \tan^{-1}\left(\frac{\rho_2}{\rho_1}\right) + \theta_g, \quad \delta = \sin^{-1}\left(\frac{\rho_3}{\rho}\right)$$

where ρ_1, ρ_2, ρ_3 are the geocentric coordinates of the $\bar{\rho}$ vector.

The remaining measurements are in the topocentric horizon coordinate system. These all require the $\hat{N}$, $\hat{Z}$, and $\hat{E}$ (north, zenith and east baseline) unit vectors which describe the coordinate system.

Direction cosines: There are three direction cosines associated with the station-satellite vector in the topocentric system. These are

$$\ell = \hat{u} \cdot \hat{E}, \; m = \hat{u} \cdot \hat{N}, \text{ and } n = \hat{u} \cdot \hat{Z}$$

X and Y angles: The X and Y angles are computed by

$$X_a = \tan^{-1}\left(\frac{\ell}{n}\right), Y_a = \sin^{-1}(m)$$

Azimuth and elevation are computed by:

$$A_z = \tan^{-1}\left(\frac{\ell}{m}\right), E_\ell = \sin^{-1}(n)$$

A1-3.2 Variational Partials of the Measurements

The partial derivatives for each of the calculated geometric equivalents with respect to the satellite positions and velocity are given here. All are in the geocentric, earth-fixed system. (The r_i refer to the earth-fixed components of $\bar{r}$.)

Range:

$$\frac{\partial \rho}{\partial r_i} = \frac{\rho_i}{\rho}$$

Range-rate:

$$\frac{\partial \dot{\rho}}{\partial r_i} = \frac{1}{\rho}\left[\dot{r}_i - \frac{\dot{\rho}\rho_i}{\rho}\right], \frac{\partial \dot{\rho}}{\partial \dot{r}_i} = \frac{\rho_i}{\rho}$$

Right ascension:

$$\frac{\partial \alpha}{\partial r_1} = \frac{-\rho_2}{\sqrt{\rho_1^2 + \rho_2^2}}, \frac{\partial \alpha}{\partial r_2} = \frac{\rho_1}{\sqrt{\rho_1^2 + \rho_2^2}}, \frac{\partial \alpha}{\partial r_3} = 0$$

Declination:

$$\frac{\partial \delta}{\partial r_1} = \frac{-\rho_1 \rho_3}{\rho^2\sqrt{\rho_1^2 + \rho_2^2}}, \frac{\partial \delta}{\partial r_2} = \frac{-\rho_2 \rho_3}{\rho\sqrt{\rho_1^2 + \rho_2^2}}, \frac{\partial \delta}{\partial r_3} = \frac{\sqrt{\rho_1^2 + \rho_2^2}}{\rho^2}$$

Direction cosines:

$$\frac{\partial \ell}{\partial r_i} = \frac{1}{\rho}[E_i - \ell u_i], \frac{\partial m}{\partial r_i} = \frac{1}{\rho}[N_i - m u_i], \frac{\partial n}{\partial r_i} = \frac{1}{\rho}[Z_i - n u_i]$$

X and Y angles:

$$\frac{\partial X_a}{\partial r_i} = \frac{nE_i - \ell Z_i}{\rho\,(1-m^2)}, \quad \frac{Y_a}{\partial r_i} = \frac{N_j - mu_i}{\rho\sqrt{1-m^2}}$$

Azimuth and elevation:

$$\frac{\partial A_z}{\partial r_i} = \frac{mE_i - \ell N_i}{\rho\sqrt{1-n^2}}, \quad \frac{\partial E_\ell}{\partial r_i} = \frac{Z_i - nu_i}{\rho\,(1-n^2)}$$

The derivatives of each measurement type with respect to time are presented below. All are in the geocentric earth-fixed system.

Range:

$$\dot{\rho} = \hat{u} \cdot \dot{\bar{r}}$$

Range-rate: The range rate derivative deserves special attention. Remembering that $\dot{\bar{\rho}} = \dot{\bar{r}}$, we write $\dot{\rho} = \hat{u} \cdot \dot{\bar{\rho}}$. Thus $\ddot{\rho} = \dot{\hat{u}} \cdot \dot{\bar{\rho}} + \hat{u} \cdot \ddot{\bar{\rho}}$. Because $\dot{\hat{u}} = d/dt(\rho\hat{u}) = \dot{\rho}\,\hat{u} + \rho\dot{\hat{u}}$, we may substitute above for $\dot{\hat{u}}$: $\ddot{\rho} = 1/\rho\,(\dot{\bar{\rho}} \cdot \dot{\bar{\rho}} - \dot{\rho}\,\hat{u} \cdot \ddot{\bar{\rho}}) + \hat{u} \cdot \ddot{\bar{\rho}}$ or, as $\dot{\rho} = \hat{u} \cdot \dot{\bar{\rho}}$, we may write $\ddot{\rho} = 1/\rho\,(\dot{\bar{\rho}} \cdot \dot{\bar{\rho}} - \dot{\rho}^2 + \bar{\rho} \cdot \ddot{\bar{\rho}})$. In order to obtain $\ddot{\bar{\rho}}$, we use the limited gravitational potential

$$U = \frac{GM}{r}\left(1 - \frac{C_{20}\,a_e^{\,2}}{r^2}\,P_2^0\,(\sin\phi')\right)$$

The gradient of this potential with respect to the earth-fixed position coordinates of the satellite is the part of $\ddot{\bar{\rho}}$ due to the potential

$$\frac{\partial U}{\partial r_i} = -\frac{GM}{r^3}\left[1 - \frac{3\,a_e^2\,C_{20}}{2\,r^2}\left(5\sin^2\phi' - 1 - 2\,\frac{z}{r_i}\right)\right] r_i$$

We must add to this the effect of the rotation of the coordinate system. (The earth-fixed coordinate system rotates with respect to the true coordinates of date with a rate $\dot{\theta}_g$, the time rate of change of the Greenwich hour angle.)

The components of $\ddot{\bar{\rho}}$ are then

$$\ddot{\rho}_1 = \frac{\partial U}{\partial r_1} + [\dot{x}\cos\theta_g + \dot{y}\sin\theta_g]\,\dot{\theta}_g + \dot{r}_2\,\dot{\theta}_g$$

$$\ddot{\rho}_2 = \frac{\partial U}{\partial r_2} + [-\dot{x} \sin\theta_g + \dot{y} \cos\theta_g]\ \dot{\theta}_g - \dot{r}_1\ \dot{\theta}_g$$

$$\ddot{\rho}_3 = \frac{\partial U}{\partial r_3} = \frac{\partial U}{\partial z}$$

these transforms are used on the satellite velocity components $\dot{x}$ and $\dot{y}$ in the true coordinates of date.

It should be noted that all quantities in this formula, with the exception of those quantities in brackets, are earth-fixed values. (The magnitude r is invariant with respect to the coordinate system transformations.)

The remaining time derivatives are tabulated here:

Right ascension:

$$\dot{\alpha} = \frac{u_1\ \dot{r}_2 - u_2\ \dot{r}_1}{\rho\ (1 - u_3^2)}$$

Declination:

$$\dot{\delta} = \frac{r_3 - \dot{\rho}\ u_3}{\rho \sqrt{1 - u_3^2}}$$

Direct cosines:

$$\dot{\ell} = \frac{\dot{\bar{\rho}} \cdot \hat{E} - \ell\dot{\rho}}{\rho}, \dot{m} = \frac{\dot{\bar{\rho}} \cdot \hat{N} - m\dot{\rho}}{\rho}$$

X and Y angles:

$$\dot{X}_a = \frac{\dot{\bar{\rho}} \cdot (n\hat{E} - \ell\hat{Z})}{\rho\ (1 - m^2)}, \dot{Y}_a = \frac{\dot{\bar{\rho}} \cdot \hat{N} - m\dot{\rho}}{\rho \sqrt{1 - m^2}}$$

Azimuth:

$$\dot{A}_z = \frac{\dot{\bar{\rho}} \cdot (m\hat{E} - \ell\hat{N})}{\rho\ (1 - m^2)}$$

Elevation:

$$\dot{E}_\ell = \frac{\dot{\bar{\rho}} \cdot \hat{Z} - m\dot{\rho}}{\rho \sqrt{1 - m^2}}$$

A1-3.3 Corrections to Measurements

The function of data preprocessing is to convert and correct the data. These corrections and conversions relate the data to the physical model and to the coordinate and time reference systems used in GEODYN. The data corrections and conversions implemented in GEODYN are to: transform all observation times to A1 time at the satellite, refer right ascension and declination observations to the true equator and equinox of date, correct range measurements for transponder delay and gating effects, correct SAO right ascension and declination observations for diurnal aberration, correct for refraction, and convert TRANET Doppler observations into range-rate measurements. These conversions and corrections are applied to the data on the first iteration of each arc.

A1-3.3.1 Time Preprocessing—The time reference system used to specify the time of each observation is determined by a time identifier on the data record. This identifier also specifies whether the time recorded was the time at the satellite or at the observing station.

The preprocessing in GEODYN transforms all observations to A1 time. If the time recorded is the time at the station, it is converted to time at the satellite, by computing the propagation time between the spacecraft and the observing station. The station-satellite distance used for this correction is computed from the initial estimate of the trajectory.

There is special preprocessing for right ascension and declination measurements for the GEOS satellites when input in National Space Science Data Center format. If the observation is passive, the image recorded is an observation of light reflected from the satellite and the times are adjusted for propagation delay as above. If the observation is active, the image recorded is an observation of light transmitted from the optical beacon on the satellite. The beacons on the GEOS satellites are programmed to produce a sequence of seven flashes at four second intervals starting on an even minute. For the active observations, the times are set equal to the programmed flash time with a correction applied for known clock errors, plus half a millisecond, the time allowed for flash buildup.

A1-3.3.2 Reference System Conversion to True of Date—The camera observations, right ascension and declination, may be input referred to the mean equator and equinox of date, to the true equator and equinox of date, or to the mean equator and equinox of some standard epoch.

A1-3.3.3 Transponder Delay and Gating Effects—The range observations may be corrected on option for transponder delay or gating errors.

The transponder delay correction is computed as a polynomial in the range rate:

$$\Delta\rho = a_0 + a_1 \dot{\rho} + a_2 (\dot{\rho})^2$$

where a_0, a_1, and a_2 depend on the characteristics of the particular satellite.

A gating error is due to the fact that actual range measurements are either time delays between transmitted and received radar pulses or the phase shifts in the modulation of a received signal with respect to a coherent transmitted signal. Thus there is the possibility of incorrectly identifying the returned pulse or the number of integral phase shifts. The difference between the observed range and the computed range on the first iteration of the arc is used to determine the appropriate correction. The correction is such that there is less than half a gate, where the gate is the range equivalent of the pulse spacing or phase shift. The appropriate gate depends on the particular station.

A1-3.3.4 Aberration—Optical measurements may require corrections for the effects of annual aberration and diurnal aberration.

Annual Aberration—The corrections to right ascension and declination measurements for annual aberration effects are given by

$$\alpha = \alpha' - \frac{20''.5 \, (\cos\alpha' \cos\odot \cos\epsilon_T + \sin\alpha' \sin\odot)}{\cos\delta'}$$

$$\delta = \delta' - 20''.5 \, [\cos\odot \cos\epsilon_T \, (\tan\epsilon_T \cos\delta' - \sin\alpha' \sin\delta')$$

$$+ \cos\alpha' \sin\delta' \sin\odot]$$

where: α is the true right ascension of the satellite, α' is the observed right ascension of the satellite, δ is the true declination of the satellite, δ' is the observed declination of the satellite, ϵ_T is the true obliquity of date, and $\odot$ is the geocentric longitude of the sun in the ecliptic plane.

Diurnal Aberration—The corrections to right ascension and declination measurements for diurnal aberration effects are given by

$$\alpha = \alpha' + 0''.320 \cos\phi' \cos h_s \sec\delta'$$

$$\delta = \delta' + 0''.320 \cos\phi' \sin h_s \sin\delta'$$

where: ϕ' is the geocentric latitude of the station, h_s is the local hour angle measured in the westward direction from the station to the satellite, α is the

true right ascension of the satellite, α' is the observed right ascension of the satellite, δ is the true declination of the satellite, and δ' is the observed declination of the satellite.

A1-3.3.5 Refraction Corrections—The GEODYN system can apply corrections to all of the observational types significantly affected by refraction.

Right Ascension and Declination—Optical measurements may require corrections for the effects of parallactic refraction. These corrections are given by

$$\alpha = \alpha' - \Delta R \sin q/\cos \delta$$

$$\delta = \delta' - \Delta R \cos q$$

where the change in the zenith angle, ΔR, in radians is given by

$$\Delta R = - \frac{0.435\ (4.84813) \tan Z_o}{\rho \cos Z_o} \left[1 - e^{(-1.385)\ 10^{-4}\ \rho \cos Z_o}\right]$$

and α is the true right ascension of the satellite, α' is the observed right ascension of the satellite, δ is the true declination of the satellite, δ' is the observed declination of the satellite, Z_o is the observed zenith angle in radians, ρ is the range from the station to the satellite in meters, and q is the parallactic angle in radians.

The parallactic angle q is defined by the intersection of two planes represented by their normal vectors $\overline{P}_1$ and $\overline{P}_2$.

$$\overline{P}_1 = \hat{C}_P \times \hat{u}$$

$$\overline{P}_2 = \hat{v} \times \hat{u}$$

where $C_P = (0,0,1)$, $\hat{v}$ is the unit local vertical at the station, and $\hat{u}$ is the unit vector pointing from the station to the satellite in inertial space.

Therefore, the sine and cosine of the parallactic angle are given by

$$\cos q = \hat{P}_1 \cdot \hat{P}_2$$

$$\sin q = \hat{P}_3 \cdot \hat{P}_2$$

where $\hat{P}_1$ is the unit vector in the $\overline{P}_1$ direction, $\hat{P}_2$ is the unit vector in the $\overline{P}_2$ direction, and $\hat{P}_3 = \overline{P}_1 \times \hat{u} / |\overline{P}_1 \times \hat{u}|$.

The parallactic angle, q, is measured in the clockwise direction about the station-satellite vector (i.e., a left-handed system is used to define this angle). All vectors and vector cross products used in this formulation conform to a right-handed system.

Range:

The refraction correction applied to CNES laser range data is

$$\Delta\rho = \frac{\Delta\rho_n}{\sin E_\ell + (\cot E_\ell)\, 10^{-3}}$$

and the correction applied to range data from all other tracking systems is

$$\Delta\rho = - \frac{2.77\, n_s}{328.5\, (0.026 + \sin E_\ell)}$$

where $\Delta\rho_n$ is that correction associated with a range observation measured along the direction of the satellite zenith, and is provided along with each observation on the data tape, E_ℓ is the elevation angle computed from the initial estimate of the trajectory and n_s is the PPM deviation from unity of the surface index of refraction (default value equals 328.5).

Range Rate:

For range-rate, the correction $\Delta\dot{\rho}$ is derived from the range correction:

$$\Delta\dot{\rho} = \frac{2.77\, n_s \cos E_\ell}{328.5\, (0.026 + \sin E_\ell)^2}\, \dot{E}_\ell$$

where $\dot{E}_\ell$ is the computed rate of change of elevation.

Elevation:

For elevation observations the correction ΔE_ℓ is computed as follows:

$$\Delta E_\ell = \frac{n_s\, 10^3}{16.44 + 930 \tan E_\ell}$$

Azimuth is not affected by refraction.

Direction Cosines:

The corrections $\Delta\ell$ and Δm are derived from the elevation correction:

$$\Delta\ell = -\sin A_z \sin(E_\ell)\,\Delta E_\ell$$

$$\Delta m = -\cos A_z \sin(E_\ell)\,\Delta E_\ell$$

where A_z is the azimuth angle computed from the intitial estimate of the trajectory.

X and Y Angles:

For X and Y angles the corrections ΔX and ΔY are computed as follows:

$$\Delta X_a = -\frac{\sin A_z\,\Delta E_\ell}{(\sin^2 E_\ell + \sin^2 A_z \cos^2 E_\ell)}$$

$$\Delta Y_a = -\frac{\cos A_z \sin E_\ell\,\Delta E_\ell}{\sqrt{1-\cos^2 A_z \cos^2 E_\ell}}$$

Note that these are also derived from the elevation correction.

A1-3.3.6 TRANET Doppler Observations—TRANET Doppler observations are received as a series of measured frequencies with an associated base frequency for each station pass. Using the following relationship, the GEODYN system converts these observations to range-rate measurements.

$$\dot{\rho} = \frac{c\,(F_B - F_M)}{F_M}$$

where F_M is the measured frequency, F_B is the base frequency, and c is the velocity of light.

A1-4.0 FORCE MODEL AND VARIATIONAL EQUATIONS

The system requires computing positions and velocities of the spacecraft at each observation time and therefore requires a force model. The dynamics of the situation are expressed by the equations of motion, which provide a relationship between the orbital elements at any given instant and the initial conditions of epoch. There is an additional requirement for variational partials, which are the partial derivatives of the instantaneous orbital elements with respect to the parameters at epoch and other parameters defined below. These partials are generated using the variational equations, which are analogous to the equations of motion.

In a geocentric inertial rectangular coordinate system, the equations of motion for a spacecraft are of the form

$$\ddot{\bar{r}} = \frac{\mu \bar{r}}{r^3} + \bar{A}$$

where $\bar{r}$ is the position vector of the satellite, μ is GM, where G is the gravitational constant and M is the mass of the earth, and $\bar{A}$ is the acceleration caused by the asphericity of the earth, extraterrestrial gravitational forces, atmospheric drag and solar radiation.

This provides a system of second order equations which, given the epoch position and velocity components, may be integrated to obtain the position and velocity at any other time. The direct integration of these accelerations in Cartesian coordinates is known as Cowell's method and is the technique used in the orbit generator.

There is an alternative way of expressing the above equations of motion:

$$\ddot{\bar{r}} = \nabla U + \bar{A}_D + \bar{A}_R$$

where U is the potential field due to gravity, $\bar{A}_D$ contains the accelerations due to drag, and, $\bar{A}_R$ contains the accelerations due to solar radiation pressure. This is just a regrouping of terms coupled with a recognition of the existence of a potential field. This is the form used in the program.

The inertial coordinate system in which these equations of motion are integrated is that system corresponding to the true of date system of 0^h0 of the reference day.

The evaluation of the accelerations for $\ddot{\bar{r}}$ is performed in the true of date system. Thus there is a requirement that the inertial position and velocity output

from the integrator be transformed to the true of date system for the evaluation of the accelerations, and a requirement to transform the computed accelerations from the true of date system to the inertial system.

The variational equations have the same relationship to the variational partials as the satellite position vector does to the equations of motion. The variational partials are defined as the $\partial \bar{x}_t / \partial \bar{\beta}$ where $\bar{x}_t$ spans the true of date position and velocity of the satellite at a given time, and $\bar{\beta}$ spans the epoch parameters, geopotential coefficients, drag parameters, and solar radiation parameters.

The variational partials may be partitioned according to the satellite position and velocity vectors at the given time. Thus the required partials are $\partial \bar{r} / \partial \bar{\beta}$, $\partial \dot{\bar{r}} / \partial \bar{\beta}$, where $\bar{r}$ is the satellite position vector (x, y, z) in the true of date system, and $\dot{\bar{r}}$ is the satellite velocity vector ($\dot{x}$, $\dot{y}$, $\dot{z}$) in the same system. The first of these, $\partial \bar{r} / \partial \bar{\beta}$, can be obtained by the double integration of

$$\frac{d^2}{dt^2} \frac{\partial \bar{r}}{\partial \bar{\beta}}$$

or rather, since the order of differentiation may be exchanged, $\partial \ddot{\bar{r}} / \partial \bar{\beta}$. Note that the second set of partials, $\partial \dot{\bar{r}} / \partial \bar{\beta}$, may be obtained by the first order integration of $\partial \ddot{\bar{r}} / \partial \bar{\beta}$. Hence we recognize that the quantity to be integrated is $\partial \ddot{\bar{r}} / \partial \bar{\beta}$. Using the second form given for the equations of motion in the previous subsection, the variational equations are given by

$$\frac{\partial \ddot{\bar{r}}}{\partial \bar{\beta}} = \frac{\partial}{\partial \bar{\beta}} \left(\nabla U + \bar{A}_D + \bar{A}_R \right)$$

where U is the potential field due to gravitational effects, $\bar{A}_R$ is the acceleration due to radiation pressure, and $\bar{A}_D$ is the acceleration due to drag. At this point we must consider a few items:

1. The potential field is a function only of position. Thus we have

$$\frac{\partial}{\partial \bar{\beta}} \left(\frac{\partial U}{\partial r_i} \right) = \sum_{m=1}^{3} \left(\frac{\partial^2 U}{\partial r_i \, \partial r_m} \right) \frac{\partial r_m}{\partial \bar{\beta}}$$

2. The partials of solar radiation pressure with respect to the geopotential coefficients, the drag coefficient, and the satellite velocity are zero, and the partials, with respect to satellite position, are negligible.

3. Drag is a function of position, velocity, and the drag coefficients. The partials, with respect to the geopotential coefficients and satellite emissivity, are zero, but we have

$$\frac{\partial \bar{A}_D}{\partial \bar{\beta}} = \frac{\partial A_D}{\partial \bar{x}_t} \frac{\partial \bar{x}_t}{\partial \bar{\beta}} + \frac{\partial \bar{A}_D}{\partial C_D} \frac{\partial C_D}{\partial \bar{\beta}} + \frac{\partial \bar{A}_D}{\partial \dot{C}_D} \frac{\partial \dot{C}_D}{\partial \bar{\beta}}$$

Let us write our variational equations in matrix notation. We define

n to be the number of epoch parameters in $\bar{\beta}$

F is a 3 x n matrix whose j^{th} column vectors are $\partial \ddot{\bar{r}}/\partial \beta_j$

U_{2c} is a 3 x 6 matrix whose last 3 columns are zero and whose first 3 columns are such that the i, j^{th} element is given by $\partial^2 U/\partial r_i \, \partial r_j$

D_r is a 3 x 6 matrix whose j^{th} column is defined by $\partial \bar{A}_D/\partial x_{t_j}$

X_m is a 6 x n matrix whose i^{th} row is given by $\partial \bar{x}_t/\partial \beta_j$. Note that X_m contains the variational partials.

f is a 3 x n matrix whose first six columns are zero and whose last n-6 columns are such that the i, j^{th} element is given by $\partial/\partial \beta_j \; (\nabla U + \bar{A}_D + \bar{A}_R)$. Note that the first six columns correspond to the first six elements of $\bar{\beta}$ which are the epoch position and velocity. (This matrix contains the direct partials of $\bar{x}_t$ with respect to $\bar{\beta}$.) We may now write $F = [U_{2c} + D_r] \; X_m + f$. This is a matrix form of the variational equations.

Note that U_{2c}, D_r, and f are evaluated at the current time, whereas X_m is the output of the integration. Initially, the first six columns of X_m plus the six rows form an identity matrix; the rest of the matrix is zero (for i = j, $X_{m_{ij}} = 1$; for $i \neq j$, $X_{m_{ij}} = 0$).

A1-4.1 The Geopotential Field of the Earth

In GEODYN the earth's potential is described by a spherical harmonic expansion and it is most conveniently expressed in a spherical coordinate system where ϕ' is the satellite's geocentric latitude, λ is the satellite's east longitude, and r is the geocentric range of the satellite.

The earth's gravity field is represented by the normal potential of an ellipsoid of revolution and small irregular variations, expressed by a sum

of spherical harmonics. This formulation, used in the GEODYN system, is

$$U = \frac{GM}{r}\left\{1 + \sum_{n=2}^{nmax}\sum_{m=0}^{n}\left(\frac{a_e}{r}\right)^n P_n^m(\sin\phi')\left[C_{nm}\cos m\lambda + S_{nm}\sin m\lambda\right]\right\}$$

where G is the universal gravitational constant, M is the mass of the earth, r is the geocentric satellite distance, nmax is the upper limit for the summation (highest degree), a_e is the earth's mean equatorial radius, $P_n^m(\sin\phi')$ indicate the associated Legendre functions, and C_{nm} and S_{nm} are the unnormalized coefficients.

The relationships between the normalized coefficients ($\bar{C}_{nm}$, $\bar{S}_{nm}$) and the unnormalized coefficients are as follows:

$$C_{nm} = \left[\frac{(n-m)!\,(2n+1)\,(2-\delta_{om})}{(n+m)!}\right]^{1/2}\bar{C}_{nm}$$

where δ_{om} is the Kronecker delta, and $\delta_{om} = 1$ for $m = 0$ and $\delta_{om} = 0$ for $m \neq 0$. A similar expression is valid for the relationship between $\bar{S}_{nm}$ and S_{nm}.

The gravitational accelerations in true of date coordinates ($\ddot{x}$, $\ddot{y}$, $\ddot{z}$) are computed from the geopotential, $U(r, \phi', \lambda)$, by the chain rule; e.g.,

$$\ddot{x} = \frac{\partial U}{\partial r}\frac{\partial r}{\partial x} + \frac{\partial U}{\partial \phi'}\frac{\partial \phi'}{\partial x} + \frac{\partial U}{\partial \lambda}\frac{\partial \lambda}{\partial x}$$

The accelerations $\ddot{y}$ and $\ddot{z}$ are determined likewise. The partial derivatives of U with respect to r, ϕ', and λ are given by

$$\frac{\partial U}{\partial r} = \frac{GM}{r^2}\left[1 + \sum_{n=2}^{nmax}\left(\frac{a_e}{r}\right)^n\sum_{m=0}^{n}\left(C_{nm}\cos m\lambda + S_{nm}\sin m\lambda\right)(n+1)\,p_n^m(\sin\phi')\right]$$

$$\frac{\partial U}{\partial \lambda} = \frac{GM}{r}\sum_{n=2}^{nmax}\left(\frac{a_e}{r}\right)^n\sum_{m=0}^{n}\left(S_{nm}\cos m\lambda - C_{nm}\sin m\lambda\right)m\,P_n^m(\sin\phi')$$

$$\frac{\partial U}{\partial \phi'} = \frac{GM}{r}\sum_{n=2}^{nmax}\left(\frac{a_e}{r}\right)^n\sum_{m=0}^{n}\left(C_{nm}\cos m\lambda + S_{nm}\sin m\lambda\right)$$

$$\left[P_n^{m+1}(\sin\phi') - m\tan\phi'\,P_n^m(\sin\phi')\right]$$

The partials derivatives of r, ϕ', and λ with respect to the true of date satellite position components are

$$\frac{\partial r}{\partial r_i} = \frac{r_i}{r}$$

$$\frac{\partial \phi'}{\partial r_i} = \frac{1}{\sqrt{x^2 + y^2}} \left[- \frac{z r_i}{r^2} + \frac{\partial z}{\partial r_i} \right]$$

$$\frac{\partial \lambda}{\partial r_i} = \frac{1}{\sqrt{x^2 + y^2}} \left[\frac{\partial y}{\partial r_i} - \frac{y}{x} \frac{\partial x}{\partial r_i} \right]$$

The Legendre functions are computed via recursion formulae:

Zonals: $m = 0$

$$P_n^o (\sin \phi') = \frac{1}{n} \left[(2n - 1) \sin \phi' P_{n-1}^o (\sin \phi') - (n - 1) P_{n-2}^o (\sin \phi') \right]$$

$$P_1^o (\sin \phi') = \sin \phi'$$

Tesserals: $m \neq 0$ and $m \leqslant n$.

$$P_n^m (\sin \phi') = P_{n-2}^m (\sin \phi') + (2n - 1) \cos \phi' P_{n-1}^{m-1} (\sin \phi')$$

$$P_1^1 (\sin \phi') = \cos \phi'$$

Sectorials: $m = n$

$$P_n^n = (2n - 1) \cos \phi' P_{n-1}^{n-1} (\sin \phi')$$

The relationship for the derivatives is given by

$$\frac{d}{d\phi'} \left(P_n^m (\sin \phi') \right) = P_n^{m+1} (\sin \phi') - m \tan \phi' P_n^m (\sin \phi')$$

It should also be noted that multiple-angle formulas are used for evaluating the sine and cosine of $m\lambda$.

The variational equations require the computation of the matrix U_{2c}, whose elements are given by

$$(U_{2c})_{i,j} = \frac{\partial^2 U}{\partial r_i \, \partial r_j}$$

where $r_i = \{x, y, z\}$, the true of date satellite position, and U is the geopotential.

Because the Earth's field is in terms of r, sin ϕ', and λ, we write

$$U_{2c} = C_1^T U_2 C_1 + \sum_{k=1}^{3} \frac{\partial U}{\partial e_k} C_{2k}$$

where e_k ranges over the elements r, sin ϕ', and λ, U_2 is the matrix whose i, j^{th} element is given by $\partial^2 U/\partial e_i \partial e_j$, C_1 is the matrix whose i, j^{th} element is given by $\partial e_i/\partial r_j$, and C_{2k} is a set of three matrices whose i, j^{th} elements are given by $\partial^2 e_k/\partial r_i \partial r_j$.

We compute the second partial derivatives of the potential U with respect to r, ϕ', and λ:

$$\frac{\partial^2 U}{\partial r^2} = \frac{2GM}{r^3} + \frac{GM}{r^3} \sum_{n=2}^{nmax} (n+1)(n+2) \left(\frac{a_e}{r}\right)^n \sum_{m=0}^{n}$$

$$(C_{nm} \cos m\lambda + S_{nm} \sin m\lambda) P_n^m (\sin \phi')$$

$$\frac{\partial^2 U}{\partial r \partial \phi'} = -\frac{GM}{r^2} \sum_{n=2}^{nmax} (n+1) \left(\frac{a_e}{r}\right)^n \sum_{m=0}^{n} (C_{nm} \cos m\lambda$$

$$+ S_{nm} \sin m\lambda) \frac{\partial}{\partial \phi'} \left(P_n^m (\sin \phi')\right)$$

$$\frac{\partial^2 U}{\partial r \partial \lambda} = \frac{GM}{r^2} \sum_{n=2}^{nmax} (n+1) \left(\frac{a_e}{r}\right)^n \sum_{m=0}^{n} m$$

$$(-C_{nm} \sin m\lambda + S_{nm} \cos m\lambda) P_n^m (\sin \phi')$$

$$\frac{\partial^2 U}{\partial \phi'^2} = \frac{GM}{r} \sum_{n=2}^{nmax} \left(\frac{a_e}{r}\right)^n \sum_{m=0}^{n} (C_{nm} \cos m\lambda + S_{nm} \sin m\lambda)$$

$$\frac{\partial^2}{\partial \phi'^2} \left(P_n^m (\sin \phi')\right)$$

$$\frac{\partial^2 U}{\partial \phi' \partial \lambda} = \frac{GM}{r} \sum_{n=2}^{nmax} \left(\frac{a_e}{r}\right)^n \sum_{m=0}^{n} m \left(- C_{nm} \sin m\lambda \right.$$

$$\left. + S_{nm} \cos m\lambda \right) \frac{\partial}{\partial \phi'} \left(P_n^m (\sin \phi') \right)$$

$$\frac{\partial^2 U}{\partial \lambda^2} = - \frac{GM}{r} \sum_{n=2}^{nmax} \left(\frac{a_e}{r}\right)^n \sum_{m=0}^{n} m^2 \left(C_{nm} \cos m\lambda \right.$$

$$\left. + S_{nm} \sin m\lambda \right) P_n^m (\sin \phi')$$

where

$$\frac{\partial}{\partial \phi'} \left(P_n^m (\sin \phi') \right) = P_n^{m+1} (\sin \phi') - m \tan \phi' \, P_n^m (\sin \phi')$$

$$\frac{\partial^2}{\partial \phi'^2} \left(P_n^m (\sin \phi') \right) = P_n^{m+2} (\sin \phi') - (m + 1) \tan \phi' \, P_n^{m+1} (\sin \phi')$$

$$- m \tan \phi' \left[P_n^{m+1} (\sin \phi') - m \tan \phi' \, P_n^m (\sin \phi') \right]$$

$$- m \sec^2 \phi' \, P_n^m (\sin \phi')$$

The elements of U_2 have almost been computed. What remains is to transform from (r, ϕ', λ) to $(r, \sin \phi', \lambda)$. This affects only the partials involving ϕ':

$$\frac{\partial U}{\partial \sin \phi'} = \frac{\partial U}{\partial \phi'} \frac{\partial \phi'}{\partial \sin \phi'}$$

$$\frac{\partial^2 U}{\partial \sin \phi'^2} = \frac{\partial \phi'}{\partial \sin \phi'} \left(\frac{\partial^2 U}{\partial \phi'^2} \right) \frac{\partial \phi'}{\partial \sin \phi'} + \frac{\partial U}{\partial \phi'} \frac{\partial^2 \phi'}{\partial \sin \phi'^2}$$

where

$$\frac{\partial \phi'}{\partial \sin \phi'} = \sec \phi', \quad \frac{\partial^2 \phi'}{\partial \sin \phi'^2} = \sin \phi' \sec^3 \phi'$$

For the C_1 and C_{2k} matrices, the partials of r, $\sin \phi'$, and λ are obtained from the formulas

$$r = \sqrt{x^2 + y^2 + z^2}, \sin \phi' = \frac{z}{r}, \lambda = \tan^{-1} \left(\frac{y}{x}\right) - \theta_g.$$

We have for C_1:

$$\frac{\partial r}{\partial r_i} = \frac{r_i}{r}$$

$$\frac{\partial \sin \phi'}{\partial r_i} = \frac{-z\, r_i}{r^3} + \frac{1}{r}\frac{\partial z}{\partial r_i}$$

$$\frac{\partial \lambda}{\partial r_i} = \frac{1}{x^2 + y^2}\left[x \frac{\partial y}{\partial r_i} - y \frac{\partial x}{\partial r_i}\right]$$

The C_{2k} are symmetric. The necessary elements are given by

$$\frac{\partial^2 r}{\partial r_i\, \partial r_j} = \frac{r_i\, r_j}{r^3} + \frac{1}{r}\frac{\partial r_i}{\partial r_j}$$

$$\frac{\partial^2 \sin \phi'}{\partial r_i\, \partial r_j} = \frac{3z\, r_i\, r_j}{r^5} - \frac{1}{r^3}\left[r_j \frac{\partial z}{\partial r_i} + r_i \frac{\partial z}{\partial r_j} + z \frac{\partial r_i}{\partial r_j}\right]$$

$$\frac{\partial^2 \lambda}{\partial r_i\, \partial r_j} = \frac{-2r_j}{(x^2 + y^2)^2}\left[x \frac{\partial y}{\partial r_i} - y \frac{\partial x}{\partial r_i}\right] + \frac{1}{x^2 + y^2}\left[\frac{\partial x}{\partial r_j}\frac{\partial y}{\partial r_j} - \frac{\partial y}{\partial r_j}\frac{\partial x}{\partial r_j}\right].$$

If the gravitational constants, C_{nm} or S_{nm} are being estimated, we require their partials in the f matrix for the variational equations computations. These partials are

$$\frac{\partial}{\partial C_{nm}}\left(-\frac{\partial U}{\partial r}\right) = (n+1)\frac{GM}{r^2}\left(\frac{a_e}{r}\right)^n \cos(m\lambda)\, P_n^m(\sin\phi')$$

$$\frac{\partial}{\partial C_{nm}}\left(-\frac{\partial U}{\partial \lambda}\right) = m\frac{GM}{r}\left(\frac{a_e}{r}\right)^n \sin(m\lambda)\, P_n^m(\sin\phi')$$

$$\frac{\partial}{\partial C_{nm}}\left(-\frac{\partial U}{\partial \phi'}\right) = -\frac{GM}{r}\left(\frac{a_e}{r}\right)^n \cos(m\lambda)\left[P_n^{m+1}(\sin\phi') - m\tan\phi'\, P_n^m(\sin\phi')\right]$$

The partials for S_{nm} are identical with C_{nm} when $\cos(m\lambda)$ replaced by $\sin(m\lambda)$ and when $\sin(m\lambda)$ replaced by $-\cos(m\lambda)$.

These partials are converted to inertial true of date coordinates using the chain rule; e.g.,

$$\frac{\partial}{\partial C_{nm}}\left(-\frac{\partial U}{\partial x}\right) = \frac{\partial}{\partial C_{nm}}\left(\frac{-\partial U}{\partial r}\right)\frac{\partial r}{\partial x} + \frac{\partial}{\partial C_{nm}}\left(\frac{-\partial U}{\partial \lambda}\right)\frac{\partial \lambda}{\partial x} + \frac{\partial}{\partial C_{nm}}\left(\frac{-\partial U}{\partial \phi'}\right)\frac{\partial \phi'}{\partial x}$$

A1-4.1.1 Solid Earth Tides—The gravitational potential originating from solid earth tides caused by a single disturbing body is given by

$$U_D(r) = \frac{k_2}{2}\frac{GM_d}{R_d^3}\frac{R_e^5}{r^3}\left[3(\hat{R}_d \cdot \hat{r})^2 - 1\right]$$

$$= \frac{k_2}{2}\frac{GM_e}{R_e}\left(\frac{M_d}{M_e}\right)\left(\frac{R_e}{R_d}\right)^3\left(\frac{R_e}{r}\right)^3\left[3(\hat{R}_d \cdot \hat{r})^2 - 1\right]$$

and the resultant accelerations on a satellite due to this potential are

$$\nabla U_D = \frac{k_2}{2}\frac{GM_d}{R_d^3}\frac{R_e^5}{r^4}\left\{\left[3 - 15(\hat{R}_d \cdot \hat{r})^2\right] r + 6(\hat{R}_d \cdot \hat{r}) R_d\right\}$$

where k_2 is the tidal coefficient of degree 2 called the "Love Number," G is the universal gravitational constant, M_e is the mass of the Earth, R_e is the mean earth radius, M_d is the mass of the disturbing body, R_d is the distance from the center of mass of the earth to the center of mass of the disturbing body, r is the distance from the center of mass of the earth to the satellite, $\hat{R}_d$ is the unit vector and $\hat{r}$ is the unit vector from the center of mass of the earth to the satellite.

A1-4.2 Luni-Solar-Planetary Ephemeris

Precomputed equi-spaced ephemeris data in true of date coordinates for the Moon, the Sun, Venus, Mars, Jupiter and Saturn is used. The actual ephemerides are computed using Everett's fifth-order interpolation formula. The interval between ephemerides; i.e., the tabular interval, h, is 0.5 days for the Moon and the equation of the equinoxes and 4.0 days for the other bodies.

The GEODYN ephemeris tape contains all coordinates in true of date. The quantities on the tape are, the geocentric lunar positions and the corresponding 2nd and 4th differences, the solar positions relative to the Earth-Moon barycenter and the corresponding 2nd and 4th differences, the helicentric positions of Venus, Mars, Jupiter and Saturn and the corresponding 2nd and 4th differences, and the equation of the equinoxes and its 2nd and 4th differences. This ephemeris tape was prepared from a JPL planetary ephemeris tape corresponding to "JPL Development Ephemeris Number 69." (Devine, 1957.)

The formulation for Everett's fifth-order interpolation is:

$$y(t_j + sh) = y_j F_0(1-s) + d_j^2 F_2(1-s) + d_j^4 F_4(1-s)$$

$$+ y_{j+1} F_0(s) + d_{j+1}^2 F_2(s) + d_{j+1}^4 F_4(s)$$

where

$$F_0(s) = s; F_2(s) = [(s-1)(s)(s+1)]/6; F_4(s) = [(s-2)(s-1)(s)(s+1)(s+2)]/120.$$

The quantity s is the fractional interval for the interpolation. The quantities d_j are obtained from the ephemeris tape.

A1-4.3 Third Body Gravitational Perturbations (Luni-Solar Forces)

The gravitational perturbations caused by a third body on a satellite orbit are treated by defining a function, R_d, which is the third-body disturbing potential. This potential takes on the following form:

$$R_d = \frac{GMm_d}{r_d}\left[\left(1 - \frac{2r}{r_d}S + \frac{r^2}{r_d^2}\right)^{-1/2} - \frac{r}{r_d}S\right]$$

where m_d is the mass of the disturbing body, $\bar{r}_d$ is the geocentric true of date position vector to the disturbing body, S is equal to the cosine of the angle between $\bar{r}$ and $\bar{r}_d$, $\bar{r}$ is the geocentric true of date position vector of the satellite, G is the universal gravitational constant, and M is the mass of the earth. All perturbations are computed by,

$$\bar{a}_d = -GMm_d\left[\frac{\bar{d}}{D_d} + \frac{1}{r_d}\left(\frac{\bar{r}_d}{r_d}\right)\right]$$

where

$$\bar{d} = \bar{r} - \bar{r}_d, D_d = \left[r_d^2 - 2r\, r_d\, S + r^2\right]^{3/2}$$

Then compute the matrix U_{2c} whose i, j^{th} element is given by

$$\frac{\partial^2 R_d}{\partial r_i\, \partial r_j} = -\frac{GMm_d}{D_d}\left[\frac{\partial r_i}{\partial r_j} + \frac{3d_i\, d_j}{D_d^{2/3}}\right]$$

This matrix is a fundamental part of the variational equations.

A1-4.4 Solar Radiation Pressure

The force due to solar radiation can have a significant effect on the orbits of satellites with a large area to mass ratio. The accelerations due to solar radiation pressure are

$$\bar{A}_R = -\nu C_R \frac{A_s}{m_s} P_s \hat{r}_s$$

where ν is the eclipse factor, such that $\nu = 0$ when the satellite is in the earth's shadow and $\nu = 1$ when the satellite is illuminated by the Sun. C_R is a factor depending on the reflectivity of the satellite, A_s is the cross sectional area of the satellite, m_s is the mass of the satellite, P_s is the solar radiation pressure in the vicinity of the earth, and $\hat{r}_s$ is the (geocentric) true of date unit vector pointing to the Sun.

The unit vector $\hat{r}_s$ is determined as part of the luni-solar-planetary ephemeris computations (see A1-4.2).

The eclipse factor, ν, is determined as follows: Compute $D = \bar{r} \cdot \hat{r}_s$ where $\bar{r}$ is the true of date position vector of the satellite. If D is positive, the satellite is always in sunlight. If D is negative, compute the vector $\bar{P}_R \cdot \bar{P}_R = \bar{r} - D\hat{r}_s$. This vector is perpendicular to $\hat{r}_s$. If its magnitude is less than an earth radius, or if $P_R \cdot P_R < a_e^2$, the satellite is in shadow.

The satellite is assumed to be specularly reflecting with reflectivity ρ_s; thus $C_R = 1 + \rho_s$.

When a radiation pressure coefficient C_R is being determined the partials for the f matrix (see A1-4.0) in the variational equations computations must be computed. The i^{th} element of this column matrix is given by

$$f_i = -\nu \frac{A_s}{m_s} P_s r_{s_i}$$

A1-4.5 Atmospheric Drag

A satellite moving through an atmosphere experiences an atmospheric drag force. The acceleration due to this force is given by

$$\bar{A}_D = -\frac{1}{2} C_D \frac{A_s}{m_s} \rho_D v_r \bar{v}_r$$

where C_D is the satellite drag coefficient, A_s is the cross-sectional area of the satellite, m_s is the mass of the satellite, ρ_D is the density of the atmosphere at the satellite position, and $\bar{v}_r$ is the velocity vector of the satellite relative to the atmosphere.

Both A_s and C_D are treated as constants in GEODYN. Although A_s depends somewhat on satellite attitude, the use of a mean cross-sectional area does not lead to significant errors at this time. The factor C_D varies slightly with satellite shape and atmospheric composition. However, it has been treated as a satellite dependent constant.

The relative velocity vector, $\bar{v}_r$, is computed assuming that the atmosphere rotates with the Earth. The true of date components of this vector are then

$$\dot{x}_r = \dot{x} - \dot{\theta}_g \dot{y}, \dot{y}_r = \dot{y} - \dot{\theta}_g x, \dot{z}_r = \dot{z}$$

The quantities $\dot{x}$, $\dot{y}$, and $\dot{z}$ are the components of $\dot{\bar{r}}$, the satellite velocity in true of date coordinates.

The direct partials for the f matrix of the variational equations when the drag coefficient C_D is being determined are given by

$$f = -\frac{1}{2}\frac{A_s}{m_s}\rho_D v_r \bar{v}_r$$

The direct partials for the f matrix of the variational equations when the drag rate $\dot{C}_D$ is being determined are given by:

$$f = -\frac{1}{2}\frac{A_s}{m_s}\rho_D \Delta t\, v_r \bar{v}_r$$

where Δt is the time from epoch.

When drag is present the D_r matrix in the variational equations must also be computed. This matrix, which contains the partial derivatives of the drag acceleration with respect to the Cartesian orbital elements, is

$$D_r = -\frac{1}{2} C_D \frac{A_s}{m_s}\left[\rho_D v_r \frac{\partial \bar{v}_r}{\partial \bar{x}_t} + \rho_D \frac{\partial v_r}{\partial \bar{x}_t}\bar{v}_r + \frac{\partial \rho_D}{\partial \bar{x}_t} v_r \bar{v}_r\right]$$

where $\bar{x}_t$ is (x, y, z, $\dot{x}$, $\dot{y}$, $\dot{z}$);

$$\frac{\partial \bar{v}_r}{\partial \bar{x}_t} = \begin{bmatrix} 0 & -\dot{\theta}_g & 0 \\ \dot{\theta}_g & 0 & 0 \\ 0 & 0 & 0 \\ 1 & 0 & 0 \\ 0 & 1 & 0 \\ 0 & 0 & 1 \end{bmatrix}$$

$$\frac{\partial v_r}{\partial \bar{x}_t}\,\bar{v}_r = \frac{1}{v_r} \begin{bmatrix} -\dot{y}_r\ \dot{\theta}_g\ \dot{x}_r & -\dot{y}_r\ \dot{\theta}_g\ \dot{y}_r & -\dot{y}_r\ \dot{\theta}_g\ \dot{z}_r \\ \dot{x}_r\ \dot{\theta}_g\ \dot{x}_r & \dot{x}_r\ \dot{\theta}_g\ \dot{y}_r & \dot{x}_r\ \dot{\theta}_g\ \dot{z}_r \\ 0 & 0 & 0 \\ \dot{x}_r\ \dot{x}_r & \dot{x}_r\ \dot{y}_r & \dot{x}_r\ \dot{z}_r \\ \dot{y}_r\ \dot{x}_r & \dot{y}_r\ \dot{y}_r & \dot{y}_r\ \dot{z}_r \\ \dot{z}_r\ \dot{x}_r & \dot{z}_r\ \dot{y}_r & \dot{z}_r\ \dot{z}_r \end{bmatrix}$$

and $\partial \rho_D / \partial \bar{x}_t$ is the matrix containing the partial derivatives of the atmospheric density with respect to $\bar{x}_t$. Because the density is not a function of the satellite velocity, the required partials are $\partial \rho_D / \partial \bar{r}$.

A1-4.5.1 Atmospheric Density—The atmospheric density is the factor which is least well known in the computation of drag. The program uses the Jacchia-Nicolet model. This model gives densities between 120km and 1000km with an extrapolation formula for higher altitudes. (Jacchia, 1965.)

The formulae for computing the exospheric temperature have been modified according to Jacchia's later papers. The density computed from the exospheric temperature is based on density data provided in that report which presents density distribution versus altitude and exospheric temperature.

The model of the atmosphere proposed by Nicolet considers that the fundamental parameter is the temperature. Other physical parameters such as the pressure and density were derived from the temperature.

To calculate the fundamental parameter, the exospheric temperature, Jacchia considered the four factors of solar activity variation, semi-annual variation, diurnal variation, and geomagnetic activity variation.

In addition to the density, the partial derivatives of the density with respect to the Cartesian position coordinates are required. These partials are used in computing the drag contribution to the variational equations. The density is given by

$$\rho_D = \exp\left(C_0 + C_1\, h + C_2\, h^2 + C_3\, h^3\right)$$

where h is the spheroid height, and the C_i are coefficients which are polynomials in temperature as determined by the model. We then have

$$\frac{\partial \rho_D}{\partial \bar{r}} = \rho_D \left(C_1 + 2\, C_2\, h + 3\, C_3\, h^2\right) \frac{\partial h}{\partial \bar{r}}$$

where $\bar{r}$ is the true of date position vector of the satellite (x, y, z).

A1-5.0 ADJUSTMENT PROCEDURES

A1-5.1 Bayesian Least Squares Method

It should be noted that the functional relationships between the observations and parameters being solved for are in general non-linear; thus an iterative procedure is necessary to solve the resultant non-linear normal equations. The Newton-Raphson iteration formula is used to solve these equations.

In a multi-satellite, multi-arc estimation program, it is necessary to formulate the estimation scheme in a manner such that the information for all satellite arcs are not in core simultaneously. The procedure used is a partitioned Bayesian Estimation Scheme which requires only common parameter information and the information for a single arc to be in machine memory at any given time. The development of the solution is given here.

The Bayesian estimation formula is

$$\underline{dx}^{(n+1)} = (B^T WB + V_A^{-1})^{-1} [B^T W\underline{dm} + V_A^{-1} (x^{(n)} - \underline{x}_A)]$$

where $\underline{x}_A$ is the a priori estimate of $\underline{x}$; V_A is the a priori covariance matrix associated with x_A; W is the weighting matrix associated with the observations; $\underline{x}^{(n)}$ is the n^{th} approximation to $\underline{x}$; $\underline{dm}$ is the vector of residuals (O-C) from the n^{th} approximation; $\underline{dx}^{(n+1)}$ is the vector of corrections to the parameters; i.e.,

$$\underline{x}^{n+1} = \underline{x}^n + \underline{dx}^{(n+1)}$$

B is the matrix of partial derivatives of the observations with respect to the parameters where the i, j^{th} element is given by $\partial m_i / \partial x_j$.

The iteration formula given by this equation solves the non-linear normal equations formed by minimizing the sum of squares of the weighted residuals.

In the application for GEM models no a priori information is employed, thus V_A^{-1} and $\underline{x}_A$ vanishes from the above Bayesian formula which then describes the usual least squares process. After convergence of the above orbital parameters the normal equations, M, are formed for all parameters including the geodetic parameters as a contributory set to GEM 5. Therefore the normal equations for the given arc of satellite data are

$$M = B^T WB \underline{dx} - B^T W dm$$

where $\underline{dx}$ refers to adjustments for all parameters.

For certain types of satellite tracking data for which a bias parameter is adjusted in the data, a reduced form of the above normal equations is obtained as described in the next section.

A1-5.2 Measurement Bias Separation (Electronic Instruments)

For certain types of electronic tracking data (e.g., Doppler data), biases exist which are different from one pass to the next. In many cases, these biases are of no interest per se, although their existence must be appropriately accounted for if the data is to be used in an orbit or geodetic estimation. In addition, a desired arc of data involving hundreds of passes of the satellite over various stations of such electronic data, and the complete solution for each bias would require the use of an excessively large amount of computer core for storing the normal matrix for the complete set of adjusted parameters.

The effects of electronic biases can be removed, with the use of only a small amount of additional core, by partitioning of the biases from the other parameters being adjusted in the Bayesian least squares estimation. The forms which this partitioning takes can be seen from the solution of the basic measurement equation $\delta m = B_e \Delta b + B \Delta x + \epsilon$ where δm = the vector of residuals (O-C), Δb = the set of corrections that should be made to the electronic biases, B_e = the matrix of partial derivatives of the measurements with respect to the biases (the elements of this matrix are either 1's or 0's), Δx = the set of corrections to be made to all the other adjustable parameters, B = the matrix of partial derivatives of the measurements with respect to the x parameters, and ϵ = the measurement noise vector.

The least squares solution of the above equation is

$$\begin{bmatrix} \Delta\hat{b} \\ \Delta\hat{x} \end{bmatrix} = \begin{bmatrix} B_e^T W B_e & B_e^T W B \\ B^T W B_e & B^T W B \end{bmatrix}^{-1} \begin{bmatrix} B_e^T W \delta m \\ B^T W \delta m \end{bmatrix}$$

with W the weight matrix ($W^{-1} = E(\epsilon\epsilon^T)$), taken to be completely diagonal in GEODYN. The $\Delta\hat{x}$ part can be shown to be

$$\Delta\hat{x} = \left[B^T W B - B^T W B_e \left(B_e^T W B_e\right)^{-1} B_e^T W B\right]^{-1} \cdot \left[B^T W \delta m - B^T W B_e \left(B_e^T W B_e\right)^{-1} B_e^T W \delta m\right]$$

To effectively remove the electronic bias effects, the last equation states that the normal matrix $B^T W B$ must have $B^T W B_e (B_e^T W B_e)^{-1} B_e^T W \delta m$ subtracted from it. Due to the assumed independence of different measurements, it follows that these quantities which must be subtracted are a sum of contributions

for different satellite passes over various stations

$$B^T W B_e \left(B_e^T W B_e\right)^{-1} B_e^T W B = \sum_{p=1}^{n_b} B_p^T W_p B_{e_p} \left(B_{e_p}^T W_p B_{e_p}\right)^{-1} B_{e_p}^T W_p B_p$$

$$B^T W B_e \left(B_e^T W B_e\right)^{-1} B_e^T W \delta m = \sum_{p=1}^{n_b} B_p^T W_p B_{e_p} \left(B_{e_p}^T W_p B_{e_p}\right) B_{e_p}^T W_p \delta m_p$$

where n_b is the total number of passes with electronic biases in the equipment and the subscript p denotes an array for measurements of pass p. The computation of the equational right hand sides requires the arrays $B_p^T W_p B_p$ = na x 1 array, $B_{e_p}^T W_p B_{e_p}$ = 1 x 1 array, $B_{e_p}^T W_p \delta m_p$ = 1 x 1 array where na is the number of adjusted parameters other than biases affecting the arc in which the biases occur. Thus, na + 2 storage locations must be assigned for every bias which exists at any one time.

The individual biases may be adjusted, based on the previous iteration orbital elements and force model parameters. This bias can then be used, along with the above accumulated arrays to properly correct the sum of weighted squared residuals upon which the program does dynamic editing. Otherwise, however, it will not be possible for the statistical summaries to incorporate the adjusted values of the electronic biases unless substantial additional core is allocated.

A1-6.0 NUMERICAL INTEGRATION PROCEDURE

Cowell's Sum method is used for direct numerical integration of both the equations of motion and the variational equations to obtain the position and velocity and the attendant variational partials at each observation time. Values at the actual observation time are obtained by interpolation between values at even-numbered steps in the integration.

Let us first consider the integration of the equations of motion. These equations are three second order differential equations in position, and would be formulated as six first order equations in position and velocity if a first order integration scheme were used for their solution. For reasons of increased accuracy and stability, the position vector $\bar{r}$ is obtained by a second order integration of the accelerations $\ddot{\bar{r}}$, where as the velocity vector $\dot{\bar{r}}$ is obtained as the solution of a first order system. These are both multi-step methods requiring at least one derivative evaluation on each step.

A1-6.1 Integration for Position and Velocity Components

To integrate the position components, the predictor formula

$$\bar{r}_{n+1} = \left(S_2 + \sum_{p=0}^{q} \gamma_p^* \ddot{\bar{r}}_{n-p} \right) h^2$$

is applied, followed by a Cowell corrector formula

$$\bar{r}_{n+1} = \left(S_2 + \sum_{p=0}^{q} \gamma_p \ddot{\bar{r}}_{n-p+1} \right) h^2$$

The velocity components are obtained using the predictor formula

$$\dot{\bar{r}}_{n+1} = \left(S_1 + \sum_{p=0}^{q+1} \beta_p^* \ddot{\bar{r}}_{n-p} \right) h$$

followed by an Adams-Moulton corrector formula

$$\dot{\bar{r}}_{n+1} = \left(S_1 + \sum_{p=0}^{q+1} \beta_p \ddot{\bar{r}}_{n-p+1} \right) h,$$

where S_1 and S_2 are the first and second sums of the accelerations.

In these integration formulae, h is the integration step size, q is the order of the integration less 2, and γ_p, γ_p^*, β_p and β_p^* are coefficients of integration.

A1-6.2 Integration of the Variational Equations

Let us next consider the integration of the variational equations (see A1-4.0). These equations may be written as

$$\ddot{Y} = [AB] \begin{bmatrix} Y \\ \dot{Y} \end{bmatrix} + f$$

where

$$\begin{bmatrix} Y \\ \dot{Y} \end{bmatrix} = X_m$$

and, partitioning according to position and velocity partials,

$$[A\ B] = [U_{2c} + D_r].$$

See A1-4.0 for definitions of matrices involved.

Because A, B, and f are functions only of the orbital parameters, the integration can be and is performed using only corrector formulae. (Note that A, B and f must be evaluated with the final correction values of $\bar{r}_{n+1}$ and $\dot{\bar{r}}_{n+1}$.)

In the above corrector formulae, we substitute the equation for $\ddot{Y}$ and solve explicitly for Y and $\dot{Y}$:

$$\begin{bmatrix} Y_{n+1} \\ \dot{Y}_{n+1} \end{bmatrix} = (I - H)^{-1} \begin{bmatrix} \bar{X}_n \\ \bar{V}_n \end{bmatrix}.$$

Under certain conditions, a reduced form of this solution is used. It can be see from the variational and observation equations that if drag is not a factor and there are no range-rate or doppler measurements, the velocity variational partials are not used. There is then no need to integrate the velocity variational equations. In the integration algorithm, the B matrix is zero and (I-H) is reduced to a three-by-three matrix.

Backwards integration involves only a few simple modifications to these normal or forward integration procedures. The step size is made negative and

the time completion test needs to be rephrased. The step size for these integration procedures can be selected on the basis of perigee height and the eccentricity of the orbit if it is desired.

For a starting scheme, a Taylor series approximation is used to predict initial values of position and velocity. With these starting values, the Sum array (S_1 and S_2 variables) is evaluated. The loop is closed by interpolating for the positions and velocities not at epoch and their accelerations evaluated. The sums are now again evaluated.

A1-6.3 Interpolation

In this procedure interpolation is used for two functions. The first is the interpolation of the orbit elements and variational partials to the observation times; the second is the interpolation for mid-points when the integrator is decreasing the step size in the varistep mode of integration.

The formulas used are:

$$X(t+\Delta t) = \left(S_2(t) + \left(\frac{\Delta t}{h} - 1 \right) S_1(t) + \sum_{i=0}^{n} C_i(\Delta t) f_{n-i} \right) h^2$$

for positions and

$$\dot{X}(t+\Delta t) = \left(S_1(t) + \sum_{i=0}^{n} C_i'(\Delta t) f_{n-i} \right) h$$

for velocities.

S_1 and S_2 are the first and second sums carried along by the integration, f's are the back values of acceleration, h the step size, and C_i, C_i' are the interpolation coefficients. See Velez and Brodsky, 1969, for more complete information.

REFERENCES TO APPENDIX A1.

1. Devine, C. J., JPL Development Ephemeris Number 19, JPL Technical Report 32-1181, Pasadena, California, 1967.

2. Explanatory Supplement to the Astronomical Ephemeris and the American Ephemeris and Nautical Almanac, H. M. Nautical Almanac Office, 1961.

3. Jacchia, L. G., Static Diffusion Models of the Upper Atmosphere with Empirical Temperatures Profiles, Special Report 170, Smithsonian Institution Astrophysical Observatory, Cambridge, Massachusetts, 1965.

4. Martin, T. V., C. C. Goad, M. M. Chin and N. C. Mullins, GEODYN, Vol. I, II, III and IV, Wolf Research and Development Corporation, Riverdale, Maryland, 1972.

5. Maury, Jr., J. L. and G. D. Brodsky, Cowell Type Numerical Integration as Applied to Satellite Orbit Computations, Goddard Space Flight Center, X-553-69-46, 1969.

6. Velez, C. E. and G. P. Brodsky, Geostar-1, A Geopotential and Station Position Recovery System, Goddard Space Flight Center, X-553-69-544, 1969.

7. Wolf Research and Development Corporation, Error Models for Solid Earth and Ocean Tidal Effects in Satellite Systems Analysis, Riverdale, Maryland, 1972.

APPENDIX A2 . . . . . GEOMETRIC METHOD

APPENDIX A2

GEOMETRIC METHODS FOR SIMULTANEOUS OBSERVATIONS INCLUDING CONSTRAINTS FROM DATUM SURVEY

CONTENTS

		Page
A2-1.0	TECHNIQUE FOR THE NORMAL EQUATIONS	A2-3
A2-2.0	COORDINATE SYSTEM	A2-6
A2-3.0	COPLANARITY EQUATION	A2-6
A2-4.0	LENGTH EQUATION	A2-8
A2-5.0	CONDITION EQUATIONS FOR CONSTRAINTS	A2-13
A2-6.0	CORRELATED OBSERVATIONS	A2-15

APPENDIX A2

Geometric Methods for Simultaneous Observations
Including Constraints from Datum Survey

Least squares normal equations are derived for the adjustment of station coordinates. The method is based upon the technique of formulating reduced condition equations where the satellite parameters have been eliminated. The data considered consists of simultaneous events from MOTS (Minitrack Optical Tracking System) and laser systems on GEOS-I and II, the BC-4 worldwide camera network on PAGEOS, and local datum survey ties and baselines. The reduced condition equations are developed in this appendix and a case is considered for the treatment of correlated observations.

A2-1.0 TECHNIQUE FOR THE NORMAL EQUATIONS

The mathematical analysis leading to the formation of normal equations for the geometric adjustment of coordinates of tracking stations is based on the following type of events:

1. Two cameras observe the satellite simultaneously
2. Three cameras observe the satellite simultaneously
3. Four cameras observe the satellite simultaneously
4. Two cameras and one laser observe the satellite simultaneously.

Condition equations resulting from a given set of simultaneous observations are of two types:

- Coplanarity equation, which requires that two observing stations and their directions to the satellite lie in the same plane.
- Length equation, which requires that the satellite position satisfying the two-station coplanarity relationship also agrees with the range from a third station.

Corresponding to each event condition equations of the following form are used:

$$\sum_{i}^{m} a_i v_i + \sum_{j}^{n} b_j x_j + c = 0 \qquad (1)$$

where a_i, b_j, and c are known constants derived in the subsequent sections, c is the discrepancy in the condition equation

v_i are the unknown residuals (adjusted minus observed values)

x_j are the unknown corrections to stations' Cartesian coordinates (adjusted minus initial values)

m is the number of observed quantities

n is the number of unknown coordinates.

The number and types of condition equations for events 1 through 4 above are as follows:

- For a two-camera event, one coplanarity equation is used.
- For a three-camera event, three coplanarity equations are used.
- For a four-camera event, five coplanarity equations are used.
- For a two-camera, single-laser event, one coplanarity equation and one length equation are used.

The number of condition equations for each event corresponds to the number of observations less three, since the observation equations are reduced to a form where the three satellite position coordinates are eliminated. Each observing camera contributes two observations in an event and an observing laser contributes one observation. Each of the coplanarity equations for an event involves distinct pairs of observing stations.

Additional condition (constraint) equations specify coordinate differences and also take the form of equation (1). Constraints are treated statistically, similar to observation equations, where values and accuracies are obtained from a priori information based on datum survey. Two types of constraint equations are applied:

- Distance equations (baselines), which require the distance between two stations to remain near a given value
- Coordinate-shift equations, which require the differences between coordinates of two nearby stations to remain near a given value. This constraint is used to connect the stations in the geometric geodesy with those in the dynamic satellite geodesy.

For a geometric only solution a third type of statistical constraint may be applied on individual station coordinates in order to fix the origin of the system. A priori values for these constraints should be taken from a different source than datum survey such as from a previously determined geocentric solution in

a center of mass reference frame. This constraint is not used in the combination solution with dynamic satellite geodesy.

For each event (or constraint) k, denote the associated condition equations of the form (1) in matrix notation as

$$A_k V_k + B_k X + C_k = 0, \tag{2}$$

for which an example of the dimensions and elements of the matrices are given below. Minimizing Q below w.r.t. the unknown station coordinates in X and residuals in V_k will lead to the formation of the normal matrix equation. The form Q is

$$Q = \sum_{k=1}^{K} (V_k^T W_k V_k - 2\lambda_k^T (A_k V_k + B_k X + C_k)) \tag{3}$$

where W_k is the diagonal weight matrix for the observations in V_k and each λ_k is a column vector of Lagrangian multipliers corresponding to the number of condition equations in event k. The resulting normal matrix equation to be combined with the gravimetric and dynamic satellite geodesy systems is

$$JX + \sum_{k=1}^{K} B_k^T M_k^{-1} C_k = N, \tag{4}$$

where

$$J = \sum_{k=1}^{K} (B_k^T M_k^{-1} B_k), \tag{5}$$

$$M_k = (A_k W_k^{-1} A_k^T) \tag{6}$$

The largest dimension of M_k is 5×5 corresponding to event of type 3 where there are 5 coplanarity equations of condition. This case has 8 observations and the dimensions of A_k, V_k, B_k, and C_k are respectively 5×8, 8×1, $5 \times N_x$, and 5×1. N_x is the total number of all station coordinates and B_k ($5 \times N_x$) would contain for each of the 5 rows only 6 non-zero elements, corresponding to the b_j coefficients in (1) for each distinct coplanarity equation involving two observing stations. Each row of A_k has 4 non-zero elements corresponding to the a_i coefficients in (1), associated with the two observing stations in each coplanarity equation.

By employing a suitable set of constraints including those that fix the origin, N may be set equal to zero and a geometric only solution for X can be derived from (4).

Condition equations for coplanarity, length, and constraints are developed in sections 2 through 5 and section 6 treats a case for correlated observations.

A2-2.0 COORDINATE SYSTEM

Camera observations in α and δ are transformed from right ascension α and declination δ to earth-fixed angles β and γ. The conversion of α and δ, as corrected for precession, nutation, and polar motion, to the angles β and γ is straightforward. The topocentric angle γ is measured with respect to the equatorial plane and is equivalent to δ, i.e., $\gamma = \delta$. The angle β is measured from the Greenwich meridian in a plane parallel to the equator and is

$$\beta = \alpha - \text{GHA} \tag{7}$$

where GHA is the Greenwich Hour Angle at the epoch of the observation.

A2-3.0 COPLANARITY EQUATION

The coplanarity equation requires that the volume of the parallelepiped defined by the two station-to-satellite vectors and the station-to-station vector and their respective errors be zero. The two station-to-satellite vectors are defined in the local terrestrial coordinates as

$$\vec{p}_i = u_i \hat{i} + v_i \hat{j} + w_i \hat{K} \tag{8}$$

where

$$u_i = \cos \gamma_i \cos \beta_i$$

$$v_i = \cos \gamma_i \sin \beta_i \qquad (i = 1, 2)$$

$$w_i = \sin \gamma_i$$

The station-to-station direction vector $\vec{p}_3$ is similarly defined in spherical coordinates by use of

$$\beta_3 = \tan^{-1}\left(\frac{y_2 - y_1}{x_2 - x_1}\right) \qquad 0 \le \beta_3 \le 2\pi \tag{9}$$

$$\gamma_3 = \tan^{-1}\left[\frac{z_2 - z_1}{((x_2 - x_1)^2 + (y_2 - y_1)^2)^{1/2}}\right] \quad -\frac{\pi}{2} \leq \gamma_3 < \frac{\pi}{2}, \tag{10}$$

where x, y, z are the Cartesian coordinates and the range between the station is

$$r_3 = ((x_2 - x_1)^2 + (y_2 - y_1)^2 + (z_2 - z_1)^2)^{1/2} \tag{11}$$

The volume of the parallelepiped defined by these vectors ($\vec{p}_1$, $\vec{p}_2$, $\vec{p}_3$) is given by their triple scalar product, which is the determinant

$$F_0 = \begin{vmatrix} \cos\gamma_1 \cos\beta_1 & \cos\gamma_2 \cos\beta_2 & \cos\gamma_3 \cos\beta_3 \\ \cos\gamma_1 \sin\beta_1 & \cos\gamma_2 \sin\beta_2 & \cos\gamma_3 \sin\beta_3 \\ \sin\gamma_1 & \sin\gamma_2 & \sin\gamma_3 \end{vmatrix} \tag{12}$$

and the adjusted volume through linear expansion is

$$F = F_0 + \Delta F = 0$$

The coefficients of the expansion are then given by

$$a_1 \equiv \frac{\partial F_0}{\partial \beta_1} = \cos\gamma_1 \sin\gamma_2 \cos\gamma_3 \cos(\beta_3 - \beta_1) - \cos\gamma_1 \cos\gamma_2 \sin\gamma_3 \cos(\beta_2 - \beta_1) \tag{13}$$

$$a_2 \equiv \frac{\partial F_0}{\partial \gamma_1} = \cos\gamma_1 \cos\gamma_2 \cos\gamma_3 \sin(\beta_3 - \beta_2) - \sin\gamma_1 \cos\gamma_2 \sin\gamma_3 \sin(\beta_2 - \beta_1)$$
$$+ \sin\gamma_1 \sin\gamma_2 \cos\gamma_3 \sin(\beta_3 - \beta_1) \tag{14}$$

$$a_3 \equiv \frac{\partial F_0}{\partial \beta_2} = \cos\gamma_2 [\cos\gamma_1 \sin\gamma_3 \cos(\beta_2 - \beta_1) - \sin\gamma_1 \cos\gamma_3 \cos(\beta_3 - \beta_2)] \tag{15}$$

$$a_4 \equiv \frac{\partial F_0}{\partial \gamma_2} = -\cos\gamma_1 \cos\gamma_2 \cos\gamma_3 \sin(\beta_3 - \beta_1) - \sin\gamma_1 \sin\gamma_2 \cos\gamma_3 \sin(\beta_3 - \beta_2)$$

$$- \cos\gamma_1 \sin\gamma_2 \sin\gamma_3 \sin(\beta_2 - \beta_1) \tag{16}$$

$$b_1 \equiv \frac{\partial F_0}{\partial \beta_3} = \cos\gamma_3 [\sin\gamma_1 \cos\gamma_2 \cos(\beta_3 - \beta_2) - \cos\gamma_1 \sin\gamma_2 \cos(\beta_3 - \beta_1)] \tag{17}$$

$$b_2 \equiv \frac{\partial F_0}{\partial \gamma_3} = \cos\gamma_1 \cos\gamma_2 \cos\gamma_3 \sin(\beta_2 - \beta_1) - \sin\gamma_1 \cos\gamma_2 \sin\gamma_3 \sin(\beta_3 - \beta_2)$$

$$+ \cos\gamma_1 \sin\gamma_2 \sin\gamma_3 \sin(\beta_3 - \beta_1) \tag{18}$$

Since β_1, γ_1, β_2, and γ_2 are observations, $\Delta\beta_1$, $\Delta\gamma_1$, $\Delta\beta_2$, and $\Delta\gamma_2$ are residuals and are designated v_1, v_2, v_3, and v_4, respectively. $\Delta\beta_3$ and $\Delta\gamma_3$ are the inter-station direction adjustments. The variables to be solved for are corrections to the stations Cartesian coordinates. The transformation of unknowns from inter-station direction to Cartesian coordinate corrections are given by equation 26. Then there results an equation of the form of (1).

A2-4.0 LENGTH EQUATION

The length equation is developed for two cameras and a laser DME observing the satellite simultaneously. Assume the existence of two cameras (A and B), the laser DME (L), and the satellite (S), where directions from the cameras to the satellite are observed simultaneously (A to S and B to S) and a range is observed at the same time from L to S. These quantities and auxiliary vectors and angles are shown in Figure A-1. Assumed values of coordinates of the cameras and the laser system are used to calculate initial estimates of the directions and distances between the cameras and the laser. By taking scalar products of the station-to-station and station-to-satellite vectors the cosines of the angles, ξ, η, and ζ are obtained as follows:

$$\cos\xi = \vec{\rho}_1 \cdot \vec{\rho}_2 = \sin\gamma_1 \sin\gamma_2 + \cos\gamma_1 \cos\gamma_2 \cos(\beta_2 - \beta_1) \tag{19}$$

$$\cos\eta = \vec{\rho}_1 \cdot \vec{\rho}_3 = \sin\gamma_1 \sin\gamma_3 + \cos\gamma_1 \cos\gamma_3 \cos(\beta_3 - \beta_1) \tag{20}$$

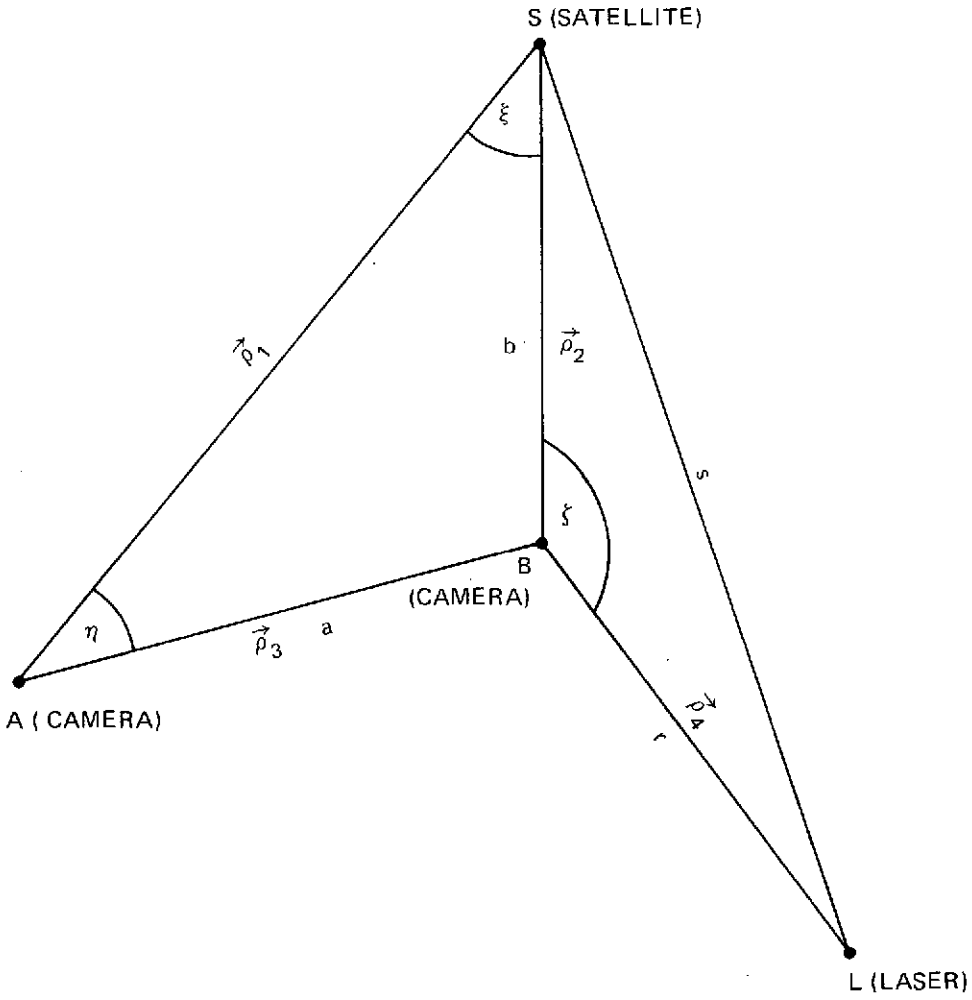

Figure A-1. Geometry for Two-Camera and One Laser DME Observing Simultaneously

$$\cos \zeta = \vec{\rho}_2 \vec{\rho}_4 = \sin \gamma_2 \sin \gamma_4 + \cos \gamma_2 \cos \gamma_4 \cos(\beta_4 - \beta_2) \tag{21}$$

where $\beta_1, \gamma_1, \beta_2$, and γ_2 are directions to the satellite,

β_3, γ_3 are the inter-station angles for the two cameras, and

β_4, γ_4 are the inter-station angles for one camera and the laser system.

From Figure A-1 the law of cosines will give, corresponding to the laser length s

$$F = r^2 + b^2 - 2br \cos \zeta - s^2 = 0, \tag{22}$$

and the law of sines will give for b above

$$b = a \frac{\sin \eta}{\sin \xi}.$$

Through the use of (19) through (21) we expand F linearly about the values of a, r, β_3, γ_3, β_4, γ_4, obtained from the initial station coordinates, and the values of β_1, γ_1, β_2, γ_2, and s_0 from the observations. Then we have using differentials as adjustments ($d \equiv \Delta$)

$$F = F_0 + \frac{\partial F}{\partial a} da + \frac{\partial F}{\partial r} dr + \frac{\partial F}{\partial \beta_3} d\beta_3 + \ldots + \frac{\partial F}{\partial s} ds = 0$$

Divide F through by $q = 2(b - r \cos \zeta)$ and denote the result by

$$a_1 d\beta_1 + a_2 d\gamma_1 + a_3 d\beta_2 + a_4 d\gamma_2 + a_5 ds + b_1 d\beta_3 + b_2 d\gamma_3 + b_3 da + b_4 d\beta_4 + b_5 d\gamma_4$$

$$+ b_6 dr + C = 0 \tag{23}$$

where $C = F_0 / q$, and the differentials on the a_i coefficients are the observation residuals v_i for i = 1 to 5. This represents the laser length equation. The coefficients and C are evaluated from the initial values, where F_0 is obtained from the misclosure of (22) and the coefficients in (23) are as follows:

$$a_1 = P_1/\sin\xi - P_5/\sin\eta \qquad b_1 = P_5/\sin\eta \tag{24}$$

$$a_2 = P_2/\sin\xi - P_6/\sin\eta \qquad b_2 = -P_8/\sin\eta$$

$$b_3 = \sin\eta/\sin\xi$$

$$a_3 = -P_1/\sin\xi - P_9/\sin\zeta \qquad b_4 = P_9/\sin\zeta$$

$$a_4 = P_4/\sin\xi - P_{10}/\sin\zeta \qquad b_5 = -P_{12}/\sin\zeta$$

$$a_5 = -s/(b - r\cos\zeta) \qquad b_6 = (r - b\cos\zeta)/(b - r\cos\zeta)$$

and where the P's are given as

$$P_1 = b\cot\xi[\cos\gamma_2 \sin(\beta_2 - \beta_1)] \cos\gamma_1$$

$$P_2 = b\cot\xi[\cos\gamma_1 \sin\gamma_2 - \sin\gamma_1 \cos\gamma_2 \cos(\beta_2 - \beta_1)]$$

$$P_3 = -P_1$$

$$P_4 = b\cot\xi[\sin\gamma_1 \cos\gamma_2 - \cos\gamma_1 \sin\gamma_2 \cos(\beta_2 - \beta_1)]$$

$$P_5 = \frac{a\cos\eta}{\sin\xi}[\cos\gamma_1 \cos\gamma_3 \sin(\beta_3 - \beta_1)]$$

$$P_6 = \frac{a\cos\eta}{\sin\xi}[\cos\gamma_1 \sin\gamma_3 - \sin\gamma_1 \cos\gamma_3 \cos(\beta_3 - \beta_1)]$$

$$P_7 = -P_5$$

$$P_8 = \frac{a\cos\eta}{\sin\xi}[\sin\gamma_1 \cos\gamma_3 - \cos\gamma_1 \sin\gamma_3 \cos(\beta_3 - \beta_1)]$$

$$P_9 = \left(\frac{br\sin\zeta}{b - r\cos\zeta}\right)[\cos\gamma_2 \cos\gamma_4 \sin(\beta_4 - \beta_2)]$$

$$P_{10} = \left(\frac{br \sin \zeta}{b - r \cos \zeta}\right) [\cos \gamma_2 \sin \gamma_4 - \sin \gamma_2 \cos \gamma_4 \cos(\beta_4 - \beta_2)]$$

$$P_{11} = - P_9$$

$$P_{12} = \left(\frac{br \sin \zeta}{b - r \cos \zeta}\right) [\sin \gamma_2 \cos \gamma_4 - \cos \gamma_2 \sin \gamma_4 \cos(\beta_4 - \beta_2)]$$

In order to obtain the desired form (1) for Cartesian station coordinates, the coplanarity and length equations are transformed from γ, β, r variables to x, y, z variables by using the relationships

$$\begin{aligned} x_2 - x_1 &= r \cos \gamma \cos \beta \\ y_2 - y_1 &= r \cos \gamma \sin \beta \\ z_2 - z_1 &= r \sin \gamma \end{aligned} \tag{25}$$

Differentiating these expressions yields

$$\begin{bmatrix} dx_2 - dx_1 \\ dy_2 - dy_1 \\ dz_2 - dz_1 \end{bmatrix} = \begin{bmatrix} - r \cos \gamma \sin \beta & - r \sin \gamma \cos \beta & \cos \gamma \cos \beta \\ r \cos \gamma \cos \beta & - r \sin \gamma \sin \beta & \cos \gamma \sin \beta \\ 0 & r \cos \gamma & \sin \gamma \end{bmatrix} \begin{bmatrix} d\beta \\ d\gamma \\ dr \end{bmatrix} \tag{26}$$

Inverting Equation 26 produces the transformation

$$\begin{bmatrix} d\beta \\ d\gamma \\ dr \end{bmatrix} = \begin{bmatrix} \frac{-\sin \beta}{r \cos \gamma} & \frac{\cos \beta}{r \cos \gamma} & 0 \\ \frac{-\sin \gamma \cos \beta}{r} & \frac{-\sin \gamma \sin \beta}{r} & \frac{\cos \gamma}{r} \\ \cos \gamma \cos \beta & \cos \gamma \sin \beta & \sin \gamma \end{bmatrix} \begin{bmatrix} dx_2 - dx_1 \\ dy_2 - dy_1 \\ dz_2 - dz_1 \end{bmatrix} \tag{27}$$

A2-5.0 CONDITION EQUATIONS FOR CONSTRAINTS

The three types of condition equations are: (1) coordinate equations, (2) distance equations, and (3) coordinate-shift equations. As indicated previously constraints for station coordinates, distances (baselines), and coordinate shifts (local datum ties) are based upon a priori information. Such information is treated statistically as in the case of satellite observations, and hence weights are applied corresponding to a priori errors.

A2-5.1 Coordinate Equation

Assume the input coordinates of the ith station are coordinates for which a priori information is available. Let the input values of X_i, Y_i, Z_i be X_{io}, Y_{io}, Z_{io}, and denote the adjusted coordinates as

$$\begin{aligned} dx_i &= X_1 - X_{io} \equiv x_{i-2} \\ dy_i &= Y_i - Y_{io} \equiv x_{i-1} \\ dz_i &= Z_i - Z_{io} \equiv x_i \end{aligned} \tag{28}$$

then the constraint equations in the form of equation (1) are simply

$$\begin{aligned} v_{i-2} - x_{i-2} &= 0 \\ v_{i-2} - x_{i-1} &= 0 \\ v_i - x_i &= 0 \end{aligned} \tag{29}$$

A2-5.2 Distance Equations (Baselines)

The condition equation for the baseline distance q between the rth and sth ground stations is

$$-dq + \cos\gamma\cos\beta(dx_s - dx_r) + \cos\gamma\sin\beta(dy_s - dy_r) + \sin\gamma(dz_s - dz_r) = 0 \tag{30}$$

where γ and β are used as in (9) and (10) and the differentials are the unknown station adjustments. The adjustment

$$\begin{aligned} dq &= q - q_c = (q - q_0) - (q_c - q_0) \\ &= v - C \end{aligned} \tag{31}$$

where q is the solution value, q_c is the computed value based upon the initial station coordinates, and q_0 is the a priori value for the constraint.

In conformity with the previous notation the terms dx_s, dy_s, dz_s, dx_r, dy_r, and dz_r are replaced by x_{s-2}, x_{s-1}, x_s, x_{r-2}, x_{r-1}, s_r, and dq by (31) to obtain

$$-v + \cos\gamma\cos\beta(x_{s-2} - x_{r-2}) + \cos\gamma\sin\beta(x_{s-1} - x_{r-1}) + \sin\gamma(x_s - x_r) + C = 0 \quad (32)$$

A2-5.3 Coordinate-Shift Equations

For two nearby stations denote the difference in coordinates as

$$\begin{aligned} D_x &= x_2 - x_1 \\ D_y &= y_2 - y_1 \\ D_z &= z_2 - z_1 \end{aligned} \quad (33)$$

Since the results are similar for the three equations we will treat just one equation of condition. For the x component the differential is

$$-dD_x + dx_2 - dx_1 = 0, \quad (34)$$

and as in the case of the distance equation (31)

$$dD_x = v_x - C_x, \qquad v_x = D_x - D_{x_0}, \qquad C_x = D_{x_c} - D_{x_0} \quad (35)$$

where D_x is the unknown difference, D_{x_0} is obtained from local survey station coordinates, and D_{x_c} is computed from the initial input of the station coordinates. For the ith and jth stations, using the notation of the form (1) where differentials are replaced by corrections x_q and x_p, the condition equations for (33) are

$$\begin{aligned} -v_x + x_{j-2} - x_{i-2} + C_x &= 0 \\ -v_y + x_{j-1} - x_{i-1} + C_y &= 0 \\ -v_z + x_j \quad - x_i \quad + C_z &= 0 \end{aligned} \quad (36)$$

A2-6.0 COORELATED OBSERVATIONS

The model described above was developed for camera systems that observed simultaneously the flashing lamps on GEOS-I and II, and then the model was employed to include the BC-4 camera network that observed the PAGEOS satellite. A BC-4 photograph taken on PAGEOS by an observing station, s, was reduced to 7 time points (k = 1 to 7) of satellite observation angles (γ_k^s, β_k^s). The reduced observations γ_k^s and β_k^s are correlated separately* in each type among the points k = 1 to 7. The modeling for the correlated observations is presented.

Consider 7 events of the type (1), (2), or (3) described in section 1, where respectively 2, 3, or 4 stations (S = 2, 3, or 4) observe the satellite simultaneously at each of the 7 reduced photographic points k = 1 to 7. Thus for each event there are 2S simultaneous observations, namely (γ_k^s, β_k^s) for s = 1 to S. Let p denote this configuration of S stations and 7 events, then for each p there are 7 sets of matrix condition equations of the form (2). Denote these as

$$A_p V_p + B_p X + C_p = 0 \tag{37}$$

where by row partitioning for k = 1 to 7

$$\begin{aligned} V_p &= [V_k^p] \\ C_p &= [C_k^p] \\ B_p &= [B_k^p] \end{aligned} \tag{38}$$

and A_k^p lies along the diagonal submatrix path of A_p (with zero submatrices for off diagonal blocks)

$$A_p = [\text{DIAG } A_k^p] \tag{39}$$

The submatrices V_k^p, B_k^p, and A_k^p are given as before in (2) for a particular event, but here the event type for S = 2, 3, or 4 stations is fixed for the 7 events for a given configuration p.

Denote the variance-covariance matrix of the observation errors as

$$P_p = E(\bar{V}_p \bar{V}_p^T) \tag{40}$$

where $\bar{V}_p$ corresponds to the observation errors (noise) in V_p.

*Cross correlations between γ and β are assumed negligible in this analysis.

The normal equations for the BC-4 observations is obtained by minimizing

$$Q = \sum_{p} Q_p \tag{41}$$

for the unknowns V_p and X, where

$$Q_p = V_p^T P_p^{-1} V_p - 2(A_p V_p + V_p X + C_p)^T \lambda_p \tag{42}$$

and

$$\lambda_p = [\lambda_{\ell k}^p]$$

for which $\lambda_{\ell k}^p$ is a vector of Lagrangian multipliers defined as in (3) for a given event. Hence the normal equations will have the form given in (4) through (6). Thus for each p the normal equations are

$$J_p X + B_p^T M_p^{-1} C_p = N_p \tag{43}$$

where

$$J_p = B_p^T M_p^{-1} B_p$$

$$M_p = (A_p P_p A_p^T), \tag{44}$$

and the total set of normal equations for all p are then

$$N' = \sum_{p} N_p.$$

It is of interest to compare the matrix M_p derived from 7 events to that of $M_{\ell k}$ given in (6) for a single event k. Take the case of S = 4 for which the dimensions $A_{\ell k}$, $V_{\ell k}$, and $W_{\ell k}$ were given under (6) respectively as 5×8, 8×1, and 8×8, and for which there were 8 observations and 5 coplanarity equations of condition from the 4 observing stations in a given event. Consider 7 events of the same type as in the configuration p for S = 4, denote $M_{\ell k}$ as $M_{\ell k}^p$ for k = 1 to 7, and assume correlations are absent as in the previous modeling. Then

$$M_p = \begin{bmatrix} M_1^p & & & 0 \\ & M_2^p & & \\ & & \ddots & \\ 0 & & & M_7^p \end{bmatrix}_{35\times 35} \equiv [\mathrm{DIAG}\, M_k^p] \tag{45}$$

where

$$M_k^p = [A_k^p (W_k^p)^{-1} (A_k^p)^T]_{5\times 5} \tag{46}$$

and since correlations are assumed absent here

$$P_p = [\mathrm{DIAG}(W_k^p)^{-1}].$$

With correlations the same diagonal blocks in (45) arise for M_p in (44) since in each event k all observations are uncorrelated, but similar off diagonal blocks also exist which is now shown. Using the submatrices V_k^p for V_p in (38) and dropping the superscript p on the submatrices, then the variance-covariance matrix in (40) becomes

$$P_p = E(\bar{V}_p \bar{V}_p^T) = [E(\bar{V}_k \bar{V}_\ell^T)] \quad \text{for } k = 1 \text{ to } 7 \text{ and } \ell = 1 \text{ to } 7, \tag{47}$$

which corresponds to 49 sublocks or submatrices in P_p. For a given event k and ℓ the only covariances occur when the station s and the angle γ_k^s or β_k^s are the same. Denote the observation errors for a given k as (where T ≡ true, o ≡ observed)

$$\bar{V}_k = \begin{bmatrix} \gamma_k^1(T) - \gamma_k^1(0) \\ \beta_k^1(T) - \gamma_k^1(0) \\ \vdots \\ \gamma_k^s(T) - \gamma_k^s(0) \\ \beta_k^s(T) - \beta_k^s(0) \end{bmatrix}_{2S\times 1} \equiv [\bar{v}_{ik}], \quad i = 1 \text{ to } 2S, \tag{48}$$

then for a given k and ℓ

$$E(\bar{V}_k \bar{V}_\ell^T) = [E(\bar{v}_{ik} \bar{v}_{j\ell})]_{2S \times 2S} \quad i = 1 \text{ to } 2S, \quad j = 1 \text{ to } 2S, \tag{49}$$

and from the definition of the correlations

$$\begin{aligned} E(\bar{v}_{ik} \bar{v}_{j\ell}) &= \sigma^2_{ij}(k, \ell) = 0 \quad \text{for } i \neq j \text{ for all } k \text{ and } \ell \\ &= \sigma^2_{ii}(k, \ell) \qquad \text{for covariances } k \neq \ell, \\ &= \sigma^2_{ii}(k, k) \qquad \text{for variances } k = \ell. \end{aligned} \tag{50}$$

Thus, in each sublock of a given k and ℓ, the off diagonal elements are zero and

$$\begin{aligned} E(\bar{V}_k \bar{V}_\ell^T) &= [\text{DIAG } \sigma^2_{ij}(k, \ell)]_{2S \times 2S} \\ &\equiv D_{k\ell} \end{aligned} \tag{51}$$

and

$$P_p = [D_{k\ell}] \quad (k, \ell = 1 \text{ to } 7), \tag{52}$$

Denote

$$M_p = [M_{k\ell}] \quad (k, \ell = 1 \text{ to } 7), \tag{53}$$

and with use of (38), (39), and (52) in (44) then by (53)

$$M_{k\ell} = [A_k D_{k\ell} A_\ell^T]_{(2S-3) \times (2S-3)} \tag{54}$$

Now

$$\begin{aligned} M_{kk} &= A_k D_{kk} A_k^T \\ &= A_k W_k^{-1} A_k^T = M_k, \end{aligned} \tag{55}$$

which is the same as in (46) for the uncorrelated case.

The block form $[M_{k\ell}]$ for M_p, where $M_{k\ell}$ is given in (54), provides a convenient method for the computations of M_p. However in the present case of correlated observations there are 49 such blocks, whereas only the 7 diagonal blocks M_{kk} are computed for uncorrelated observations as in (45) or (55). The largest inverse matrix M_p to be inverted occurs for the case of $S = 4$ and which has dimension 35×35, whereas previously for the case of uncorrelated observations the largest matrix was 5×5. Correlations are generally large among the

reduced observations of a photograph. Thus the geometric normal equations should be analyzed further to investigate the overall effect of the correlation on the final combination solution.

APPENDIX A3 . . . . . GRAVIMETRIC METHOD

APPENDIX A3

GRAVIMETRIC METHOD FOR MEAN ANOMALY DATA

CONTENTS

		Page
A3-1.0	INTRODUCTION TO TECHNIQUE	A3-3
A3-1.1	Synopsis of the Method and Procedure	A3-3
A3-2.0	GRAVITY FUNCTIONS FOR THE EARTH	A3-5
A3-2.1	Gravity Potential for the Geoid	A3-5
A3-2.2	Reference Potential and Earth Ellipsoid	A3-6
A3-3.0	GRAVITY FUNCTIONS BASED UPON INITIAL CONDITIONS	A3-7
A3-3.1	Initial Potential and Gravity System for GEM 6	A3-7
A3-3.2	Geometry of the Gravity System	A3-7
A3-3.3	Initial Constants and Reference Parameters	A3-8
A3-4.0	EXPANSION OF THE GRAVITY FUNCTION FOR THE GEOID	A3-10
A3-4.1	Computations for Gravity and Geoid Height	A3-12
A3-5.0	OBSERVATION EQUATION AND NORMAL EQUATIONS	A3-15
A3-5.1	Data Point of Gravity Anomaly	A3-15
A3-5.2	Conversion of Rapp's Gravity Formula	A3-15
A3-5.3	Observation Equation for Mean Gravity Anomaly	A3-16
A3-5.3.1	Truncation, Modeling, and Data Errors in the Observation Equation	A3-17
A3-5.4	Normal Equations for Gravity Data	A3-18
A3-6.0	ADJUSTMENT OF REFERENCE PARAMETERS	A3-20

CONTENTS (Continued)

Page

A3-7.0 FORMULAE EMPLOYED FOR ANALYSIS OF MODELS WITH USE OF MEAN GRAVITY ANOMALY DATA A3-23

A3-7.1 Derivation of Gravity Anomaly Formula A3-23
A3-7.2 Mean Gravity Anomaly Residual and Errors A3-25
A3-7.3 Degree Variances of Gravity Anomaly and Error of Commission in Anomaly A3-26

REFERENCES A3-27

APPENDIX A3

GRAVIMETRIC METHOD FOR MEAN ANOMALY DATA

A3-1.0 INTRODUCTION TO TECHNIQUE

A global set of 5° equal-area (300 n.m. sq.) mean gravity anomalies, formed by Rapp (1972), are modeled to provide for adjustment of potential coefficients through degree and order 16 and a mean value of gravity. Normal equations are prepared in a form to be combined with those obtained from the satellite data. For compatibility and subsequent adjustment of basic earth parameters, the gravity data is modeled with respect to the same initial parameters of the earth and initial values of potential coefficients as used in the satellite normal equations.

Along with the mean gravity anomaly, the data of Rapp includes an error estimate for the anomaly and a center point in terms of geodetic latitude (ϕ') and longitude (λ). The error estimates are employed for weighting the data in the normal equations. The data was based principally upon 1° x 1° mean free-air anomalies, which approximate the undulation of gravity at mean sea level (geoid). In the modeling the gravitational potential for the geoid is expressed in spherical harmonics with coefficients compatible with the gravitational potential of the satellite model.

A3-1.1 Synopsis of the Method and Procedure

The anomaly of gravity for a point p on the geoid is defined as follows:

$$\Delta g_E = g(p) - \gamma_E(q) \tag{1}$$

where q is the normal projection of the point p onto the ellipsoid of the earth and where

$$g(p) = |\nabla W(p)|, \gamma_E(q) = |\nabla U(q)|$$

for which W(p) is the gravity potential for the geoid and U(q) is a reference potential for the earth's ellipsoid of revolution, based upon a set of earth parameters $E = (GM, a_e, f, \omega)$. Functions for the above quantities and their relation to the reference parameters are to be defined, including a gravitational potential which is expressed in spherical harmonics with coefficients ($\bar{C}_{nm}$, $\bar{S}_{nm}$) for degree n and order m.

Similar functions to the above are to be established based upon initial conditions. Initial potential coefficients ($\bar{C}'_{nm}$, $\bar{S}'_{nm}$) and reference parameters E' are

employed which are the same as used with the satellite data, providing for a simultaneous solution of gravity and satellite data for GEM 6. A computed anomaly Δg_c (P), analogous to (1), is formulated based upon the initial conditions.

Mean gravity anomaly data, $\Delta\bar{g}_{OBS}(p)$, is referred to the reference system of GEM 6 and an observation equation is established in the form of the following linear expansion:

$$\Delta\bar{g}_{OBS}(p) - \Delta g_c(P) = \delta g_0 + \delta g_1 (p) + T_N(p) + \bar{e}(p)$$

$$\delta g_1 (p) = \frac{GM}{r^2} \sum_{n=2}^{N} \sum_{m=0}^{n} (n-1) \left(\frac{a_e}{r}\right)^n P_n^m (\sin \phi) \cdot$$

$$(\delta\bar{C}_{nm} \cos (m\lambda) + \delta\bar{S}_{nm} \sin (m\lambda),) \qquad (2)$$

where the spherical coordinates (r, ϕ, λ) refer to the point P, δg_0 is an adjustment to a mean value of gravity and ($\delta\bar{C}_{nm}$, $\delta\bar{S}_{nm}$) are adjustments to potential coefficients from initial values. The truncation error $T_N(p)$ and errors $\bar{e}(p)$, due to the data and the technique, are discussed.

Least squares normal equations are formed with the gravity data for coefficient adjustments complete through degree and order 16 (N = 16). These normal equations are then to be combined with those from the satellite data to give the solution for GEM 6. Adjustments to certain basic earth constants are then formulated from the solution parameters of GEM 6.

The derivation of the method, the gravity functions employed including related constants, and the computational process are presented. Additional gravity formulae, which were used in the report for comparing different potential solutions with use of mean gravity anomaly data, are also derived herein.

A3-2.0 GRAVITY FUNCTIONS FOR THE EARTH

A3-2.1 Gravity Potential for the Geoid

The gravity potential for a point p on the geoid is expressed as follows:

$$W(p) = V(p) + \Phi(p) \tag{3}$$

where the rotational potential is

$$\Phi(p) = \frac{1}{2}\,\omega^2\, r^2 \cos^2\phi$$

and the gravitational potential is given in spherical harmonics as

$$V(p) = \frac{GM}{r}\left\{1 + \sum_{n=2}^{\infty}\sum_{m=0}^{n}\left[\left(\frac{a_e}{r}\right)^n P_n^m(\sin\phi)\right.\right.$$
$$\left.\left.(\bar{C}_{nm}\cos(m\lambda) + \bar{S}_{nm}\sin(m\lambda))\right]\right\}, \tag{4}$$

and where

(r, ϕ, λ)	are respectively the spherical coordinates of distance, latitude, and longitude for the point p
$P_n^m(\sin\phi)$	is the normalized Legendre polynomial of degree n and order m
$\bar{C}_{nm}$, $\bar{S}_{nm}$	are the normalized harmonic coefficients
GM	product of gravitational constant and earth's mass
a_e, f	semi-major axis (a_e) of a mean earth ellipsoid and associated flattening f
ω	angular rotation rate of the earth.

The equipotential surface for the geoid (mean sea level) is

$$W(p) = W_o(E) \tag{5}$$

and gravity thereon is

$$g(p) = |\nabla W(p)|, \tag{6}$$

where E denotes the basic set of earth constants

$$E = (GM, a_e, f, \omega). \tag{7}$$

The constant W_0 is related functionally to the set of constants E and is considered to be determined by them.

A3-2.2 Reference Potential and Earth Ellipsoid

A reference potential for the geoid is employed to define gravity on the earth's ellipsoid, which in turn will be needed to formulate gravity anomaly. The potential is similar in form to W(p) in (3) and is given simply by

$$U(p) = \frac{GM}{r}\left[1 + \bar{C}^*_{20}\left(\frac{a_e}{r}\right)^2 P^0_2(\sin\phi) + \bar{C}^*_{40}\left(\frac{a_e}{r}\right)^4 P^0_4(\sin\phi)\right] + \Phi(p), \tag{8}$$

where $\bar{C}^*_{20}$ and $\bar{C}^*_{40}$ are determined by the basic constants, $E = (GM, a_e, f, \omega)$. For a point q on the earth's ellipsoid, gravity thereon is defined by

$$\gamma_E(q) = |\nabla U(q)| \tag{9}$$

and the ellipsoid has equipotential surface

$$U(q) = U_0(E) = W_0(E). \tag{10}$$

The latter relation $U_0(E) = W_0(E)$, for which $W_0(E) = W(p)$ for mean sea level as in (5), provides for a mean earth ellipsoid with mean equatorial radius a_e. Formulae for the above constants $\bar{C}^*_{20}$, $\bar{C}^*_{40}$, and W_0, as a function of the set $E = (GM, a_e, f, \omega)$, are given in Heiskanen and Moritz (1967).

A gravity formula for $\gamma_E(q)$, in (9), is given as a function of geodetic latitude ϕ' as follows:

$$\gamma_E(q) = \gamma_E(\phi') = g_e(1 + f_1 \sin^2\phi' + f_2 \sin^2 2\phi') \tag{11}$$

where g_e, f_1 and f_2 are constants. The quantity g_e is equitorial gravity on the ellipsoid with an approximate value of 978 cm/sec^2. The constants f_1 and f_2 are in magnitude respectively of the order of flattening f and f^2.

Similar functions as described above are employed based upon initial values for the set E.

A3-3.0 GRAVITY FUNCTIONS BASED UPON INITIAL CONDITIONS

A3-3.1 Initial Potential and Gravity System for GEM 6

Variation of the gravity potential W(p) in (3) will be derived with respect to a computed potential $W_c(P)$. $W_c(P)$ has the same form as W(p) in (3) and is based upon initial potential coefficients and reference parameters E′ corresponding to the set $E = (GM, a_e, f, \omega)$. Analogous to the gravity system for the geoid and the earth's ellipsoid as described in A3-2.0, a computed system for gravity based upon the initial conditions for GEM 6 is defined as follows:

Reference System of Gravity for GEM 6

approximate geoid

$$W_c(P) = U_o(E'), \quad g_c(P) = |\nabla W_c(P)| \tag{12}$$

approximate reference potential

$$U_c(P) = U(P, \bar{C}^{*\prime}_{20}, \bar{C}^{*\prime}_{40}, E') \tag{13}$$

$$U_c(Q) = U_o(E'), \quad \gamma_c(Q) = |\nabla U_c(Q)| \tag{14}$$

where the point P lies on the approximate geoid and the point Q lies on the reference ellipsoid for GEM 6 with parameters E′. The reference potential $U_c(P)$ is given by the form (8) with coefficients $(\bar{C}^{*\prime}_{20}, \bar{C}^{*\prime}_{40})$ and parameters E′. A formula for $\gamma_c(Q)$ is given in the form (11) as

$$\gamma_c(\phi') = g'_e (1 + f'_1 \sin^2 \phi' + f'_2 \sin^2 2\phi'). \tag{15}$$

The geometry relating a point P on the equipotential surface (12) to a point Q on the reference ellipsoid is presently described for the GEM 6 system.

A3-3.2 Geometry of the Gravity Systems

The geometry relating a point p on the geoid with a point q on the ellipsoid for the earth is shown in Figure A3-1. The point p has geodetic coordinates (hg, ϕ', λ) relative to the earth's ellipsoid at the point q (ϕ', λ). The gravity system is based upon the potential coefficients $(\bar{C}, \bar{S})$ for the geoid and the constants $E = (GM, a_e, f, \omega)$. A similar geometry exists for the points P and Q for the gravity system of GEM 6, which is based upon initial potential coefficients $(\bar{C}', \bar{S}')$ and initial parameters E′. The potential $W_c(P)$ is an initial approximation to the geoid and its reference potential $U_c(Q)$ is an initial approximation for that in (8) of the earth. The two systems will be related through a linear expansion of gravity g(p) for the geoid about $g_c(P)$ in terms of adjustments $(\delta\bar{C}, \delta\bar{S})$ and the reference parameters $\delta E = E - E'$.

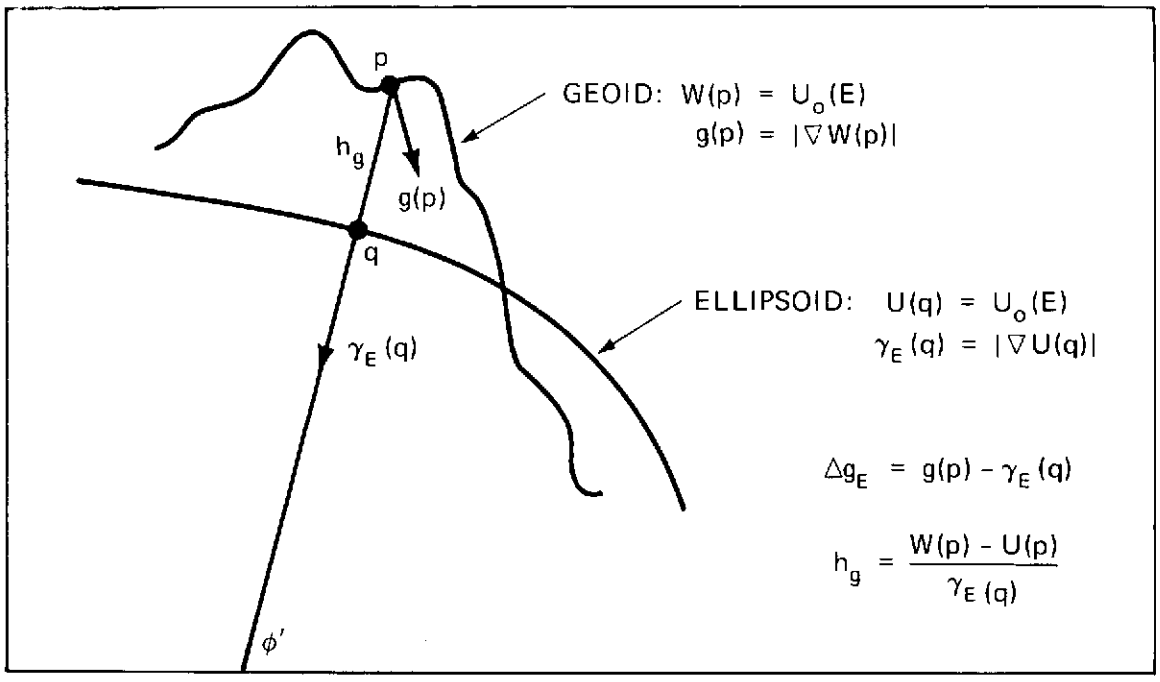

Figure A3-1. Geometry of the Geoid and Earth's Ellipsoid

The gravity anomaly for the earth is defined by (1) as

$$\Delta g_E = g(p) - \gamma_E(q)$$

and that for GEM 6, based upon initial conditions, is

$$\Delta g_c = g_c(P) - \gamma_c(Q)$$

A3-3.3 Initial Constants and Reference Parameters

Initial reference parameters employed for the gravity data are the same set as employed with the satellite data, since both the satellite and gravity data are to be combined simultaneously in GEM 6.

The basic reference constants for GEM 6 are as follows:

$$GM' = 398601.3\,km^3/sec^2$$

$$a_e' = 6378155\,m$$

$$f = 1/298.255$$

$$\omega = 0.7292115146 \times 10^{-4}\ rad/sec \qquad (16)$$

$$E' = (GM', a'_e, f, \omega)$$

Initial constants, derived from the set E′ and used for the computed functions described under (13) and (15), are as follows:

$$\bar{C}^{*\prime}_{20} = -484.17104 \times 10^{-6}$$

$$\bar{C}^{*\prime}_{40} = 0.7903 \times 10^{-6}$$

$$g'_e = 978029.1 \text{ mgal}$$

$$f'_1 = .0053025$$

$$f'_2 = -.00000585 \qquad (17)$$

The above value of flattening f and rotation rate ω are sufficiently accurate for modeling the gravity data. Hence only GM′ and a'_e differ from the set E.

The reference value of GM′ was derived from analysis of satellite data on deep space probes and contains the mass of the atmosphere and earth. This value as indicated was employed for the satellite data on the close earth satellites in GEM 6, but it requires a nominal adjustment to remove the mass of the atmosphere for use with surface gravity data. The adjustment is given by

$$\frac{\delta GM}{GM} = \frac{\delta M}{M} = -.87 \times 10^{-6} \qquad (18)$$

Essentially the value of GM′ is accepted except for the nominal adjustment of the atmosphere.

The remaining parameter a'_e is to be adjusted by $\delta a'_e$. Its adjustment will be related with use of (18) to an adjustment δg_o of a mean value of gravity, which is directly related to the gravity data. Since the computed functions and associated constants refer to the set $E' = (GM', a'_e, f, \omega)$, GM and a_e are regarded as parameters in the variation of W(p).

A3-4.0 EXPANSION OF THE GRAVITY FUNCTION FOR THE GEOID

Denote the functional form for W(p) in (3) as

$$W(p) = W(p, \bar{C}, \bar{S}, E) = U_o(E)$$

and its gravity as

$$g(p) = |\nabla W(p, \bar{C}, \bar{S}, E)| \equiv g(p, \bar{C}, \bar{S}, E) \tag{19}$$

where $(\bar{C}, \bar{S})$ denotes the potential coefficients and $E = (GM, a_e, f, \omega)$ the reference constants. For the system of gravity (12) based upon initial conditions, denote from (19) above

$$W_c(P) = W(P, \bar{C}', \bar{S}', E') = U_o(E'), \quad g_c(P) = |\nabla W_c(P)| = g(P, \bar{C}', \bar{S}', E') \tag{20}$$

where $(\bar{C}', \bar{S}')$ denote initial potential coefficients and constants $E' = (GM', a_e', f, \omega)$. We wish to expand g(p) about $g_c(P)$ in terms of adjustments $(\delta C, \delta S)$ for the potential coefficients from initial values and an adjustment δg_o of a mean value of gravity in terms of δGM and δa_e from initial values. The expansion is given under (35) and it is derived in the remainder of this section.

Since flattening f is the same in each system, the points, p and P, differ only in geoid height relative to their respective ellipsoids. In geodetic coordinates denote

$$p = (hg, \phi', \lambda), \quad P = (hg', \phi', \lambda) \tag{21}$$

and to a sufficient approximation denote their radial coordinates respectively as

$$r = a_e \left[1 - f \sin^2 \phi' + 0(f^2)\right] + hg, \quad r' = a_e' \left[1 - f \sin^2 \phi' + 0(f^2)\right] + hg' \tag{22}$$

In the expansion for g(p) the partial derivatives will be obtained to within terms of the order of flattening relative to their magnitudes. The expansion is made from the functional forms (19) and (20) as follows:

$$g(p) = g_c(P) + \delta\left(\frac{GM}{r^2}\right) + \frac{\partial g}{\partial(\bar{C}, \bar{S})}(\delta\bar{C}, \delta\bar{S}) \tag{23}$$

where for the central term of gravity and by use of (22)

$$\delta \frac{GM}{r^2} = \frac{\delta GM}{r^2} - 2\frac{GM}{r^2}\frac{\delta a_e}{r} - 2\frac{GM}{r^2}\frac{hg - hg'}{r} \tag{24}$$

To within terms of the order of flattening the first two terms in (24) become

$$\frac{\delta GM}{r^2} - 2\frac{GM}{r^2}\frac{\delta a_e}{r} = \frac{GM}{a_e{}^2}\left(\frac{\delta GM}{GM} - 2\frac{\delta a_e}{a_e}\right) \equiv \delta g_o \tag{25}$$

From the relationship in (19), namely

$$W(p, \bar{C}, \bar{S}, E) = U_o(E),$$

we have by holding the parameters E fixed, $\delta U_o(E) = 0$ and in terms of the varying quantities (hg, $\bar{C}$, $\bar{S}$)

$$\delta U_o(E) = 0 = \delta W(p, \bar{C}, \bar{S}, E) = W(p, \bar{C}, \bar{S}, E) - W(P, \bar{C}', \bar{S}', E)$$

or

$$0 = -\frac{GM}{r^2}(hg - hg') + \frac{\partial W}{\partial(\bar{C}, \bar{S})}(\delta\bar{C}, \delta\bar{S}) \tag{26}$$

where from (22) use is made of $\delta r = hg - hg'$ for a_e fixed. Equation (26) establishes the last term in (24) and with use of (25) then (24) becomes

$$\frac{\delta GM}{r^2} = \delta g_o - \frac{2}{r}\frac{\partial W}{\partial(\bar{C}, \bar{S})}(\delta\bar{C}, \delta\bar{S}), \tag{27}$$

and substituting this result into (23) then

$$g(p) = g_c(P) + \delta g_o - \frac{2}{r}\frac{\partial W}{\partial(\bar{C}, \bar{S})}(\delta\bar{C}, \delta\bar{S}) + \frac{\partial g}{\partial(\bar{C}, \bar{S})}(\delta\bar{C}, \delta\bar{S}) \tag{28}$$

For the harmonic terms of W(p) in (3) denote

$$W(p) = \frac{GM}{r} + \sum_{n,m} W_{nm}(p, \bar{C}_{nm}, \bar{S}_{nm}) + \Phi(p), \tag{29}$$

where

$$W_{nm}(p, \bar{C}_{nm}, \bar{S}_{nm}) = \frac{GM}{r}\left(\frac{a_e}{r}\right)^n P_n^m(\sin\phi)\,[\bar{C}_{nm}\cos m\lambda + \bar{S}_{nm}\sin m\lambda], \tag{30}$$

then

$$\frac{\partial W(p)}{\partial(\bar{C}_{nm}, \bar{S}_{nm})}\,\delta(\bar{C}_{nm}, \bar{S}_{nm}) = W_{nm}(p, \delta\bar{C}_{nm}, \delta\bar{S}_{nm}) \tag{31}$$

Denoting the direction of the local vertical by n′ for a point p on the geoid, then since n′ has small deviations from the normal to the ellipsoid we have

$$g(p) = |\nabla W(p)| = -\frac{\partial W(p)}{\partial n'} \doteq -\frac{\partial W(p)}{\partial hg} \tag{32}$$

For the last term in (28), with use of (32)

$$\frac{\partial g(p)}{\partial(\bar{C}, \bar{S})} = -\frac{\partial}{\partial(\bar{C}, \bar{S})}\left[\frac{\partial W(p)}{\partial hg}\right] \doteq -\frac{\partial}{\partial(\bar{C}, \bar{S})}\left[\frac{\partial W(p)}{\partial r}\right] \tag{33}$$

where the spherical approxmation in brackets gives terms to within an order of flattening by (22). With use of the results from (29) through (33) we have

$$\frac{\partial g(p)}{\partial(\bar{C}_{nm}, \bar{S}_{nm})}\,\delta(\bar{C}_{nm}, \bar{S}_{nm}) = \frac{(n+1)}{r}\,W_{nm}\,(p, \delta\bar{C}_{nm}, \delta\bar{S}_{nm}). \tag{34}$$

Substituting (31) and (34) into (28) and with use of (30) we have the following result for the expansion:

$$g(p) - g_c(P) = \delta g(p) = \delta g_o + \delta g_1(p)$$

$$\delta g_1(p) = \frac{GM}{r^2}\left[\sum_{n=2}^{N}\sum_{m=0}^{n}(n-1)\left(\frac{a_e}{r}\right)^n P_n^m(\sin\phi)\,(\delta\bar{C}_{nm}\cos m\lambda + \delta\bar{S}_{nm}\sin m\lambda)\right] \tag{35}$$

and from (25)

$$\delta g_o = \frac{GM}{a_e^2}\,\frac{\delta GM}{GM} - 2\,\frac{\delta a_e}{a_e}\,.$$

For use in the normal equations for mean gravity anomaly, a value of N = 16 is employed in (35) for the adjustments of spherical harmonic coefficients ($\delta\bar{C}$, $\delta\bar{S}$).

A3-4.1 Computations for Gravity and Geoid Height

In the expansion of g(p) in (35), the computed value $g_c(P)$ and the partial derivatives of g(p) with respect to the coefficients require the point P to be

determined. Initial values of GM and a_e, including the radial coordinate $r = r'$ for P, are used in the expression for $\delta g(p)$ under (35) for computations. Coordinates of (ϕ', λ), as defined in (21) for the points p and P, are given with the gravity anomaly data. Hence only geoid height (hg') for P needs to be obtained to establish the point P. The result for the computation of hg' is given below in (40) where Brun's formula is applied and the computation for gravity $g_c(P)$ is given in (41). The description and derivation for the computation of geoid height is given in the remainder of this section.

Geoid height for the point P is derived from the condition (12) with use of the reference potential $U_c(P)$ as defined under (13). By expansion

$$U_c(P) = U_o(E') - \gamma_c \, hg' \tag{36}$$

where γ_c is defined in (14) and a gravity formula for $\gamma_c(\phi')$ is given in (15). Related constants (g_e', f_1', f_2') for $\gamma_c(\phi')$ and those ($\bar{C}_{20}^{*\prime}$, $\bar{C}_{40}^{*\prime}$) for $U_c(P)$ are given numerically in (17).

With use of (12) there results from (36)

$$hg' = \frac{W_c(P) - U_c(P)}{\gamma_c(\phi')} = \frac{T_c(P)}{\gamma_c} \tag{37}$$

$$T_c(P) = W_c(P) - U_c(P),$$

which is an application of Brun's formula.

$T_c(P)$ is the disturbance potential for the gravity system under (12) and is given as follows through use of the forms of W(p) in (3) and U(p) in (8):

$$T_c(P) = \frac{GM'}{r'}\left(\sum_{n=2}^{N}\sum_{m=0}^{n}\left(\frac{a_e'}{r'}\right)^n P_n^m(\sin\phi)\left[C_{nm}^{*}\cos m\lambda + \bar{S}_{nm}'\sin m\lambda\right]\right) \tag{38}$$

$$C_{20}^{*} = \bar{C}_{20}' - \bar{C}_{20}^{*\prime} = 4.2 \times 10^{-9}$$

$$C_{40}^{*} = \bar{C}_{40}' - \bar{C}_{40}^{*\prime} = -0.2593 \times 10^{-6} \tag{39}$$

and for all other coefficients $C_{nm}^{*} = \bar{C}_{nm}'$. The coefficient C_{20}^{*} is quite small and all other coefficients are approximately $10^{-5}/n^2$ in magnitude using Kaula's rule of thumb. Since geoid height hardly exceeds 100 meters and N = 16, $T_c(P)$ is

evaluated by replacing the point P with its subnormal point Q on the reference ellipsoid of GEM 6. Geoid height is computed with use of (38) by

$$hg' = \frac{T_c(Q)}{\gamma_c(\phi')} \quad . \tag{40}$$

The point P in spherical coordinates (r', ϕ, λ) is obtained from customary formula for transforming geodetic coordinates to spherical coordinates.

With the point P in spherical coordinates $g_c(P)$ is computed to sufficient accuracy from

$$g_c(P) = \sqrt{\left(\frac{\partial W_c}{\partial r}\right)^2 + \frac{1}{r^2}\left(\frac{\partial W_c}{\partial \phi}\right)^2} \tag{41}$$

where $r = r'$, and the term for $\partial W_c/\partial \lambda$ is negligible.

A3-5.0 OBSERVATION EQUATION AND NORMAL EQUATIONS

A3-5.1 Data Point of Gravity Anomaly

Gravity anomaly is defined theoretically in (1). With use of (11) it may be expressed as

$$\Delta g_E = g(p) - \gamma_E(\phi')$$

where $\gamma_E(\phi')$ depends upon the constants $E = (GM, a_e, f, \omega)$, g(p) is gravity at a point p on the geoid, and (hg, ϕ', λ) are the geodetic coordinates of the point p relative to the earth's ellipsoid. In practice a data point of gravity anomaly $\Delta g_R(\phi', \lambda)$ is referred to a gravity formula $\gamma_R(\phi')$ based upon a known set of constants E_R, and the anomaly is expressed by

$$\Delta g_R(\phi', \lambda) = g(p) - \gamma_R(\phi'), \tag{42}$$

where (ϕ', λ) refer to the point p as defined above.

For the system of constants E′ as in GEM 6, let the data point of gravity anomaly be designated as

$$\Delta g_D(\phi', \lambda) = g(p) - \gamma_c(\phi'), \tag{43}$$

then from (42)

$$\Delta g_D(\phi', \lambda) = \Delta g_R(\phi', \lambda) + \gamma_R(\phi') - \gamma_c(\phi'). \tag{44}$$

Hence by (44), given the constants E_R, a data point of gravity anomaly may be converted to the system of GEM 6 and referred to the gravity formula for $\gamma_c(\phi')$ as designated in (43).

From (15), the difference in the gravity formulae, based upon the constants E′ and E_R, is expressed by

$$\gamma_R(\phi') - \gamma_c(\phi') = \Delta g_e + \Delta f_1\, g_e \sin^2 \phi' + \Delta f_2\, g_e \sin^2 2\phi'. \tag{45}$$

Numerical results are given in the next section for two gravity formulae employed for use with Rapp's gravity data.

A3-5.2 Conversion of Rapp's Gravity Formula

The data of Rapp refers to a gravity formula γ_R consistent with the following constants:

$$a_e = 6378137.8 \text{ meters}$$

$$f = 1/298.258$$

$$GM = 398601.3 \text{ km}^3/\text{sec}^2 \tag{46}$$

The gravity formula given by Rapp (1972) consistent with these constants and including a term of -0.87 mgal for eliminating the mass of the atmosphere in GM is

$$\gamma_R = 978033.5\ (1 + .00530243 \sin^2 \phi' - .00000587 \sin^2 2\phi')\ (\text{mgal}) \tag{47}$$

From (15) and the constants in (17), the gravity formula in the GEM 6 system is

$$\gamma_c = 978029.1\ (1 + .0053025 \sin^2 \phi' - .00000585 \sin^2 2\phi')\ (\text{mgal}), \tag{48}$$

and from (47) and (48)

$$\gamma_R - \gamma_c = \Delta g_e = 4.4 \text{ mgal} \tag{49}$$

to within one-tenth of a milligal.

The difference of $\gamma_R - \gamma_c$ given in (49) may be explained by the following relationship among the parameters, namely

$$\Delta g_e = \frac{GM}{a_e^2}\left(\frac{\delta GM}{GM} - 2\,\frac{\Delta a_e}{a_e}\right) = 4.4 \text{ mgal} \tag{50}$$

where Rapp applied the nominal atmospheric correction $\delta GM/GM$, given in (18), for his derived value of g_e.

It is noted that in the computation of γ from the reference formula of gravity, such as in (47), the value for ϕ' need not be precisely known. A lateral displacement of 100 meters, corresponding to an error in ϕ', produces a maximum effect of 0.1 mgal on γ. Such an effect is not greatly significant in the modeling for the gravity data which is at best accurate to about 1 mgal.

A3-5.3 Observation Equation for Mean Gravity Anomaly

From (35)

$$g(p) - g_c(P) = \delta g(p), \tag{51}$$

where $\delta g(p)$ is given in terms of adjustments of the potential coefficients ($\delta\bar{C}$, $\delta\bar{S}$) and an adjustment Δg_o of a mean value of gravity. The relation (51) may be written as

$$[g(p) - \gamma_c(\phi')] - [g_c(P) - \gamma_c(\phi')] = \delta g(p), \tag{52}$$

and with use of (43) for a data point of gravity anomaly, $\Delta g_D(\phi, \lambda)$, this relation (52) becomes

$$\Delta g_D(\phi', \lambda) - \Delta g_c(P) = \delta g(p) \tag{53}$$

where

$$\Delta g_c(P) = g_c(P) - \gamma_c(\phi'). \tag{54}$$

Mean gravity anomaly over a given area on a reference ellipsoid is an average point anomaly, as defined in (42), for a region of the geoid. In practice the mean anomaly is centered in geodetic coordinates (ϕ', λ). Let the mean gravity anomaly data of Rapp for 5° equal area blocks be designated as $\Delta\bar{g}_R(\phi', \lambda)$. Then similar to (44) the data is referred to the GEM 6 system as

$$\Delta\bar{g}_D(\phi', \lambda) = \Delta\bar{g}_R(\phi', \lambda) + \gamma_R(\phi') - \gamma_c(\phi') \tag{55}$$

where $\gamma_R - \gamma_c$ is given in (45) and numerically in (49).

A3-5.3.1 Truncation, Modeling, and Data Errors in Observation Equation
In Equation (53) we replace the point anomaly $\Delta g_D(\phi', \lambda)$ by the mean anomaly $\Delta \bar{g}_D(\phi', \lambda)$ from (55) and form the observation equation as follows:

$$\Delta\bar{g}_D(\phi', \lambda) - \Delta g_c(P) = \delta g(p) + T_N(p) + e(p) + e_D \tag{56}$$

where:

$\delta g(p)$ is given in (35) as an harmonic expansion expressed in terms of adjustments Δg_o and ($\delta\bar{C}$, $\delta\bar{S}$) for coefficients complete through degree and order N, $T_N(p)$ denotes the error due to truncation, e(p) denotes the error induced by approximating a mean anomaly centered at (ϕ', λ) by a point anomaly evaluated at the center point (ϕ', λ), and e_D denotes errors in the data which vary from 1 to 20 mgal.

The modeling error for e(p) would certainly be significant for harmonic terms of degree n which experience a complete cycle in a 5° block, namely

$$n \geqslant \bar{n} = \frac{360}{5} = 72.$$

This error would vanish by averaging the computed anomaly $\Delta g_c(P)$ and the variation $\delta g(p)$ over the 5° block, and the averaging is recommended for terms with use of the present data where

$$n \geqslant \frac{1}{4}\,\bar{n} = 18. \tag{57}$$

Effects of the error e(p) are discussed in A3-7.1 where some numerical results are given, which show a small effect for a test case with truncation of N = 20.

Since N = 16 is employed for the truncation, the error e(p) is not significant. However the truncation error $T_N(p)$ is large. The effect of $T_N(p)$ on the modeled coefficients is not significant in the normal equations because of the orthogonality property of the spherical harmonics. Nevertheless, some aliasing effect is experienced particularly on coefficients of degree 15 and 16, which have neighboring frequencies to those just beyond the point of truncation. The aliasing effect results because of the inhomogeneous set of gravity data with variable accuracy, from 1 to 20 mgals of error, which is applied in the weighting for the normal equations. The weighting is necessary so that solution conforms appropriately to the better data, but it tends to degrade the orthogonality condition between distinct pairs of harmonics.

A3-5.4 Normal Equations for Gravity Data

Denote from (56), for the global set of anomaly data at each point i, the residual

$$\nu_i = \Delta\bar{g}_D\,(\phi_i', \lambda_i) - \Delta g_c\,(P_i) \tag{58}$$

From the form of $\delta g(p)$ given under (35), let the point p_i correspond to the computed point P_i above, x_j correspond to an adjustment parameter for the set $(\delta\bar{C}, \delta\bar{S})$ and Δg_o and A_{ij} the corresponding spherical harmonic factor for the parameter x_j, then

$$\delta g(p_i) = \sum_j A_{ij}\, x_j, \tag{59}$$

and with use of (58) the residual for the observation equation becomes

$$\nu_i = \sum_j A_{ij}\, x_j - \tag{60}$$

For all observation data, namely $\Delta\bar{g}_D(\phi_i', \lambda_i)$ for all i, (60) becomes in matrix form

$$\nu = A\,x, \quad \nu = [\nu_i], \quad A = [A_{ij}], \quad x = [x_j]. \tag{61}$$

The computations for the point P_i, and its gravity $g_c(P_i)$ are discussed in A3-4.1, including the elements A_{ij}.

The normal equations are formed with use of a diagonal weight matrix, namely

$$W = [w_i] \tag{62}$$

where $w_i = 1/\sigma_i^2$ (OBS) and σ_i(OBS) are given with the data $\Delta\bar{g}_R(\phi_i', \lambda_i)$. The normal equations for the gravity data, which are to be combined with the satellite data in GEM 6, are given in matrix form from (60), (61), and (62) as

$$A^T W\nu = A^T WA\,x. \tag{62}$$

A3-6.0 ADJUSTMENT OF REFERENCE PARAMETERS

Based upon the adjustments δg_o and $\delta \bar{C}_{20}$ from the combined solution of GEM 6, an adjustment for equitorial gravity g_e, and adjustments for the semi-major axis a_e and flattening f are derived. The variational equations are given below for the adjustment and numerical results are provided for the adjusted quantities. It is shown that a_e depends upon the reference value of GM, while g_e is independent of this value to within first order, and that the new value of flattening is essentially the same as that of the reference value employed. Initial values of parameters are given under (16) and (17).

A complete set of formulae relating the above quantities may be obtained from Heiskanen and Moritz (1967). Their variational relationships result in a set of simultaneous equations of first order. Results are derived below which are accurate to within the numerical values listed.

From (25) and the solution value of δg_o from GEM 6

$$\delta g_o = \left(\frac{GM}{a_e^2}\right)\left(\frac{\delta GM}{GM} - 2\,\frac{\delta a_e}{a_e}\right) = 3.0 \text{ mgal}, \tag{63}$$

where, with use of the nominal correction for the atmosphere in (18) for which $\delta GM/GM = -.87 \times 10^{-6}$ and use of the constants in (16),

$$\delta a_e = -12.5 \tag{64}$$

From the relationship

$$\frac{\delta g_o}{g_e} = \frac{\delta GM}{GM} - 2\,\frac{\delta a_e}{a_e} \tag{65}$$

and (63)

$$\delta g_e \doteq \delta g_o = 3.0 \text{ mgal}. \tag{66}$$

The adjustment for flattening f is obtained from the relation

$$\delta f = \frac{3}{2}\,\delta J_2 + \frac{1}{2}\,\delta m, \tag{67}$$

where

$$\delta J_2 = J_2 - J_2' = -\sqrt{5}\,(\bar{C}^*_{20} - \bar{C}^{*\prime}_{20})$$

$$\bar{C}^*_{20} \equiv \bar{C}_{20} = -484.16608 \times 10^{-6}$$

$$\bar{C}^{*\prime}_{20} = -484.17104 \times 10^{-6}$$

$$\delta J_2 = -11.1 \times 10^{-9}$$

and where

$$m \doteq \omega^2 a_e / g_e, \tag{68}$$

$$\delta m = m\left(\frac{\delta a_e}{a_e} - \frac{\delta g_e}{g_e}\right) = -17.3 \times 10^{-9} \tag{69}$$

and thus

$$\delta f = -25 \times 10^{-9} \tag{70}$$

The new value for flattening, namely

$$f_{NEW} = f + \Delta\delta$$

will give

$$f_{NEW} = 1/298.257 \tag{71}$$

where for the reference value

$$f = 1/298.255.$$

Adjusted values for a_e and g_e, based upon the adjustments obtained above, are

$$a_e = 6378142.5 \text{ m}$$

$$g_e = 978032.1 \text{ mgal.} \tag{72}$$

Rapp (1974) has provided new estimates for all the above basic parameters. Of principal concern here are his new values for g_e and f, since our value for g_e is derived directly from the gravity data as indicated by (66) and our reference value for flattening was assumed sufficiently accurate for modeling the gravity data. His new values for these two parameters are given as

$$g_e = 978031.7 \pm .77 \text{ mgal}$$

$$1/f = 298.2564 \pm .0015$$

$$\sigma_f = \pm 17 \times 10^{-9}$$

which agree well with our results.

A3-7.0 FORMULAE EMPLOYED FOR ANALYSIS OF MODELS WITH USE OF MEAN GRAVITY ANOMALY DATA

Certain formulae were employed for the analysis of potential solutions, among different models, with use of mean gravity anomaly data for which results are given in the report. Let the potential coefficients of the models be designated as ($\bar{C}$, $\bar{S}$) for coefficients complete through degree and order N, for N = 12, 16, or 20. The models were based upon the same initial parameters as in GEM 6, $E' = (GM', a'_e, f, \omega)$, hence the gravity anomaly data is referred to the GEM 6 gravity formula $\gamma_c(\phi')$ as in (43), namely

$$\Delta g_D(\phi', \lambda) = g(p) - \gamma_c(\phi') \tag{73}$$

where g(p) as before is gravity on the geoid.

A3-7.1 Derivation of Gravity Anomaly Formula

Let the normalized potential coefficients for the geoid be designated as (C, S), and its reference parameters by $E = (GM, a_e, f, \omega)$ as before. Hence the functional form, given in (19) for g(p), is now designated as

$$g(p) = g(p, C, S, E),$$

and from the expansion in (35) g(p) may be represented in terms of parameters E' by

$$g(p) = g(p, C, S, E') + \delta g_o, \tag{74}$$

since the only difference is given by δg_o in (25) due to the two sets of parameters E and E'.

Let gravity $g(\bar{P})$ for a solution with coefficients ($\bar{C}$, $\bar{S}$) be similarly designated as in g(p) above, for parameters E and E', as follows:

$$g(\bar{P}) = g(\bar{P}, \bar{C}, \bar{S}, E) = g_c(\bar{P}, \bar{C}, \bar{S}, E') + \delta g_o. \tag{75}$$

We may write an identity relation for (74) as

$$g(p) = g_c(\bar{P}, \bar{C}, \bar{S}, E') + \delta g_2(p) + \delta g_o,$$

$$\delta g_2(p) = g(p, C, S, E') - g(\bar{P}, \bar{C}, \bar{S}, E'), \tag{76}$$

and again with use of the form of the expansion in (35)

$$\delta g_2(p) = \delta g_1(p) + T_N \tag{77}$$

where $\delta g_1(p)$ now represents the effect of the errors (δC, δS) committed in the coefficients ($\bar{C}$, $\bar{S}$) through degree N, and where T_N designates the effect of the errors of omission for the coefficients (C, S) in g(p) beyond degree N. In the new context it is more appropriate to designate $\delta g_1(p)$ as ϵ_N, hence (77) becomes

$$\delta g_2(p) = \epsilon_N + T_N \tag{78}$$

where ϵ_N represents the errors in gravity committed by the errors in the solution parameters ($\bar{C}$, $\bar{S}$) through degree N.

Substituting the result for $\delta g_2(p)$ from (78) into (76) for g(p), then (73) may be expressed as

$$\Delta g_D(\phi', \lambda) = g_c(\bar{P}, \bar{C}, \bar{S}, E') - \gamma_c(\phi') + \delta g_o + \epsilon_N + T_N \tag{79}$$

The quantity $g_c(\bar{P}, \bar{C}, \bar{S}, E')$ may be computed analogous to $g_c(P)$ as described in A3-4.1. It is convenient in the remaining analysis to use an alternative method, which is more customary, for computing the gravity anomaly

$$\Delta g_c(\bar{P}, \bar{C}, \bar{S}, E') = g_c(\bar{P}, \bar{C}, \bar{S}, E') - \gamma_c(\phi') \tag{80}$$

corresponding to these two terms in (79).

The result for $\Delta g_c(\bar{P}, \bar{C}, \bar{S}, E')$ is given in (85) below and it is established from use of the expansion given in (35), where $g_c(\bar{P}, \bar{C}, \bar{S}, E')$ replaces g(p) and $\gamma_c(\bar{P})$ replaces $g_c(P)$. The expressions for the gravity quantities are obtained from their respective potentials as follows:

$$g_c(\bar{P}, \bar{C}, \bar{S}, E') = |\nabla W_c(\bar{P}, \bar{C}, \bar{S}, E')| \tag{81}$$

$$\gamma_c(\bar{P}) = |\nabla U_c(\bar{P})|, \tag{82}$$

where, analogous to the reference system of GEM 6 in (12) through (14), $W_c(\bar{P}, \bar{C}, \bar{S}, E')$ is given by the form for W(p) in (3) and $U_c(P)$ is given by the form (8) with use of the constants ($\bar{C}^{*'}_{20}$, $\bar{C}^{*'}_{40}$) in (17). As in (37), geoid height $\bar{h}g$ for $\bar{P}$ is related as

$$\bar{h}g = \frac{W_c(\bar{P}, \bar{C}, \bar{S}, E') - U_c(\bar{P})}{\gamma_c(\phi')} \tag{83}$$

and is computed as in (40). With use of the approximation

$$\gamma_c(\bar{P}) = \gamma_c(\phi') - 2\frac{GM'}{r^2}\frac{\bar{h}g}{r} \tag{84}$$

and the above relations (81) through (83), we obtain from the technique given for the expansion in (35) the following result for (80):

$$\Delta g_c\,(\bar{P}, \bar{C}, \bar{S}, E') = \frac{GM'}{r}\left[\sum_{n=2}^{N}\sum_{m=0}^{n}(n-1)\left(\frac{a_e'}{r}\right)^n P_n^m(\sin\phi)\,(C^*_{nm}\cos m\lambda + \bar{S}_{nm}\sin m\lambda)\right] \tag{85}$$

where C^*_{nm} is defined by

$$C^*_{20} = \bar{C}_{20} - \bar{C}^{*\prime}_{20}, \quad C^*_{40} = \bar{C}_{40} - \bar{C}^{*\prime}_{40}$$

and for all other (nm), $C^*_{nm} = \bar{C}_{nm}$. The spherical coordinates (r, ϕ, λ) for the point $\bar{P}$ are obtained from its geodetic coordinates $(\bar{h}g, \phi', \lambda)$ relative to the reference ellipsoid for GEM 6 with parameters $E' = (GM', a_e', f, \omega)$.

A3-7.2 Mean Gravity Anomaly Residual and Errors

As in the observation equation (56) for mean gravity anomaly, we replace the point anomaly $\Delta g_D(\phi', \lambda)$ in (79) by the mean anomaly $\Delta\bar{g}_D(\phi', \lambda)$. We then obtain from (79) and (80) the residual ν_s for a given solution of potential coefficients, namely

$$\Delta\bar{g}_D(\phi', \lambda) - \Delta g_c\,(\bar{P}, \bar{C}, \bar{S}, E') - \delta g_o = \nu_s \tag{86}$$

where in terms of the errors in (79) and (56)

$$\nu_s = \epsilon_N + T_N + e(p) + e_D. \tag{87}$$

In the report the mean square of the residuals, $M(\nu_s^2)$, was compared among different models, which are truncated at degrees N = 12, 16, and 20.

The errors e_D for the data, T_N for the truncation of the solution, and e(p) were discussed previously. Gravity anomaly Δg_c in (85) is computed at the center point (ϕ', λ) of the data $\Delta\bar{g}_D(\phi', \lambda)$, as opposed to averaging the anomaly Δg_c over the 5° equal-area block of data, resulting formally in an error e(p) as previously described. Gravity anomaly Δg_c was computed by both averaging and employing the center point only, for cases of N = 12, 16, and 20. Only a slight difference of less than one mgal^2 was seen in $M(\nu_s^2)$ for the case of N = 20. Also Δg_c, as computed directly by (80) or by (85), gives no essential difference.

The value of $\delta g_o = 3.0$ mgals was used in (86) which best fits the data relative to the reference constants E′ of GEM 6. Hence, for a given potential model, all quantities in (86) are computed w.r.t. the set E′.

The principal source of error of interest in (87) is ϵ_N, which is the effect of the errors (δC, δS) in the potential coefficients of a given solution. For two models with solutions s1 and s2, truncated at degree N, the only difference in the residuals from (87) is

$$\nu_{s1} - \nu_{s2} = \epsilon_N(s1) - \epsilon_N(s2) \tag{88}$$

since the other errors are the same. By the orthogonality property of the spherical harmonics and by the assumption of randomness of data errors (e_D), then for a solution independent of the data we have from (87)

$$M(\nu_s^2) = M(\epsilon_N^2) + M(T_N^2) + M(e_D^2). \tag{89}$$

For two solutions independent of the data, such as different satellite solutions,

$$M(\nu_{s1}^2) - M(\nu_{s2}^2) = M\left[\epsilon_N^2(s1)\right] - M\left[\epsilon_N^2(s2)\right]. \tag{90}$$

Hence the difference in the mean square residuals give a direct measure of the errors in gravity as committed by the coefficient errors in the two models.

A3-7.3 Degree Variances of Gravity Anomaly and Error of Commission in Anomaly

Solutions were compared in the report based upon degree variances of gravity anomaly. $\sigma_n^2(\Delta g)$, which are derived directly from the coefficients of degree n, ($\bar{C}_{nm}$, $\bar{S}_{nm}$). They are particularly of interest for high degree n, where greater variability is seen among different models. These irregularities occur in σ_n^2 for values of n bordering near the truncation point at degree N, and these are usually due to the aliasing effect in the solution arising from the truncation error T_N.

By setting $r = a_e'$ in (85) for gravity anomaly and taking the mean square value over the earth, we have

$$\sigma^2(\Delta g) = \sum_{n=2}^{N} \sigma_n^2(\Delta g), \tag{91}$$

for all n ($\neq$ 2 or 4)

$$\sigma_n^2(\Delta g) = g_e^2 \sum_{m=0}^{n} (n-1)^2 \, (\bar{C}_{nm}^2 + \bar{S}_{nm}^2)$$

and for n = (2, 4), $\bar{C}_{nm}$ is replaced by $\bar{C}_{20}^*$ and $\bar{C}_{40}^*$ as given under (85).

Cross term effects from (85) vanish in (91) due to the orthogonality of the harmonics. Similarly to (91) we have for the errors in gravity anomaly (ϵ), due to the commision errors in the coefficients $\sigma^2(\delta C_{nm})$ and $\sigma^2(\delta S_{nm})$, the following result:

$$\sigma^2[\epsilon(\Delta g)] = \sum_{n=2}^{N} \sigma_n^2[\epsilon(\Delta g)]$$

$$\sigma_n^2[\epsilon(\Delta g)] = g_e^2 \sum_{m=0}^{n} (n-1)^2 \left[\sigma^2(\delta C_{nm}) + \sigma^2(\delta S_{nm})\right]. \qquad (92)$$

REFERENCES

Heiskanen, W. A., and H. Moritz, Physical Geodesy, W. H. Freeman, San Francisco, 1967.

Rapp, R. H., "The Formation and Analysis of a 5° Equal Area Block Terrestial Gravity Field," Dept. of Geodetic Science Report No. 178, Ohio State University Research Foundation, Columbus, Ohio, June 1972.

Rapp, R. H., "Current Estimates of Mean Earth Ellipsoid Parameters," Geophysical Research Letters, Vol. 1, No. 1, AGU, May 1974.

APPENDIX A4 . . . . . TECHNIQUES IN COMBINED SOLUTION

APPENDIX A4

METHOD OF COMBINED SOLUTION

CONTENTS

		Page
A4-1.0	COMBINATION OF DIFFERENT SETS OF DATA	A4-3
A4-1.1	Combined Set of Normal Equations for GEM 5	A4-3
A4-1.2	Combined System of Normal Equations for GEM 6	A4-5
A4-2.0	NUMERICAL TECHNIQUES	A4-6
A4-3.0	STATISTICS OF SOLUTION FOR THE GEODETIC PARAMETERS	A4-9

APPENDIX A4

METHOD OF COMBINED SOLUTION

Described herein are, (1) the techniques employed for combining the normal equations for GEM 5 and GEM 6, (2) the numerical techniques for the solution of the geodetic parameters, and (3) the variance-covariance matrix for the solution parameters.

A4-1.0 COMBINATION OF DIFFERENT SETS OF DATA

For GEM 5, the gravitational potential and stations' coordinates are computed using only orbital (dynamical) theory. For GEM 6, the orbital theory is combined with geometric theory and gravimetric theory.

A4-1.1 Combined Set of Normal Equations for GEM 5

The dynamical theory is used to generate systems of arc-specific normal equations, i.e., the system of normal equations is generated for a given orbit. These systems of normal equations are written in terms of arc-dependent (orbital elements) and arc-independent variables (gravitational potential and station parameters). Processing continues by reducing these systems of normal equations to systems written in arc-independent variables only. Once this is done, normal equations using any number of arcs and/or surface and geometric data are combined. The elimination of orbital elements from satellite-specific systems of normal equations is described herein.

The normal equations formed for individual arcs are of the form

$$\begin{bmatrix} B_1 & B_3^T \\ B_3 & B_2 \end{bmatrix} \begin{bmatrix} X_1 \\ X_2 \end{bmatrix} = \begin{bmatrix} b_1 \\ b_2 \end{bmatrix} \tag{1}$$

where

B_1 is the k-by-k matrix of coefficients involving partial derivatives with respect to arc-independent variables only

B_2 is the (n-k)-by-(n-k) matrix of coefficients involving arc-dependent partial derivatives only

B_3 is the (n-k)-by-k matrix of coefficients involving product-term partial derivatives of arc-independent and arc-dependent variables

X_1 is the k-dimensional vector $X_1, \ldots, X_k$ involving arc-independent variables (gravitational parameters and tracking station coordinates)

X_2 is the (n-k)-dimensional vector $X_{k+1}, \ldots, X_n$ involving arc-dependent variables (satellite vectors, tracking system biases, and drag and radiation pressure coefficients)

b_1 is the k-dimensional portion of the right-hand side vector associated with the arc-independent and product term partial derivatives (B_1 and B_3^T)

b_2 is the (n-k)-dimensional portion of the right-hand side vector associated with the arc-dependent and product term partial derivatives (B_2 and B_3).

The back substitution solution for X_2 gives

$$X_2 = B_2^{-1} (b_2 - B_3 X_1) \tag{2}$$

Using this result to find X_1 produces the expression

$$B_1 X_1 + B_3^T \left[B_2^{-1} (b_2 - B_3 X_1) \right] = b_1 \tag{3}$$

which yields the equation

$$\left(B_1 - B_3^T B_2^{-1} B_3 \right) X_1 = b_1 - B_3^T B_2^{-1} b_2 \tag{4}$$

Equation 4 is the reduced system of normal equations in arc-independent variables only. A reduced set of normal equations is formed for each arc prior to its aggregation to form a multi-arc solution for the arc-independent variables. Once equation 4 is solved, the result is substituted into equation 2 to produce an estimate of X_2, the arc-dependent variables.

A notational simplification is obtained by

$$\begin{aligned} B^* &= B_1 - B_3^T B_2^{-1} B_3, \\ b^* &= b_1 - B_3^T B_2^{-1} b_2, \\ x^* &= X_1, \end{aligned} \tag{5}$$

which produces a reduced set of normal equations of the form

$$B^* x^* = b^* \tag{6}$$

The combined reduced normal equations are formed by simple matrix addition, where

$$C = \sum_{i=1}^{N} B_i^*, \quad c = \sum_{i=1}^{N} b_i^* \tag{7}$$

and where N is the number of systems of normal equations to be combined. In the GEM solutions, the capability exists for weighting each set of the N normal equations. Through this technique a weight factor can be applied to each set of normal equations to accomplish any desired relative weights between the various satellite arcs, and between the dynamic, geometric, and gravimetric normal equations. The resulting combined normal equations are of the form,

$$Cx^* = c \tag{8}$$

Solving Equation 8 now yields

$$x^* = C^{-1} c \tag{9}$$

from which x* is used to obtain estimates of the gravitational potential and the coordinates of the stations.

A4-1.2 Combined System of Normal Equations for GEM 6

The normal equations produced using geometric and gravimetric theory involve only geodetic parameters, i.e., station coordinates and geopotential terms, respectively. The geometric and gravimetric normal equations are computed in a form comparable to (6), and are compatible for directly combining with the GEM 5 normal equations. This system of equations, combined as in (7) and (8), contain the combination of effects from dynamical, geometric, and gravimetric data and are used to produce GEM 6.

A4-2.0 NUMERICAL TECHNIQUES

The numerical method employed for solving the system (8),

$$Cx^* = c,$$

is discussed.

The approach described here uses single-precision arithmetic to estimate the x* vector iteratively without first finding the C^{-1} matrix. Single-precision arithmetic permits substantial reductions of core storage and does not increase computer utilization time. Test cases have shown that the single-precision iterative improvement yields solutions that agree to within 4 to 5 significant places with double-precision inversion schemes when as many as 400 parameters were estimated simultaneously.

A decomposition of the matrix C is computed by the Cholesky method such that

$$C = LL^T \tag{10}$$

where L is a lower triangular matrix (all elements of L above the diagonal are equal to zero). This decomposition is unique because C is symmetric and positive definite.

Let the elements of the matrices above be denoted for row i and column j as

$$L = [\ell_{ij}], C = [c_{ij}], c = [c_i].$$

The matrix L has $\ell_{ij} = 0$ for $i < j$, and remaining elements defined by

$$\ell_{ii} = \sqrt{c_{ii} - \sum_{j=1}^{i-1} \ell_{ij}^2} \tag{11}$$

$$\ell_{ij} = \frac{c_{ij} - \sum_{m=1}^{j-1} \ell_{im}\,\ell_{jm}}{\ell}, \quad i > j \tag{12}$$

for i = 1 to N where N is the order of the matrix.

Substituting (10) into (8) gives

$$LL^T x^* = c \tag{13}$$

letting

$$y = L^T x^* \tag{14}$$

and substituting this expression in (13) yields

$$Ly = c$$

Because L is a lower triangular matrix, a solution for the y vector is found through use of the "forward elimination" algorithm

$$y_i = \frac{c_i - \sum_{j=1}^{i-1} \ell_{ij} y_j}{\ell_{ii}} \tag{15}$$

for i = 1 to N.

Using this estimate of y, an estimate of x* is computed through use of the "backward elimination" algorithm, where i = N to 1,

$$x_i^* = \frac{y_i - \sum_{j=i+1}^{N} \ell_{ji} x_j^*}{\ell_{ii}} \tag{16}$$

where ℓ_{ji} is the element in the j^{th} row and i^{th} column of the L^T matrix.

Letting the original estimate of the x* vector be designated $x^*_{(1)}$, a residual vector $r_{(1)}$ is computed from substitution of $x^*_{(1)}$ in (13)

$$r_{(1)} = c - LL^T x^*_{(1)} \tag{17}$$

A correction, $d_{(1)}$, to the solution vector is computed by solving the equation

$$LL^T d_{(1)} = r_{(1)} \tag{18}$$

by forward and backward elimination and letting

$$x^*_{(2)} = x^*_{(1)} + d_{(1)} \tag{19}$$

A new residual vector $r_{(2)}$ is computed from (17) and (19) and the solution improvement vector is computed by forward and backward elimination until the process converges. Usually 3 iterations are required for a system such as GEM 6.

-3.0 STATISTICS OF SOLUTION FOR THE GEODETIC PARAMETERS

The statistics are computed from the inverse of the single-precision array, in (10). Approximate values of the statistics are obtained to sufficient accu-cy without the use of an iterative improvement process as employed for the lution vector.

Denoting the inverse matrix of C as,

$$[\sigma_{ij}] = C^{-1},$$

ıere σ_{ij} is the element in the i^{th} row and j^{th} column of the matrix), statistics ɜ computed for the estimated parameters as follows:

1. Variance (σ_{ii})
2. Covariance (σ_{ij})
3. Standard deviation $\left(\sigma_i = \sqrt{\sigma_{ii}}\right)$
4. Correlation coefficient ($\sigma_{ij}/\sigma_i\,\sigma_j$) (20)

To obtain C^{-1} from (10) a matrix Q is defined such that

$$LQ = I \tag{21}$$

$$Q = L^{-1} \tag{22}$$

ɜre Q is also a lower triangular matrix. The matrix C^{-1} can then be written

$$C^{-1} = (L^T)^{-1}\, L^{-1} \tag{23}$$

$$= Q^T\, Q \equiv [\sigma_{ij}] \tag{24}$$

The elements of Q are

$$q_{ii} = \frac{1}{\ell_{ii}} \tag{25}$$

$$q_{ij} = -\frac{1}{\ell_{ii}} \sum_{k=j}^{i-1} \ell_{ik}\, q_{kj} \quad (i = 2,\ldots,N,\ i > j) \tag{26}$$

where ℓ_{ij} and q_{ij} are the elements of the i^{th} row and j^{th} column of the matrices L and Q, respectively. The elements of the inverse matrix C^{-1}, which is symmetric, are given by the lower triangular elements

$$\sigma_{ij} = \sum_{k=j}^{N} q_{ki}\, q_{kj}, \; (i \geq j = 1, 2, \ldots, N) \tag{27}$$

APPENDIX B. . . . . SATELLITE AND GRAVITY DATA DISTRIBUTIONS

APPENDIX B

SATELLITE AND GRAVITY DATA DISTRIBUTIONS

This appendix presents detailed tabulations of the data employed in GEM 5 and 6. A summary of this data was presented in Section 2.

CONTENTS

Table		Page
B-1	Baker-Nunn Observations by Station and Satellite in 7-Day Arcs	B-3
B-2	7-Day Electronic-Optical Arcs	B-4
B-3	Satellite Time Periods of Baker-Nunn Arcs	B-6
B-4	Station Passes in 2-Day Arcs	B-9
B-5	MOTS and SPEOPTS Camera Observations in 7-Day Arcs	B-11
B-6	BC-4 Simultaneous Photographic Events	B-12
B-7	MOTS Geometric Events	B-16
B-8	MOTS & Laser Geometric Events	B-20
B-9	Survey Ties Employed	B-21
B-10	5° Equal Area Surface Gravimetric Data of Rapp (1972)	B-23
Figure B-1.	Distribution and Errors (mgal) of 5° Mean Gravity Anomalies, Rapp (1972)	B-28

Table B-1
Baker-Nunn Observations by Station and Satellite in 7-Day Arcs

SATELLITE	SAO BAKER-NUNN STATIONS																					
	9001	9002	9003	9004	9005	9006	9007	9008	9009	9010	9011	9012	9021	9023	9025	9028	9031	9050	9091	9424	9425	9426	9427
TELSTAR-1	135	117	101	57	55	73	65	71	71	44	78	103											
GEOS-I	996	658		779	66	138	429	107	307	1127	424	255		809				96		108		15	13
SECOR-5	11	22		9	2	11	7	10	11	6	23	10		23									
OVI-2	57	35		35	16	63	43			48	2	30		69		66							
ECHO-1RB	68	121	202	97	59	51	63	112	56	83	158	50											
DID	789	73		603	67	534	53			327		245		134		139	85			6	69		65
BE-C	170	340		179	10	434	73	60	47	148	145	171		503		37	95				27		10
DIC	42	44		40	21	70	5			55		43		95		7					15		15
ANNA-1B	350	143		150		168		51	88		238	109		210									
GEOS-II		572		843		80	321			68		371	331	370	66	204	438		894	14	183		34
OSCAR-7	28	59		34		176	97	49	47	17	93	207		123									
5BN-2	27	24		3	5	19	9	11	16	8	18	18		21									
COURIER-1B	52	168		106	36	154	176			125		132		243		218	47						
GRS	30	6		34			12	31	7	9	13	18		15									
TRANSIT-4A	93	82	142	64	31	10	26	16	21	33	64	59											
BE-B	11	26		26	1	1	5			25		10		57		12	60						
OGO-2	37	7		30	7	21	13	27	12	15	9	43		4						3			3
INJUN-1	33	62	36	18	54		3	15	41	22	21	75											
AGENA-R	90	46	33	51	5	36	47	16	16	47	51	51		21									
MIDAS-4	1180	74		675	530	820	212	595	573	631	169	650		118						323		255	576
VANG-2-ROC	19	21	18	1	5	17	18	8	11		24	27		20									
VANG-2-SAT	72	16	13	101	10	30	17	6	12	14	6	8											
VANG-3-SAT	16	51	120	51	25	4	17	9	48	30	63	36											
TOTAL	4306	2767	665	3986	1005	2910	1711	1194	1381	2882	1599	2721	331	2835	66	683	725	96	894	454	294	270	716

Each count refers to obs. pairs (right ascension and declination).

Table B-2

7-Day Electronic-Optical Arcs (by Satellite and Time Period)

Satellite	Time Period	Number of Stations ① & Station Passes ② Used							
		GRARR		Doppler		Laser		Camera	
		①	②	①	②	①	②	①	②
DIC	4/22/67 - 4/28/67					2	6	6	25
DIC	4/30/67 - 5/ 8/67					2	12	8	68
DID	5/ 9/67 - 5/17/67					2	27	7	98
BE-B	12/23/64 - 12/29/64			4	113				
BE-B	1/ 2/65 - 1/ 8/65			4	122				
BE-B	1/25/65 - 1/31/65			4	124				
BE-B	2/24/65 - 3/ 3/65			4	85				
BE-B	3/21/65 - 3/28/65			3	108				
BE-B	5/12/67 - 5/19/67			1	2	1	5	4	18
BE-C	6/29/65 - 7/ 6/65			6	203				
BE-C	7/ 9/65 - 7/15/65			6	216				
BE-C	7/25/65 - 7/31/65			6	221				
BE-C	8/29/65 - 9/ 5/65			6	200				
BE-C	4/ 2/67 - 4/10/67					2	6	5	30
BE-C	4/20/67 - 4/27/67					2	7	6	23
GEOS-I	11/17/65 - 11/24/65			8	271			10	39
GEOS-I	11/25/65 - 12/ 1/65			8	237			16	70
GEOS-I	1/21/66 - 1/27/66			8	311			16	59
GEOS-I	1/28/66 - 2/ 5/66			8	213			22	68
GEOS-I	4/17/66 - 4/24/66			7	284			27	133
GEOS-I	5/11/66 - 5/18/66			6	243			13	67
GEOS-I	6/16/66 - 6/23/66			6	234			6	6
GEOS-I	7/ 2/66 - 7/ 9/66			7	258			7	16
GEOS-I	7/23/66 - 7/30/66			7	185			15	94
GEOS-I	8/13/66 - 8/21/66			6	217			17	68
GEOS-I	10/29/66 - 11/ 5/66			6	208			3	7
GEOS-I	11/15/66 - 11/22/66			6	142			12	55
GEOS-II	2/25/68 - 3/ 1/68	3	12	4	47	1	1	23	81
GEOS-II	3/16/68 - 3/24/68	4	29	3	50			23	82
GEOS-II	3/28/68 - 4/ 4/68	4	23	4	40	1	2	24	92
GEOS-II	4/22/68 - 4/29/68	4	25	3	116	1	3	27	82
GEOS-II	6/ 3/68 - 6/10/68	3	29	5	110	1	4	22	73
GEOS-II	6/13/68 - 6/19/68	1	2	6	141	1	3	27	132
GEOS-II	6/21/68 - 6/28/68	3	33	5	136	1	3	28	140
GEOS-II	7/12/68 - 7/18/68	3	45	4	107			1	2
GEOS-II	7/25/68 - 8/ 1/68	4	30	4	92			15	41
GEOS-II	8/ 9/68 - 8/16/68	3	18	4	131			8	15
GEOS-II	8/31/68 - 9/ 7/68	3	20	3	31	1	5	22	67

Table B-2 (Continued)

Satellite	Time Period	GRARR		Doppler		Laser		Camera	
GEOS-II	10/19/68 - 10/26/68	3	20	2	51	1	4	22	73
GEOS-II*	2/ 5/69 - 2/12/69					2	10		
PEOLE**	6/ 3/71 - 6/ 5/71					4	13		
PEOLE	6/ 6/71 - 6/10/71					1	9		
PEOLE	6/11/71 - 6/15/71					2	41		
PEOLE	6/16/71 - 6/19/71					2	13		

*C-Band tracking data from 8 stations with 105 station passes are also included.

**MINITRACK data were also used with each PEOLE arc.

In addition to the above arcs, 4 SAS-A arcs, 14 TIROS arcs, and 6 ALOUETTE arcs with MINITRACK data only were used in the GEM solutions.

Table B-3

Satellite Time Periods of Baker-Nunn Arcs

TELSTAR	ECHO	BE-C	OSCAR-7
8/10 - 8/17/62	9/13 - 9/20/60	3/ 2 - 3/ 7/66	4/ 1 - 4/ 7/66
10/ 7 - 10/14	9/20 - 9/27	3/14 - 3/19	4/ 8 - 4/14
10/24 - 10/31	9/27 - 10/ 4	3/25 - 3/31	4/15 - 4/22
11/ 7 - 11/15	10/ 4 - 10/11	3/31 - 4/ 5	4/22 - 4/28/66
11/15 - 11/23	10/11 - 10/18	4/ 5 - 4/11	
11/23 - 12/ 1	10/18 - 10/24	4/11 - 4/17	5BN-2
12/ 1 - 12/ 9	11/30 - 12/ 6	4/17 - 4/23	2/26 - 3/ 5/65
12/ 9 - 12/17	12/13 - 12/20/60	4/23 - 4/29	3/ 4 - 3/11
12/17 - 12/25/62	4/10 - 4/17/61	4/29 - 5/ 4	3/11 - 3/18
12/25 - 1/ 1/63	4/17 - 4/24	5/ 4 - 5/10	4/19 - 4/26
1/ 1 - 1/ 9	4/24 - 4/30	5/10 - 5/16	4/26 - 5/2
1/ 9 - 1/17	5/11 - 5/18	5/16 - 5/21	5/25 - 5/31/65
1/26 - 2/ 2	6/19 - 6/26	5/22 - 5/27	
5/23 - 5/30	8/ 8 - 8/15	5/27 - 6/ 2/66	COURIER
6/ 9 - 6/16	8/15 - 8/22	3/12 - 3/17/67	12/23 - 12/29/66
6/23 - 6/30/63	8/22 - 8/29	3/17 - 3/23	12/31 - 1/ 6/67
	9/ 8 - 9/15	3/23 - 3/29	1/ 8 - 1/15
SECOR	9/15 - 9/22/61	3/29 - 4/ 4	1/15 - 1/20
		4/ 4 - 4/ 9	1/27 - 2/ 2
3/ 1 - 3/ 8/65	DID	4/ 9 - 4/15	6/ 2 - 6/ 9
3/15 - 3/22		4/15 - 4/20	6/ 9 - 6/15
12/ 1 - 12/ 8	2/19 - 2/26/67	4/20 - 4/25/67	6/16 - 6/22
12/15 - 12/22/65	2/26 - 3/ 4		6/23 - 6/29
	3/ 5 - 3/12	BE-B	6/30 - 7/ 6
OVI-2	3/19 - 3/25		7/ 7 - 7/13
	4/30 - 5/ 7	2/26 - 3/ 3/67	7/14 - 7/20
10/28 - 11/ 3/66	5/ 7 - 5/13	3/ 4 - 3/ 9	7/21 - 7/27/67
11/ 4 - 11/10	5/14 - 5/21	3/10 - 3/15	
11/11 - 11/17	5/21 - 5/28	3/16 - 3/21/67	OGO-2
11/18 - 11/24/66	5/28 - 6/ 3/67		
		DIC	5/15 - 5/21/66
GRS	VANGUARD-2 (Sat.)		5/21 - 5/27
		2/24 - 3/ 3/67	5/27 - 6/ 2
6/16 - 6/23/65	4/ 7 - 4/14/60	3/ 3 - 3/11	6/ 3 - 6/ 8
6/23 - 6/30	4/14 - 4/21	3/10 - 3/17	6/ 9 - 6/15
6/30 - 7/ 7	4/21 - 4/28	3/17 - 3/25/67	6/15 - 6/21
7/ 7 - 7/13	4/28 - 5/ 5		6/23 - 6/29/66
7/14 - 7/21/65	5/ 5 - 5/12/60		

Table B-3 (Continued)

ANNA-1B	GEOS-I	GEOS-II	TRANSIT
11/ 5 - 11/10/63	11/ 8 - 11/15/65	3/31 - 4/ 7/68	9/ 2 - 9/10/61
11/16 - 11/21	11/16 - 11/23	4/ 7 - 4/14	9/10 - 9/18
11/21 - 11/27	11/23 - 12/ 1	4/14 - 4/21	9/19 - 9/27
11/27 - 12/ 2	12/ 1 - 12/ 8	5/11 - 5/18	11/17 - 11/25
12/ 2 - 12/ 8	12/ 9 - 12/16	5/25 - 5/31	11/26 - 12/ 3
12/ 8 - 12/13	12/16 - 12/24	6/ 8 - 6/14	12/ 4 - 12/11
12/19 - 12/25/63	12/31 - 1/ 8/66	6/24 - 7/ 2	12/13 - 12/19
2/29 - 3/ 5/64	1/ 8 - 1/15	7/18 - 7/26	12/21 - 12/29/61
3/ 5 - 3/11	1/16 - 1/23	9/ 1 - 9/ 7	7/16 - 7/23/62
3/11 - 3/16	1/23 - 1/31	9/15 - 9/22	8/ 1 - 8/ 9
3/16 - 3/22	1/31 - 2/ 7	9/30 - 10/ 6	8/ 7 - 8/16
3/22 - 3/27	2/ 8 - 2/16	10/ 6 - 10/13	11/ 1 - 11/ 8
4/ 2 - 4/ 7	2/16 - 2/23	10/13 - 10/20	11/ 9 - 11/16
4/13 - 4/17	2/24 - 3/ 3	10/20 - 10/27	11/17 - 11/24/62
4/19 - 4/24	3/ 3 - 3/11	11/ 3 - 11/10/68	AGENA
5/31 - 6/ 5	3/11 - 3/18	1/31 - 2/ 6/69	6/ 1 - 6/ 8/64
6/ 5 - 6/11	3/19 - 3/26	MIDAS	6/ 8 - 6/15
6/11 - 6/16	3/26 - 4/ 3	11/ 3 - 11/10/64	6/15 - 6/22
6/16 - 6/21	4/ 3 - 4/10	11/10 - 11/17	6/22 - 6/29
6/22 - 6/25	4/26 - 5/ 3	11/17 - 11/24	7/16 - 7/23
7/31 - 8/ 6	5/ 4 - 5/11	11/24 - 12/ 1	7/30 - 8/ 7
8/ 6 - 8/11	5/11 - 5/19	12/ 1 - 12/ 8	11/18 - 11/25/64
8/11 - 8/15	5/19 - 5/27	12/ 8 - 12/15	INJUN
8/15 - 8/21	6/16 - 6/23	12/15 - 12/23/64	9/ 3 - 9/11/61
8/21 - 8/25	7/ 9 - 7/16	1/21 - 1/28/65	9/ 9 - 9/16
11/ 1 - 11/ 5	8/ 1 - 8/ 9	1/28 - 2/ 4	9/16 - 9/22
11/ 5 - 11/11	8/ 7 - 8/14	2/ 4 - 2/11	12/21 - 12/28
11/11 - 11/16	8/21 - 8/28	2/11 - 2/18	12/28 - 1/ 3/62
11/16 - 11/22	8/28 - 9/ 4	2/25 - 3/ 4	2/ 4 - 2/11
11/22 - 11/27	9/ 4 - 9/11	3/ 4 - 3/11	2/11 - 2/18
11/27 - 12/ 3	9/25 - 10/ 2	3/11 - 3/18	2/21 - 2/28
12/ 3 - 12/ 7	10/18 - 10/25	3/19 - 3/26	5/16 - 5/23
12/ 7 - 12/14	11/ 1 - 11/ 8	3/26 - 4/ 2	5/23 - 5/30/62
12/14 - 12/19/64	11/ 8 - 11/15	4/ 2 - 4/ 9	
11/30 - 12/ 6/65	11/15 - 11/22/66	4/ 9 - 4/16	
12/11 - 12/17		4/16 - 4/23	
12/22 - 12/27/65		4/23 - 5/ 1/65	
1/ 2 - 1/ 7/66			
1/13 - 1/17/66			

Table B-3 (Continued)

VANGUARD-2 (RB)	VANGUARD-3	
4/ 3 - 4/10/60	1/ 8 - 1/15/60	
4/ 9 - 4/17/60	1/15 - 1/22	
2/11 - 2/18/64	1/22 - 1/29	
11/17 - 11/25/65	1/29 - 2/ 5	
12/11 - 12/18	2/ 5 - 2/12	
12/29 - 1/ 5/66	2/12 - 2/19	
1/ 5 - 1/12	2/22 - 2/29	
1/13 - 1/20	2/29 - 3/ 7	
1/20 - 1/28	3/ 7 - 3/14	
1/28 - 2/ 4	3/14 - 3/21	
2/ 4 - 2/11	3/21 - 3/28	
2/11 - 2/18/66	3/28 - 4/ 4	
	4/ 4 - 4/11	
	4/11 - 4/18	
	4/18 - 4/25/60	

Table B-4

Station Passes in 2-Day Arcs (Used for GEM Station Position Solutions)

Station		GEOS-I	GEOS-II
	MOTS		
1021	Blossom Pt.	49	
1022	Ft. Myers	68	50
1024	Woomera	31	
1028	Santiago	12	35
1030	Goldstone	76	87
1031	Johannesburg	26	28
1032	St. John's	6	15
1034	East Grand Forks	70	
1035	Winkfield	4	16
1036	Fairbanks		53
1037	Rosman		78
1038	Orroral		31
1042	Rosman	60	
1043	Tananarive	4	13
	GRARR		
1123	Tananarive		14
1126	Rosman		34
1128	Fairbanks		95
1152	Carnarvon		43
	Doppler		
2014	Anchorage	149	
2017	Tafuna	81	
2018	Thule		253
2100	Wahiawa	119	
2103	Las Cruces	135	
2106	Lasham	139	
2111	Howard County	152	
2115	Pretoria		26
2117	Tafuna		81
2817	Mashhad		84
2822	Fort Lamy		26
2837	Natal		27
	SPEOPTS		
7034	East Grand Forks		35
7036	Edinburg	45	33
7037	Columbia	78	40

Table B-4 (Continued)

Station	GEOS-I	GEOS-II
7039 Bermuda	25	28
7040 San Juan	47	30
7043 Greenbelt	42	
7045 Denver	63	37
7050 Greenbelt (laser)		25
7052 Wallops Island (laser)		13
7054 Carnarvon (laser)		33
7072 Jupiter	36	
7075 Sudbury	13	14
7076 Kingston	18	22
Baker-Nunn		
9001 Organ Pass	47	
9002 Olifantsfontein	44	38
9004 San Fernando	42	62
9005 Tokyo	31	
9006 Naini Tal	51	11
9007 Arequipa	24	45
9008 Shiraz	48	
9009 Curaçao	26	
9010 Jupiter	39	4
9011 Villa Dolores	35	
9012 Maui	50	32
9023 Woomera	41	42

Table B-5

MOTS and SPEOPTS Camera Observations* in 7-Day Arcs
(Used for GEM Gravitational and Station Solutions)

Station	GEOS-I	GEOS-II
1021 Blossom Pt.	636	
1022 Ft. Myers	1737	1021
1024 Woomera	616	
1028 Santiago	233	382
1030 Goldstone	1569	1405
1031 Johannesburg	690	328
1032 St. John's	46	56
1033 Fairbanks	129	
1034 East Grand Forks	1531	
1035 Winkfield	145	263
1036 Fairbanks		434
1037 Rosman	112	1179
1038 Orroral		617
1042 Rosman	861	421
1043 Tananarive	95	170
7034 East Grand Forks		564
7036 Edinburg	1272	704
7037 Columbia	1765	1074
7039 Bermuda	651	555
7040 San Juan	914	472
7043 Greenbelt	601	
7045 Denver	1349	999
7071 Jupiter	145	
7072 Jupiter	615	
7073 Jupiter	108	
7074 Jupiter	151	
7075 Sudbury	484	47
7076 Kingston	638	20
7077 Greenbelt	90	41
7079 Carnarvon		14

*Observation pairs of right ascension and declination.

Table B-6

BC-4 Simultaneous Photographic Events

Two Station Events					
Stations	No. of Events	Stations	No. of Events	Stations	No. of Events
6002 - 6003	6*	6009 - 6019	8	6019 - 6020	4
6002 - 6006	1	6009 - 6020	3	6019 - 6043	11
6002 - 6007	8	6009 - 6038	7	6019 - 6061	9
6002 - 6008	14	6009 - 6043	1	6019 - 6067	12
6002 - 6009	4			6019 - 6069	2
6002 - 6038	4	6011 - 6012	9		
6002 - 6111	4	6011 - 6022	1	6020 - 6038	8
6002 - 6134	3	6011 - 6038	5	6020 - 6039	3
		6011 - 6059	13	6020 - 6043	7
6003 - 6004	6	6011 - 6134	4		
6003 - 6011	2			6022 - 6023	1
6003 - 6012	1	6012 - 6013	5	6022 - 6031	7
6003 - 6038	8	6012 - 6022	6	6022 - 6039	2
6003 - 6111	1	6012 - 6023	8	6022 - 6059	10
6003 - 6123	5	6012 - 6059	8	6022 - 6060	5
				6022 - 6078	2
6004 - 6011	1	6013 - 6015	2		
6004 - 6012	3	6013 - 6040	1	6023 - 6031	2
6004 - 6013	5	6013 - 6047	6	6023 - 6047	4
6004 - 6123	6	6013 - 6072	4	6023 - 6060	18
		6013 - 6078	1	6023 - 6072	2
6006 - 6007	2			6023 - 6078	3
6006 - 6015	8	6015 - 6016	11		
6006 - 6016	11	6015 - 6040	2	6031 - 6032	3
6006 - 6065	5	6015 - 6042	8	6031 - 6039	3
		6015 - 6064	2	6031 - 6052	5
6007 - 6016	12	6015 - 6065	6	6031 - 6053	8
6007 - 6063	10	6015 - 6072	8	6031 - 6060	13
6007 - 6065	3	6015 - 6073	4	6031 - 6078	4
6007 - 6067	2	6015 - 6075	3		
				6032 - 6040	8
6008 - 6009	6	6016 - 6042	3	6032 - 6044	4
6008 - 6019	11	6016 - 6063	3	6032 - 6045	3
6008 - 6063	1	6016 - 6064	6	6032 - 6047	8
6008 - 6067	3	6016 - 6065	4	6032 - 6051	3

*Each photographic event consists of 7 points of satellite position observed simultaneously by the stations designated.

Table B-6 (Continued)

Two Station Events

Stations	No. of Events	Stations	No. of Events	Stations	No. of Events
6032 - 6052	5	6044 - 6045	2	6055 - 6061	2
6032 - 6053	1	6044 - 6051	4	6055 - 6063	8
6032 - 6060	1	6044 - 6052	1	6055 - 6064	14
6032 - 6072	1			6055 - 6067	9
		6045 - 6051	4	6055 - 6068	2
6038 - 6039	5	6045 - 6068	11	6055 - 6069	7
6038 - 6059	3	6045 - 6073	5		
6038 - 6134	10	6045 - 6075	3	6061 - 6067	3
				6061 - 6068	3
6039 - 6059	5	6047 - 6072	9	6061 - 6069	3
		6047 - 6078	1		
6040 - 6045	8			6063 - 6064	5
6040 - 6047	2	6050 - 6051	1	6063 - 6067	6
6040 - 6060	1	6050 - 6052	2		
6040 - 6072	3	6050 - 6053	4	6064 - 6068	8
6040 - 6073	3	6050 - 6061	4		
6040 - 6075	4			6067 - 6069	1
		6051 - 6052	8		
6042 - 6045	2	6051 - 6053	12	6068 - 6069	2
6042 - 6064	6	6051 - 6061	5	6068 - 6075	1
6042 - 6068	7	6051 - 6068	12		
6042 - 6073	1			6072 - 6073	1
6042 - 6075	6	6052 - 6053	10	6072 - 6075	1
		6062 - 6060	6		
6043 - 6050	10			6073 - 6075	7
6043 - 6061	8	6053 - 6060	3		
		6053 - 6061	1		

Three Station Events

Stations	No. of Events	Stations	No. of Events
6002 - 6003 - 6038	4	6003 - 6004 - 6123	1
6002 - 6003 - 6111	8	6003 - 6011 - 6012	1
6002 - 6008 - 6009	1	6003 - 6011 - 6038	2
6002 - 6009 - 6038	1	6003 - 6011 - 6111	2
		6003 - 6011 - 6134	5

Table B-6 (Continued)

Three Station Events			
Stations	No. of Events	Stations	No. of Events
6004 - 6012 - 6013	3	6019 - 6020 - 6043	3
		6019 - 6043 - 6061	4
6006 - 6015 - 6016	2		
6006 - 6015 - 6065	3	6022 - 6023 - 6060	2
		6022 - 6023 - 6078	1
6007 - 6016 - 6063	3	6022 - 6031 - 6059	1
6007 - 6016 - 6064	1	6022 - 6039 - 6059	2
6007 - 6016 - 6065	2		
6007 - 6055 - 6067	2	6023 - 6031 - 6032	2
6007 - 6063 - 6064	2	6023 - 6031 - 6060	2
6007 - 6064 - 6065	1	6023 - 6032 - 6060	12
6007 - 6064 - 6067	1	6023 - 6040 - 6047	1
6008 - 6009 - 6019	1	6031 - 6032 - 6060	9
6008 - 6019 - 6061	1	6031 - 6051 - 6053	1
6008 - 6019 - 6067	2	6031 - 6052 - 6053	1
		6031 - 6053 - 6060	3
6009 - 6019 - 6043	3		
6009 - 6020 - 6038	2	6032 - 6040 - 6044	2
		6032 - 6040 - 6045	1
6011 - 6012 - 6059	1	6032 - 6040 - 6047	1
6011 - 6022 - 6059	2	6032 - 6051 - 6052	3
6011 - 6038 - 6059	3	6032 - 6052 - 6053	1
6013 - 6040 - 6072	1	6040 - 6045 - 6073	4
6013 - 6047 - 6072	2	6040 - 6045 - 6075	1
6015 - 6016 - 6042	1	6042 - 6045 - 6068	2
6015 - 6016 - 6064	8	6042 - 6045 - 6075	4
6015 - 6016 - 6065	3	6042 - 6064 - 6068	9
6015 - 6040 - 6045	1	6042 - 6068 - 6075	1
6015 - 6040 - 6075	1		
6015 - 6042 - 6045	4	6043 - 6050 - 6061	1
6015 - 6045 - 6073	1		
6015 - 6072 - 6073	2	6044 - 6051 - 6068	1
6015 - 6072 - 6075	2		
		6045 - 6051 - 6068	2
6016 - 6063 - 6064	2	6045 - 6068 - 6075	1
		6045 - 6073 - 6075	5

Table B-6 (Continued)

Three Station Events			
Stations	No. of Events	Stations	No. of Events
6051 - 6052 - 6053	3	6055 - 6063 - 6064	3
		6055 - 6063 - 6067	4
6052 - 6053 - 6060	2	6055 - 6063 - 6069	2

Four Station Events	
Stations	No. of Events
6007 - 6016 - 6063 - 6064	1
6012 - 6022 - 6023 - 6060	1
6015 - 6016 - 6042 - 6064	1
6015 - 6042 - 6045 - 6073	2
6015 - 6042 - 6045 - 6075	1
6015 - 6045 - 6073 - 6075	1
6023 - 6031 - 6032 - 6060	3
6023 - 6032 - 6047 - 6060	2
6040 - 6045 - 6073 - 6075	1

Table B-7

MOTS Geometric Events

Two-Station Simultaneous Optical Observations

Two Stations Observing	Number of Flashes Observed	Two Stations Observing	Number of Flashes Observed
1021-1022	20	1030-7075	8
1021-1034	16	1034-1042	41
1021-1042	10	1034-7036	33
1021-7036	5	1034-7037	220
1021-7037	29	1034-7045	100
1021-7039	21	1034-7075	60
1021-7040	16	1042-7036	34
1021-7045	1	1042-7037	25
1021-7075	81	1042-7039	9
1022-1030	58	1042-7040	13
1022-1034	16	1042-7045	24
1022-1042	64	1042-7075	19
1022-7036	109	7036-7037	92
1022-7037	124	7036-7045	94
1022-7039	48	7036-7076	50
1022-7040	106	7037-7039	35
1022-7045	44	7037-7045	168
1022-7076	151	7037-7075	91
1030-1034	134	7037-7076	16
1030-1042	6	7039-7040	95
1030-7036	254	7039-7075	25
1030-7037	114	7045-7075	14
1030-7045	358		

Table B-7 (Continued)

Three-Station Simultaneous Optical Observations

Three Stations Observing	Number of Flashes Observed
1021-1034-7037	12
1021-1034-7075	12
1021-1042-7037	14
1022-1034-1042	39
1022-1034-7045	10
1022-1034-7075	14
1022-1042-7037	35
1022-7037-7039	21
1022-7039-7040	26
1022-7040-7076	47
1022-7045-7076	13
1030-1034-7036	10
1030-1034-7037	39
1030-1034-7045	14
1030-7036-7037	43
1030-7036-7045	45
1030-7037-7045	76
1034-1042-7037	17
1034-1042-7045	13
1034-7037-7045	44
1034-7037-7075	40
7036-7037-7045	30

Table B-7 (Continued)

Four-Station Simultaneous Optical Observations

Four Stations Observing	Number of Flashes Observed	Four Stations Observing	Number of Flashes Observed
1021 1022 1042 7043	6	1022 1034 1042 7075	6
1021 1022 7034 7040	1	1022 1034 7036 7039	5
1021 1022 7040 7043	4	1022 1034 7036 7072	5
1021 1022 7043 7045	3	1022 1034 7037 7075	6
1021 1030 1034 7037	6	1022 1034 7039 7074	3
1021 1034 1042 7037	8	1022 1034 7072 7074	3
1021 1034 1042 7045	5	1022 1034 7072 7076	4
1021 1034 7037 7043	7	1022 1037 7034 7036	8
1021 1034 7037 7075	6	1022 1037 7037 7040	2
1021 1034 7043 7045	6	1022 1037 7037 7075	2
1021 1042 7036 7037	6	1022 1037 7039 7075	2
1021 1042 7037 7045	14	1022 1037 7075 7077	5
1021 1042 7040 7043	6	1022 1037 7076 7077	5
1021 7036 7037 7039	1	1022 1042 7036 7037	5
1021 7043 7072 7074	1	1022 1042 7036 7045	3
1021 7045 7072 7076	1	1022 1042 7037 7072	10
1022 1030 1037 7037	5	1022 1042 7039 7072	1
1022 1030 7034 7037	7	1022 1042 7043 7076	1
1022 1030 7036 7037	7	1022 1042 7071 7072	4
1022 1030 7036 7045	7	1022 1042 7072 7076	5
1022 1030 7045 7072	5	1022 7036 7037 7039	6
1022 1034 1042 7036	7	1022 7036 7037 7045	17
1022 1034 1042 7043	5	1022 7036 7037 7076	3
1022 1034 1042 7045	7	1022 7037 7039 7040	7

Table B-7 (Continued)

Four-Station Simultaneous Optical Observations

Four Stations Observing	Number of Flashes Observed	Four Stations Observing	Number of Flashes Observed
1022 7037 7039 7043	7	1034 1042 7037 7043	6
1022 7037 7040 7072	4	1034 1042 7037 7045	2
1022 7037 7040 7077	4	1034 1042 7037 7075	1
1022 7037 7043 7045	7	1034 1042 7039 7045	1
1022 7037 7045 7072	7	1034 1042 7045 7075	7
1022 7039 7040 7076	14	1034 7036 7037 7043	5
1022 7071 7072 7073	5	1034 7037 7039 7075	13
1022 7071 7072 7074	2	1034 7037 7045 7075	4
1022 7072 7073 7074	13	1037 7034 7036 7037	7
1030 1034 7036 7037	23	1037 7034 7037 7045	20
1030 1034 7036 7045	12	1037 7034 7039 7045	7
1030 1034 7037 7045	33	1037 7036 7037 7045	3
1030 1034 7037 7075	6	1037 7036 7037 7076	6
1030 1037 7034 7036	11	1037 7036 7076 7078	3
1030 1037 7034 7045	1	1037 7037 7039 7045	5
1030 1037 7036 7045	6	1042 7036 7037 7075	7
1030 1042 7036 7075	1	1042 7036 7043 7045	7
1030 7034 7036 7037	6	1042 7040 7043 7076	2
1030 7034 7036 7045	2	7034 7036 7037 7045	7
1030 7034 7037 7045	35	7034 7036 7037 7077	1
1030 7034 7045 7075	7	7036 7037 7043 7076	7
1030 7036 7037 7045	20	7036 7039 7075 7076	1
1030 7045 7071 7072	4	7039 7040 7071 7072	4
1034 1042 7037 7039	1		

Table B-8

MOTS & LASER Geometric Events

Three-Station Simultaneous Optical-LASER Observations

Three Stations Observing	Number of Flashes Observed
7040-7077-7050	1
7075-7077-7050	2
1037-7077-7050	19
1037-7075-7050	7
1022-7034-7052	4
1037-7034-7052	6
1037-7078-7052	1

Table B-9

Survey Ties Employed

Station Pair	Relative Position Constraints (Meters)			Est. Stand. Dev. (Meters)
	Δx	Δy	Δz	σ
2017 2117	-3.75	6.28	-2.02	4.23
2822 6064	-12.06	13.60	23.74	3.00
2837 6067	46.13	290.25	-1248.20	3.00
1038 6060	304147.18	114912.15	494900.60	2.04
2019 6053	-130.35	808.62	87.15	3.00
2722 6055	-78.06	-172.20	-160.45	3.00
2723 6040	19.71	0.69	14.10	3.00
1152 6032	-47149.40	-424141.91	676055.82	2.50
6019 9011	-52.01	-37.07	18.82	0.01
1021 7043	12681.43	44984.51	51158.99	0.49
1022 7071	168409.91	50582.89	45732.81	0.93
1034 7034	0.08	0.66	-0.74	0.01
1037 1042	-7.58	-0.59	0.50	0.01
7043 7050	-38.21	-36.26	-31.23	0.01
7043 7052	130836.64	-50256.13	-100969.38	0.90
7043 7077	-652.92	-1710.84	-1877.61	0.06
7043 7078	130867.90	-50025.41	-100693.72	0.90
7071 7072	4.08	5.48	11.42	0.01
7071 7073	10.32	6.62	9.32	0.01
7071 7074	11.03	8.97	15.81	0.01
2738 6003	3.96	-23.90	21.87	3.00
1025 6009	17214.35	4034.43	58089.41	0.46
2817 6015	7.76	4.05	-16.20	3.00

Table B-9 (Continued)

Station Pair	Relative Position Constraints (Meters)			Est. Stand. Dev. (Meters)
	Δx	Δy	Δz	σ
6111 6134	-53.77	-90.12	-305.26	0.01
6002 7043	-56.27	-499.54	-586.43	0.02
6011 9012	-49.58	118.93	-35.81	0.01
7071 9010	19.05	3.07	3.92	0.01
9003 9023	6011.64	-17986.56	-27467.42	0.30
4740 7039	-674.06	699.92	1476.31	0.04
4760 7039	-683.27	706.55	1488.25	0.04
1037 1126	-334.06	-403.53	-571.31	0.02
1152 7054	54.96	-51.86	-135.62	0.01
2203 7052	-116.78	-336.48	-389.60	3.00
2115 4050	354.70	970.65	296.73	3.00
4082 7071	65691.26	62291.57	137735.55	0.87
4840 4860	-2384.64	711.85	1660.19	0.06
4840 7052	-2425.68	685.03	1630.22	0.06
1024 4946	-21762.84	24680.80	54300.42	0.46
1031 6068	59.69	-55.46	51.19	0.01
6068 9002	28722.17	46167.12	-7673.38	0.42
7072 9049	4.82	-3.60	-12.97	0.01
6111 9425	-1159.33	43554.59	52281.60	0.48
6042 9028	2992.55	-3032.66	-2462.26	0.08
2100 6011	32128.97	-180272.68	-83071.46	3.04
9005 9025	36256.49	10061.56	30386.63	0.38
7901 9001	0.00	0.00	0.00	4.23
2106 1035	-22330.33	23266.93	17999.44	3.02

Table B-10

5° Equal Area Surface Gravimetric Data of Rapp (1972)

PHI	LAMDA	DELG	M	N	PHI	LAMDA	DELG	M	N	PHI	LAMDA	DELG	M	N	PHI	LAMDA	DELG	M	N	PHI	LAMDA	DELG	M	N
87.5	60.0	2.	13.	3	87.5	180.0	5.	7.	13	87.5	300.0	4.	8.	8	82.5	20.0	10.	10.	7	82.5	60.0	18.	14.	2
82.5	180.0	-1.	6.	16	82.5	220.5	5.	4.	23	82.5	260.0	6.	10.	7	82.5	300.0	-12.	5.	15	82.5	340.0	9.	13.	4
77.5	11.5	-8.	10.	8	77.5	34.0	-2.	12.	3	77.5	56.5	-10.	9.	5	77.5	79.0	-9.	12.	4	77.5	146.5	-15.	15.	1
77.5	169.0	-7.	10.	7	77.5	191.5	4.	3.	24	77.5	214.0	-12.	2.	25	77.5	236.5	-2.	2.	25	77.5	259.0	-8.	2.	25
77.5	281.5	1.	5.	18	77.5	304.0	15.	6.	12	77.5	326.5	-8.	8.	7	77.5	349.0	19.	11.	4	72.5	8.0	17.	10.	13
72.5	24.5	-3.	5.	19	72.5	41.0	0.	12.	3	72.5	57.0	-7.	7.	11	72.5	73.5	-8.	10.	5	72.5	90.0	-7.	10.	9
72.5	106.5	-11.	4.	20	72.5	123.0	5.	3.	25	72.5	172.0	-1.	15.	1	72.5	188.0	-4.	6.	16	72.5	204.5	-16.	3.	25
72.5	221.0	-12.	2.	25	72.5	237.0	-8.	4.	19	72.5	253.5	-19.	6.	13	72.5	270.0	-6.	3.	23	72.5	286.5	-3.	4.	22
72.5	303.0	-6.	5.	16	72.5	319.0	16.	11.	7	72.5	335.5	9.	9.	8	72.5	352.0	13.	13.	2	67.5	6.5	11.	4.	24
67.5	19.5	-1.	2.	24	67.5	32.5	-0.	7.	15	67.5	45.0	-3.	10.	6	67.5	57.5	-8.	9.	7	67.5	83.5	-9.	5.	18
67.5	96.5	-16.	3.	25	67.5	109.5	-23.	3.	25	67.5	122.5	-20.	3.	25	67.5	135.5	3.	3.	25	67.5	147.5	8.	3.	25
67.5	150.5	13.	3.	25	67.5	173.5	19.	3.	25	67.5	186.5	2.	3.	25	67.5	199.5	-3.	3.	22	67.5	212.5	14.	3.	25
67.5	225.0	4.	4.	21	67.5	237.5	-3.	2.	25	67.5	250.5	-24.	2.	25	67.5	263.5	-29.	7.	14	67.5	276.5	-34.	5.	15
67.5	289.5	-20.	2.	25	67.5	302.5	19.	3.	25	67.5	315.0	1.	12.	5	67.5	327.5	20.	12.	3	67.5	340.5	27.	9.	11
62.5	5.5	11.	2.	25	62.5	16.5	-10.	2.	24	62.5	27.5	-7.	4.	23	62.5	38.5	-1.	4.	19	62.5	49.5	1.	4.	20
62.5	60.0	-4.	12.	4	62.5	70.5	-11.	13.	2	62.5	81.5	-19.	5.	18	62.5	92.5	-30.	3.	25	62.5	103.5	-37.	4.	25
62.5	114.5	-27.	3.	25	62.5	125.5	-24.	3.	25	62.5	136.5	1.	3.	25	62.5	147.5	19.	3.	25	62.5	158.5	17.	4.	24
62.5	169.5	24.	4.	22	62.5	180.0	18.	11.	6	62.5	190.5	-2.	5.	19	62.5	201.5	12.	5.	19	62.5	212.5	24.	3.	24
62.5	223.5	27.	6.	17	62.5	234.5	10.	5.	18	62.5	245.5	-19.	2.	25	62.5	256.5	-31.	2.	25	62.5	267.5	-39.	3.	25
62.5	278.5	-28.	3.	25	62.5	289.5	-12.	3.	21	62.5	300.0	3.	4.	19	62.5	310.5	-12.	5.	17	62.5	321.5	6.	14.	3
62.5	332.5	27.	9.	9	62.5	343.5	27.	5.	18	62.5	354.5	16.	5.	19	57.5	4.5	1.	2.	24	57.5	13.5	0.	1.	25
57.5	23.0	-19.	5.	18	57.5	32.5	-2.	3.	24	57.5	41.5	2.	5.	18	57.5	50.5	6.	4.	19	57.5	60.0	7.	2.	25
57.5	69.5	-17.	2.	25	57.5	78.5	-17.	2.	25	57.5	87.5	-17.	3.	25	57.5	97.0	-30.	3.	25	57.5	106.5	-16.	4.	25
57.5	115.5	-36.	3.	25	57.5	124.5	-33.	3.	25	57.5	133.5	-10.	3.	25	57.5	143.0	2.	12.	5	57.5	152.5	12.	13.	3
57.5	161.5	17.	4.	22	57.5	170.5	4.	7.	13	57.5	180.0	-15.	8.	12	57.5	189.5	12.	5.	20	57.5	198.5	25.	9.	10
57.5	207.5	9.	3.	24	57.5	217.0	6.	5.	15	57.5	226.5	12.	5.	18	57.5	235.5	13.	4.	20	57.5	244.5	-5.	3.	25
57.5	253.5	-13.	2.	25	57.5	263.0	-26.	2.	25	57.5	272.5	-40.	3.	25	57.5	281.5	-39.	3.	25	57.5	290.5	-27.	3.	24
57.5	300.0	-15.	6.	16	57.5	309.5	7.	3.	9	57.5	318.5	6.	12.	5	57.5	327.5	24.	11.	5	57.5	346.5	5.	8.	12
57.5	355.5	16.	3.	24	52.5	4.0	-7.	1.	25	52.5	12.0	8.	1.	25	52.5	20.5	-0.	2.	23	52.5	29.0	4.	3.	24
52.5	37.0	0.	4.	21	52.5	45.0	-2.	4.	22	52.5	53.0	-8.	3.	25	52.5	61.0	4.	1.	25	52.5	69.5	-1.	6.	15
52.5	78.0	-21.	3.	23	52.5	86.0	-11.	3.	25	52.5	94.0	-23.	3.	25	52.5	102.0	-33.	3.	25	52.5	110.5	-10.	11.	7
52.5	119.0	3.	12.	4	52.5	127.0	4.	10.	8	52.5	159.5	15.	8.	12	52.5	168.0	6.	8.	9	52.5	176.0	-4.	4.	24
52.5	184.0	-24.	3.	24	52.5	192.0	3.	3.	23	52.5	200.5	-1.	6.	15	52.5	209.0	7.	13.	3	52.5	217.0	5.	9.	9
52.5	225.0	-2.	5.	20	52.5	233.0	12.	2.	25	52.5	241.0	6.	2.	25	52.5	249.5	-3.	1.	25	52.5	258.0	1.	2.	25
52.5	266.0	-9.	2.	25	52.5	274.0	-26.	2.	25	52.5	282.0	-32.	3.	24	52.5	290.5	-10.	2.	25	52.5	299.0	-20.	3.	25
52.5	307.0	-1.	5.	20	52.5	323.0	21.	9.	9	52.5	331.0	12.	10.	7	52.5	339.5	-3.	12.	4	52.5	348.0	15.	5.	21
52.5	356.0	11.	3.	24	47.5	3.5	5.	1.	25	47.5	11.0	10.	0.	25	47.5	18.5	18.	2.	24	47.5	25.5	20.	4.	21
47.5	33.0	9.	3.	24	47.5	40.5	-4.	3.	25	47.5	47.5	-14.	6.	14	47.5	55.0	-23.	6.	14	47.5	62.5	-11.	5.	15
47.5	69.5	-14.	2.	25	47.5	77.0	-27.	3.	25	47.5	84.5	-35.	3.	25	47.5	92.0	-16.	3.	25	47.5	99.5	-20.	4.	25
47.5	106.5	0.	9.	10	47.5	114.0	-4.	12.	5	47.5	121.5	10.	5.	13	47.5	128.5	8.	6.	15	47.5	136.0	6.	10.	7
47.5	143.5	-1.	10.	10	47.5	165.5	13.	14.	1	47.5	172.5	5.	9.	9	47.5	180.0	11.	10.	10	47.5	187.5	16.	9.	10
47.5	194.5	12.	10.	6	47.5	202.0	6.	9.	8	47.5	209.5	-2.	11.	4	47.5	216.5	-5.	12.	3	47.5	224.0	-2.	10.	8
47.5	231.5	-10.	4.	23	47.5	238.5	-7.	1.	25	47.5	246.0	8.	1.	25	47.5	253.5	14.	2.	25	47.5	260.5	7.	2.	25
47.5	268.0	2.	1.	25	47.5	275.5	-11.	1.	25	47.5	283.0	-15.	2.	25	47.5	290.5	-7.	1.	25	47.5	297.5	-10.	2.	25
47.5	305.0	12.	3.	24	47.5	312.5	18.	4.	22	47.5	319.5	6.	4.	20	47.5	327.0	23.	3.	24	47.5	334.5	35.	5.	20
47.5	341.5	16.	4.	22	47.5	349.0	4.	3.	24	47.5	356.5	-0.	2.	25	42.5	3.5	12.	3.	23	42.5	10.5	13.	3.	23
42.5	17.0	22.	4.	20	42.5	23.5	21.	7.	11	42.5	30.5	-8.	6.	15	42.5	37.5	-23.	5.	17	42.5	44.5	10.	5.	15
42.5	51.0	-30.	11.	6	42.5	57.5	-7.	3.	20	42.5	64.5	-20.	2.	25	42.5	71.5	-32.	3.	25	42.5	78.5	-7.	4.	25
42.5	85.0	-20.	4.	25	42.5	91.5	-28.	4.	25	42.5	98.5	-5.	4.	25	42.5	105.5	4.	9.	10	42.5	112.0	-2.	14.	2
42.5	118.5	4.	12.	4	42.5	125.5	18.	5.	16	42.5	132.5	4.	5.	18	42.5	139.5	13.	3.	25	42.5	146.0	-17.	7.	15
42.5	166.5	-2.	13.	3	42.5	173.5	4.	10.	7	42.5	180.0	1.	12.	3	42.5	186.5	-5.	13.	2	42.5	193.5	-3.	15.	1

PHI – Latitude, LAMDA – Longitude, DELG – 5° mean gravity anomaly, M – accuracy of DELG in mgal, N – number of 1° equal area observed anomalies used to form DELG.

Table B-10 (Continued)

PHI	LAMDA	DELG	M	N	PHI	LAMDA	DELG	M	N	PHI	LAMDA	DELG	M	N	PHI	LAMDA	DELG	M	N	PHI	LAMDA	DELG	M	N
42.5	200.5	-4.	7.	12	42.5	207.5	0.	11.	4	42.5	214.0	-1.	13.	3	42.5	220.5	-11.	9.	11	42.5	227.5	-7.	6.	20
42.5	234.5	-11.	2.	25	42.5	241.5	10.	1.	25	42.5	248.0	22.	1.	25	42.5	254.5	15.	2.	25	42.5	261.5	-2.	2.	25
42.5	268.5	-10.	0.	25	42.5	275.0	-11.	1.	25	42.5	281.5	-11.	1.	25	42.5	288.5	0.	1.	25	42.5	295.5	-6.	4.	23
42.5	302.5	-18.	4.	25	42.5	309.0	12.	5.	19	42.5	315.5	4.	4.	23	42.5	322.5	13.	3.	25	42.5	329.5	27.	4.	25
42.5	336.5	25.	3.	25	42.5	343.0	2.	3.	24	42.5	349.5	5.	3.	23	42.5	356.5	8.	2.	25	37.5	3.0	14.	4.	21
37.5	9.5	23.	5.	18	37.5	16.0	7.	4.	23	37.5	22.0	-3.	7.	14	37.5	28.5	-1.	8.	11	37.5	35.0	25.	9.	11
37.5	41.0	9.	8.	8	37.5	47.5	42.	5.	13	37.5	54.0	1.	6.	17	37.5	60.0	-15.	3.	25	37.5	66.0	-25.	4.	23
37.5	72.5	-6.	4.	24	37.5	79.0	-11.	4.	25	37.5	85.0	-8.	4.	25	37.5	91.5	9.	4.	25	37.5	98.0	10.	5.	25
37.5	104.0	6.	7.	15	37.5	110.5	-13.	10.	6	37.5	117.0	-18.	8.	9	37.5	123.0	8.	8.	10	37.5	129.5	14.	4.	20
37.5	136.0	24.	3.	25	37.5	142.0	23.	3.	24	37.5	148.5	1.	9.	9	37.5	155.0	3.	8.	8	37.5	161.0	-2.	5.	13
37.5	167.5	-3.	9.	8	37.5	174.0	1.	11.	7	37.5	180.0	-3.	13.	3	37.5	192.5	-9.	11.	5	37.5	199.0	-7.	9.	8
37.5	205.0	-4.	7.	13	37.5	211.5	4.	10.	10	37.5	218.0	-20.	5.	21	37.5	224.0	-18.	7.	15	37.5	230.5	-25.	2.	25
37.5	237.0	-17.	1.	25	37.5	243.0	-1.	1.	25	37.5	249.5	7.	2.	25	37.5	256.0	9.	2.	25	37.5	262.0	-11.	3.	25
37.5	268.5	-7.	1.	25	37.5	275.0	-5.	0.	25	37.5	281.0	-0.	1.	25	37.5	287.5	-22.	2.	25	37.5	294.0	-22.	4.	22
37.5	300.0	-17.	5.	19	37.5	306.0	-14.	5.	20	37.5	312.5	-2.	4.	21	37.5	319.0	16.	4.	25	37.5	325.0	33.	4.	25
37.5	331.5	40.	3.	25	37.5	338.0	15.	4.	23	37.5	344.0	5.	5.	17	37.5	350.5	6.	4.	22	37.5	357.0	11.	3.	25
32.5	3.0	3.	1.	25	32.5	9.0	-10.	4.	19	32.5	15.0	0.	5.	18	32.5	21.0	8.	6.	16	32.5	27.0	-35.	4.	24
32.5	32.5	-17.	4.	25	32.5	38.0	25.	5.	17	32.5	44.0	-4.	12.	5	32.5	50.0	13.	4.	23	32.5	56.0	17.	4.	25
32.5	62.0	25.	7.	15	32.5	68.0	12.	7.	14	32.5	74.0	-38.	3.	25	32.5	80.0	42.	4.	25	32.5	86.0	24.	5.	25
32.5	91.5	8.	5.	25	32.5	97.0	11.	4.	25	32.5	103.0	-10.	5.	20	32.5	109.0	-22.	10.	7	32.5	115.0	-26.	7.	14
32.5	121.0	0.	9.	9	32.5	127.0	17.	9.	10	32.5	133.0	19.	6.	14	32.5	139.0	-20.	5.	17	32.5	145.0	-4.	7.	14
32.5	150.5	-5.	9.	9	32.5	156.0	-7.	7.	12	32.5	162.0	-13.	8.	11	32.5	168.0	-16.	8.	9	32.5	174.0	-10.	12.	5
32.5	180.0	-4.	14.	1	32.5	186.0	-24.	11.	6	32.5	192.0	-14.	13.	3	32.5	198.0	-4.	8.	9	32.5	204.0	-4.	13.	4
32.5	209.5	-3.	7.	13	32.5	215.0	-13.	11.	8	32.5	221.0	-9.	6.	17	32.5	227.0	-18.	4.	23	32.5	233.0	-19.	7.	15
32.5	239.0	-22.	3.	23	32.5	245.0	-12.	2.	25	32.5	251.0	-1.	2.	25	32.5	257.0	-4.	2.	25	32.5	263.0	-7.	3.	25
32.5	268.5	0.	3.	25	32.5	274.0	-2.	2.	25	32.5	280.0	-5.	2.	24	32.5	286.0	-38.	4.	22	32.5	292.0	-26.	4.	22
32.5	298.0	-9.	4.	22	32.5	304.0	-15.	5.	20	32.5	310.0	-4.	5.	20	32.5	316.0	10.	4.	23	32.5	322.0	27.	4.	24
32.5	327.5	17.	7.	14	32.5	333.0	5.	10.	10	32.5	339.0	-3.	7.	13	32.5	345.0	5.	4.	23	32.5	351.0	26.	3.	23
32.5	357.0	41.	2.	25	27.5	3.0	-10.	1.	25	27.5	8.5	4.	3.	23	27.5	14.0	3.	5.	9	27.5	20.0	2.	8.	12
27.5	25.5	1.	8.	11	27.5	31.0	6.	7.	13	27.5	36.5	1.	7.	12	27.5	42.0	6.	9.	11	27.5	48.0	-10.	4.	23
27.5	53.5	-15.	4.	25	27.5	59.0	8.	4.	25	27.5	65.0	8.	4.	24	27.5	70.5	-10.	3.	25	27.5	76.0	-19.	3.	25
27.5	81.5	-71.	4.	24	27.5	87.0	-27.	4.	25	27.5	93.0	-31.	4.	25	27.5	98.5	-7.	5.	25	27.5	104.0	-25.	5.	21
27.5	110.0	-20.	7.	14	27.5	115.5	-8.	3.	10	27.5	121.0	4.	8.	9	27.5	126.5	26.	8.	9	27.5	132.0	-17.	13.	3
27.5	138.0	16.	8.	9	27.5	143.5	-11.	11.	5	27.5	149.0	0.	13.	4	27.5	155.0	29.	10.	8	27.5	160.5	-4.	14.	3
27.5	156.0	-9.	11.	6	27.5	171.5	-9.	9.	10	27.5	177.0	-4.	10.	9	27.5	183.0	-13.	13.	3	27.5	188.5	-1.	8.	12
27.5	194.0	6.	10.	7	27.5	200.0	8.	10.	6	27.5	205.5	-2.	11.	7	27.5	211.0	-5.	6.	16	27.5	216.5	2.	7.	15
27.5	222.0	-13.	10.	10	27.5	228.0	-14.	10.	6	27.5	233.5	-17.	9.	8	27.5	239.0	-23.	8.	12	27.5	245.0	-18.	5.	21
27.5	250.5	-7.	2.	25	27.5	256.0	15.	1.	25	27.5	261.5	-4.	1.	25	27.5	267.0	-9.	2.	25	27.5	273.0	-2.	4.	20
27.5	278.5	3.	2.	25	27.5	284.0	-18.	5.	21	27.5	290.0	-25.	7.	11	27.5	295.5	-17.	5.	16	27.5	301.0	-29.	5.	20
27.5	306.5	-21.	4.	22	27.5	312.0	-2.	4.	21	27.5	318.0	8.	5.	18	27.5	323.5	-2.	4.	22	27.5	329.0	0.	5.	21
27.5	335.0	-10.	5.	20	27.5	340.5	0.	5.	20	27.5	346.0	14.	5.	18	27.5	351.5	11.	5.	18	27.5	357.0	-3.	6.	17
22.5	2.5	20.	2.	25	22.5	8.0	26.	2.	25	22.5	13.5	3.	3.	25	22.5	18.5	3.	5.	17	22.5	24.0	-17.	7.	13
22.5	29.5	4.	15.	1	22.5	35.0	-3.	9.	11	22.5	40.5	33.	9.	8	22.5	45.5	-10.	11.	6	22.5	51.0	-31.	4.	21
22.5	56.5	-15.	13.	3	22.5	67.0	-6.	8.	11	22.5	72.5	2.	3.	25	22.5	78.0	1.	3.	25	22.5	83.5	-1.	4.	25
22.5	88.5	-9.	4.	21	22.5	94.0	-22.	5.	23	22.5	99.5	-19.	5.	25	22.5	104.5	-19.	5.	20	22.5	110.0	-11.	7.	11
22.5	115.5	-9.	9.	8	22.5	121.0	0.	7.	10	22.5	126.5	-1.	7.	12	22.5	131.5	1.	11.	6	22.5	137.0	1.	9.	5
22.5	142.5	1.	11.	4	22.5	153.0	8.	13.	4	22.5	158.5	-13.	10.	7	22.5	164.0	-10.	10.	5	22.5	174.5	-6.	11.	5
22.5	180.0	-9.	8.	13	22.5	185.5	2.	8.	10	22.5	190.5	6.	6.	15	22.5	196.0	10.	6.	13	22.5	201.5	24.	6.	17
22.5	207.0	5.	6.	18	22.5	212.5	-7.	8.	10	22.5	217.5	-5.	8.	11	22.5	223.0	-8.	8.	10	22.5	228.5	-12.	8.	13
22.5	233.5	-9.	10.	6	22.5	244.5	-9.	13.	5	22.5	250.0	-10.	6.	17	22.5	255.5	11.	3.	23	22.5	260.5	20.	3.	25
22.5	256.0	1.	3.	25	22.5	271.5	12.	2.	24	22.5	276.5	-1.	3.	24	22.5	282.0	-6.	3.	25	22.5	287.5	-53.	5.	25

Table B-10 (Continued)

PHI	LAMDA	DELG	M	N	PHI	LAMDA	DELG	M	N	PHI	LAMDA	DELG	M	N	PHI	LAMDA	DELG	M	N	PHI	LAMDA	DELG	M	N
22.5	293.0	-35.	4.	24	22.5	298.5	-28.	5.	21	22.5	303.5	-22.	4.	24	22.5	309.0	-23.	4.	23	22.5	314.5	5.	6.	18
22.5	319.5	0.	5.	18	22.5	325.0	0.	3.	19	22.5	330.5	8.	5.	20	22.5	336.0	-3.	4.	21	22.5	341.5	4.	5.	21
22.5	346.5	-3.	4.	21	22.5	352.0	-14.	5.	16	22.5	357.5	-5.	6.	15	17.5	2.5	7.	1.	25	17.5	7.5	6.	2.	25
17.5	13.0	-3.	2.	24	17.5	18.5	-11.	5.	11	17.5	23.5	5.	7.	12	17.5	34.0	10.	10.	6	17.5	39.5	4.	8.	13
17.5	44.5	8.	8.	11	17.5	49.5	-20.	3.	12	17.5	54.5	3.	11.	6	17.5	60.0	2.	15.	1	17.5	65.5	-11.	8.	9
17.5	70.5	-19.	8.	10	17.5	75.5	-23.	4.	24	17.5	80.5	-10.	3.	24	17.5	86.0	-13.	7.	14	17.5	91.5	-20.	8.	11
17.5	96.5	-9.	5.	20	17.5	101.5	-17.	2.	24	17.5	107.0	-10.	6.	14	17.5	112.5	-2.	14.	2	17.5	117.5	15.	14.	2
17.5	122.5	34.	8.	11	17.5	127.5	5.	12.	4	17.5	133.0	3.	11.	6	17.5	138.5	1.	8.	9	17.5	143.5	24.	9.	10
17.5	148.5	17.	10.	8	17.5	154.0	-7.	15.	1	17.5	159.5	-9.	12.	5	17.5	164.5	-8.	11.	6	17.5	169.5	-6.	9.	11
17.5	174.5	-9.	8.	10	17.5	180.0	-2.	7.	12	17.5	185.5	0.	12.	5	17.5	190.5	-11.	8.	11	17.5	195.5	1.	12.	4
17.5	200.5	8.	8.	11	17.5	206.0	22.	8.	8	17.5	211.5	1.	11.	6	17.5	216.5	2.	13.	3	17.5	221.5	-11.	9.	9
17.5	227.0	-8.	13.	3	17.5	232.5	-10.	13.	4	17.5	237.5	-12.	12.	3	17.5	242.5	-15.	8.	8	17.5	247.5	-13.	11.	6
17.5	253.0	-12.	4.	23	17.5	258.5	-7.	4.	23	17.5	263.5	30.	4.	22	17.5	268.5	14.	3.	24	17.5	274.0	21.	4.	23
17.5	279.5	4.	4.	25	17.5	284.5	-2.	4.	25	17.5	289.5	16.	4.	24	17.5	294.5	-45.	3.	25	17.5	300.0	-36.	4.	25
17.5	305.5	-17.	10.	7	17.5	310.5	-12.	11.	6	17.5	315.5	-12.	10.	6	17.5	320.5	-16.	11.	4	17.5	326.0	-5.	14.	2
17.5	331.5	2.	15.	1	17.5	336.5	24.	8.	8	17.5	341.5	1.	9.	10	17.5	347.0	12.	3.	22	17.5	352.5	1.	9.	11
17.5	357.5	6.	4.	21	12.5	2.5	1.	3.	22	12.5	7.5	8.	7.	15	12.5	12.5	8.	4.	18	12.5	18.0	2.	11.	4
12.5	23.5	-4.	12.	3	12.5	28.5	5.	10.	5	12.5	33.5	-4.	15.	1	12.5	38.5	22.	5.	16	12.5	43.5	4.	6.	17
12.5	48.5	3.	5.	15	12.5	54.0	-4.	4.	21	12.5	59.5	-9.	5.	17	12.5	64.5	-5.	13.	3	12.5	69.5	-35.	6.	16
12.5	74.5	-30.	6.	16	12.5	79.5	-24.	6.	17	12.5	90.0	-6.	9.	7	12.5	95.5	-10.	5.	20	12.5	100.5	-6.	5.	19
12.5	105.5	-6.	3.	25	12.5	110.5	1.	8.	13	12.5	115.5	8.	7.	14	12.5	120.5	29.	5.	17	12.5	126.0	36.	7.	14
12.5	131.5	8.	13.	3	12.5	136.5	1.	10.	7	12.5	141.5	25.	10.	9	12.5	146.5	-22.	5.	16	12.5	151.5	-3.	8.	13
12.5	156.5	11.	8.	9	12.5	162.0	-6.	10.	5	12.5	167.5	-5.	13.	3	12.5	177.5	17.	12.	5	12.5	182.5	13.	14.	2
12.5	187.5	-9.	13.	4	12.5	192.5	-6.	9.	8	12.5	198.0	6.	6.	14	12.5	213.5	2.	11.	6	12.5	218.5	0.	13.	4
12.5	244.5	-9.	12.	5	12.5	254.5	-3.	13.	4	12.5	259.5	2.	11.	6	12.5	264.5	5.	9.	10	12.5	270.0	7.	5.	18
12.5	275.5	33.	5.	20	12.5	280.5	-8.	7.	14	12.5	285.5	-17.	4.	23	12.5	290.5	-33.	6.	19	12.5	295.5	-25.	5.	21
12.5	300.5	-36.	4.	24	12.5	306.0	-34.	3.	20	12.5	311.5	-23.	7.	12	12.5	316.5	-11.	5.	19	12.5	321.5	-16.	12.	5
12.5	326.5	-9.	12.	3	12.5	331.5	-4.	9.	8	12.5	336.5	-9.	7.	13	12.5	342.0	11.	6.	14	12.5	347.5	10.	7.	15
12.5	352.5	11.	3.	23	12.5	357.5	3.	2.	25	7.5	2.5	17.	6.	15	7.5	7.5	23.	6.	12	7.5	12.5	19.	9.	11
7.5	17.5	2.	12.	2	7.5	22.5	-5.	12.	3	7.5	28.0	25.	6.	12	7.5	43.5	5.	13.	3	7.5	48.5	-10.	15.	1
7.5	53.5	-36.	5.	19	7.5	58.5	-10.	5.	15	7.5	63.5	-24.	6.	13	7.5	68.5	-41.	5.	18	7.5	73.5	-43.	5.	18
7.5	78.5	-29.	5.	21	7.5	83.5	-35.	5.	17	7.5	88.5	-14.	7.	14	7.5	93.5	-23.	4.	23	7.5	98.5	8.	3.	25
7.5	103.5	5.	12.	4	7.5	109.0	0.	7.	12	7.5	114.5	7.	6.	16	7.5	119.5	42.	11.	6	7.5	124.5	54.	7.	12
7.5	129.5	4.	10.	7	7.5	134.5	23.	8.	11	7.5	139.5	5.	8.	10	7.5	144.5	7.	8.	11	7.5	149.5	-5.	7.	13
7.5	154.5	-59.	7.	10	7.5	159.5	5.	15.	1	7.5	159.5	37.	15.	1	7.5	180.0	5.	9.	5	7.5	185.5	-9.	14.	3
7.5	190.5	-6.	6.	15	7.5	195.5	-1.	13.	3	7.5	200.5	22.	9.	7	7.5	240.5	-6.	13.	4	7.5	245.5	-4.	13.	5
7.5	251.0	-4.	12.	5	7.5	256.5	0.	11.	6	7.5	251.5	2.	12.	5	7.5	266.5	3.	12.	6	7.5	271.5	10.	8.	12
7.5	276.5	25.	4.	23	7.5	281.5	21.	5.	19	7.5	286.5	27.	3.	22	7.5	291.5	3.	8.	11	7.5	296.5	-2.	11.	5
7.5	301.5	-12.	11.	4	7.5	306.5	-23.	9.	9	7.5	311.5	-34.	7.	15	7.5	316.5	-23.	7.	14	7.5	322.0	-12.	9.	11
7.5	327.5	7.	8.	11	7.5	332.5	-1.	6.	13	7.5	342.5	7.	8.	8	7.5	347.5	29.	6.	13	7.5	352.5	27.	3.	25
7.5	357.5	15.	2.	25	2.5	7.5	17.	10.	8	2.5	12.5	10.	12.	4	2.5	17.5	-11.	9.	8	2.5	22.5	-29.	7.	13
2.5	27.5	-4.	8.	10	2.5	32.5	2.	4.	20	2.5	37.5	-2.	12.	4	2.5	42.5	-11.	13.	2	2.5	47.5	-30.	7.	14
2.5	52.5	-29.	5.	17	2.5	57.5	-19.	4.	20	2.5	62.5	-21.	4.	20	2.5	67.5	-24.	10.	9	2.5	72.5	-42.	5.	17
2.5	77.5	-43.	9.	10	2.5	82.5	-30.	3.	12	2.5	87.5	-16.	8.	10	2.5	92.5	-12.	5.	19	2.5	97.5	-13.	6.	18
2.5	102.5	14.	8.	9	2.5	107.5	16.	6.	14	2.5	112.5	13.	11.	6	2.5	117.5	1.	15.	1	2.5	122.5	24.	8.	11
2.5	127.5	9.	8.	11	2.5	132.5	23.	13.	3	2.5	137.5	-1.	14.	2	2.5	142.5	4.	7.	15	2.5	147.5	11.	7.	13
2.5	152.5	11.	8.	11	2.5	157.5	2.	11.	5	2.5	177.5	4.	12.	5	2.5	182.5	3.	8.	12	2.5	187.5	-1.	8.	13
2.5	192.5	3.	14.	2	2.5	197.5	14.	12.	5	2.5	267.5	2.	15.	1	2.5	272.5	0.	14.	2	2.5	277.5	8.	7.	13
2.5	282.5	24.	3.	25	2.5	287.5	26.	2.	25	2.5	292.5	3.	15.	1	2.5	302.5	-11.	14.	2	2.5	307.5	-4.	12.	5
2.5	312.5	-2.	15.	1	2.5	317.5	-11.	11.	6	2.5	322.5	-5.	8.	13	2.5	327.5	10.	6.	18	2.5	332.5	5.	9.	13
2.5	342.5	-7.	9.	5	2.5	347.5	-8.	10.	5	2.5	352.5	5.	12.	4	2.5	357.5	2.	15.	1	-2.5	7.5	14.	15.	1

Table B-10 (Continued)

PHI	LAMDA	DELG	M	N	PHI	LAMDA	DELG	M	N	PHI	LAMDA	DELG	M	N	PHI	LAMDA	DELG	M	N	PHI	LAMDA	DELG	M	N
-2.5	12.5	-9.	11.	6	-2.5	17.5	-21.	5.	18	-2.5	22.5	-37.	2.	25	-2.5	27.5	1.	5.	20	-2.5	32.5	-7.	4.	23
-2.5	37.5	13.	7.	16	-2.5	42.5	-31.	3.	19	-2.5	47.5	-19.	6.	12	-2.5	52.5	-13.	4.	20	-2.5	57.5	-15.	4.	23
-2.5	62.5	-20.	6.	17	-2.5	67.5	-24.	10.	8	-2.5	72.5	-39.	5.	14	-2.5	77.5	-37.	9.	9	-2.5	82.5	-54.	5.	20
-2.5	87.5	-32.	6.	15	-2.5	92.5	-19.	8.	11	-2.5	97.5	4.	6.	15	-2.5	102.5	9.	9.	11	-2.5	107.5	30.	6.	17
-2.5	112.5	12.	13.	3	-2.5	117.5	8.	7.	13	-2.5	122.5	-3.	7.	16	-2.5	127.5	9.	5.	21	-2.5	132.5	24.	7.	17
-2.5	137.5	2.	7.	11	-2.5	142.5	28.	3.	23	-2.5	147.5	37.	3.	25	-2.5	152.5	17.	6.	16	-2.5	157.5	18.	10.	7
-2.5	177.5	-6.	8.	11	-2.5	182.5	4.	13.	3	-2.5	187.5	-1.	9.	8	-2.5	197.5	15.	12.	5	-2.5	202.5	6.	15.	1
-2.5	277.5	0.	9.	7	-2.5	282.5	8.	8.	11	-2.5	287.5	25.	11.	5	-2.5	292.5	15.	13.	3	-2.5	297.5	-2.	15.	1
-2.5	302.5	-8.	13.	2	-2.5	307.5	-0.	12.	4	-2.5	312.5	-30.	5.	22	-2.5	317.5	-29.	6.	19	-2.5	322.5	-1.	9.	10
-2.5	327.5	-7.	6.	16	-2.5	332.5	-5.	6.	19	-2.5	337.5	-10.	8.	14	-2.5	342.5	-12.	10.	7	-2.5	347.5	6.	10.	8
-2.5	352.5	3.	12.	3	-7.5	7.5	-7.	12.	4	-7.5	12.5	10.	11.	3	-7.5	17.5	-4.	14.	2	-7.5	22.5	-11.	9.	12
-7.5	27.5	-9.	5.	21	-7.5	32.5	5.	4.	23	-7.5	38.0	-1.	5.	20	-7.5	43.5	-35.	5.	19	-7.5	48.5	-18.	6.	14
-7.5	53.5	-2.	8.	9	-7.5	58.5	-6.	10.	8	-7.5	63.5	-8.	12.	5	-7.5	68.5	-5.	7.	12	-7.5	73.5	-4.	11.	6
-7.5	78.5	-15.	13.	3	-7.5	83.5	-13.	13.	4	-7.5	88.5	-6.	13.	2	-7.5	93.5	-11.	11.	5	-7.5	98.5	8.	10.	10
-7.5	103.5	-15.	4.	23	-7.5	109.0	18.	4.	21	-7.5	114.5	17.	5.	20	-7.5	119.5	-4.	5.	21	-7.5	124.5	-5.	5.	24
-7.5	129.5	-26.	5.	25	-7.5	134.5	8.	5.	15	-7.5	139.5	16.	4.	21	-7.5	144.5	25.	3.	25	-7.5	149.5	20.	3.	25
-7.5	154.5	36.	3.	25	-7.5	159.5	23.	3.	25	-7.5	154.5	-36.	4.	25	-7.5	169.5	-23.	10.	9	-7.5	174.5	0.	9.	9
-7.5	180.0	1.	8.	8	-7.5	185.5	-5.	14.	2	-7.5	190.5	-2.	9.	5	-7.5	200.5	22.	10.	6	-7.5	220.5	10.	14.	1
-7.5	276.5	-8.	12.	3	-7.5	281.5	-8.	12.	4	-7.5	286.5	-13.	9.	8	-7.5	291.5	5.	13.	3	-7.5	296.5	2.	14.	1
-7.5	311.5	-26.	7.	17	-7.5	316.5	-28.	4.	25	-7.5	322.0	-4.	4.	25	-7.5	327.5	-17.	6.	15	-7.5	332.5	-5.	14.	3
-7.5	337.5	-4.	11.	8	-7.5	342.5	-4.	6.	18	-7.5	347.5	3.	6.	18	-7.5	352.5	-4.	13.	2	-7.5	357.5	-3.	12.	3
-12.5	12.5	6.	13.	2	-12.5	18.0	4.	14.	1	-12.5	23.5	2.	11.	4	-12.5	28.5	-15.	7.	13	-12.5	33.5	-6.	9.	12
-12.5	38.5	-13.	11.	7	-12.5	43.5	-26.	5.	13	-12.5	48.5	11.	8.	10	-12.5	54.0	-5.	6.	14	-12.5	59.5	-27.	11.	4
-12.5	64.5	4.	8.	10	-12.5	69.5	2.	11.	4	-12.5	79.5	-12.	13.	3	-12.5	84.5	-9.	13.	3	-12.5	90.0	-17.	12.	4
-12.5	95.5	-10.	5.	15	-12.5	100.5	-8.	5.	17	-12.5	105.5	3.	7.	12	-12.5	110.5	-8.	4.	20	-12.5	115.5	-26.	5.	21
-12.5	120.5	2.	3.	23	-12.5	126.0	23.	2.	25	-12.5	131.5	27.	2.	24	-12.5	136.5	19.	4.	21	-12.5	141.5	15.	3.	25
-12.5	146.5	11.	3.	25	-12.5	151.5	19.	4.	25	-12.5	156.5	25.	4.	23	-12.5	162.0	11.	4.	25	-12.5	167.5	16.	6.	18
-12.5	172.5	-5.	15.	1	-12.5	177.5	-2.	11.	5	-12.5	182.5	17.	9.	7	-12.5	187.5	14.	8.	11	-12.5	192.5	17.	9.	10
-12.5	198.0	9.	12.	5	-12.5	260.5	-10.	10.	5	-12.5	285.5	-2.	10.	6	-12.5	290.5	13.	11.	6	-12.5	295.5	33.	11.	6
-12.5	306.0	-16.	15.	1	-12.5	311.5	5.	3.	15	-12.5	316.5	-8.	4.	25	-12.5	321.5	-3.	5.	20	-12.5	326.5	-15.	7.	14
-12.5	342.0	-4.	11.	5	-12.5	347.5	-5.	8.	12	-12.5	352.5	-3.	12.	3	-12.5	357.5	-2.	13.	2	-17.5	7.5	2.	14.	2
-17.5	13.0	5.	12.	2	-17.5	18.5	4.	15.	1	-17.5	23.5	-0.	10.	6	-17.5	28.5	10.	7.	14	-17.5	34.0	-1.	7.	13
-17.5	39.5	-15.	8.	10	-17.5	44.5	4.	6.	17	-17.5	49.5	18.	8.	12	-17.5	54.5	-8.	6.	14	-17.5	60.0	21.	6.	15
-17.5	65.5	-4.	9.	7	-17.5	70.5	1.	14.	2	-17.5	75.5	8.	13.	4	-17.5	80.5	-8.	7.	12	-17.5	86.0	-15.	8.	10
-17.5	91.5	-29.	6.	15	-17.5	96.5	-20.	7.	12	-17.5	101.5	-22.	8.	10	-17.5	107.0	-12.	9.	6	-17.5	112.5	-21.	7.	15
-17.5	117.5	-5.	4.	20	-17.5	122.5	11.	2.	25	-17.5	127.5	13.	1.	25	-17.5	133.0	4.	1.	25	-17.5	138.5	9.	2.	25
-17.5	143.5	20.	1.	25	-17.5	148.5	15.	3.	25	-17.5	154.0	11.	4.	25	-17.5	159.5	1.	5.	20	-17.5	164.5	18.	9.	10
-17.5	169.5	24.	10.	8	-17.5	174.5	20.	10.	5	-17.5	180.0	18.	8.	11	-17.5	190.5	6.	9.	7	-17.5	200.5	9.	15.	1
-17.5	206.0	16.	15.	1	-17.5	211.5	22.	13.	1	-17.5	216.5	1.	14.	1	-17.5	268.5	1.	15.	1	-17.5	279.5	-11.	14.	1
-17.5	284.5	4.	13.	3	-17.5	289.5	57.	3.	11	-17.5	294.5	33.	6.	17	-17.5	300.0	19.	9.	7	-17.5	305.5	1.	13.	4
-17.5	310.5	-21.	8.	13	-17.5	315.5	-23.	4.	25	-17.5	320.5	-14.	4.	23	-17.5	326.0	-16.	6.	13	-17.5	357.5	0.	11.	3
-22.5	2.5	4.	9.	8	-22.5	8.0	-4.	12.	3	-22.5	13.5	4.	12.	3	-22.5	18.5	10.	10.	6	-22.5	24.0	2.	13.	7
-22.5	29.5	8.	4.	20	-22.5	35.5	-14.	10.	8	-22.5	40.5	-14.	5.	18	-22.5	45.5	22.	5.	21	-22.5	51.0	9.	8.	10
-22.5	56.5	7.	5.	21	-22.5	61.5	19.	6.	15	-22.5	57.0	30.	5.	16	-22.5	72.5	16.	6.	15	-22.5	78.0	-0.	11.	8
-22.5	83.5	-8.	13.	3	-22.5	88.5	-11.	12.	5	-22.5	94.0	-14.	12.	5	-22.5	99.5	-28.	8.	10	-22.5	104.5	-7.	14.	3
-22.5	110.0	5.	11.	6	-22.5	115.5	5.	3.	21	-22.5	121.0	-1.	4.	21	-22.5	126.5	-11.	1.	25	-22.5	131.5	-9.	2.	25
-22.5	137.0	8.	2.	25	-22.5	142.5	5.	2.	25	-22.5	147.5	22.	2.	25	-22.5	153.0	8.	10.	8	-22.5	158.5	7.	12.	5
-22.5	164.0	34.	6.	15	-22.5	169.5	23.	10.	6	-22.5	174.5	24.	11.	5	-22.5	180.0	4.	15.	1	-22.5	185.5	-20.	7.	15
-22.5	190.5	-19.	8.	7	-22.5	239.0	3.	13.	3	-22.5	244.5	4.	12.	5	-22.5	287.5	-1.	9.	8	-22.5	293.0	61.	5.	18
-22.5	298.5	-1.	10.	9	-22.5	303.5	0.	12.	4	-22.5	309.0	-19.	4.	22	-22.5	314.5	-4.	5.	19	-22.5	319.5	-12.	7.	15
-22.5	325.0	-14.	10.	6	-22.5	357.5	2.	15.	1	-27.5	3.0	3.	13.	3	-27.5	8.5	-2.	10.	7	-27.5	14.0	23.	7.	13

Table B-10 (Continued)

PHI	LAMDA	DELG	M	N	PHI	LAMDA	DELG	M	N	PHI	LAMDA	DELG	M	N	PHI	LAMDA	DELG	M	N	PHI	LAMDA	DELG	M	N
-27.5	20.0	15.	3.	23	-27.5	25.5	17.	2.	25	-27.5	31.0	35.	4.	20	-27.5	36.5	-10.	8.	10	-27.5	42.0	3.	7.	13
-27.5	48.5	15.	6.	15	-27.5	53.5	5.	11.	7	-27.5	59.0	3.	7.	10	-27.5	65.0	10.	12.	4	-27.5	70.5	21.	12.	4
-27.5	76.0	20.	11.	7	-27.5	81.5	-5.	13.	4	-27.5	87.0	-3.	12.	5	-27.5	93.0	-6.	12.	5	-27.5	98.5	-5.	13.	5
-27.5	104.0	-12.	10.	9	-27.5	110.0	-20.	8.	9	-27.5	115.5	-0.	3.	22	-27.5	121.0	-8.	5.	19	-27.5	126.5	-16.	4.	23
-27.5	132.0	-7.	4.	21	-27.5	138.0	-13.	1.	25	-27.5	143.5	-5.	1.	25	-27.5	149.0	12.	1.	25	-27.5	155.0	4.	5.	18
-27.5	160.5	4.	9.	8	-27.5	166.0	13.	13.	3	-27.5	171.5	5.	13.	2	-27.5	177.0	0.	13.	3	-27.5	183.0	30.	11.	6
-27.5	188.5	-11.	9.	9	-27.5	245.0	0.	13.	3	-27.5	250.5	-2.	9.	9	-27.5	256.0	2.	15.	1	-27.5	261.5	-2.	14.	2
-27.5	290.0	55.	5.	18	-27.5	295.5	8.	2.	25	-27.5	301.0	12.	5.	17	-27.5	306.5	-7.	6.	16	-27.5	312.0	-10.	5.	19
-27.5	318.0	-12.	13.	2	-27.5	323.5	-7.	10.	5	-27.5	351.5	-3.	15.	1	-32.5	3.0	4.	14.	1	-32.5	9.0	5.	10.	9
-32.5	15.0	2.	6.	15	-32.5	21.0	20.	2.	25	-32.5	27.0	12.	3.	23	-32.5	32.5	17.	8.	11	-32.5	38.0	-2.	9.	8
-32.5	44.0	35.	10.	6	-32.5	50.0	9.	12.	4	-32.5	62.0	-6.	10.	4	-32.5	74.0	20.	9.	5	-32.5	91.5	12.	15.	1
-32.5	97.0	-19.	8.	8	-32.5	103.0	-24.	8.	7	-32.5	109.0	-26.	8.	10	-32.5	115.0	-15.	4.	21	-32.5	121.0	-15.	3.	24
-32.5	127.0	-15.	6.	16	-32.5	133.0	-17.	5.	17	-32.5	139.0	-0.	2.	25	-32.5	145.0	-0.	3.	23	-32.5	150.5	21.	3.	25
-32.5	156.0	-10.	8.	11	-32.5	162.0	-1.	15.	1	-32.5	174.0	25.	13.	2	-32.5	180.0	-6.	13.	2	-32.5	186.0	-2.	13.	4
-32.5	192.0	-15.	10.	7	-32.5	215.0	1.	13.	3	-32.5	221.0	7.	12.	4	-32.5	227.0	2.	12.	5	-32.5	233.0	5.	13.	3
-32.5	239.0	3.	12.	5	-32.5	245.0	-1.	12.	5	-32.5	251.0	-3.	11.	6	-32.5	257.0	-4.	7.	12	-32.5	263.0	-10.	9.	6
-32.5	268.5	-3.	9.	5	-32.5	274.0	0.	9.	5	-32.5	280.0	-0.	8.	5	-32.5	286.0	-6.	7.	11	-32.5	292.0	30.	3.	23
-32.5	298.0	11.	1.	25	-32.5	304.0	19.	3.	24	-32.5	310.0	5.	9.	8	-32.5	316.0	0.	12.	4	-32.5	322.0	4.	10.	5
-32.5	327.5	-12.	12.	2	-32.5	333.0	4.	12.	3	-32.5	339.0	4.	15.	1	-32.5	351.0	-3.	12.	3	-32.5	357.0	11.	13.	3
-37.5	9.5	-3.	13.	3	-37.5	22.0	-3.	9.	10	-37.5	28.5	5.	7.	12	-37.5	35.0	5.	8.	7	-37.5	41.0	13.	10.	5
-37.5	55.0	-1.	12.	4	-37.5	72.5	-2.	12.	4	-37.5	79.0	-6.	7.	10	-37.5	85.0	-5.	8.	7	-37.5	91.5	-3.	9.	7
-37.5	98.0	-11.	10.	5	-37.5	104.0	-21.	12.	5	-37.5	136.0	3.	9.	5	-37.5	142.0	2.	4.	19	-37.5	148.5	18.	6.	15
-37.5	155.0	-10.	8.	8	-37.5	161.0	-7.	10.	5	-37.5	167.5	4.	11.	5	-37.5	174.0	28.	7.	14	-37.5	180.0	-16.	5.	18
-37.5	192.5	-24.	11.	5	-37.5	218.0	-3.	13.	3	-37.5	224.0	-2.	13.	3	-37.5	230.5	3.	12.	3	-37.5	237.0	4.	13.	3
-37.5	243.0	-3.	13.	2	-37.5	249.5	-4.	13.	2	-37.5	262.0	-7.	8.	9	-37.5	268.5	-1.	15.	1	-37.5	281.0	1.	15.	1
-37.5	287.5	22.	6.	17	-37.5	294.0	0.	2.	25	-37.5	300.0	11.	3.	22	-37.5	306.0	6.	7.	14	-37.5	312.5	-10.	11.	5
-37.5	319.0	-2.	15.	1	-37.5	338.0	6.	14.	2	-37.5	350.5	5.	13.	3	-42.5	30.5	70.	9.	5	-42.5	71.5	-4.	11.	4
-42.5	146.0	18.	8.	8	-42.5	152.5	-7.	12.	5	-42.5	156.5	3.	13.	3	-42.5	173.5	10.	5.	18	-42.5	180.0	12.	9.	10
-42.5	186.5	-20.	10.	7	-42.5	193.5	-14.	13.	3	-42.5	258.5	-5.	8.	9	-42.5	281.5	-0.	12.	3	-42.5	288.5	35.	6.	15
-42.5	295.5	0.	7.	13	-42.5	302.5	-9.	7.	14	-42.5	309.0	-10.	9.	8	-42.5	315.5	-4.	14.	2	-42.5	356.5	-7.	15.	1
-47.5	40.5	11.	15.	1	-47.5	69.5	15.	10.	5	-47.5	158.0	-9.	12.	5	-47.5	165.5	34.	11.	5	-47.5	172.5	17.	13.	4
-47.5	180.0	-1.	15.	1	-47.5	187.5	-19.	7.	14	-47.5	194.5	0.	15.	1	-47.5	253.5	2.	14.	2	-47.5	268.0	1.	15.	1
-47.5	275.5	10.	9.	9	-47.5	283.0	-19.	13.	2	-47.5	290.5	-6.	7.	13	-47.5	297.5	-9.	10.	7	-47.5	305.0	-12.	6.	16
-52.5	69.5	13.	12.	4	-52.5	159.5	-1.	12.	5	-52.5	158.0	12.	12.	4	-52.5	192.0	-6.	10.	6	-52.5	249.5	7.	13.	2
-52.5	282.0	4.	9.	8	-52.5	290.5	4.	8.	8	-52.5	299.0	1.	5.	18	-52.5	307.0	-3.	12.	5	-52.5	323.0	26.	14.	3
-57.5	50.5	7.	14.	1	-57.5	152.5	-1.	12.	5	-57.5	189.5	-23.	8.	10	-57.5	198.5	-11.	12.	2	-57.5	253.5	-4.	14.	2
-57.5	290.5	15.	11.	7	-57.5	300.0	15.	8.	7	-57.5	309.5	9.	6.	13	-57.5	318.5	9.	13.	3	-57.5	327.5	13.	14.	2
-57.5	337.0	14.	13.	3	-62.5	8.5	4.	14.	2	-62.5	16.5	15.	8.	8	-62.5	27.5	-0.	14.	1	-62.5	49.5	6.	15.	1
-62.5	70.5	30.	10.	4	-62.5	91.5	12.	9.	10	-62.5	92.5	-17.	11.	7	-62.5	103.5	19.	13.	3	-62.5	114.5	-28.	13.	2
-62.5	125.5	-18.	12.	3	-62.5	136.5	-5.	12.	3	-62.5	147.5	-11.	14.	1	-62.5	158.5	-3.	9.	9	-62.5	169.5	-1.	14.	1
-62.5	190.5	-10.	9.	5	-62.5	201.5	-4.	12.	2	-62.5	245.5	3.	13.	2	-62.5	256.5	-2.	15.	1	-62.5	289.5	0.	12.	3
-62.5	300.0	38.	6.	15	-62.5	310.5	28.	11.	7	-67.5	6.5	2.	12.	5	-67.5	19.5	-9.	6.	14	-67.5	32.5	26.	7.	13
-67.5	45.0	4.	6.	13	-67.5	57.5	35.	7.	13	-57.5	70.5	17.	6.	13	-57.5	83.5	14.	6.	16	-67.5	96.5	20.	5.	18
-67.5	109.5	15.	7.	15	-67.5	122.5	-15.	8.	10	-67.5	135.0	4.	13.	6	-67.5	147.5	-15.	8.	9	-67.5	160.5	-12.	5.	15
-67.5	173.5	-8.	8.	8	-67.5	186.5	-10.	6.	15	-67.5	199.5	-16.	10.	5	-67.5	212.5	2.	13.	1	-67.5	225.0	-15.	12.	3
-67.5	237.5	-16.	11.	6	-67.5	250.5	-4.	12.	2	-67.5	253.5	15.	12.	2	-67.5	276.5	-5.	10.	5	-67.5	289.5	14.	12.	5
-67.5	302.5	7.	15.	1	-72.5	8.0	10.	14.	2	-72.5	24.5	7.	10.	6	-72.5	90.0	10.	7.	12	-72.5	106.5	-31.	10.	7
-72.5	139.0	-17.	9.	8	-72.5	155.5	-23.	8.	5	-72.5	172.0	-16.	13.	2	-72.5	204.5	-17.	11.	3	-72.5	237.0	-14.	15.	2
-72.5	253.5	-2.	15.	1	-72.5	270.0	9.	11.	5	-72.5	286.5	22.	10.	8	-77.5	79.0	16.	11.	5	-77.5	101.5	-14.	8.	12
-77.5	124.0	-2.	14.	1	-77.5	146.5	-36.	6.	13	-77.5	159.0	-7.	8.	11	-77.5	191.5	-17.	9.	11	-77.5	214.0	-16.	9.	9
-77.5	236.5	-6.	4.	20	-77.5	259.0	-14.	4.	22	-77.5	281.5	5.	9.	9	-77.5	304.0	-3.	13.	3	-77.5	326.5	-15.	10.	8
-82.5	60.0	28.	9.	7	-82.5	140.0	-32.	7.	11	-82.5	180.0	-30.	5.	17	-82.5	220.0	-13.	10.	9	-82.5	260.0	-6.	3.	24
-82.5	300.0	-16.	6.	14	-87.5	180.0	-19.	6.	14	-87.5	300.0	-12.	8.	10										

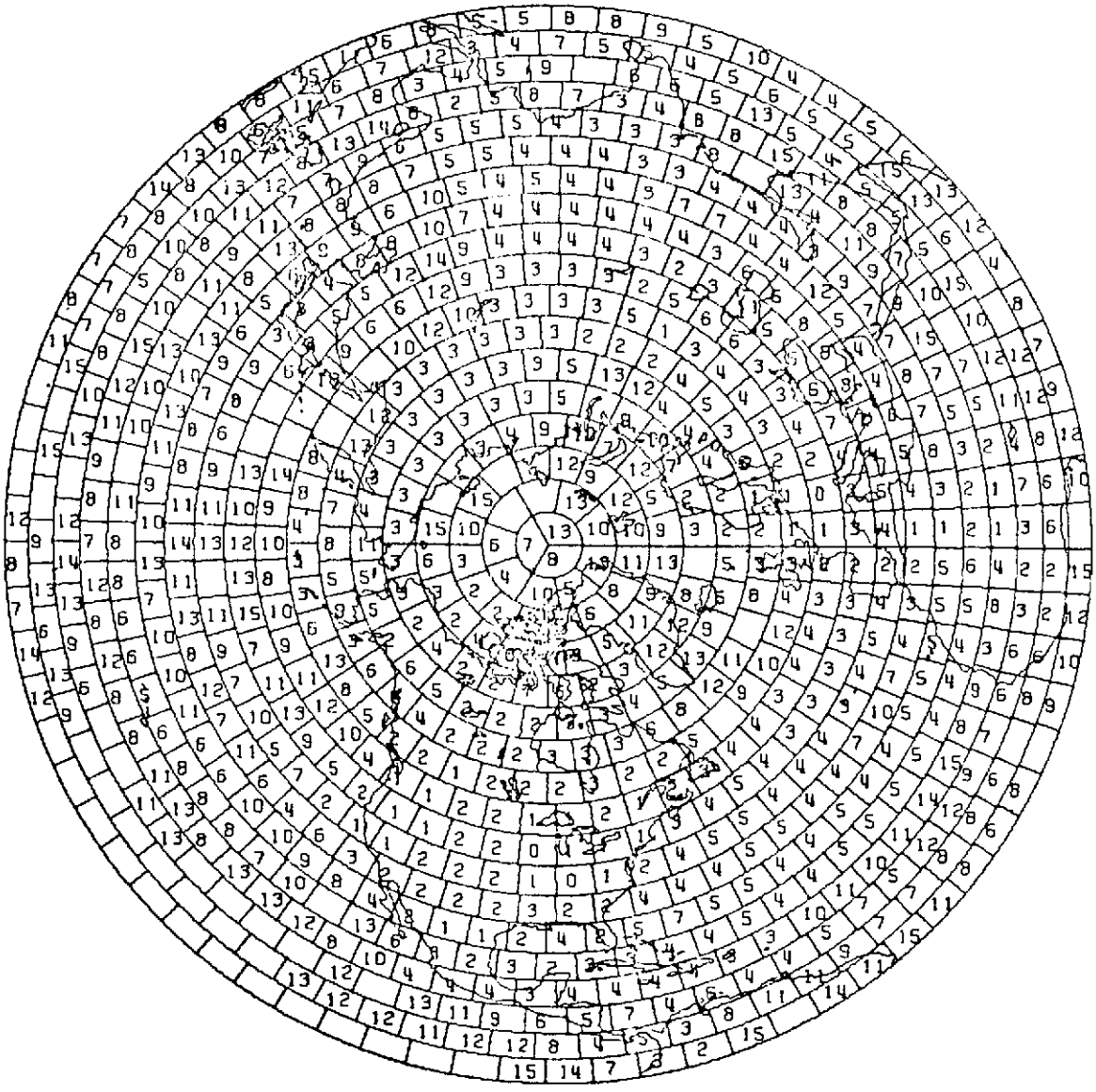

Figure B-1. Distribution and Errors (mgal) of 5°
Mean Gravity Anomalies, Rapp (1972)
(Northern Hemisphere)

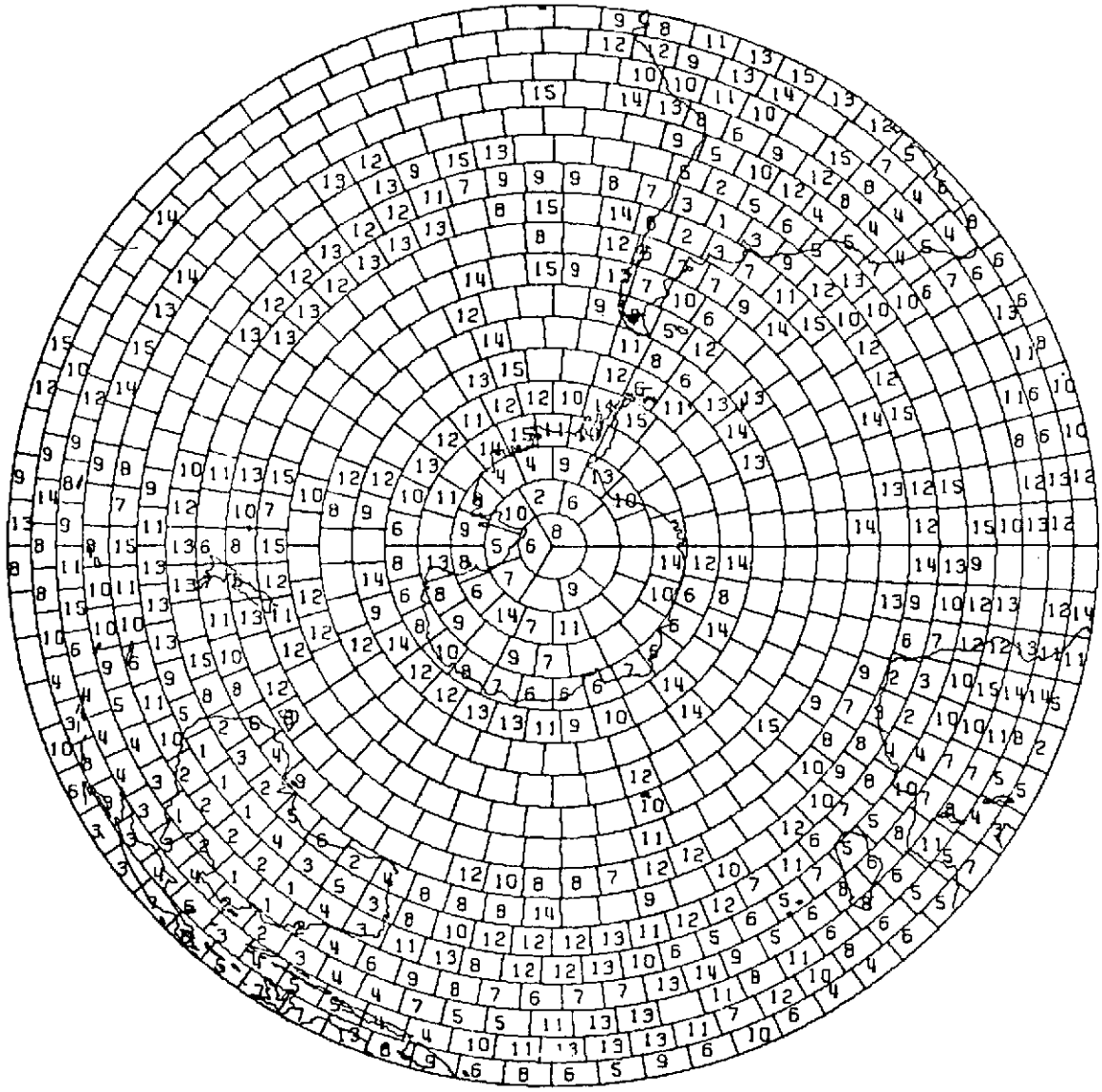

Figure B-1 (continued). Distribution and Errors (mgal) of 5° Mean Gravity Anomalies, Rapp (1972) (Southern Hemisphere)

EDGE INDEX

SECTION I . . . . . INTRODUCTION

SECTION II . . . . . DATA EMPLOYED

SECTION III . . . . . MODELING AND ANALYSIS

SECTION IV . . . . . RESULTS (GEOPOTENTIAL AND STATIONS)

SECTION V. . . . . SUMMARY AND CONCLUSIONS

REFERENCES

APPENDICES

APPENDIX A1 . . . . . ORBIT THEORY FOR GEODYN

APPENDIX A2 . . . . . GEOMETRIC METHOD

APPENDIX A3 . . . . . GRAVIMETRIC METHOD

APPENDIX A4 . . . . . TECHNIQUES IN COMBINED SOLUTION

APPENDIX B. . . . . SATELLITE AND GRAVITY DATA DISTRIBUTIONS